

UNIVERSITÀ DELLA CALABRIA



UNIVERSITA' DELLA CALABRIA

Dipartimento di Chimica e Tecnologie Chimiche

Dottorato di Ricerca in

Scienze della Vita

CICLO

XXXI

Eco-friendly Additives for Sustainable Road Pavements

Settore Scientifico Disciplinare CHIM/02

Coordinatore: Ch.mo Prof.ssa Maria Carmela Cerra

Firma

Supervisore/Tutor: Ch.mo Prof. Cesare Oliviero Rossi

Firma

Dottorando: Dott. Paolino Caputo

Firma

A mia Moglie e alle mie Figlie,

che sono “tutte le mie ragioni” (cit. J. Nash);

grazie anche a Dio che illumina il mio cammino.

Contents.

Abstract	4
----------	---

Chapter 1

1.1	Introduction	4
1.1.1	Principles of Sustainability	4
1.1.2	Sustainable pavements	4
1.1.3	Different types of additive	5
1.2	Problem statement	5
1.2.1	Sustainable materials for paving	5
1.3	REFERENCES Chapter 1	7

Chapter 2 Materials

2.1	Crude oil overview	8
2.1.1	Crude Oil Characteristics	9
2.2	Bitumen	12
2.3	Different bitumen sources	15
2.3.1	Natural bitumen	15
2.3.2	Oxidized bitumen	15
2.4	Asphalt	15
2.4.1	Asphaltic rocks	15
2.4.2	Tar	15
2.5	Reclaimed Asphalt Pavement (RAP)	16
2.6	Bitumen Modifiers	16
2.6.1	Polymer Modified Bitumen	16
2.7	Adhesion promoter for bitumen	18
2.8	REFERENCES Chapter 2	20

Chapter 3 Experimental Techniques

3.1	Nuclear Magnetic Resonance.	26
3.1.1	Basic Concepts	26
3.1.2	Spin-Spin Relaxation time measurement: Spin Echo Sequences	28
3.1.3	Inverse Laplace Transform of the echo decay	31
3.2	Atomic Force Microscopy (AFM)	32
3.2.1	Artifacts in Atomic Force Microscopy	34
3.2.2	Tip Effects	34
3.3	Fundamentals Rheology of Viscoelastic Matter	37
3.4	REFERENCES Chapter 3	43

Chapter 4

Results part I: “Investigation of new additives to reduce the fume emission of bitumen during Asphalt Concrete Processing” : Published Data	46
---	----

Chapter 5

Results part II: “Role of a food grade additive in the high temperature performance of modified bitumens” : Published Data	54
--	----

Chapter 6

Results part III: “ ¹ H-NMR Spectroscopy: A Possible Approach to Advanced Bitumen Characterization for Industrial and Paving Applications” : Published Data	61
--	----

Chapter 7

Results part IV: “Effects of Natural Antioxidant Agents on the Bitumen Aging Process: An EPR and Rheological Investigation”: Published Data	75
---	----

Chapter 8

Results part V: “A New Green Rejuvenator: Evaluation of Structural Changes of Aged and Recycled Bitumens by Means of Rheology and NMR” : Published Data	89
---	----

Chapter 9

Results part VI: Effect of high water salinity on the bitumen adhesion proprieties modified with a smart additive. : Paper submitted_____90

Chapter 10

Results part VII: “Effect of additives on the structural organization of asphaltene aggregates in bitumen” : Paper submitted_____109

Chapter 11

Results part VIII: “A new eco friendly rejuvenator and differentiation between a real rejuvenator and a softener for bitumens by means NMR techniques”: Paper submitted_____110

ABSTRACT

The main objective of the present study is to develop and to evaluate the effectiveness of new additives that are non-toxic and eco-friendly biocompatible in the road pavement industry. Currently, in the field of the road pavements there is a tendency to adopt more sustainable practices looking the health and environment. Mainly the new additives were characterized and developed in order to reduce bitumen's fume emission expelled into the atmosphere during the processing of asphalt concrete. Additionally in the present research new bioadditives were developed and tested to improve the adhesion between bitumen and stones and to modify the rheological characteristic of the binder as well as antioxidant properties of the bitumen.

Chapter 1

1.1 Introduction

1.1.1 Principles of Sustainability

Most definitions of sustainability begin with that issued by the World Commission on Environment and Development (WCED) in 1987: "Sustainable development is development that meets the needs of the present without compromising the ability of future generations to meet their own needs." Moreover, sustainability is often described as a quality that reflects the balance of three primary components: economic, environmental, and social impacts [1].

1.1.2 Sustainable pavements

"Sustainable" in the context of pavements refers to system characteristics that encompasses a pavement's ability to:

- Achieve the engineering goals for, which they were constructed.
- Preserve and (ideally) restore surrounding ecosystems.
- Use financial, human, and environmental resources economically.
- Meet human needs such as health, safety, equity, employment, comfort, and happiness.

All stakeholders in the pavement community from owner/agencies to designers, and from material suppliers to contractors and consultants are embracing the need to adopt more sustainable practices in all aspects of their work, and are continually seeking the latest technical information and guidance available to help improve those practices [2]. In this respect, asphalt has been considered as a sustainable material for constructing pavements. From the production of the paving material, to the placement of the pavement on the road, to rehabilitation, through recycling, asphalt pavements

minimize impact on the environment. Low consumption of energy for production and construction, low emission of greenhouse gases, and conservation of natural resources help to make asphalt the environmental pavement of choice. However, the ever-increasing pavement's loads and the needs for using modified binders and additives to coup the problem of heavy-duty pavements has led to both environmental and economic concerns.

1.1.3 Different types of additives

To date several types of asphalt mixture additives have been introduced and experienced in the filed practices. These additives can be mainly divided into three categories of asphalt mixture modifiers [3], asphalt mixture reinforcement materials [4] and recovering agents [5].

Asphalt mixture modifiers can be divided into direct modification with low-melting point additives [6], which are added directly to the hot mixtures and those of additives (mainly polymers), which are added to the bitumen binders, producing modified bitumen, then added to asphalt mixture [7]. While as for asphalt mixture modifier many different low-melting temperature polymers e.g. EVA have been introduced, for bitumen modification purposes elastomeric copolymers are more common. Asphalt mixture reinforcing materials are considered the latest introduced additives aiming for enhancing the asphalt mixtures for improving its shortcomings for heavy-duty pavement. Within a few research works it has been shown that this synthetic materials are capable to improve the tensile properties by providing a network through asphalt mixture. The last group of asphalt mixture additives include those of oils and resins both with plant-based resources or petroleum-based ones. These materials can be added either to bitumen binder or directly to the asphalt mixture depending on the nature of the product and functionality. The main purposes of adopting such these additives are recovering some shortcoming of aged binder [8], anti-stripping agent [9] and warm-mix additives for reducing the mix and compaction temperature [10].

2 Problem statement

1.2.1 Sustainable materials for paving

Pavement materials play an important role in overall pavement sustainability including material acquisition processing, and transportation. In this respect recycling materials and locally available by-products and plant-based resources could be considered as eco-friendly sustainable paving materials. To date many different plant-based materials such plant based fibre resources and different

vegetable oils have been successfully used as an additives for asphalt mixtures. However, there is still a long way to optimum well-recognized materials, in particular those aiming for enhancing the asphalt mixture properties.

On the other hand, producing Hot Mix Asphalt (HMA) containing commonly used SBS Polymer modified Bitumen (SBS PmB) consumes a considerable amount of energy due to high viscosity of modified binder. Bearing in mind that, even producing any kind of PmBs consumes a considerable amount of energy, which is neither economical, nor eco-friendly solution. In addition, some technical deficiencies such as the difficulties of providing a compatible polymer/bitumen aggravates the shortcomings of PmBs in asphalt pavement technology.

Regarding the abovementioned obstacles related to sustainable paving materials, bio-based recycling additives may provide a solution to coup the problems of constructing modified asphalt mixtures for heavy-duty pavements. Bearing in mind the highly developed network of roadways in Europe and the considerable amount of energy and financial resources annually used to keep the acceptable level of service of EU highways, the needs for more eco-friendly and economical solutions became more crucial.

1.3 REFERENCES Chapter 1

1. Bardeesi, M. W.; Attallah, Y. Economic and environmental considerations for pavement management systems. *European Scientific Journal* 2015, 11, No.29.
2. Kowalski, K. J.; Król, J.; Radziszewski, P.; Casado, R.; Blanco, V.; Pérez, D.; Viñas, V.M.; Brijse, Y.; Frosch, M.; Le, D.M.; Wayman M. Eco-friendly materials for a new concept of asphalt pavement. *Transportation Research Procedia* 2016, 14, 3582-3591.
3. Baldino, N.; Gabriele, G.; Lupi, F.R.; Oliviero Rossi, C.; Caputo, P.; Falvo, T. Rheological effects on bitumen of polyphosphoric acid (PPA) addition. *Construction and Building Materials* 2013. 40, 397–404.
4. Jaskuła, P.; Stienss, M.; Szydłowski, C. Effect of polymer fibres reinforcement on selected properties of asphalt mixtures. *Procedia Engineering* 2017, 172, 441 – 448.
5. Zaumanis, M.; Mallick, R.B.; Frank, R. Evaluation of different recycling agents for restoring aged asphalt binder and performance of 100 % recycled asphalt. *Materials and Structures* 2015, 48:2475–2488 DOI 10.1617/s11527-014-0332-5.
6. Merusi, F.; Giuliani, F. Rheological characterization of wax-modified asphalt binders at high service temperatures. *Materials and Structures* 2011, 44:1809–1820 DOI 10.1617/s11527-011-9739-4.
7. Yildirim, Y. Polymer modified asphalt binders, *Construction and Building Materials* 2007,21, 66–72.
8. Chen, M.; Leng, B.; Wu, S.; Sang, Y. Physical, chemical and rheological properties of waste edible vegetable oil rejuvenated asphalt binders. *Construction and Building Materials* 2014, 66, 286–298.
9. Oliviero Rossi, C.; Caputo, P.; Baldino, N.; Lupi, F.R.; Miriello, D.; Angelico, R. Effects of adhesion promoters on the contact angle of bitumen-aggregate interface. *International Journal of Adhesion & Adhesives* 2016, 70, 297–303.
10. Chowdhury, A.; Button, J.W. A Review of Warm Mix Asphalt. SWUTC/08/473700-00080-1

Chapter 2

Materials

Bitumen has been widely used in variety of applications construction included flexible pavements other for a long time. However, in some applications, the performance of conventional bitumen may not be considered satisfactory. Hence, the characterization of bitumen is a necessary step to provide a stable system especially for bitumen polymer modifications. It is well-accepted that, the inherent characteristics of bitumen are highly depended on the bitumen production and processing procedure as well as bitumen crude oil characteristics. Therefore having the knowledge on the characteristics and applied processing method of bitumen is of paramount importance. This knowledge turns to be more importance, where for some bitumen applications some difficulties such as discontinuity in phase, mal dispersion, and instability make a challenge in production and application of bituminous materials. Here the knowledge of the origin of bitumen and the used processing system will support the interpretations of the problem occurrence.

The provided review aimed to gather all the needed information regarding bitumen and bituminous systems from early steps of crude oil characterization to the latest advances and findings on bitumen modifications. As for crude oil section, the authors concentrated on crude oil chemical characterization systems as well as different distillation processing continued by bitumen fundamental chemical fractions. The second section concentrated on different bitumen modification systems. In this case, mainly three groups of Elastomers, Plastomers, and Wax added bitumens were characterised by reviewing and concluding some of the viable research works and field documented data.

2.1 Crude oil overview

Although crude oil was known and used since ancient times by the civilizations along the Euphrates river as early as 3800 B. C. [1], by Greeks, Roman and Egyptians, its real industrial use starts from 1859 with the first drill in Pennsylvania carried out by E. Drake. Previously it was recovered by natural resources in which it emerged spontaneously and used as a fuel in oil lamps as an alternative to whale oil or coal derivatives. Being recognized its potentials, nearly 340 oil wells were delved and in 1870 the first crude oil company was founded by J. D. Rockefeller; the Standard Oil Company, nowadays known as Esso. Crude oil key role in industry growth developed in the first half of XX century mostly with the advent of new industrial technologies and engines. In this case, (Fig. 2.1) represents the price evolution of crude oil.

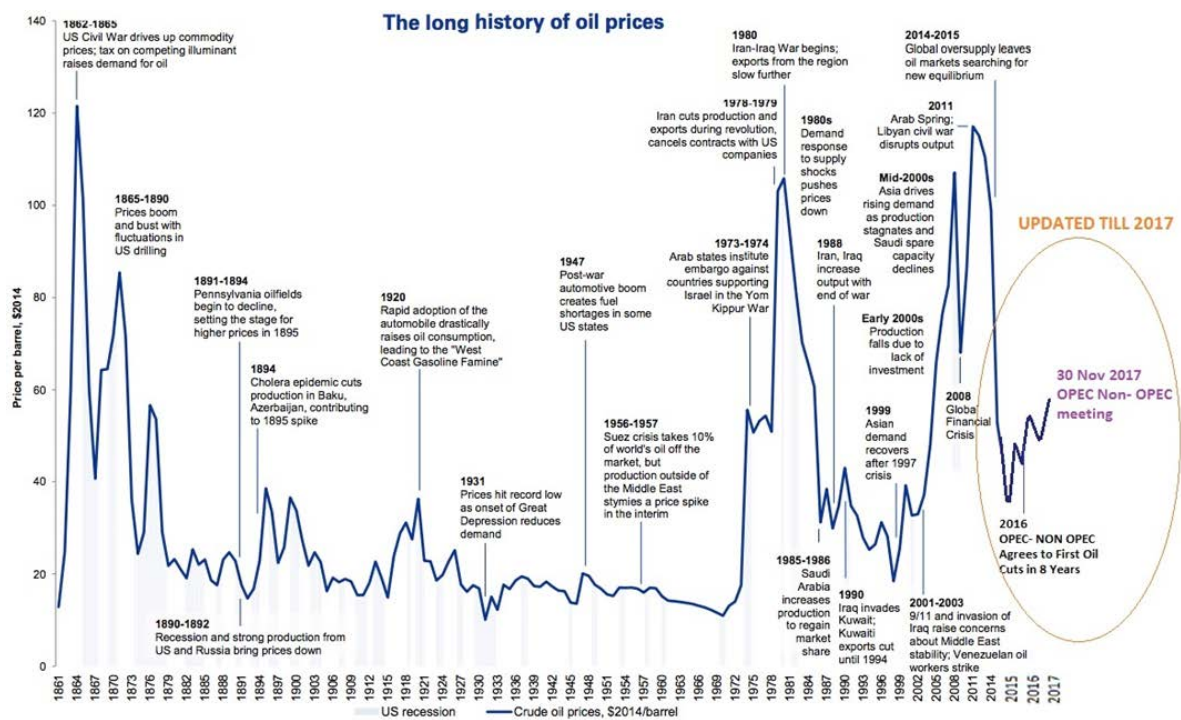


Figure 2.1. Crude oil prices' trend [2]

2.1.1 Crude Oil Characteristics

Crude oil is a complex mixture of hydrocarbons. Its physical and chemical properties are variable depending to extraction areas and sometimes from the same location. Generally, it is found in the liquid state but crude oils with high molecular mass aliphatic hydrocarbons (paraffines) are solid at ambient temperature. Its colour varies from light brown to black, the latter indicating the presence of long chain (and consequently high mass) hydrocarbons. Due to its millenary formation process, it generally does not contain unsaturated compounds. It's principally composed of:

- I. Aliphatic Hydrocarbons (paraffin C_nH_{2n+2} , n up to 35)
- II. Cycloalkanes (naphthenes typically C5-C7)
- III. Aromatic and Polyaromatic compounds.

(Table 2.1) summarizes some of the crude oils' fundamental characterizing parameters. It is noteworthy that the fundamental properties such as carbon and hydrogen content does not vary excessively by the extraction areas and location. Crude oil always contains different quantity of sulfurated compound especially thioalcohols (linear and cyclic) oxygenated and nitrogenated compounds and numerous metallic elements combined in organic compounds and dissolved in water

traces. Technological characterization of crude oils is made by determining a great number of parameters [3] some of which are indicated in the table below.

Table 2.1 Crude oil's characterising properties

Property	Principles and Definition
Density	The conventional unit measure used for the crude oil density is the °API (American Petroleum Institute), defined as: $^{\circ}API = \frac{141.5}{\delta} - 131.5$ (where δ is the density expressed in $\frac{Kg}{l}$). Crude oils have a lower density than water with a limit value of $0.75 \frac{Kg}{l}$ corresponding to 57 °API.
Sulphur content	Sulphur is always present with a percentage ranging from 0.05% to 9 % for the low quality crude oils. Commercial specifics of crude oil require low content of sulphur. Crude oils with high contents of sulphur require desulphuration process since sulphur compounds deactivate most of the catalysts used in industrial processes.
Characterization factor	It represents an empirical method to evaluate paraffins and naphthenes content. It is calculated as: $K = \frac{\sqrt[3]{T_b}}{\delta}$, where K is the characterization factor, T_b is the average boiling temperature and is the density in $\frac{Kg}{l}$ measured at 60 °F. For K values less than 11.4 crude oil has a naphthenic base, for values between 11.4 and 12.2 is mixed base while for values higher than 12.2 has a paraffinic base.
Asphaltenes content	Asphaltenes are high molecular mass and slightly less soluble compounds found in the heavy petroleum fraction with high aromaticity.
Conradson Carbon	Measures the tendency of crude oil to form residues under strong worming. It can be referred to crude oil or to fraction derive from it such as gasoils and fuel oils.
Aniline Point	Represents the aromatic content of the crude oil. It is the temperature (expressed in °F) at which the sample is completely miscible with aniline in a 1 to 1 ratio.

However, the principal analyses to gain specific information about the crude oil yields is the distillation test. The test simulates on laboratory scale the results of the Topping process, by which crude oil is industrially separated in the different fractions as shown in the simplified scheme of (Fig. 2.2).

Crude Distillation Unit (CDU)

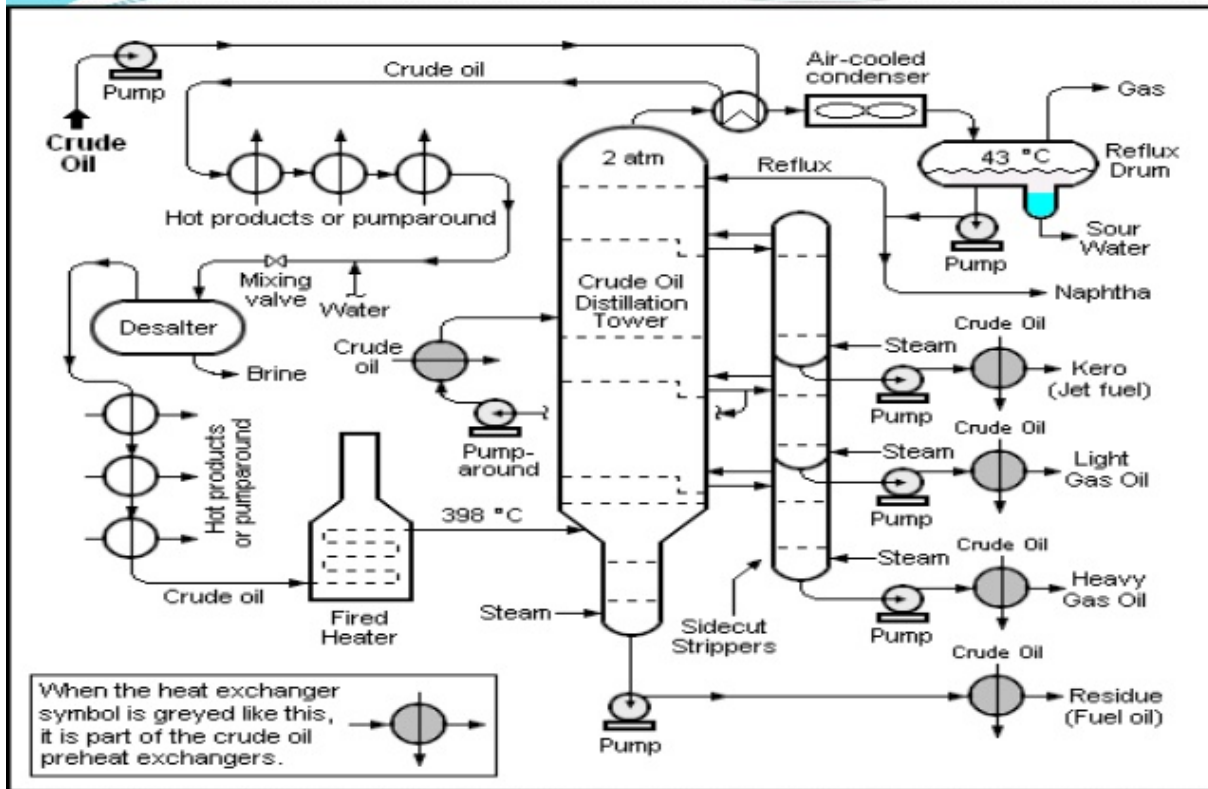


Figure 2.2 Schematic plan of crude oil distillation procedure [4]

Different standard technique can be used to simulate the Topping process in laboratory. Among them the standard of Bureau of Mine and the distillation TBP (True Boiling Point) are the most common. Through the procedure it is first characterized by a discontinuous distillation at atmospheric pressure warming the sample up to 275 °C. The produced vapours are progressively condensed and separately collected by distillation intervals of 25 °C starting from 50° °C. The residue left at the 275 °C is brought at the pressure or 40 mmHg and the distillation goes on starting from 200 °C up to 300 °C. On every fraction obtained (totally 15, see Table 2.2) specific chemical physics parameters are determinates to characterize the fraction quality. The 10 and 15 fractions are used as key fraction to determine (calculating characterization factor reported in Table 2.1) the paraffinic or naphtenic nature of the crude oil. TBP distillation instead is a discontinuous distillation in which there is a condensed vapour reflux.

Table 2.2 Principal Crude Oils Characterisation parameters

Fraction number	Distillation temperature		% (± 0.1)	Specific weight (± 0.001)	API density (± 0.1)	Correlation index (± 0.1)
	°C	°F				
Atmospheric pressure distillation 743 mmHg						
1	50	122	3.2	0.628	93.8	
2	75	167	4.6	0.659	83.2	2.3
3	100	212	4.5	0.696	71.8	10.0
4	125	257	5.9	0.724	63.9	14.0
5	150	302	6.3	0.751	56.9	19.0
6	175	347	5.5	0.773	51.6	23.0
7	200	392	5.5	0.786	48.5	23.0
8	225	437	4.7	0.797	46.0	23.0
9	250	482	5.1	0.810	43.2	23.0
10	275	527	6.0	0.827	37.6	27.0
Reduced pressure distillation (40 mmHg)						
11	200	392	4.3	0.845	36.0	31.0
12	225	437	5.2	0.855	34.0	32.0
13	250	482	5.4	0.877	29.9	39.0
14	275	527	4.7	0.894	26.8	44.0
15	300	572	5.6	0.907	24.5	47.0
residue			23.3	0.997	10.4	

In the recent years, chromatographic technique are increasingly used in distillation simulated tests. These methodologies became more common because of their rapidity and not using atmospheric and vacuum distillation. Within these techniques differences relative to average hydrocarbon molecular mass, percentages between different hydrocarbon classes, sulphur percentage etc. can be observed. Of the various Topping's distillation fractions, in this work we focus on the residue and in particular on the bitumen fraction.

2.2 Bitumen

In everyday language, terms like bitumen, tar and asphalt are used indifferently but they could be used more precisely. One of the main reason for their confusion is the different meaning they have in different countries. For example, crude oil bitumen is called asphalt in the USA, but the same term in Europe means the mixing of crude oil bitumen and aggregates used for road pave. Throught the article we adopt the European terminology. Bitumen is a brown/black material, solid or semisolid at ambient temperature with thermoplastic properties. It comprising a very great number of molecular species

that vary widely in polarity and molecular weight [5,6]. Due to its high adhesive and waterproof properties, bitumen was the first crude oil product employed in human manufactures [7]. However Good crude oils and proper distillation processes can enhance bitumen properties. According to a joint publication of Asphalt Institute and Eurobitum in 2011, the current world consumption of bitumen is approximatively 102 million tonnes per year, 85 % of which is used in various kind of pavements [8,9]. From chemical point of view, the molecular weight distribution analysis shows that bitumen is a complex mixture of about 300-2000 chemical compounds (medium value 500-700) making a complete chemical characterization very difficult. For this reason, bitumen is generally fractionated by more simple methodologies, which allow to identify two principal constituents:

Asphaltenes

Malthenes (also called Petrolenes)

The latter are split out in Resins and Oils, which are further classified as Saturated Oils and Aromatic Oils. This classification is called SARA (Saturate, Aromatic, Resin, Asphaltene). The relative abundance of the SARA fractions allows to relate the bitumen chemical composition with its internal structure and some of its macroscopic properties [10].

Asphaltenes (percentage in bitumen varies from 5-25%) are amorphous brown/black solids, insoluble in n-heptane, constituted by complex mixtures of hydrocarbons, characterized by condensed aromatic compounds. Asphaltene contains oxygen, nitrogen, sulphur and heavy metals (V, Ni etc...) with long (up to 30 carbon atoms) aliphatic chains, pyrrolic and pyridinic rings as shown in (Fig. 2.3). Asphaltene particles have dimensions between 5-30 μm and a carbon hydrogen ratio nearly to 1.

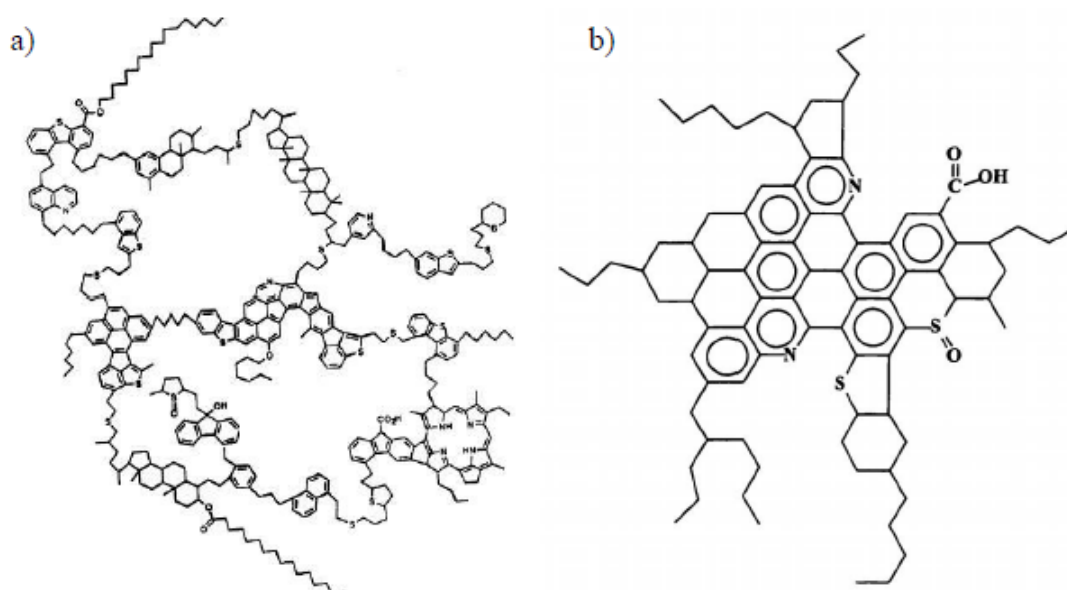


Figure 2.3 Asphaltene hypothetical structure: a) Archipelago structure: $C_{412}H_{509}O_9S_{17}N_7$ with H/C ratio 1.23 and molecular weight 6239 g/mol [11,12], b) Continent structure: $C_{84}H_{100}O_3S_2N_2$ with H/C ratio 1.19 and molecular weight 1276 g/mol [13,14].

Bitumen characteristics strongly depends on them. In particular a higher asphaltene content is responsible of a more viscous and harder bitumen. A detailed study on the asphaltene nature can be found in reference [6].

Resins are dark brown solid (or semi-solid) compounds soluble in n-heptane structurally similar to asphaltenes. Like these their molecules are prevalently composed of carbon and hydrogen. However, small quantities of oxygen, nitrogen and sulphur could be seen. Their polar nature enhances the adhesive properties of bitumen, but their principal role is as dispersing agents for the asphaltene macromolecular structures and oils, which are mutually insoluble. Resins molecular weight ranges from 500 to 5000 Dalton, with particle sizes of 1-5 nm and a Hydrogen Carbon ratio of 1:3 or 1:4. They represent the 10-25 % of bitumen. When bitumen is oxidized resins gains oxygen molecules acquiring a structure similar to asphaltenes. Bitumen characteristics is determined largely by resins asphaltenes ratio [15].

Aromatic oils are dark brown viscous liquids containing low molecular weight aromatic compounds. Their molar mass range between 300-2000 Dalton. Aromatic oils represent the highest fraction (40-65%) of bitumen. They have a high solvent power relative to high molecular weight hydrocarbons. Together with saturated oils they are considered as the plasticizing agents of bitumen.

Saturated oils are white/yellow viscous liquids essentially composed by long chain saturated hydrocarbons and naphthenes. They are non-polar compounds with molecular weight ranging between 300-1500 Dalton and representing the 5 to 20 % of bitumen's weight.

2.3 Different bitumen sources

2.3.1 Natural bitumen

Natural bitumen is the residue formed from the oxidation and evaporation of more volatile substances of crude oils. It is found in nature in cavities, outcrops, lakes, etc. It is noteworthy that despite properties of natural analogous to that of crude oil bitumen, its chemical and toxicological properties are very different.

2.3.2 Oxidized bitumen

This type of bitumen is produced by air blowing through a sample of hot residue or using a refined product obtained by de-asphalting process. The process is essentially based on an oxidative condensation which produce an increase of bitumen molar mass.

2.4 Asphalt

It is obtained by mixing bitumen and aggregates. Soaked rocks with natural bitumen are found in USA, Canada, France, Switzerland, Italy, in particular in Abruzzo and Sicily (from Scicli to Vizzini). Between the typology of Italian asphalt there is a deep difference not only for the aggregates but also for bitumen characteristics. Abruzzo's Asphalts oilfield have a calcareous nature with a hard bitumen binder. Sicilian's asphalts oilfields are composed by a more pliable calcareous rocks and a very soft bitumen binder.

2.4.1 Asphaltic rocks

Are those bitumen containing inorganic compounds in percentage above the 2% and a bitumen percentage ranging between 5% to 20% and rarely 40%. Italy gains important asphaltic rocks oilfield. For example, in Sicily (Ragusa) these oilfields are characterized by calcareous rocks impregnated of 7% to 12% of bitumen.

2.4.2 Tar

It is a material similar to bitumen but completely different from it by origin and composition. At ambient temperature it is a liquid, more or less viscous, with a brown/black colour. It is obtained industrially from destructive distillation of fossil carbon. It is composed of aliphatic hydrocarbons, aromatic compounds, and to a lesser extent by other compound containing sulphur, oxygen and nitrogen. Tar can be used directly as a source to impermeabilize the roofs and to produce carbon

black, but more frequently, after an opportune dehydration. It is fractionally distilled to produce substances with some higher practical usages. The distilled fractions are characterized by light, average and heavy oils, anthracene oils, while the residue obtained is called pitch. Compared to bitumen it has a higher content in polycyclic aromatic hydrocarbons (PAH). In the past years Tar was often used as bitumen's substitute or mixed with it in industrial applications. Table 2.3 summarizes some of the principal differences between bitumens and tar as reported in the CONCAWE dossier 92/104 [16].

Table 2.3

BITUMEN		OXIDIZED BITUMEN		TAR
<i>(Source)</i>	<i>(Walrave,1971)</i>	<i>(Brandt,1985)</i>	<i>(Brandt,1985)</i>	<i>(Brandt, 1985)</i>
N° Samples	8	4	3	2
Phenanthrene $\left(\frac{mg}{kg}\right)$	0.4÷3.5	1.7÷7.3	0.3÷2.4	$(19.8 \div 25.7) \cdot 10^3$
Chrysene $\left(\frac{mg}{kg}\right)$	< 0.1÷8.9	0.5÷3.9	0.8÷1	$(11.2 \div 22.7) \cdot 10^3$
Benzo[a]Pyrene $\left(\frac{mg}{kg}\right)$	ND÷2.5	0.2÷1.8	0.4÷0.5	$(11.4 \div 15.2) \cdot 10^3$
Benzo[ghi]Perylene $\left(\frac{mg}{kg}\right)$	< 0.1÷4.6	1.7÷4.6	1.2÷2.0	$(3.43 \div 3.53) \cdot 10^3$
Max single IPA $\left(\frac{mg}{kg}\right)$	39.0 (Perylene)	4.2 (Benzo[ghi]Perylene)	2.4 (Phenanthrene)	$76.0 \cdot 10^3$

2.5 Reclaimed Asphalt Pavement (RAP)

Reclaimed Asphalt Pavement (RAP) is the asphalt removed and processed, It is a bituminous layers which contains valuable asphalt binder and aggregates [17]. The aged bitumen is very hard and has higher transition temperature respect the virgin bitumen because some of the aromatic components and resins, which are responsible for a certain grade of mobility, are oxidized to asphaltenes. Compared with virgin bitumen, the aged bitumen is more brittle and has worse relaxation characteristics that make it vulnerable to cracking [18]. In the laboratory this process it is simulated through Pressure Aging Vessel (PAV). The first aging process takes place during the preparation of the asphalt concrete and during layering of bitumen on the road. In this case the short aging process is simulated by RollingThin Film Oven Test (RTFOT).

2.6 Bitumen Modifiers

The bitumen is viscoelastic material, an improvement of its mechanical response does represent an important factor in the design of roads. Until today, several chemical compounds has been tested as

bitumen modifiers. They generally promote an increase of the bitumen softening point, crucial point for warm geographical regions. The most common types of bitumen modifiers present on the market are classified as physical modifiers (i.e. polymers) or chemical modifiers (i.e. organo-metallic compounds, sulphur compounds).

2.6.1 Polymer Modified Bitumen

Polymer-modified Bitumens (PmBs) were developed as a response to the diminishing crude oil sources and to increase the performance properties besides mechanical properties and lifetime resistance as a road pavement material binder in flexible pavements [19]. Typical situations in which is necessary to use PmB are: heavy duty pavements, pavements being operated in critically climatic conditions, airport runways, draining and phono-absorbing pavements in which the high porosity (up to 18 % vacuum) necessitate higher bituminous binder performance. PmBs are produced by mechanical mixing or chemical reactions of bitumen and one or more polymer in a percentage usually ranging between 3 % to 10 % relatively to the bituminous fraction [20]. Modified bitumens are characterized as two-phase system: bituminous, prevalently as asphaltenic matrix, and polymeric matrix. The complex interaction mechanism between them has received particularly attentions and numerous studies relative to the interaction mechanism have been made, as well as the influence of different type of polymer modifiers has been investigated studying the rheological performance characteristics, temperature sensitivity, morphology, thermal behaviour storage stability and aging of the resulting PmBs [20-36] As indicated in reference [8], polymer modification results in a thermodynamically unstable but kinetically stable system in which the polymer is partially swollen by the light bitumen components (maltenes) and can swell up to nine times its initial volume [37]. Bitumen is generally regarded as a colloidal system consisting of a suspension of high molecular weight asphaltene micelles dispersed in a lower molecular weight oily medium (maltenes) [38] If bitumen's resins content and aromatic compounds, with good solvating power, is adequate, it tends to form a sol structure with asphaltenes fully peptized and the resulting micelles presents a good mobility within bitumen. Insufficient content of resins and aromatics with low solvating power tend to promote micelles aggregation according to the following equilibrium: molecules \rightleftharpoons micelles \rightleftharpoons clusters [39]. The dynamics of this equilibrium is disturbed by introducing a high molecular weight polymer reducing the homogeneity of the bitumen system. Competing for bitumen's light fractions, polymers tend to induce asphaltenes' micelles aggregation or increasing their degree of association, depending on the nature of the original bitumen [34]. At high temperatures, a relatively low viscosity of the melted micro heterogeneous polymer modified bitumen allows the substances with similar structure and polarity to form their domains: the swollen polymers and the asphaltenes. The

thermodynamic instability of this system induce a phase separation (or sedimentation) under the gravitational field influence. Therefore associated asphaltenes micelles may settle to the bottom of the blend during static hot storage. According to this mechanism, the degree of phase separation of polymer modified binders may be influenced by storage conditions such as temperature and time. However, the phase separation will mainly be governed by the nature of the base bitumen and the characteristics and content of the polymer [34].

Despite the complex mechanisms related to the polymer bitumen interaction, it is possible to observe that some polymers can improve the bitumen performance by reducing the thermal susceptibility and alleviating the short-term aging. In the last 20 years a wide spectrum of modifying polymeric materials has been tested with bitumens used in road construction [40-47]. For a polymer to be effective it must blend and improve resistance at high temperatures without making the bitumen too viscous at mixing temperatures or too brittle at low temperatures [48]. As a general rule, besides being affordable, in particular, polymers should be chemically and physically stable during storage and application. Moreover, they should have a good solubility in the bituminous matrix to ensure the stability of modified product.

Among the introduced and experienced polymers for bitumen modification, natural rubbers [49-51] and a cheap material such as atactic polypropylene (APP, obtained as a by-product during isotactic polypropylene production) were more concentrated in through the last decade [52,53]. Nowadays the main groups of polymers used as bitumen modifiers are: thermoplastic elastomers, natural and synthetic rubbers, and plastomers.

2.7 Adhesion promoter for bitumen

The bitumen is required to coat and bind the aggregates, consequently the adhesion properties is of great importance in all asphalt pavement applications. ASTM D907 defines ‘adhesion’ as a “state in which two surfaces are held together by valence forces or interlocking forces, or both” [54].

Fundamental theory builds the adhesion concept on the forces between atoms at an interface, but, practically, adhesion is evaluated mechanically, performing tests able to control the forces between surfaces. In fact, as reported in the literature [55], it is possible to distinguish between “basic adhesion” and “practical adhesion”. The first depends on the interatomic interactions at the interface of a film and substrate, while the second depends on a complex combination of characteristics relating to both the substrate and film. In general, adhesion defines many complex phenomena, which appear in the bitumen-aggregate union. Some are physical or physicochemical (such as aggregate surface texture and porosity, bitumen viscosity, surface tension or film thickness) and others are chemical such as bitumen composition or aggregate nature [56]. Several methods can be used to measure also

the practical adhesion for bituminous systems for which the adhesion failure is induced by water entering the bituminous mix, a phenomenon known as stripping [57,58]. Water damage causes a loss of stiffness and structural strength [59].

In order to improve adhesion, bitumen may be modified with antistripping additives. In fact, it is important to improve the capacity of the binder to cover aggregates so as to minimize stripping under water or traffic aggressions. Therefore, we define “adhesion agent” or “antistripping agent” as the product that improves the adhesion of bitumen to a specific aggregate. The quality of the adhesive bond in an asphalt-aggregate mixture is affected by mineralogy (chemical composition), surface texture, absorption surface area, surface coatings, particle shape and binder viscosity [60–63].

The water susceptibility of bituminous mixtures is evaluated by using empirical methods like boiling water tests (Riedel-and-Wieber test), rolling bottle tests, wash test, swell tests, and eventually wet-dry mechanical tests [64]. A modern surface analysis technique for investigation of the interactions at the bitumen aggregate interface was recently used, specifically the contact angle analysis [65].

A good adhesion between bitumen, the common binder used in the construction of pavements, and mineral aggregates is a key property for optimal performance of the road paving material (asphalt). The most common types of activators present on the market are classified according to the chemical nature of their active ingredient (es. basic and acid nature) and they are greatly affected by the type of mineral substrate. [66].

2.8 REFERENCES Chapter 2

1. Spielman, P. E. Bituminous Substances. Ernest Benn Ltd., London 1925, 5.
2. IFA Global, Special Report-Opec Meet And Indian's Math Behind Rising Crude Oil, 30th 2017.
3. Oliviero Rossi, C.; Caputo, P.; De Luca, G.; Maiuolo, L.; Eskandarsefat, S.; Sangiorgi, C. ¹H-NMR spectroscopy: A Possible Approach to Advanced Bitumen Characterization for Industrial and Paving Applications. *Appl. Sci.* 2018, 8(2), 229.
4. <https://www.blaknwynt.co/wiring/process-flow-diagram-crude-distillation-unit.html>
5. Lu, X.; Isacson, U.; Ekblad, J. Phase Separation of SBS Polymer Modified Bitumens. *J. Mater. Civ. Eng.* 1999, 11(1), 51-7.
6. Petersen, J. C. Chemical Composition of Asphalt as Related to Asphalt Durability: State of the Art, *Transp. Res. Rec.* 1984, 999, 13-30.
7. Morgan, P.; Mulder, A. The Shell Bitumen Industrial Handbook. Surrey: Shell Bitumen 1995.
8. Polacco, G.; Stasna, J.; Biondi, D.; Zanzotto, L. Relation Between Polymer Architecture and Nonlinear Viscoelastic Behaviour of Modified Asphalts. *Curr. Opin. Colloid Interface Sci.* 2006, 11(4), 230-45.
9. Asphalt Institute, Eurobitume. The Bitumen Industry – A Global Perspective, 2nd ed. Lexington, Kentucky: Asphalt Institute; Brussels, Belgium: Eurobitume; 2011.
10. Ashoori, S.; Sharifi, M.; Masoumi, M.; Salehi, M.M. The Relationship Between SARA Fractions and Crude Oil Stability. *Egypt. J. Petrol.* 2017, 26, 209-213.
11. Murgich, J.; Abanero, J.; Strausz, O. Molecular Recognition in Aggregates Formed by Asphaltene and Resin Molecule from the Athabasca Oil Sand. *Energy and Fuel* 1999, 13(2), 278-286.
12. Strausz, O. P.; Peng, P.; Murgich, J. The Molecular Structure Unfolding Story of Asphaltene: An Unfolding Story. *Energy and Fuel* 1992, 71, 1355-63.
13. Dickie, J. P.; Yen, T. F. Macrostructures of the Asphaltic Fractions by Variuos Instrumental Methods. *Analytical chemistry* 1967, 5213(14), 1963-68.

14. Mullins, O. Review of the Molecular Structure and Aggregation of Asphaltenes and Petroelomics. *SPE Journal* 2008, 2007, 9-12.
15. Yarranton, H.W.; Fox, W.A.; Svrcek, W.Y. Effect of Resins on Asphaltene Self-Association and Solubility. *Can. J. Chem. Eng.* 2007, 85, 635-42.
16. https://crrc.unh.edu/sites/crrc.unh.edu/files/media/docs/Workshops/liquid_asphalt/concawe_bitumen.pdf
17. Baldino, N.; Oliviero Rossi, C.; Lupi, F.R.; Gabriele, D. Rheological and structural properties at high and low temperature of bitumen for warm recycling technology. *Colloid Surf. A* 2017, 532, 592–600.
18. Baldino, N.; Gabriele, D.; Oliviero Rossi, C.; Seta, L.; Lupi, F.R., Caputo, P. Low temperature rheology of polyphosphoric acid (PPA) added bitumen. *Constr. Build. Mater.* 2012, 36, 592–596.
19. Becker, Y.; Mendez, M. P.; Rodriguez, Y. Polymer modified Asphalt. *Vision Technol.* 2001, 9(1), 39-50.
20. Lu, X. On polymer modified road bitumens [doctoral dissertation]. Stockholm: KTH Royal Institute of technology 1997.
21. Wardlaw, K.R.; Shuler, S. editors. *Polymer modified Asphalt Binders*. Philadelphia, Pennsylvania. American Society for Testing and Materials 1992
22. Aglan, H. Polymeric Additives and Their Role in Asphaltic Pavements. Part I: Effect of Additive Type on the Fracture and Fatigue Behaviour. *J. Elastomers Plast* 1993, 25(4), 307-21.
23. Bahia, H.U.; Anderson, D.A. Glass Transition Behaviour and Physical Hardening of Asphalt Binders (with discussion). In: *Asphalt Paving Technology 1993*. Journal of the Association of Asphalt Paving Technologists 1993 March 22-24; Austin Texas. St. Paul, Minnesota: Association of Asphalt Paving Technologists 1993 pp 93-129.
24. Elmore, W.E.; Kennedy, T.W.; Solaimanian, M.; Bolzan, P. Long-Term Performance Evaluation of Polymer- modified Asphalt Concrete Pavements. Report N°: FHWA-TX-94+1306-1F. Washington D. C.: Federal Highway Administration 1993 November.
25. Bonemazzi, F.; Braga, V.; Corrieri, R.; Giavarini, C.; Sartori, F. Characteristics of Polymers and Polymer-modified Binders. *Trans. Res. Rec.: J. Trans. Res. Board* 1966, 1535, 36-47.

26. Brûlé, B.; Polymer-modified Asphalt Cements Used in the Road Construction Industry: Basic Principles. *Trans. Res. Rec.: J. Trans. Res. Board* 1966, 1535, 48-53.
27. Adedeji, A.; Grünfelder, T.; Bates, F.S.; Macosko, C.W.; Stroup-Gardiner, M.; Newcomb, D.E. Asphalt Modified by SBS Triblock Copolymer: Structure and Properties, *Polym. Eng. Sci.* 1996, 36(12), 1707-23.
28. Shin, E. E.; Bhurke, A.; Scott, E.; Rozeveld, S.; Drzal, L. T. Microstructure, Morphology and Failure Modes of Polymer-Modified Asphalts. *Trans. Res. Rec.: J. Trans. Res. Board* 1966, 1535, 61-73.
29. Loeber, L.; Durand, A.; Muller, G.; Morel, J.; Sutton, O.; Bargiacchi, M. New Investigation on Mechanism of Polymer-Bitumen Interaction and Their Practical Application for Binder Formulation. In: *Proceedings of the 1st Eurasphalt and Eurobitume Congress; 1996 May 7-10; Strasbourg, France. Brussels: Eurasphalt and Eurobitume Congress; 1996. Paper N° 5115.*
30. Gahvari, F. Effects on Thermoplastic Block Copolymers on Rheology of Asphalt. *J. Mater. Civ. Eng.* 1997, 9(3), 111-6.
31. Valkering, C.P.; Vonk, W. Thermoplastic Rubber for the Modification of Bitumens. Improved Elastic Recovery for High Deformation Resistance of Asphalt Mixes. In: *Proceedings of the 15th Australian Road Research Board (ARRB) Conference; 1990 August 26-31; Darwin, Northern Territory. Vermont South, Victoria: Australian Road Research Board; 1990, pag. 1-19.*
32. Krutz, N.C.; Siddharthan, R.; Stroup-Gardiner, M. Investigation of Rutting Potential Using Static Creep Testing on Polymer-Modified Asphalt Concrete Mixtures. *Trans Res Rec: J. Trans Res. Board* 1991, 1317, 100-8.
33. Stock, A.F.; Arand, W. Low Temperature Cracking in Polymer modified Binders. In: *Asphalt Paving Technology 1993: Journal of the Association of Asphalt Paving Technologists; 1993 March 22-24; Austin, Texas. St Paul, Minnesota: Association of Asphalt Paving Technologists; 1993 pag. 23-53.*
34. Lu, X.; Isacsson, U.; Ekblad, J. Phase Separation of SBS Polymer Modified Bitumens. *J. Mater. Civ. Eng.* 1999, 11(1), 51-7.
35. Boudin, M.G.; Collins, J.H.; Berker, A. Rheology and Microstructure of Polymer/Asphalt Blends. *Rubber Chem. Technol.* 1991, 64(4), 577-600.

36. Oliviero Rossi, C.; Spadafora, A.; Teltayev, B.; Izmailova, G.; Amerbayev, Y.; Bortolotti, V. Polymer Modified Bitumen: Rheological Properties and Structural Characterization. *Colloid and Surface A: Physicochemical and Engineering Aspects* 2015, 480, 390-97.
37. Walkering, C.P.; Vonk, W.C.; Whiteoak, C.D. Improved Asphalt Properties Using SBS modified Bitumens. *Shell Bitumen Review* 1992, 66, 9-11.
38. Whiteoak, D. *The Shell Bitumen Handbook*. Shell Bitumen, Chertsey, U. K. 1991.
39. Yen, T.F. A macrostructure of petroleum asphalt. Preprints of the Symp.: Chemistry and Characterization of Asphalts, Div. of Petroleum Chemistry, American Chemistry Society, Washington, D.C. 1990, 35, 314–319.
40. Lu, X.; Isacson, U. Rheological Characterization of Styrene-Butadiene-Styrene Copolymer Modified Bitumens. *Constr. and Build. Mat.* 1997, 11, 23–32.
41. Collins, J.H.; Bouldin, M.G.; Gelles, R.; Berker, A. Improved Performance of Paving Asphalts by Polymer Modification (with discussion). In: *Asphalt Paving Technology 1991: Journal of the Association of Asphalt Paving Technologists: 1991 Seattle Washington*. St. Paul, Minnesota: Association of Asphalt Paving Technologists 1991 pag. 43-79.
42. *Proceedings of International Symposium on Chemistry of Bitumens, Roma, Sect. G 1991, Vol. 2, pp. 859-1032.*
43. *Proceedings of the 3rd Eurobitume Symposium, The Hague, Sect. IV, 1985, Vol. 1, pp. 479-700.*
44. *Proceedings of the 3rd Eurobitume Symposium, Madrid, Sect. I, 1989, Vol. 1, pp. 25-237.*
45. *Rilem Seminar on Formulation, Control and Behaviour of Polymer Modified Bitumens either for waterproofing or for Road Construction, Dubrovnik, 1988.*
46. Boutevin, B.; Pietrasanta, Y.; Robin, J.J. Bitumen-Polymer Blends for Coatings Applied to Roads and Public Constructions. *Prog. Org. Coatings* 1989, 17, 221.
47. Giavarini, C. In: *Asphaltene and Asphalts*, Edited by T. F. Yen, Elsevier Science, Amsterdam, 1994, Vol. 1, pp. 381-400.
48. Giavarini, C.; De Filippis, P.; Santarelli, M.L.; Scarsella, M. Production of Stable Polypropylene-Modified Bitumens. *Fuel*, 1996, 75(6), 681-686.

49. Isacsson, U.; Lu, X. Testing and Appraisal of Polymer Modified Road Bitumens-State of the Art. *Mater. Struct.* 1995, 28(3), 139-59.
50. Lewandowski, L.H. Polymer Modification of Paving Asphalt Binders. *Rubber Chem. Technol.* 1994, 67(3), 447-80.
51. Yildirim, Y. Polymer modified Asphalt Binders. *Constr. Build Mater.* 2007, 21(1), 66-72.
52. Costantinides, G.; Lomi, C.; Schromek, N. Studio su Messcole con APP. *Riv. Combust.* 1985, 39, 1.
53. Johnson, R. Hystory and Development of Modified Bitumen. In: *Proceedings of the 8th Conference on Roofing Technology*; 1987, April 16-17; Gaithersburg, Maryland. Rosemont, Illinois: National Roofing Contractors Association; 1987, pp.81-4.
54. Moraes, R.; Velasquez, R.; Bahia, H.U. Measuring the effect of moisture on asphalt aggregate bond with the bitumen bond strength test. *Transp Res Rec* 2011:70–81.
55. Ollendorf, H.; Schneider, D. A comparative study of adhesion-test methods for hard coatings. *Surf Coat Technol* 1999;113:86–102.
56. Oliviero Rossi, C.; Caputo, P.; Baldino, N.; Lupi, F.R.; Miriello, D.; Angelico, R. Effects of adhesion promoters on the contact angle of bitumen-aggregate interface. *Int J Adhes Adhes* 2016;70:297–303.
57. Grenfell, J.; Ahmad, N.; Liu, Y.; Apeageyi, A.; Large, D.; Airey, G. Assessing asphalt mixture moisture susceptibility through intrinsic adhesion, bitumen stripping and mechanical damage. *Road Mater Pavement Des* 2014;15:131–52.
58. Airey, G.D.; Collop A.C.; Zoorob, S.E.; Elliott R.C. The influence of aggregate, filler and bitumen on asphalt mixture moisture damage. *Constr Build Mater* 2008, 22:2015–24.
59. Cui, S.; Blackman, B.R.K.; Kinloch, A.J.; Taylor, A.C. Durability of asphalt mixtures: effect of aggregate type and adhesion promoters. *Int J Adhes Adhes* 2014, 54:100–11.
60. Abo-Qudais, S.; Al-Shweily, H. Effect of aggregate properties on asphalt mixtures stripping and creep behavior. *Constr Build Mater* 2007, 21:1886–98.
61. Taylor, M.A.; Khosla, N.P. Stripping of asphalt pavements: state of the Art. *J Res Transp Board* 1983, 1:150–8.

62. Zhang, J.; Apeageyi, A.K.; Airey, G.D.; Grenfell, J.R.A. Influence of aggregate mineralogical composition on water resistance of aggregate–bitumen adhesion. *Int J Adhes Adhes* 2015, 62:45–54.
63. Majidzadeh, K.; Brovald, F.N. State of the Art: effects of Water on Bitumen-Aggregate Mixtures Highway Research Board Special Report 98 1968.
64. Krchma, L.C.; Loomis, R.J. Bituminous-aggregate water resistance studies. *J Assoc Asph Paving Technol* 1943, 15:153–87.
65. Oliviero Rossi, C.; Caputo, P.; Baldino, N.; Ildyko Szerb., E.; Teltayevd, B. Quantitative evaluation of organosilane-based adhesion promoter effect on bitumen-aggregate bond by contact angle test. *International Journal of Adhesion & Adhesives* 2017, 72, 117–122.
66. Oliviero Rossi, C.; Caputo, P.; Baldino, N.; Lupi, F.R.; Miriello, D.; Angelico, R. Effects of adhesion promoters on the contact angle of bitumen-aggregate interface. *International Journal of Adhesion & Adhesives* 2016 70, 297–303.

Chapter 3

Experimental Techniques

3.1 Nuclear Magnetic Resonance.

3.1.1 Basic Concepts

It is well known from elementary NMR theory [1] that a nucleus of spin I has $2I+1$ energy levels, equally spaced with a separation

$$\Delta E = \mu H_0 / I \quad \mathbf{3.1}$$

where H_0 is the applied magnetic field, and μ , the nuclear magnetic moment, is given by

$$\mu = \frac{\gamma \hbar I}{2\pi} \quad \mathbf{3.2}$$

Here γ is the magnetogyric ratio, a constant for a given nucleus, and h is Planck's constant. From the usual Bohr relation, the frequency of radiation that induces a transition between adjacent levels is

$$\nu_0 = \frac{\Delta E}{h} = \gamma H_0 / 2\pi \quad \mathbf{3.3}$$

At equilibrium, nuclei are distributed among the energy levels according to a Boltzmann distribution. Following any process that disrupts this distribution (e.g., moving the sample into or out of the magnetic field, or absorption of rf energy), the nuclear spin system returns to equilibrium with its surroundings (the "lattice") by a first-order relaxation process characterized by a time T_1 , the spin-lattice relaxation time. To account for processes that cause the nuclear spins to come to equilibrium with each other, a second time T_2 , the spin-spin relaxation time, is defined so that

$$\nu_{1/2} \approx 1/T_2 \quad \mathbf{3.4}$$

with $\nu_{1/2}$ being a spectrum line of full width at half maximum intensity. If the magnetic field is not perfectly homogeneous, nuclei in different parts of the sample experience slightly different values of the field, hence by equation 3.3 resonate at slightly different frequencies. This leads to a contribution to the line width due to inhomogeneity (ΔH_0) of

$$\nu_{\frac{1}{2}}(inhom) = \gamma \Delta H_0 / 2\pi \quad \mathbf{3.5}$$

So we can define a time T_2^* in terms of the observed line width as

$$\nu_{\frac{1}{2}}(\text{obsd}) = 1/\pi T_2^* \quad 3.6$$

Thus T_2^* includes contributions from both natural line width and magnetic field inhomogeneity :

$$\frac{1}{T_2^*} = \frac{1}{T_2} + \left(\frac{\gamma \Delta H_0}{2}\right) \quad 3.7$$

It is easily shown by classical mechanics that the torque exerted on a magnetic moment by a magnetic field inclined at any angle θ relative to the moment (Figure 3.1) causes the nuclear magnetic moment to precess about the direction of the field with a frequency given by the well-known Larmor equation

$$\nu_0 = -\gamma H_0 / 2\pi \quad 3.8$$

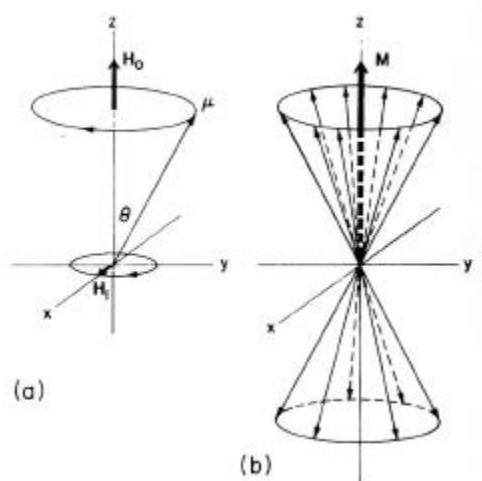


Figure 3.1 (a) Precession of a magnetic moment μ about a fixed magnetic field H_0 . The radio frequency field H_1 rotates in the xy plane. (b) Precession of an ensemble of identical magnetic moments of nuclei with $I = 1/2$, The net macroscopic magnetization is oriented along H_0 (the z axis) and has the equilibrium value M_0 .

Free Induction Decay (FID).

Suppose a 90° pulse is applied along the x' axis in the frame rotating at the radiofrequency (rf). Following the pulse, M lies entirely along the y' axis, as indicated in Figure 3.2 a. Since the apparatus is normally arranged to detect signals induced in a coil along the fixed x or y axis , the magnitude of M_{xy} determines the strength of the observed signal (called a free induction signal, since the nuclei precess "freely" without applied rf). As transverse relaxation occurs, the signal decays. In a perfectly homogeneous field the time constant of the decay would be T_2 ; but, in fact, the free induction signal decays in a time T_2^* that often is determined primarily by field inhomogeneity, since nuclei in

different parts of the field precess at slightly different frequencies, hence quickly get out of phase with each other. Thus the signal decays with a characteristic time T_2^* as defined in equation 3.7.

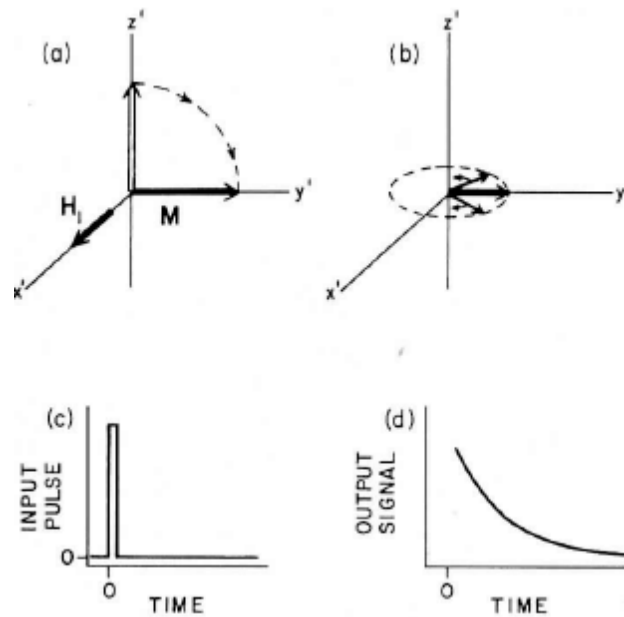


Figure 3.2. (a) A 90° pulse along z' rotates M from the equilibrium position to the y' axis. (b) M decreases as magnetic moments dephase. (c) Input signal, at 90° pulse, corresponding to (a). (d) Exponential free induction decay, corresponding to (b).

3.1.2 Spin-Spin Relaxation time measurement: Spin Echo Sequences.

Unless $T_2 \ll \left(\frac{2}{\gamma\Delta H_0}\right)$ (see equation 3.7), the contribution of inhomogeneity in H_0 to the free induction decay precludes the use of this decay time, T_2^* as a measure of T_2 . An ingenious method for overcoming the inhomogeneity problem was first, proposed by Hahn [2] who called it the spin-echo method. The method consists of the application of a $90^\circ, \tau, 180^\circ$ sequence and the observation at a time 2τ of a free induction "echo." The rationale of the method is shown in Figure 3.3, which depicts the behavior of the magnetization in the rotating frame.

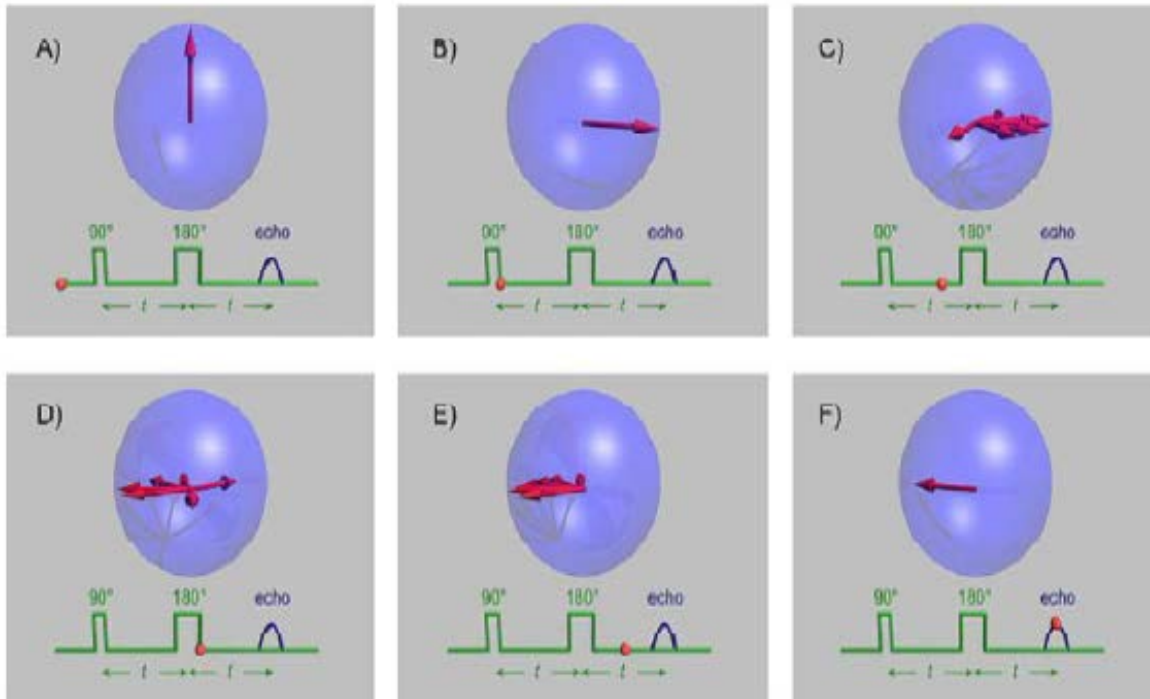


Figure 3.3. Behaviour of Magnetization during Hanh Pulse sequence.

In (b) M is shown being tipped through 90° by application of H_1 along the positive x' axis. The total magnetization M can be thought of as the vector sum of individual macroscopic magnetizations arising from nuclei in different parts of the sample and hence experiencing slightly different values of the applied field, which is never perfectly homogeneous. There is thus a range of precession frequencies centered about ν_0 , which we have taken as the rotation frequency of the rotating frame. In (c) then, the m_i begin to fan out, as some nuclei precess faster and some slower than the frame. At a time τ after the 90° pulse, a 180° pulse is applied, also along the positive x' axis, as shown in (d). The effect of this pulse is to rotate each m_i by 180° about the x' axis. Thus those m_i that are moving faster than the frame moving toward the observer or clockwise looking down the z' axis naturally continue to move faster, but in (e) their motion is now away from the observer. At time 2τ all m_i come into phase along the negative y' axis, as shown in (f). Then the phase coherence is lost again. The rephrasing of the m_i causes a free induction signal to build to a maximum at 2τ but the signal is, of course, negative relative to the initial free induction decay since rephrasing of the m_i occurs along the negative y' axis. If transverse relaxation did not occur, the echo amplitude might be just as large as the initial value of the free induction following the 90° pulse. However, each m_i decreases in magnitude during the time 2τ because of the natural processes responsible for transverse relaxation in the time T_2 . Thus the echo amplitude depends on T_2 , and this quantity may in principle be determined from a plot of peak echo amplitude as a function of τ . It is necessary to carry out separate pulse sequences at different τ and wait between pulse sequences an adequate time, at least $5T_1$.

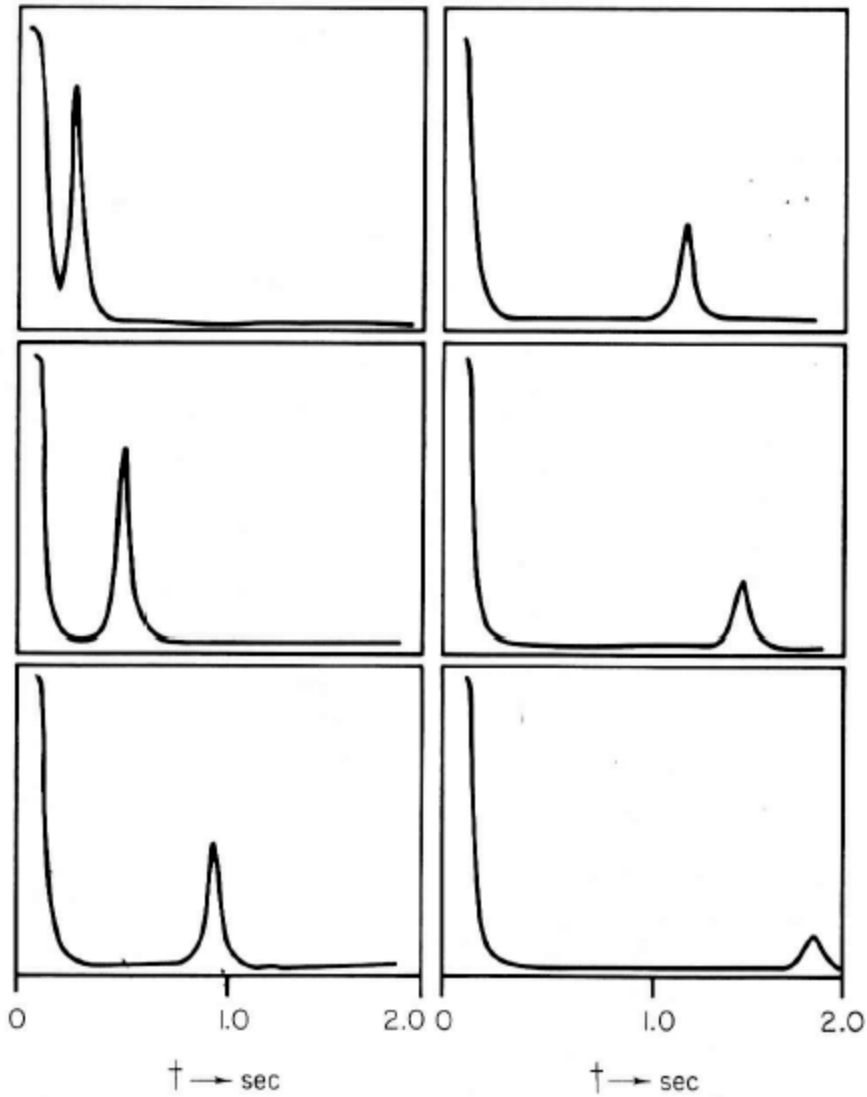


Figure 3.4. Typical Hahn experiment.

Carr and Purcell [3] showed that a simple modification of Hahn's spin-echo method reduces drastically the effect of diffusion on the determination of T_2 . This method may be described as a 90° , τ , 180° , 2τ , 180° , 2τ , 180° , 2τ ,..... sequence (or, more commonly, a Carr—Purcell sequence). As in the spin-echo method described previously, all pulses are applied along the positive x' axis. The result is the same as that shown in Figure 3.3 except that following the dephasing of the m_i another 180° pulse at time 3τ after the initial 90° pulse causes a rephasing of the m_i along the positive y' axis at time 4τ . Subsequent 180° pulses at 5τ , 7τ -, etc. cause echoes at 6τ , 8τ , etc., alternately positive and negative, as shown in Figure 3.4 (a).

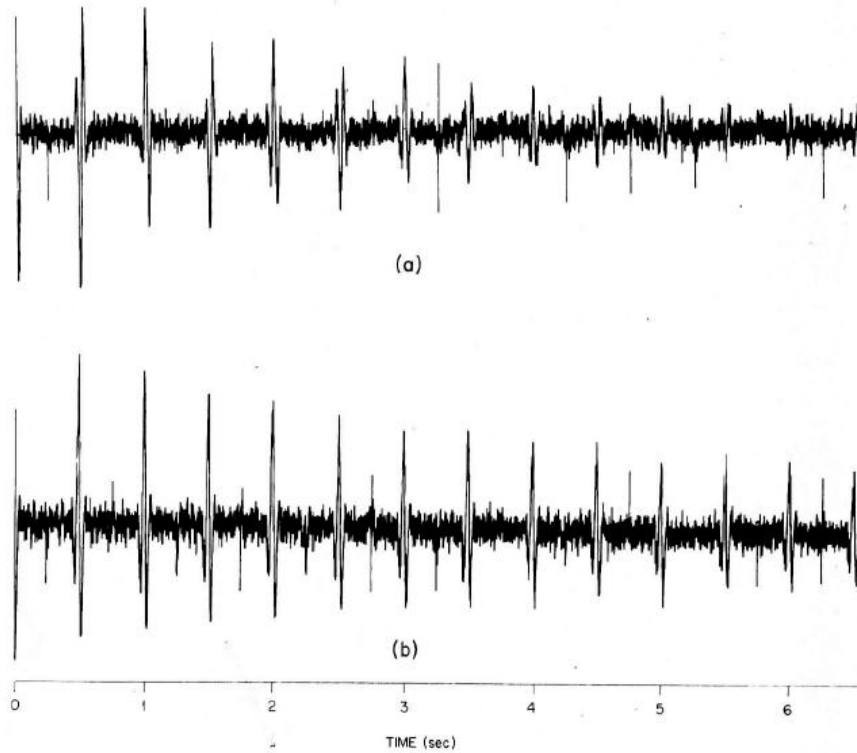


Figure 3.4. (a) Carr-Purcell experiment. (b) Meiboom-Gill method.

Another method, which is often easier experimentally, was proposed by Meiboom and Gill [4]. This method uses the same pulse sequence as the Carr-Purcell technique, but the 180° pulses are applied along the positive y' axis, i.e., at 90° phase difference relative to the initial 90° pulse. Hence, for pulses that are exactly 180° the spins are rotated about the y' axis, and for all echoes focus along the positive y' axis, so that only positive echo signals are obtained, Figure 3.4 (b).

3.1.3 Inverse Laplace Transform of the echo decay.

In the previous paragraph it has been mentioned that the T_2 time can be obtained by plotting the peak echo amplitude as a function of τ . The envelope of the echo amplitudes give rise to an exponential decay of the signal. If the Carr-Purcell envelope has a mono-exponential decay, the relaxation time T_2 of the sample can be obtained by fitting the n data to the following equation:

$$A_n = A_0 e^{-2n\tau/T_2} \quad \mathbf{3.9}$$

The Laplace transform is a powerful tool for solving ordinary and partial differential equations, linear difference equations and linear convolution equations. The Laplace transform $F(s)$ of a function $f(t)$ is defined by [5–7]

$$F(s) = \int_0^{\infty} f(t)e^{-st} dt \quad \mathbf{3.10}$$

In the equation 3.9 A_n is the amplitude of the n th echo in the echo train and A_0 is a constant depending on the sample magnetization, filling factor, and other experimental parameters. Usually the T_2 relaxation time varies all over the sample because of the sample heterogeneity or surface relaxation differences; then a multiexponential attenuation of the CP envelope should be observed. Hence, if inside the sample a continuous distribution of relaxation times exists, the amplitude of the n th echo in the echo train is given by

$$A_n = A_0 \int_0^{\infty} P(T_2)e^{-2n\tau/T_2} dT_2 \quad \mathbf{3.11}$$

In 3.11, $P(T_2)$ is the Inverse Laplace transform (ILT) of the unknown function that fit the plot of the echo amplitudes. Hence $P(T_2)$ can be understood as a distribution of rate constants, strictly, a probability density function, PDF. The ILT can give the answers required where it needs to face the inverse problem of estimating the desired function from noisy experiments. As an integration, the Laplace transform (eq. 3.10) is a highly stable operation, in the sense that small fluctuations (or errors) in $f(t)$ are averaged out in the determination of the area under a curve. Furthermore, the exponential factor, e^{-st} , means that the behaviour of $f(t)$ at large t is in practice unimportant, unless s is very small. As a result of these two aspects, a large change in $f(t)$ at large t indicates a small (perhaps insignificant) change in $F(s)$. On the contrary, the inverse transformation from $F(s)$ to $f(t)$ is a highly unstable process: a tiny change in $F(s)$ may result in an uncontrolled variation of $f(t)$ and all significant trends may disappear [8].

This kind of problems are known as ill-posed problems which means that errors in an unregularized inversion are unbounded. The problem was well faced by Provencher [9,10], who wrote down a computer program that uses numerical stable algorithms which are able to find regularized solution. In the present work a little adjustment of this computational program has been made (unpublished data) on the basis of the Tikhonov regularization [11].

3.2 Atomic Force Microscopy (AFM)

The atomic force microscopy (AFM) was introduced in 1986 [12] and originated with the invention of the scanning tunneling microscope in 1982 by Binnig and Rohrer [13,14]. These efemerids greatly enhanced the development of surface science and opened the field of nanoscience and nanotechnology as they allow to access to the molecular and atomic features. Nowadays several

apparatus have been implemented and extensively used for surface analysis and manipulation at the atomic level, operating at different interface media, in several modes, such as contact non-contact tapping, allowing go further in the discovery of surfaces features occurring at the nanoscale level. Due to the tunneling effect, either electrical or optical in nature, being itself the base mechanism for detecting surface details, probed via a cantilever-tip or tuning fork mechanical systems, together with scanning features, attention has to be paid in what concerns to both handling and data processing in looking for consistency in results. In fact, the knowledge of the approaches in both measurement and data analysis when using AFM technique are essential for the correct interpretation of surface topographic features.

Concerning to handling details, one of the most important factors come from the tip. In fact, both tip geometry and composition are known to influence the image quality. The major effects with regards to tip geometry are those leading surface feature broadening as a result of tip curvature's radius being smaller or larger than the size of features. The tip to surface interaction local forces, for a given scanned area, may also affect the image as they are changing the tip compression conditions, which could cause the tip to move far from the optimum working distance for feature observation. This effect might lead the tip to move far away from the surface or too much close to it or even to hit it. Surface and tip contamination may also influence the measurement, namely if the size of the contaminant is close to that of the surface features. Other mechanical factors as those related with the cantilever's calibration can also affect the results, mainly in what concerns to the determination of the appropriated elastic constant for a given cantilever-tip system. This could be relevant when force modulation mode is used as in measurement of force-distance curves which are relevant for studying surface molecular interactions and bond strength. Finally, there are other experimental factors that influence the accuracy in the attainment of the correct image, and are worth to refer, these are: image resolution, electric noise due to the tip-induced electric field fluctuation and image data processing. All of these experimental aspects determine the data quality and could give rise to artifacts in the analysis of surface texture parameters such as roughness, grain size and surface fractal dimension.

Concerning to data treatment as a result of a measurement, the choice of a data analysis method is always a complex issue requiring a quantitative statistical data analysis together with factors that are influencing it. Essentially this analysis is carried out at a single profile region and/or extended to the surface. In the first stage it is important to obtain the roughness parameters based on quantities as root mean square roughness, average height and grain diameter. In the case of kinetics studies, the overall surface roughness values can be obtained and roughness growth exponents determined allowing infer about the surface growth behavior. In addition, correlations between measurements, taken at different surface points, are calculated for a complete description of surface morphology. These will involve

the calculation of the Power Spectrum Density (PSD) function, which provides a more reliable topography description and allows the determination surface's fractal dimension, Autocovariance Function (ACF), giving an indication of the probability distribution of the random quantity. In addition, the determination of distribution of heights, skewness and kurtosis moment are fundamental for describing surface asymmetry and flatness features.

In this chapter one intends to address some of the above issues concerning good experimental practices and data analysis capabilities, particularly when applied to the characterization of soft condensed matter surfaces observed mainly by using the non-contact mode.

3.2.1 Artifacts in Atomic Force Microscopy

The atomic force microscopy (AFM) belongs to a family of techniques dedicated to nanoscale surface characterization based in the concepts developed by Binnig and Rohrer [12-14] for the scanning tunneling microscope (STM). Basically the AFM consists in the attainment of topographic images making probe scans over a surface, in a surface plane, x - y , while the distance between the surface and the probe, is being controlled [15-18]. The obtained topography image corresponds to the measured height values, $z(x,y)$, for a given area, A , defined by a window scan size L . Each height value is associated to a pair of surface coordinates, (x,y) , and the image may be described by a matrix with N lines and M columns which corresponds to the surface (x,y) points being the matrix elements the height $z(x,y)$. The validity and accuracy of surface properties achieved via AFM are greatly influenced by both the measuring features as tip, cantilever, scan feature, and image data analysis procedure. By its importance in the achievement of results these factors will be discussed below.

3.2.2 Tip Effects

During the topography acquisition with an atomic force microscope (AFM), the interaction between the tip and the surface is dependent on the distance between both. When the interatomic distance is large, the attractive force between the tip and the surface is weak. As the tip is approaching further the attraction increases until the atoms are so close together that the electron clouds start to repel each other electrostatically. This signifies that the interaction force goes to zero at a distance of about few angstroms. Generally the topographies are obtained maintaining the interactions magnitude constant during the tip scanning, in both direct contact (contact) and intermittent contact (tapping) modes. In the contact mode, the tip wearing comes as a result of abrasive and adhesive contact with the surface which can lead to both tip contamination and surface damage. During the measurement in non contact mode deformations can also occur contributing for elastic wear out. Therefore the interactions between tip and surfaces may cause image artifacts and even surface damage. Moreover, the tip type

to be used for a determined measurement is an important issue towards a good result, namely because the tip shape and composition is conditioned by sample nature. With respect to shape, tip artifacts may occur if the surface features have the same or smaller size than the AFM tip. In these cases the tip will not be able to correctly draw the profile contours giving rise to the so called convolution effects. One of the well known convolution effect is the feature broadening. This occurs when the tip curvature radius is comparable or greater than the feature size. For example, the silicon probes have radii of curvature in the range 5 to 15 nm, with half cone angles of about 10-30°, when used in the observation of biological samples, where normally the feature sizes are smaller than those of the tip, topographic profiles tend to be apart from real. To overcome the limitation of silicon tips during the observation of biological features, carbon nanotube tips have been successfully used to solve convolution effects. The diameter of these tips is close to that of major small organic molecules and additionally offer good mechanical properties [19-21]. As a reference to minimize tip convolution, McEuen et al [22] used carbon nanotube technology (CNT) to image protein complex in a mica surface. The CNT tips, with 1 to 2 nm of diameter, were prepared via chemical vapor deposition and were mounted onto standard Pt/Ir coated AFM tips. This technology demonstrated that when tip structure has the same properties of the surface to be analyzed the results are very reproducible. In addition, other desirable properties of CNT tips for analyzing biological samples were revealed, these are low tip-sample adhesion, ability to resist large forces, possibility of achieving high lateral imaging resolution and capability of being chemically functionalized. In fact, DNA AFM images scanned with silicon tip, Pt/Ir coated tip and single-walled CNT tip were compared and the last one demonstrated notable resolution and reproducibility.

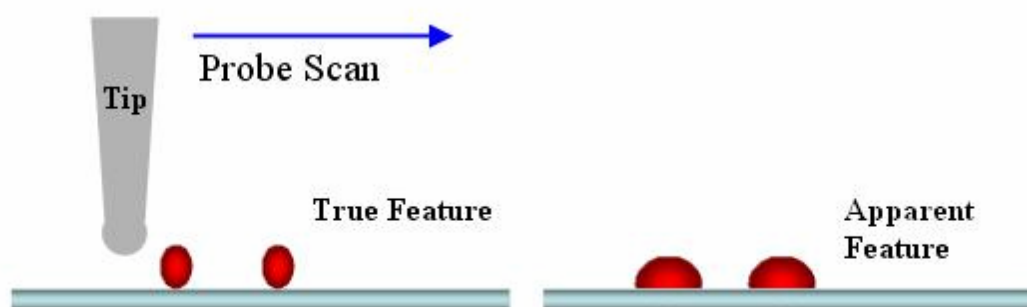


Fig. 3.5 Schematization of broadening effect in AFM image due to tip size effect, observable when tip size is comparable with the surface feature size.

Tip contamination may also give rise to convolution which is related with the contaminant size relative to surface size features to be measured. Therefore, before each measurement the verification of the tip state has to be addressed. McIntyre et al [23] proposed a method to evaluate the tip status,

using the scan of a biaxially oriented polypropylene (BOPP) film for reference. If the tip is contaminated or even damaged the characteristic fiber-like network source will not be detected. In fact, BOPP is a good reference for testing tips because is soft, hydrophobic and has low surface energy, which are important factors preventing the tip contamination [24]. Another negative influence in the image is the tip compression on the feature to be observed. This happens when the tip is over the feature compressing it.

This compression may give rise to surface damage and consequently causing an artifact in the obtained image. At this point it is worth to remark that carbon nanotube tips have demonstrated good flexibility, which limits the maximum force applied to the sample and prevents surface damage [25]. Computational calculations of the flexibility of CNT tips lead to values of maximum force of about 50 pN instead of the value of 100 nN found when using a standard AFM tip. Generally in looking for high-resolution in AFM imaging of a soft or fragile surface a sharp tip and a soft cantilever is recommended. Cantilever features will be discussed in the next section.

AFM micrography taken in tapping mode is shown in Figure 3.6

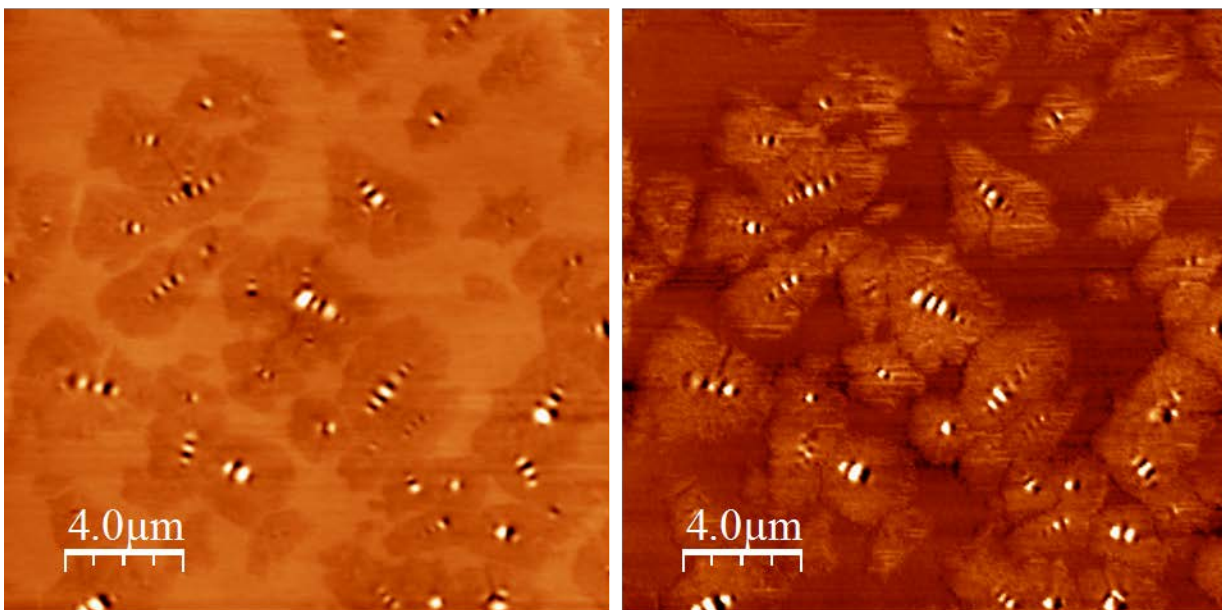


Figure 3.6 AFM Image of Bitumen 50/70 (left) topography. (right) phase contrast.

In early atomic force microscopy (AFM) work on bitumen, the bee-like structure, called catana phase, was attributed to asphaltene. The bee structure does not have a defined pattern but usually it can be visualized by AFM as composed of a series of aligned protrusions and depressions. They can be either isolated or in star shape. However more recent studies attributed to the presence of wax a substantial contribution to the bee-like structures [26]. The phase-contrast image is produced by monitoring the phase difference between the cantilever's oscillations and the standard signal, it also arises from compositional variations of the surface as well as the topographical variations caused by changes in

adhesion between the tip and, in this case, the bitumen surface. In general, the phase contrast image contains information about variations of sample mechanical properties. [27].

3.3 Fundamentals Rheology of Viscoelastic Matter.

Fluids deform irreversibly under shear; in other words, they flow. In contrast, solids deform elastically when subjected to a small shearing force and recover their original shape when the force is removed. The behavior of what is termed soft matter is somewhere in between. Soft matter systems are typically viscoelastic, that is they display a combination of viscous (fluid-like) and elastic (solid-like) behavior. Measuring the flow behavior and the mechanical response to deformation of viscoelastic materials provides us with information that can be interpreted in terms of their smallscale structure and dynamics. The mechanical properties of soft materials depend on the length scale probed by the measurements due to the fact that the materials are structured on length scales intermediate between the atomic and bulk scales [28]. For example, a colloidal suspension has structure on the scale of the spacing between the colloidal particles; a concentrated polymer system, on the scale of the entanglements between large molecules. As a result, their bulk properties can be quite different from properties on length scales smaller than or comparable to the structural scale. Making measurements on both macroscopic and microscopic length scales can help us to develop a better understanding of the relationship between microstructure and bulk properties in soft materials.

Following a brief introduction to viscoelasticity, this chapter will focus on two methods of measuring the viscoelastic properties of soft matter. On the macroscopic scale, rotational shear rheometry provides a well-established set of techniques for determining the mechanical properties of complex fluids. We will summarize the principles of rheology and describe the types of measurements one can perform [29–31]. Typically shear rheometry will be performed using a commercial rheometer, and we will discuss the types of instrument commonly available. We will not discuss extensional rheology or other rheometrical methods; the interested reader is referred to a number of excellent textbooks [29–31]. Techniques for making rheological measurements on the microscopic scale have been developed more recently, and the field of microrheology is still evolving. Several reviews of the field have been published recently [32–36]. We will summarize the theoretical background and describe a frequently used experimental method based on tracking the motion of micron-sized tracer particles as they diffuse through the material of interest [33-38]. Such experiments are typically home-built, and we will describe one implementation. In both cases, we will provide examples that illustrate how rheological measurements can provide information about the structure and dynamics of soft materials.

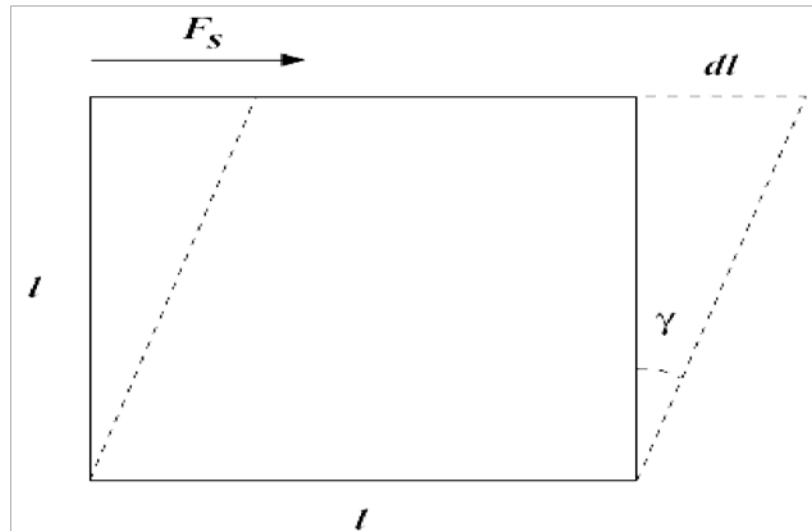


Figure 3.7 A small element of material subject to a shear force F_s . The bottom edge of the material is held fixed. The material experiences a shear strain $\gamma = dl/l$.

Consider a small solid cube having sides of length l and area $A = l^2$, as shown in Figure 3.7. Suppose that the bottom surface is held in place, and that we apply a shear force F_s parallel to plane of the top surface. The shear stress σ is the shear force divided by the surface area:

$$\sigma = F_s/A \quad \mathbf{3.12}$$

In response to the applied shear force, the solid will deform by an amount dl . The shear strain γ is the relative deformation, given by:

$$\gamma = dl/l \quad \mathbf{3.13}$$

For small strains, this is the same as the angle γ shown in Figure 3.7. For a perfectly elastic solid, Hooke's Law tells us that stress and strain are linearly proportional, that is:

$$\sigma = G'\gamma \quad \mathbf{3.14}$$

where the elastic modulus G' is a measure of the elastic energy stored in the material when it is deformed. Hooke's Law implies reversibility – the deformation immediately returns to zero when the shear stress is removed. Now imagine applying the same shear stress to a cubic element of a Newtonian fluid. In this case, the material flows continuously – the strain continues to increase for as long as the stress is applied. If the stress is increased, the fluid flows faster. Newton's law of viscosity states that:

$$\sigma = \eta\dot{\gamma} \quad \mathbf{3.15}$$

where $\dot{\gamma} = d\gamma/dt$ is the strain rate. Here the strain rate, not the strain, is proportional to the stress. Equation (3.15) can be considered to define the viscosity η , which is related to the dissipation of energy in the flow. η can be thought of as the tendency of a material to resist flow. The discussion above (and throughout this chapter) is very much simplified by our neglect of the fact that stress, strain, and strain rate are all, in general, tensor quantities. For example, the shear stress σ referred to in the above equations is really just one component of a symmetric second-rank stress tensor. Since the focus of this book is on experimental techniques, we will ignore this rather important

detail and use a simple scalar description. This implies a neglect of any material anisotropy and, more seriously, of several interesting and important physical phenomena, some of which will be mentioned very briefly below. More mathematically rigorous discussions can be found in textbooks such as references [29, 30, 39]. In general, the response of soft matter systems or complex fluids to an applied deformation or stress is time-dependent, they typically behave as solids on short time scales or at high frequencies and as viscous liquids over long times or at low frequencies. For example, when a viscoelastic material is subjected to a step increase in strain by an amount γ_0 , the stress σ in the material undergoes a step change followed by, in the simplest case, an exponential relaxation. For small strains, one can define a relaxation modulus $G(t) = \sigma(t)/\gamma_0$, which is independent of γ_0 , so

$$d\sigma = G(t)dy \quad \mathbf{3.16}$$

Analogously, in a creep experiment, the stress is suddenly increased from zero to some value σ_0 . In this case, the strain will initially change rapidly in response, then continue to evolve more slowly as a function of time. The creep compliance $J(t)$ is defined as.

$$J(t) = \gamma(t)/\sigma_0 \quad \mathbf{3.17}$$

and is conceptually equivalent to the reciprocal of the relaxation modulus $G(t)$.

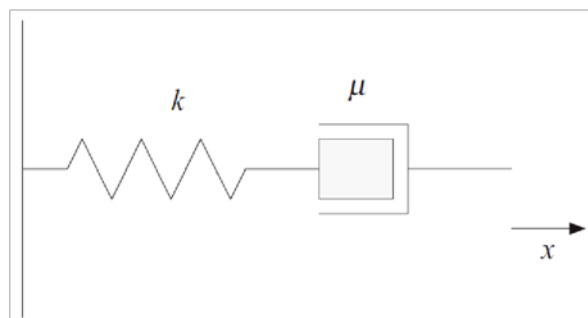


Figure 3.8 The spring-dashpot representation of the Maxwell model for a viscoelastic medium. The viscous and elastic elements are combined in series and stretched by a distance x .

The range of strains in which stress and strain are linearly related is called the linear viscoelastic regime. In this regime, the strain is small enough that it does not seriously disrupt any structure in the material, and one thus probes the response of the material to small perturbations of its equilibrium configuration. At higher strains, the structure is disrupted and the response of the material changes accordingly. In particular, the material properties become functions of strain or strain rate, and often functions of time as well. For example, outside of the linear regime, the

viscosity of polymer solutions typically decreases as the strain rate is increased (shear thinning), because the shear stretches out the polymer molecules and allows them to partially disentangle. On the other hand, a concentrated clay suspension, which is a gel at rest, will become liquid when subjected to a large enough strain as the small-scale arrangement of the interacting clay particles is changed. It will then slowly gel again over time [40] as the clay particles rearrange and reorient. The interpretation of rheological measurements in the nonlinear regime is complex, and a subject of substantial current research [41, 42]. The simplest model of a viscoelastic material is originally due to Maxwell [43], and is mechanically equivalent to a spring in series with a viscous damper (a dashpot), as in Figure 3.8. If we stretch this combined system by a displacement x , a force F is developed that obeys the differential equation

$$F + \frac{\mu}{k} \frac{dF}{dt} = \mu \frac{dx}{dt} \quad 3.18$$

where k is the spring constant and μ the viscosity of the dashpot. In terms of the viscoelastic properties of a complex fluid, the Maxwell model takes the form

$$\sigma + \phi \frac{d\sigma}{dt} = \eta \frac{d\gamma}{dt} \quad 3.19$$

where the viscosity η is assumed to be constant and ϕ is a time scale for the relaxation of the material. We can derive the integral form of the Maxwell model by imagining that the stress in a material depends on the strain to which it has been subjected over all time, from the distant past to the present [29]. The stress due to an arbitrary deformation can be calculated by integrating over contributions due to a series of small deformations as long as the relaxation modulus $G(t)$ depends only on time and not on γ . In this case, we can rewrite Equation (3.16) in the form

$$d\sigma = G \frac{d\gamma}{dt} dt = G \dot{\gamma} dt \quad 3.20$$

Integrating, we have

$$\sigma = \int_{-\infty}^t G(t-t') \dot{\gamma}(t') dt' \quad 3.21$$

where t' runs from $-\infty$ to the present time t , and in general the strain rate $\dot{\gamma}$ is a function of time. In this context, the relaxation modulus $G(t-t')$ is referred to as a memory function. If $G(t)$ can be represented by an exponential decay with a decay time ϕ , that is, $G(t) = G_0 e^{-t/\phi}$, then Equation (3.21) becomes

$$\sigma = \int_{-\infty}^t G_0 e^{-(t-t')/\phi} \dot{\gamma}(t') dt' \quad 3.22$$

which gives the stress as a sum of infinitesimal contributions weighted by the memory function. Differentiating Equation (3.22) with respect to time recovers Equation (3.19), showing that the two formulations are equivalent. At steady state, $d\sigma/dt = 0$ and Equation (3.19) becomes Newton's law of viscosity, while for rapid changes, $d\sigma/dt \gg \sigma/\phi$ and Hooke's law is recovered.

The principle of shear rheometry is straightforward: the material of interest is subjected to shear in a controlled way, and the mechanical response measured. Typically one either applies a controlled shear strain and measures the resulting shear stress, or applies a known shear stress and measures the strain. A schematic representation of a layer of fluid subjected to simple shear is shown in Figure 3.9.

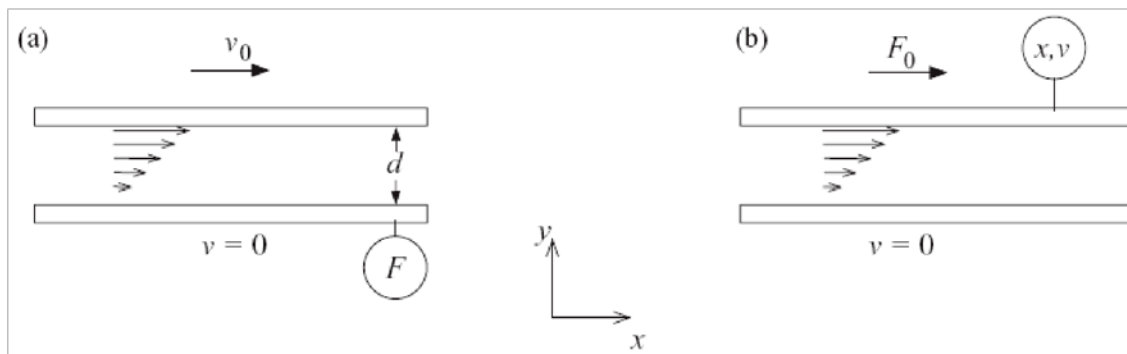


Figure 3.9 The distinction between strain- and stress-controlled deformation.

In figure 3.9(a) in a strain-controlled measurement, a fluid sample sandwiched between two plates is deformed by moving the upper plate at a controlled velocity v_0 , while the bottom plate is kept stationary. The force required to hold the lower plate fixed is measured by a transducer, indicated by the circle. In figure 3.9(b) in a stress-controlled measurement, a controlled shear force is applied to the top plate, and the resulting velocity is measured. The difference between stress and strain-controlled measurements is analogous to the difference between voltage and current-controlled measurements in electronics. In many cases, the same information can be obtained with either technique, a resistor has the same resistance no matter whether one measures it using a voltage supply or a current supply.

Typical rheological tests on bitumen samples are carried out using a controlled shear stress rheometer equipped with a parallel plate geometry (gap 2 mm, $r = 25$ mm) and a Peltier system ($\pm 0.1^\circ\text{C}$) for temperature control. Dynamic tests, carried out in conditions of linear material behavior where measured material functions are independent of the amplitude of applied load and are the only function of microstructure [44,45], are adopted for material characterization. Aimed at investigating the material phase transition, temperature sweep tests are performed at 1 Hz increasing temperature from 25 °C to 120 °C at 1 °C/min and applying the proper stress values to guarantee

linear viscoelastic conditions (previously determined by stress sweep tests, figure 3.11) at all tested temperatures.

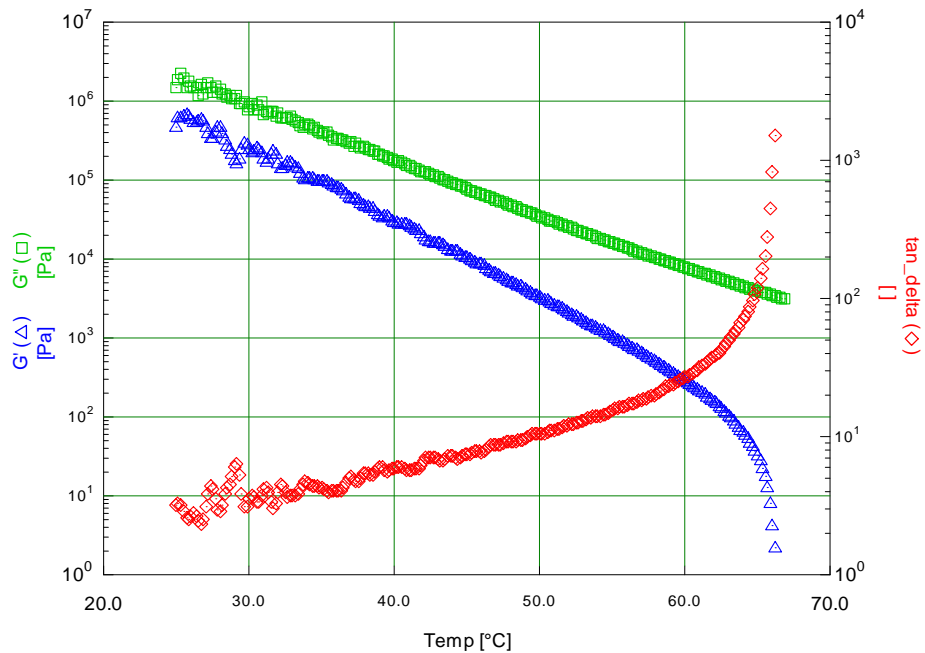


Figure 3.10 – Time cure test of Bitumen 50-70

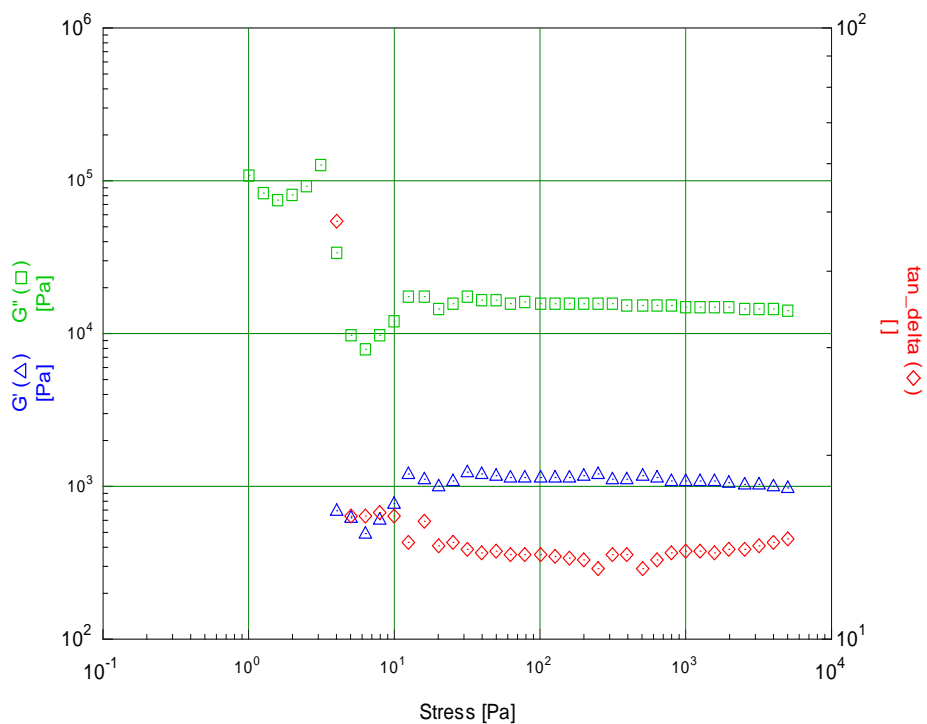


Figure 3.11 – Stress Sweep test of Bitumen 50-70 at 50°C

3.4 REFERENCES Chapter 3

1. Levitt MSpin dynamics : basics of nuclear magnetic resonance. 2nd Ed. N.York Wiley ed.(2008).
2. Hahn, E.L. Spin echoes. Physical Review 1950, 80, 580–594.
3. Carr, H. Y.; Purcell, E.M. Effects of Diffusion on Free Precession in Nuclear Magnetic Resonance Experiments. Physical Review 1954, 94, 630–638.
4. Meiboom, S.; Gill, D. Modified Spin-Echo Method for Measuring Nuclear Relaxation. Times Rev. Sci. Instrum. 1958, 29, 688.
5. Widder, D.V. Advanced Calculus, 2nd ed. Prentice-Hall, Englewood Cliffs, (1947).
6. Bellman, R.E.; Roth, R.S. The Laplace Transform World Scientific, Singapore, (1984).
7. McQuarrie, D.A. Mathematical Methods for Scientists and Engineers, University Science Books, Sausalito, (2003).
8. Bellman, R.; Kalaba., R.E.; Lockett, J.A. Numerical Inversion of the Laplace Transform: Applications to Biology, Economics. Engineering and Physics, Elsevier, New York, (1966).
9. Provencher, S.W. : A constrained regularization method for inverting data represented by linear algebraic or integral equations. Comput. Phys. Commun. 1982, 27, 213.
10. Provencher, S.W. : CONTIN: A general purpose constrained regularization program for inverting noisy linear algebraic and integral equations. Comput. Phys. Commun. 1982, 27, 229.
11. Tikhonov, A. N.; Arsenin, V. Y. Solutions of Ill-Posed Problems. John Wiley & Sons: New York 1977.
12. Binning, G.; Quate, C.; Gerber, Ch. Phys. Rev. Lett. 56, 930, 1986.
13. Binnig, G.; Rohrer, H.; Gerber, CH.; Weibel, E. Phys. Rev. Lett. 49, 57, 1982.
14. Binnig, G.; Rohrer, H. Reviews of Modern Physics 71, S324, 1999.
15. Binnig, G.; Smith, D.P.E. Rev. Sci. Instrum. 57, 1688 (1986).
16. Gustafsson, M.G.L.; Clarke, J. J. Appl. Phys. 76, 172, 1994.
17. Magonov, S.N.; Whangbo, M.H. Surface analysis with STM and AFM, (VCH, Weinheim 1996).
18. Raposo, M.; Ribeiro, P.A.; Pereira da Silva, M.A.; Oliveira Jr., O.N. in Current Issues on Multidisciplinary Microscopy Research and Education, edited by A. Méndez-Vilas and L. Labajos-Broncano, FORMATEX Microscopy Book Series N.2, pp. 224-241, 2004.
19. Chen, L.; Cheung, C.L.; Ashby, P.D.; Lieber, C.M. Nanno Letters, 4, 1725, 2004NO.
20. Stevens, R.M.D.; Frederick, N.A.; Smith, B.L. Nanotechnology 11, 1, 2000.
21. Wanga, Y.; Chen, X. Ultramicroscopy 107, 293, 2007.

22. Bunch, J.S.; Rhodin, T.N.; McEuen, P.L. *Nanotechnology* 15, S76, 2004.
23. Nie, H.Y.; McIntyre, N.S. *Langmuir* 17, 432, 2001.
24. Nie, H.Y.; Walzak, M.J.; McIntyre, N.S. *Review of Scientific Instruments*, 73, 3831, 2002.
25. Guo, L.; Wang, R.; Xu, H.; Liang, J. *Physica E* 27, 240, 2005.
26. McCarron, B. The Investigation of 'Bee-Structures' in Asphalt Binders. Major Qualifying Project 2011-2012, Dept. of Physics, Worcester Polytechnic Institute, (2012).
27. Yu, X.; Burnham, N.A.; Tao, M. Surface microstructure of bitumen characterized by atomic force microscopy. *Advances in Colloid and Interface Science* 2016, 218, 17–33.
28. Larson, R.G. *The Structure and Rheology of Complex Fluids* (Oxford University Press, New York, 1999).
29. Macosko, C.W. *Rheology: Principles, Measurements, and Applications* (Wiley-VCH, New York, 1994).
30. Morrison, F.A. *Understanding Rheology* (Oxford University Press, New York, 2001).
31. Whorlow, R.W. *Rheological Techniques* (Ellis Horwood, New York, 1992).
32. MacKintosh, F.C.; Schmidt, C.F. "Microrheology," *Curr. Opin. Coll. Interf. Sci.* 4, 300 (1999).
33. Gardel, M.L.; Valentine, M.T.; Weitz, D.A. Microrheology, in K. Breuer (ed.), *Microscale Diagnostic Techniques* (Springer, New York, 2005).
34. Waigh, T. A. Microrheology of complex fluids, *Rep. Prog. Phys.* 2005, 68, 685.
35. Willenbacher, N.; Oelschlaeger, C. Dynamics and structure of complex fluids from high frequency mechanical and optical rheometry. *Curr. Opin. Colloid Interface Sci.* 2007, 12, 43.
36. Pipe, C.; McKinley, G.H. Microfluidic rheometry. *Mech. Res. Comm.* 2009, 36, 110.
37. Mason, T.G.; Weitz, D.A. Optical measurements of frequency-dependent linear viscoelastic moduli of complex fluids. *Phys. Rev. Lett.* 74, 1250 (1995).
38. Valentine, M.T.; Kaplan, P.D.; Thota, D.; Crocker, J.C.; Gisler, T.; Prud'homme, R.K.; Beck, M.; Weitz, D.A. Investigating the microenvironments of inhomogeneous soft materials with multiple particle tracking. *Phys. Rev. E* 64, 061506 (2001).
39. Bird, R.; Armstrong, R.; Hassager, O. *Dynamics of Polymeric Liquids, Volume 1: Fluid Mechanics* (Wiley, New York, 1987).
40. Oppong, F. K.; Coussot, P.; de Bruyn, J.R. Gelation on the microscopic scale. *Phys. Rev. E* 78, 021405 (2008).
41. Wilhelm, M. Fourier transform rheology. *Macromol. Mater. Eng.* 287, 83 (2002).
42. Ewoldt, R.H.; Hosoi, A.E.; McKinley, G.H. New measures for characterizing nonlinear viscoelasticity in large amplitude oscillatory shear. *J. Rheol.* 2008, 52, 1427.

43. Maxwell, J.C. On the dynamical theory of gases. *Phil. Trans.* 1867, 157, 49.
44. Barnes, H.A.; Hutton, J.F.; Walters, K. *An introduction to rheology*. Amsterdam: Elsevier Science; 1989.
45. Steffe, J.F. *Rheological methods in food process engineering*. 2nd ed. East Lansing: Freeman Press; 1996.



Investigation of new additives to reduce the fume emission of bitumen during Asphalt Concrete Processing

Paolino Caputo ^{1,*}, Giuseppe Antonio Ranieri ¹, Nicolas Godbert ², Iolinda Aiello ², Antonio Tagarelli ³ and Cesare Oliviero Rossi ^{1,*}

¹ Dipartimento di Chimica e Tecnologie Chimiche, Università della Calabria, Cubo 14/D, Arcavacata di Rende (CS), 87036, Italy. tel./fax. +39 0984492045

² MAT-INLAB (Laboratorio di Materiali Molecolari Inorganici), LASCAMM CR-INSTM, Unità INSTM della Calabria, Dipartimento di Chimica e Tecnologie Chimiche, Università della Calabria, Cubo 14/C, Arcavacata di Rende (CS), Italy

³ Dipartimento di Chimica e Tecnologie Chimiche, Università della Calabria, Cubo 12/C, I-87036, Arcavacata di Rende (CS), Italy

Abstract: Pavement materials play an important role in overall pavement sustainability including material acquisition processing, and transportation. The main objective of the present study is to evaluate the effectiveness of new additives, to reduce bitumen's fume emission expelled into the atmosphere, during the processing of asphalt concrete. The new additives act by trapping bitumen's volatile substances avoiding their release at high temperatures. In this paper, we have been tested the performance of 2 types of mesoporous silica-based additives (AntiSmog 1 and AntiSmog 2). The idea of using these additives to reduce the emission of fumes in bitumen has been submitted as a patent. To quantify and characterize the emitted fumes, thermogravimetry (TGA) and gas chromatography-mass spectrometry (GC-MS) technique have been used. Dynamic Shear Rheology (DSR) has been used to check the rheological properties and the possible sedimentation issues that could occur after the addition of the additives.

Keywords: fume; bitumen; mesoporous; thermogravimetry (TGA); gas chromatography-mass spectrometry (GC-MS).

Introduction

Most definitions of sustainability begin with that issued by the World Commission on Environment and Development (WCED) in 1987: "Sustainable development is a development that meets the needs of the present without compromising the ability of future generations to meet their own needs." Moreover, sustainability is often described as a quality that reflects the balance of three primary components: economic, environmental, and social impacts ¹.

"Sustainable" in the context of pavements refers to system characteristics that encompass a pavement's ability to:

- Achieve the engineering goals for which they were constructed.
- Preserve and (ideally) restore surrounding ecosystems.
- Use financial, human, and environmental resources economically.

- Meet human needs such as health, safety, equity, employment, comfort, and happiness.

All stakeholders in the pavement community from owner/agencies to designers, and from material suppliers to contractors and consultants are embracing the need to adopt more sustainable practices in all

aspects of their work, and are continually seeking the latest technical information and guidance available to help improve those practices ².

Low consumption of energy for production and construction, low emission of greenhouse gases or fumes and conservation of natural resources help to make asphalt the environmental pavement of choice ³⁻⁵. However, the ever-increasing pavement's loads and the needs for using modified binders and additives to coup the problem of heavy-duty pavements has led to both environmental and economic concerns.

In particular, this paper intends to show the benefits of new additives on the emission of bitumen

*Corresponding author: Paolino Caputo, Cesare Oliviero Rossi
Email address: paolino.caputo@unical.it, cesare.oliviero@unical.it
DOI:

Received October 11, 2018
Accepted October 23, 2018
Published November 7, 2018

fumes and a methodology to check their chemical composition.

Bitumen is a soft multicomponent material issued from the petroleum cracking industry as a residual side-product⁶. For this reason, its chemical composition is randomly composed of various substances also including volatile and toxic chemicals that are subject to be easy release into the ambient during the processing step, in particular during the layering of bitumen onto the roads. Not only these substances can be toxic for the environment, but they certainly are toxic for the workers that are processing bitumen as pure material or in mixtures such as asphalt concrete⁷.

Indeed, each time bitumen is heated either for road paving or to manage and transport it in high quantity, risks of chemicals release are present. Up to now, additives are used in asphalt concrete with the main aim to decrease the temperature of asphalt processing, thus limiting the emission of possible toxic fumes of volatile components⁸⁻¹⁰. For this reason, there is a need to devise new additives that could be injected into bitumen to reduce the emission of toxic fumes¹¹, without adversely affecting the rheological properties of the resulting concrete. To this regard, we used two different additives, both silica based mesoporous powders (AntiSmog 1 and AntiSmog 2) able to entrap volatile fumes.

Many researchers described environmental applications of mesoporous silica that have permitted their use in a diverse range of applications from biosensors¹², biomedicine^{13,14}, drug delivery¹⁵, pollutants removal¹⁶ to optical devices¹⁷. However, this article will focus on the application of mesoporous silica primarily for adsorption of organic pollutants from bitumen.

In order to quantify and identify the volatile substances released during bitumen processing, thermogravimetry (TGA)¹⁸ and gas chromatography-mass spectrometry (GC-MS) techniques¹⁹ were used along with Dynamic Shear Rheology (DSR) to check the rheological properties of the bitumen after the insertion of specific additives. The use of additives as powder state requires an integrated experimental approach to check the rheological properties of the resulting material and the eventual sedimentation that could occur within the thus formulated concrete. To this purpose shear dynamic experiments were done.

Materials and Methods

The bitumen used in this work was kindly supplied by Loprete Costruzioni Stradali (Italy). It was produced in Italy but the crude oil was coming from Saudi Arabia. Its penetration grade was 50/70. Data are shown in Table 1:

Table 1. Properties of Pristine bitumen (PB) and Modified Bitumen (BM).

		PB	BM1 - 1%	BM2 - 1%
PN (0.1 mm) Penetration depth ± 1	ASTM D 946	60	56	54
R&B (°C) Softening point ± 1	ASTM D 36	51	50.4	52.2
X _A (wt%) Asphaltene content ± 0.5	C.O. Rossi <i>et al.</i> [6]	26.8	27.1	27.3
TR (°C) Transition temperature ± 0.1		68.0	65.8	69.5

Additives:

AntiSmog1 (additive 1) and AntiSmog2 (additive 2) additives were developed by the academic Spin-Off (Kimical SRL) of the University of Calabria, commercial named Kimical NoSmogA and Kimical NoSmogB respectively, following reported procedures to synthesize mesoporous silica in basic conditions (AntiSmog1) and in acid conditions (AntiSmog2). All technical information can be obtained by Kimical SRL.

In general, the mesoporous silica materials can be characterized in terms of pore diameter, surface area and pore volume²⁰. The two additives used in the present work display different porosities.

Details of the preparation and the use of these additives to reduce the emission of toxic fumes from hot bitumen are contained in the Italian Patent (n.102016000041219). Authors of the patent are available for further feedback.

Both additives **AntiSmog1** and **AntiSmog2** were added to the investigated bitumen, under vigorous stirring (600 RPM) at the temperature of

150°C and the stirring was maintained for 30 minutes. Cooling to room temperature allowed obtaining the bitumen mixtures **BM1** and **BM2** respectively. Different concentrations of additives were studied ranging from 1 to 10 % w/w. The heating temperature (150°C) was chosen below the smoke point of the used bitumen to allow a homogeneous mixture under stirring without emission of fumes. The same experimental condition was applied to the neat bitumen (exposed to the same temperature and stirring treatment before analysis) in order to produce the reference sample called “pristine bitumen”, **PB**, throughout the article. With this reference, it will be possible, throughout the whole study, to directly assert that the observed changes in properties are related to the addition of the additives and are not due to the pre-heating period used for the preparation of the samples.

Thermogravimetric measurements:

The thermogravimetric analysis allows measuring accurately the weight loss of the sample during the linear increase of temperature.

The thermogravimetric studies were performed on a Perkin-Elmer TGA-6 instrument. Analyzed samples consisted of *ca.* 3 mg of samples taken at the end of the 30 min period of stirring as described above. Analyses were performed from 100°C to 300°C at a temperature scan rate of 2°C/min.

GC-MS analysis:

The GC-MS technique represents a reliable analytical tool because of the high separation efficiency of gas chromatographic technique and the great sensitivity and specificity of mass spectrometry. This approach represents a very specific analytical methodology that allows for the reduction of interferences and then the improvement of the reliability of the entire method.

GC-MS analyses were performed using a TSQ Quantum GC (Thermo Fischer Scientific) system constituted by a triple quadrupole mass spectrometer (QqQ) Quantum and a TRACE GC Ultra.

The capillary column was 30 m × 0.25 mm i.d., 0.25 μm film thickness Thermo TR-5MS (95% polydimethylsiloxane, 5% polydiphenylsiloxane).

4 g of bitumen mixture was directly weighted in a suitable vial (30 mL). After 300 μl of internal standard (Phenanthrene-d10) solution at 133 mg l⁻¹ were added and the vial was crimped and maintained in an oil bath at 160-170 °C for 30 minutes. Solid-phase microextraction (SPME) extraction was performed with a 100 μm PDMS (polydimethylsiloxane) fiber in headspace immersion mode for 15 min, and the extracted analytes were thermally desorbed by introducing the fiber into the injector set at 280 °C for 10 min. The GC oven temperature was initially held at 70 °C for 10 min, then ramped at 20 °C min⁻¹ to 200 °C and held at this temperature for 1.5min, then ramped again at 20 °C min⁻¹ to 260 °C and maintained at this temperature for further 2 min before being finally increased at 20 °C min⁻¹ to 340°C for 5 minutes. The carrier gas was helium at 1.2 ml min⁻¹ of purity 99.999%. For SPME analyses, a Thermo PTV straight Liner 0.75 mm × 2.75 mm × 105 mm was used as GC inlet liner. The QqQ mass spectrometer was operated in electron ionization (EI) in full scan mode.

Dynamic Shear Rheology:

Dynamic Shear Rheological (DSR) measurements on bitumen samples were carried out using a controlled shear stress rheometer (SR5, Rheometric Scientific, USA) equipped with a parallel plate geometry (gap 2 mm and diameter $\phi = 25$ mm within the temperature range 25-150 °C, while gap 2 and diameter $\phi = 8$ mm from 25 to -30°C). The Peltier system (± 0.1 °C) was used for temperature control.

Rheological dynamic experiments were performed within the linear viscoelastic region where

rheological properties are independent of the amplitude of applied load and are the only function of the microstructure of material ²¹. Aimed at investigating viscoelastic properties of the bitumen and phase transition, temperature ramp tests were performed at 1 Hz with heating rate 1°C/min and applying the proper stress values to guarantee linear viscoelastic conditions (previously determined by stress sweep tests) at all tested temperatures. More details about the mechanical characterization can be found elsewhere ²².

Sedimentation tests:

A tuben test procedure was performed to determine the sedimentation phenomenon of investigated samples.

The Tuben Test procedure was performed to determine the tendency of a powder asphalt modifier to separate from the bitumen during static storage at a controlled temperature. If a modified bitumen shows a tendency to separate during storage, this must be taken into account either by providing some sort of agitation or stirring or by reformulating the binder. The test procedure was conducted in according to EN-13399 standard (Standard Practice for Determining the Separation Tendency of Polymer from Polymer Modified Asphalt) and is fully described in Oliviero Rossi et al. ²³

Results and Discussion

Thermogravimetric analysis of all prepared samples **PB**, **BM1** and **BM2** at various concentration content of additives were performed at 100°C starting temperature, at 2°C/min temperature scan rate ²⁴.

Special attention has been paid to the weight loss occurring between 140°C-200°C temperature range, which is usually used to process the bitumen. Remarkably, concerning the pristine bitumen **PB**, both additives were able to delay and therefore reduce the weight loss of the bitumen.

Indeed, already at 100°C, **PB** shows slow but constant weight loss up to 250°C. At this temperature, the 2% of weight loss is registered for **PB**, while both **BM1** and **BM2** samples have constant weight up to 170°C, even with additive concentrations as low as 1% w/w.

Fig. 1 shows, as an example, the superimposition of TGA thermograms registered for **BM1-1% w/w**, **BM1-5% w/w**, **BM1-10% w/w** together with the TGA thermogram registered for the pristine bitumen sample **PB**.

We focus our characterization only to the sample with 1% of the additive. Considering that within the temperature range 140-200°C, the samples containing 1, 5 and 10% of additive, show the similar trends (only slight differences are observable in the TGA analysis), it was clear that 1% of additive is enough to ensure a good performance regarding fumes emission

reduction. Consequently, the objective of such approach is to minimize both the quantity of additive(s) and the possible change in physical-chemistry properties of the resulting mixture compared to PB and also to minimize the cost of final modified bitumen.

In order to check the performances of the additives in trapping capacity of volatile fumes, isothermal TGA measurements have been performed at 200°C, until a constant weight of the sample was recorded (around 40 min) ²⁵.

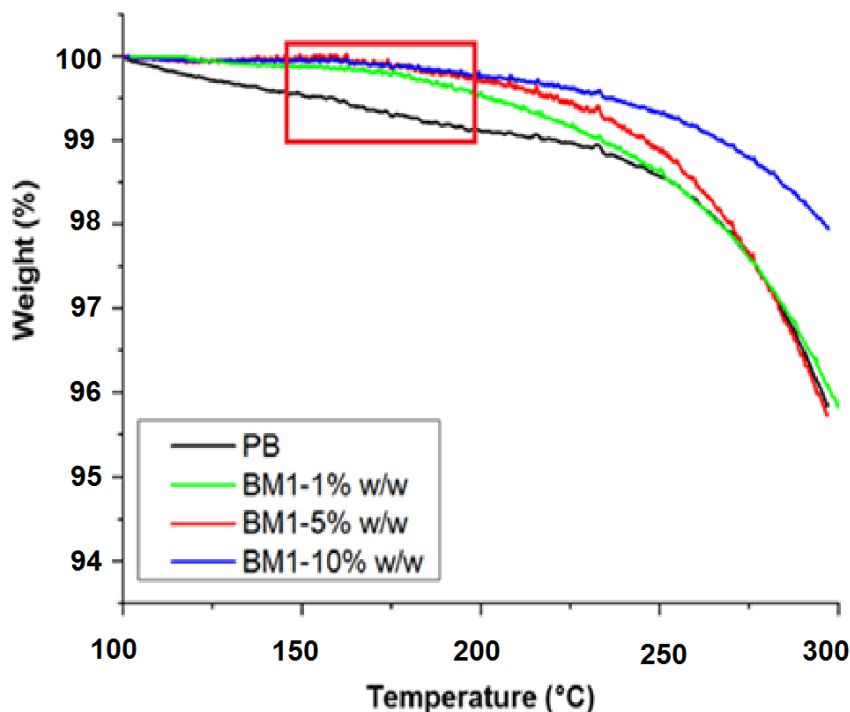


Figure 1. Thermograms of PB, BM1-5% w/w and BM1-10% w/w. The red inset shows the temperature window typically for the bitumen and pavement processing.

In Fig.2 and Table 2 data of % weight loss obtained over time required to reach a constant weight are reported. All samples reach a constant value of loss weight approximately at the same time.

For samples, BM1-1% w/w and BM2-1% w/w smaller weight loss were registered when compared to PB, consistent with less quantity of fume released.

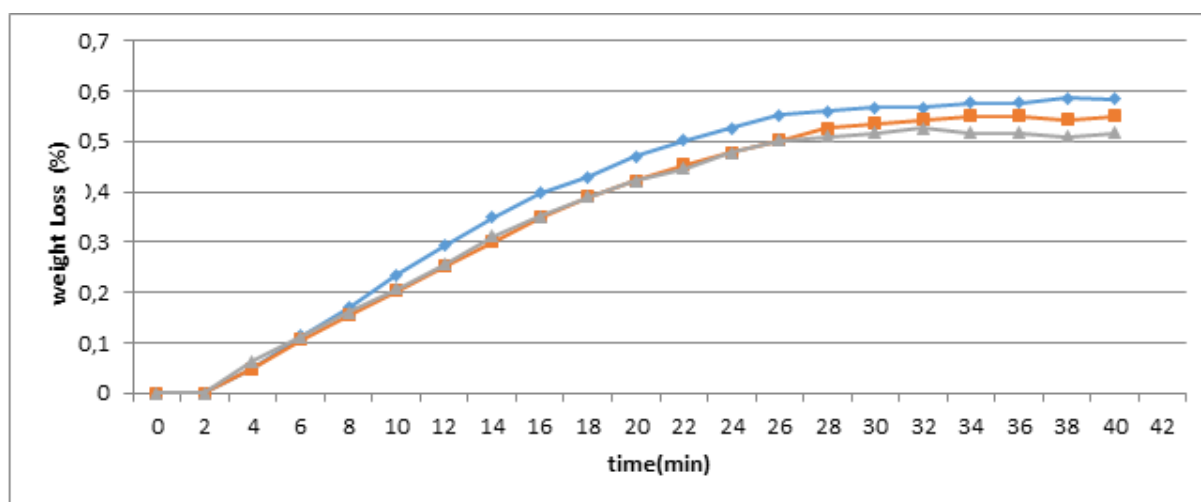


Figure 2. Additive performances in fume trapping at 200°C (—◆— Pristine Bitumen; —■— BM1-1% w/w; —▲— BM2-1% w/w)

Table. 2 Additive performances in fume trapping at 200°C.

Sample	Weight Loss (%)	Fume released (%)
Pristine Bitumen (PB)	0.560	100.0
BM1-1% w/w	0.527	94.1
BM2-1% w/w	0.510	91.7

It is worth noticing that the reducing in fume emission resulting from the use of the two additives are very similar (curves are almost overlapped). Furthermore, the modified bitumens show a delay in the fume emission. Finally, the final weight loss is lower for both **BM1** and **BM2** samples concerning **PB**.

To check the efficiency in fume trapping of the two additives **BM1** and **BM2**, GC-MS analyses of the emitted fumes were performed in order to identify their chemical content²⁶. The fume released at 160°-170°C by the pristine bitumen sample **PB**,

and the additive containing samples **BM1-1% w/w** and **BM2-1% w/w** were investigated/profiled. Specifically, the fumes emitted after 30 min from sealed samples kept at 160°C-170°C were analyzed by SPME technique²⁷.

A PDMS fiber was inserted in the headspace through the rubber disk of a sealed vial and exposed to the generated fumes for 15 minutes allowing the easy and rapid extraction of analyses which were immediately desorbed into the injector of the gas chromatography system.

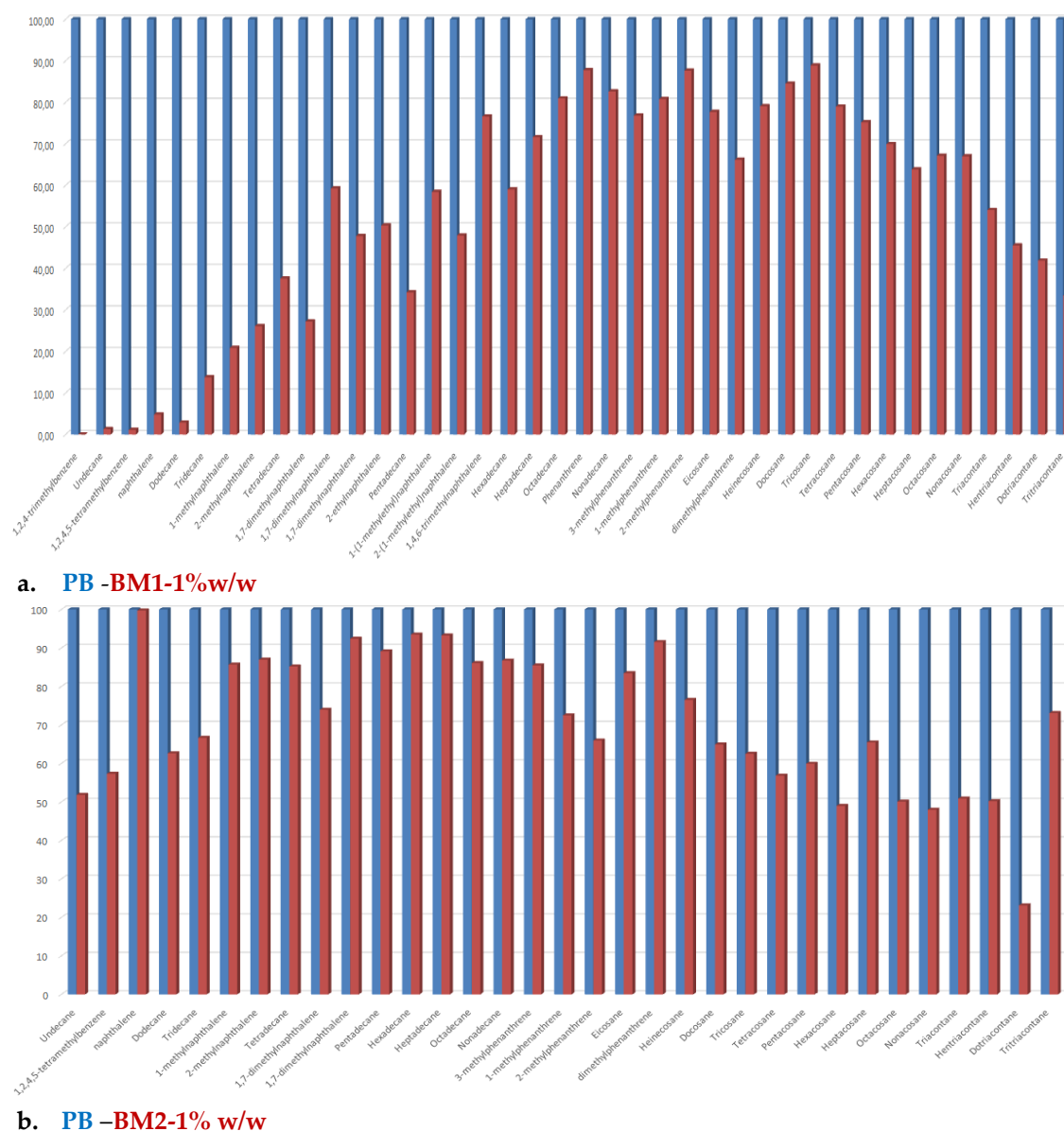


Figure 3. Selectivity of the additives towards the trappings of the chemicals present in the generated fumes of bitumen. 3a) comparison between **PB** and **BM1-1% w/w**, 3b) comparison between **PB** and **BM2-1% w/w**.

In Fig.3, the performances of both additives **AntiSmog1** (Fig.3a) and **AntiSmog2** (Fig.3b) are shown. Responses were normalized taking into account amounts in **PB** as 100% for each analysis. These results highlight the different selectivity of the two additives towards the different chemicals contained in the generated fumes. The additive **BM1** is indeed more efficient in the trapping of the smallest volatile chemicals, present in the released fumes as well as the largest ones, while the additive **BM2** is more active towards the middle-size chemicals. These results confirm that the performance of the additives strongly depends on the porosity of the mesoporous silica. Thus, both additives display complementary behavior in trapping volatile chemicals avoiding their release into the fumes emitted during bitumen processing. This behavior must be correlated to the difference in the porosity of the two additives. The gas molecules passively approach the mesoporous silica surface and by slow diffusion are physically absorbed and entrapped within the pores through van der Waals

forces (dipole-dipole interactions and London dispersion forces). Hence, the difference in pore diameter between the two additives used could explain their difference in selectivity towards specific molecules.

In order to check the integrity of physico-chemical properties of the bitumen upon addition of **BM1** and **BM2**, DSR studies were performed. Remarkably, the rheological properties of the bitumen upon increase of additive 1 and 2, up to 5 % w/w are maintained. As an example, we report data for **AntiSmog 1** (**AntiSmog 2** showed similar rheological behavior). No significant difference has indeed been observed among samples. In the next graphs is possible to observe that the rheological curves obtained at low (25°C to -30°C) and high (25°C to 80°C) temperature range for the samples prepared with additive 1 are comparable with the ones obtained for the **PB** and results are reported in Fig. 4^{28,29}.

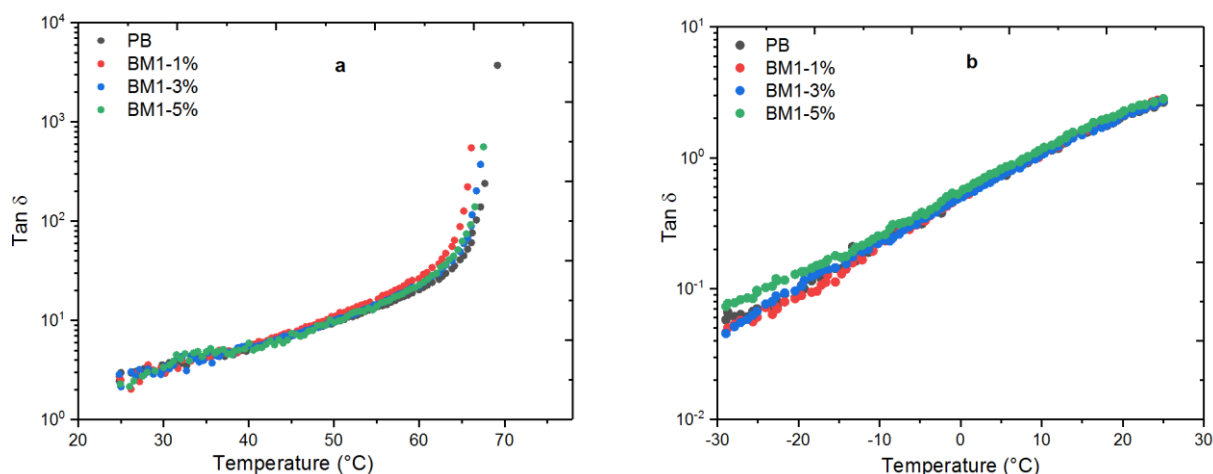


Figure 4. Rheological properties of pristine bitumen and Additive 1 containing mixtures. a) high temperature range (25°C to 80°C), b) low temperature range (25°C to -30°C).

Finally, the possible sedimentation phenomenon induced by additives was checked by Tuben Tests. The investigation method was performed according to the EN-13399 standard (Standard Practice for Determining the Separation Tendency of Polymer from Polymer Modified Asphalt)^{23,30}. Indeed, bitumen, being a soft material, can present a risk of sedimentation when additives in powder are added to it.

Both additives do not present sedimentation phenomena as can be observed as an example for

AntiSmog 1 at various concentrations. Indeed, the sedimentation tests were done at three different concentrations (1%, 3% and 5% w/w). The transition temperature of each sample was determined through DSR^{31,32} and the results between the upper part and the downer part of the examined mixtures were compared and presented in Tab.3. Noteworthy in our case, none of the samples containing additives show sedimentation during the time of the experiment, indeed, no significant difference in temperature were registered between the different observed parts.

Table 3. Temperature difference between upper and downer parts of the sedimentation tubes.

Sample	$\Delta(^{\circ}\text{C})$
BM1-1% w/w	1,1
BM1-3% w/w	0,3
BM1-5% w/w	0,5

Conclusions

This article presents the performance of the new additives to reduce the fumes generated during the processing of Asphalt concrete. The thermogravimetric studies showed the efficiency of additives towards the trapping of toxic volatile chemicals contained in bitumen, while the GC-MS analysis allowed identifying the compounds more specifically trapped by the additives highlighting the different molecular selectivity between them.

DSR studies allows checking the integrity of the physicochemical properties of the resulting mixture and DSR measurements were also employed to check eventual sedimentation phenomena that could occur upon addition of the selected additives.

Patents

An Italian patent has been filed on April, 21, 2016 (#102016000041219), untitled "ANTIFUMO PER BITUME E SUOI DERIVATI" Inventors: Giuseppe Antonio Ranieri, Cesare Oliviero Rossi, Paolino Caputo, Nicolas Godbert, Andrea Pagliuso, Haris Kaljaca. Applicant: University of Calabria, Italy and Kimical s.r.l.

References

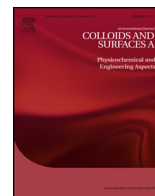
- 1- M.W. Bardeesi, Y. Attallah, Economic and environmental considerations for pavement management systems, *European Scientific Journal*, **2015**, 11, No.29.
- 2- K.J. Kowalski, J. Król, P. Radziszewski, R. Casado, V. Blanco, D. Pérez, V.M. Viñas, Y. Brijisse, M. Frosch, D.M. Le, M. Wayman, Eco-friendly materials for a new concept of asphalt pavement, *Transportation Research Procedia*, **2016**, 14, 3582-3591.
- 3- B. Peng, C. Cai, G. Yin, W. Li, Y. Zhan, Evaluation system for CO2 emission of hot asphalt mixture, *Journal of Traffic and Transportation Engineering (English edition)*, **2015**, 2 (2): 116 - 124.
- 4- P.Q Cui, S.P. Wu, Y. Xiao, M. Wan, P.D. Cui. Inhibiting Effect of Layered Double Hydroxides on the Emissions of Volatile Organic Compounds from Bituminous Materials, *Journal of Cleaner Production*, **2015**, 108, 987-991.
- 5- P.Q. Cui, S.P. Wu, Y. Xiao, H.H. Zhang. Study on the deteriorations of bituminous binder resulted from volatile organic compounds emissions, *Construction and Building Materials*, **2014**, 68, 644-649.
- 6- C. Oliviero Rossi, P. Caputo, G. De Luca, L. Maiuolo, S. Eskandarsefat, C. Sangiorgi, 1H-NMR Spectroscopy: A Possible Approach to Advanced Bitumen Characterization for Industrial and Paving Applications, *Applied Science*, **2018**, 8, 229.
- 7- L. Gate, C. Langlais, J.C. Micillino, H. Nunge, M.C. Bottin, R. Wrobel, S. Binet, Bitumen fume-induced gene expression profile in rat lung, *Toxicology and Applied Pharmacology*, **2006**, 215, 83-92.
- 8- Fall 12-17-2010 Effects of Warm-mix Asphalt Additives on Asphalt Mixture Characteristics and Pavement Performance Jun Zhang University of Nebraska-Lincoln, junzhangnj126@huskers.unl.edu.
- 9- Y. Xiao, M. Wan, K.J. Jenkins, S.P. Wu, P.Q. Cui. Using Activated Carbon to Reduce the Volatile Organic Compounds from Bituminous Materials, *Journal of Materials in Civil Engineering*, **2017**, 29(10), P: 04017166.
- 10- P.Q Cui, H.G. Zhou, C. Li, S.P. Wu, Y. Xiao. Characteristics of Using Layered Double Hydroxides to Reduce the VOCs from Bituminous Materials, *Construction and Building Materials*, **2016**, 123, 69-77.
- 11- M. Posniak, Polycyclic Aromatic Hydrocarbons in the Occupational Environment during Exposure to Bitumen Fumes, *Polish Journal of Environmental Studies*, **2005**, 14(6), 809-815.
- 12- M. Hasanzadeh, N. Shadjou, M. de la Guardia, M. Eskandani, P. Sheikhzadeh, Mesoporous silica-based materials for use in biosensors, *Trends in Analytical Chemistry*, **2012**, 33, 117-129.
- 13- R. Narayan, U.Y. Nayak, A.M. Raichur, S. Garg, Mesoporous silica nanoparticles: A comprehensive review on the synthesis and recent advances, *Pharmaceutics*, **2018**, 10, 118; doi:10.3390.
- 14- M. Manzano, M. Vallet-Regí, Mesoporous silica nanoparticles in nanomedicine applications, *Journal of Materials Science: Materials in Medicine*, **2018**, 29(5), 65.
- 15- Y. Song, Y. Li, Q. Xu, Z. Liu, Mesoporous silica nanoparticles for stimuli-responsive controlled drug delivery: Advances, challenges, and outlook, *International Journal of Nanomedicine*, **2017**, 12, 87-110.
- 16- P.N. Diagboya, E.D. Dikio, Silica-based mesoporous materials; emerging designer adsorbents for aqueous pollutants removal and water treatment, *Microporous and Mesoporous Materials*, **2018**, 266, 252-267.
- 17- P. Cheyssac, M. Klotz, E. Søndergård, Optical properties of ordered mesoporous layers of silica, *Thin Solid Films*, **2006**, 495(1-2), 237-242.
- 18- J. Miguel, J. Mateos, L.C. Quintero, C. Rial, Characterization of petroleum bitumens and their fractions by thermogravimetric analysis and differential scanning calorimetry, *Fuel*, **1996**, 75(15), 1691-1700.
- 19- G. Boczkaj, A. Przyjazny, M. Kamin, Characteristics of volatile organic compounds emission profiles from hot road bitumens, *Chemosphere*, **2014**, 107, 23-30.

- 20- L.T. Gibson, Mesosilica Materials and Organic Pollutant Adsorption: Part A Removal from Air, *Chemical Society Reviews*, **2014**, 43, 5163-5172.
- 21- H. A. Barnes, J. F. Hutton, Walters, K. An introduction to rheology, Elsevier Science, **1989**, 198.
- 22- C. Oliviero Rossi, P. Caputo, V. Loise, D. Miriello, B. Teltayev, R. Angelico, Role of a food grade additive in the high temperature performance of modified bitumens, *Colloids and Surfaces A: Physicochem. Eng. Aspects*, **2017**, 592, 618-624.
- 23- E.I. Szerb, I. Nicotera, B. Teltayev, R. Vaiana, C. Oliviero Rossi, Highly stable surfactant-crumb rubber-modified bitumen: NMR and rheological investigation, *Road Materials and Pavement Design*, **2017**, 19(5), 1192-1202.
- 24- S.S. Idris, N.A. Rahman, K. Ismail, A.B. Alias, Z.A. Rashid, M.J. Aris, Investigation on thermochemical behaviour of low rank Malaysian coal, oil palm biomass and their blends during pyrolysis via thermogravimetric analysis (TGA), *Bioresource Technology*, **2010**, 101, 4584-4592.
- 25- R.E. Zacharia, S.L. Simon, Dynamic and Isothermal Thermogravimetric Analysis of a Polycyanurate Thermosetting System, *Polymer engineering and science*, **1998**, 38(4), 566-572.
- 26- Determination by Solid-phase Micro-extraction/Gas Chromatography/Mass Spectrometry of Polycyclic Aromatic Hydrocarbons in Bitumen Fumes During Road Paving, *J. Mass Spectrom*, **1999**, 34, 1383-1384.
- 27- A. Bouaid, L. Ramos, M.J. Gonzalez, P. Fernández, C. Càmara, Solid-phase microextraction method for the determination of atrazine and four organophosphorus pesticides in soil samples by gas chromatography, *Journal of Chromatography A*, **2001**, 939, 13-21.
- 28- N. Baldino, D. Gabriele, C. Oliviero Rossi, L. Seta, F.R. Lupi, P. Caputo, Low temperature rheology of polyphosphoric acid (PPA) added bitumen, *Construction and Building Materials*, **2012**, 36, 592-596.
- 29- N. Baldino, D. Gabriele, F.R. Lupi, C. Oliviero Rossi, P. Caputo, T. Falvo, Rheological effects on bitumen of polyphosphoric acid (PPA) addition, *Construction and Building Materials*, **2013**, 40, 397-404.
- 30- G. Polacco, S. Berlincioni, D. Biondi, J. Stastna, L. Zanzotto, Asphalt modification with different polyethylene-based polymers, *European Polymer Journal*, **2005**, 41, 2831-2844.
- 31- C. Oliviero Rossi, A. Spadafora, B. Teltayev, G. Izmailova, Y. Amerbayev, V. Bortolotti, Polymer modified bitumen: Rheological properties and structural characterization, *Colloids and Surfaces. A, Physicochemical and Engineering aspects*, **2015**, 480, 390-397.
- 32- F.J. Navarro, P. Partal, F.J. X Martinez-Boza, C. Gallegos, Influence of processing conditions on the rheological behavior of crumb tire rubber-modified Bitumen, *Journal of Applied Polymer Science*, **2007**, 104, 1683-1691.



Contents lists available at ScienceDirect

Colloids and Surfaces A: Physicochemical and Engineering Aspects

journal homepage: www.elsevier.com/locate/colsurfa

Role of a food grade additive in the high temperature performance of modified bitumens



Cesare Oliviero Rossi^{a,*}, Paolino Caputo^a, Valeria Loise^a, Domenico Miriello^b, Bagdat Teltayev^c, Ruggero Angelico^{d,*}

^a Department of Chemistry and Chemical Technologies, University of Calabria, 87036, Arcavacata di Rende (CS), Italy

^b Department of Biology, Ecology and Earth Sciences, University of Calabria, 87036, Arcavacata di Rende (CS), Italy

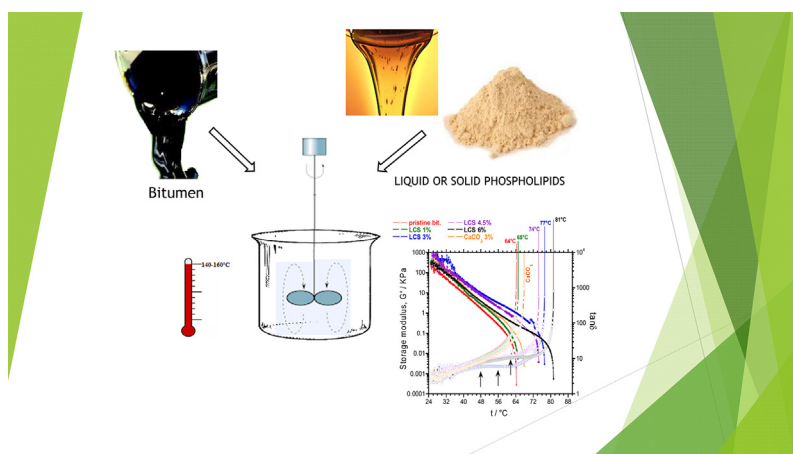
^c Kazakhstan Highway Research Institute, Nurpeisova Str., 2A, Almaty, 050061, Kazakhstan

^d Department of Agricultural, Environmental and Food Sciences (DIAAA), University of Molise, Via De Sanctis, 86100, Campobasso, CB, Italy

HIGHLIGHTS

- We investigate the effects of phospholipids on the structure of the bitumen.
- We examine the interface of modified bitumen/stone.
- We performed Rheological characterization of phospholipids modified bitumen.

GRAPHICAL ABSTRACT



ARTICLE INFO

Article history:

Received 4 November 2016

Received in revised form 9 January 2017

Accepted 10 January 2017

Available online 16 January 2017

Keywords:

Modified bitumen

Phospholipids

Quantitative performance evaluation

Rheology

Contact angle measurements

ABSTRACT

A good adhesion between bitumen, the common binder used in the construction of pavements, and mineral aggregates is a key property for optimal performance of the road paving material (asphalt). Moreover, as bituminous material is viscoelastic in nature, an improvement of its mechanical response does represent an equally important factor in the design of roads. To date, a variety of chemical compounds has been tested as bitumen modifiers and evaluated in their capacity to improve the adhesion of binder to the aggregates and promote an increase of the bitumen softening point, especially in warm ambient conditions. This contribution explores, for the first time, the potentialities of a class of lipophilic food grade additives, i.e., non-toxic and eco-friendly biocompatible compounds, acting both as adhesion promoters and as rheological modifiers. Their effects on the high temperature mechanical performance of a tested bitumen have been investigated through time cure rheological measurements and the sol-transition

* Corresponding authors.

E-mail addresses: cesare.oliviero@unical.it (C. Oliviero Rossi), angelico@unimol.it (R. Angelico).

temperature determined in a wide range of temperatures. Measurements of the contact angle between the aggregate surface and modified bitumens preventively blended with increasing amounts of food grade additives were also carried out. We believe that those results could provide an alternative opportunity to use additives from natural resources in the design of sustainable and much more performant asphalts.

© 2017 Elsevier B.V. All rights reserved.

1. Introduction

Bitumen is widely used as a binder for asphalt mixes in the construction of pavements throughout the world. The term “asphalt” denotes a semi-solid mixture of crushed stone materials, sand, filler and bitumen, which is commonly used as a road paving material [1]. Bitumen, which is a complex solid or semisolid colloidal dispersion of asphaltenes in a continuous oily phase of saturated paraffins, aromatics and resins [2–4] is a viscoelastic material whose mechanical response is both time and temperature dependent [5]. However, because of the wide variation in geographical and climatic conditions, a careful selection of asphalt materials is required to increase the useful life of the pavement and reduce the huge cost of road maintenance. The following failure modes have been identified for asphalt pavement: rutting, fatigue, moisture damage, and thermal cracking [6–8]. Rutting is the term used for the permanent deformation of a pavement surface, which happens at high temperatures during summer when the asphalt is softer [9,10]. Therefore, the increased demand for high performance and durable asphalt mixes has prompted the development of various additives and new modified bitumens. Structural modification can be achieved by adding directly at the bitumen poly-function materials capable of influencing more properties in the mix, such as mechanical modulus [11], adhesion [12], temperature of melting [13], durability, workability etc. They belong to various chemical classes such as polymers, fibers, waxes, anti-stripping agents etc. and can be tailor-made for a specific application. One group of additives used as asphalt modifiers are polymeric materials. These elastomeric materials, when they are stretched, will largely return to their original shape after the load is removed. Examples of these polymers are styrene-butadiene rubber latex (SBR), diblock styrene-butadiene (SB) and triblock styrene-butadiene-styrene (SBS). The use of crumb rubber from worn-out tires can be considered as polymer-modified bitumen [14]. The benefits of using these polymers in asphalt binders is again the mitigation of permanent deformation or rutting of asphalt binders and further a reduction in fatigue and thermal cracking distress. The use of thermoplastic polymers such as polyethylene (often the low-density polyethylene, which is identified as LDPE), ethylene-vinyl-acetate (EVA), and ethylene-acrylate (EA) must be also mentioned [15]. Those polymers are used to decrease permanent deformation or rutting in asphalt pavements. However, asphalt workability drops rapidly when using EVA in asphalt at cold ambient conditions. This is due to hardening of the EVA-modified bitumen because of EVA polymer crystallization [16]. Other commercial additives are proprietary whose composition is variable; traditionally they mostly contain either nitrogen groups such as fatty polyamines, or phosphate groups [17,18]. Acid modification such as polyphosphoric acid (PPA) has recently been a common approach to modify asphalt [19,20]. PPA is basically used to increase the softening point of a binder and to lower the penetration value. PPA has also found increasing use to raise the grading range typically at high temperature, but depending on the source of crude oil, it may have a negative effect on long-term fatigue performance [21].

A class of compounds that contain both ammine and phosphate chemical residues can be represented by natural phospholipids

such as, e.g., phosphatidyl choline, phosphatidyl inositol, phosphatidyl ethanolamine, and phosphatidic acid [22–24]. They can be efficiently dissolved in hydrocarbons due to their significant lipophilic properties [25–27]. Motivated by the demanding need to seek environmental friendly low cost and non-toxic compounds, we tested commercial food grade phospholipids as additives to bitumen and their effect on the high temperature mechanical performance, which should be taken into special consideration particularly if the binder is intended for use under warm climatic conditions. We expect that phospholipids based food grade additives can act as both modifiers to improve the asphalt concrete mechanical properties as well as adhesive promoters to enhance the adhesion efficiency of the binder onto aggregate surfaces. For this purpose, time cure rheological measurements have been performed to determine the sol-transition temperature of modified bitumens. In the present contribution, we illustrate also experimental results based on the determination of the contact angle between the aggregate surface and modified binders blended with increasing amounts of phospholipids [28]. Indeed, previous investigations demonstrated the feasibility of the contact angle method to test the bitumen adhesion capacity and provided results in agreement with usual empirical standard methods [29,30] such as, e.g., the boiling water test (Riedel-and-Wieber test) [31]. Therefore, according to the protocol described in ref. [12], a relative decrease of the contact angle between modified bitumen and aggregate surface (better wettability) can be correlated to the efficiency of phospholipids as adhesion promoters.

Finally, since adhesion between asphalt and aggregate is affected by mineralogy (rock chemical composition) [32,33], Scanning Electron Microscopy with energy-dispersive X-ray Spectroscopic Microanalysis (SEM-EDS), X-ray Powder Diffraction (XRPD) and polarized light microscopy, were carried out in order to characterize the mineralogical and chemical composition of a tested aggregate (crushed rock).

2. Materials and methods

2.1. Materials

The bitumen was kindly supplied by Loprete Costruzioni Stradali (Italy) and was used as fresh standard. It was produced in Italy and the crude oil was from Saudi Arabia. Its penetration grade (50/70) was measured by the usual standardized procedure [34] in which a standard needle is loaded with a weight of 100 g and the length traveled into the bitumen specimen is measured in tenths of a millimeter for a known time, at fixed temperature. The bitumen was modified by adding commercial phospholipids provided by Somercom srl (Catania (CT), Italy), namely, a) phospholipids in form of light yellow powder (hereafter LCS) and b) phospholipids in form of amber-yellow viscous liquid (hereafter LCL). According to product data sheets, they were mixtures of non-polar (triglycerides) and polar- (phospho- and glycol-) lipids with small amounts of carbohydrates. As inert filler, calcium carbonate CaCO_3 was also tested for comparison. All detailed information on those compounds were proprietary and unavailable to the investigators.

Table 1
XRPD analysis of the aggregate (sample PT) used as tested stone material. In order of decreasing abundance: quartz (Qtz); plagioclase (Pl); Orthoclase (Or); biotite (Bt); chlorite (Chl).

Sample	Max. (-----) Min.				
PT	Qtz	Pl	Or	Bt	Chl

An acidic stone chosen as tested stone material, was kindly furnished by the company “Porfido Trentino SRL” (Albiano, Northern Italy); the rock sample (commercial name: “Porfido del Trentino”) will be abbreviated hereafter with the term “sample PT”.

2.2. Sample preparation

Both LCS and LCL additives were mixed separately to hot bitumen (140–160 °C) in the following wt% ratios: 1, 3, 4.5 and 6.

The bitumen was modified by using a mechanical stirrer (IKA RW20, Germany). Firstly, 100 g of bitumen was heated up to 140–160 °C until it flowed fully, then a given amount of additive was added to the melted bitumen under a high-speed shear mixer of 500–700 rpm. Furthermore, the mixture was stirred again at 140–160 °C for 30 min. After mixing, the resulting bitumen was poured into a small sealed can and then stored in a dark chamber thermostated at 25 °C to retain the obtained morphology.

2.3. S.A.R.A. determination

The Iatroskan MK 5 Thin Layer Chromatography (TLC) was used for the chemical characterization of bitumen by separating it into four fractions: Saturates, Aromatics, Resins and Asphaltenes (S.A.R.A.) [35]. During the measurement, the separation took place on the surface of silica-coated rods. The detection of the amount of different groups were according to the flame ionization. The sample was dissolved in peroxide-free tetrahydrofuran solvent to reach a 2% (w/v) solution. Saturated components of the sample were developed in *n*-heptane solvent while the aromatics in a 4:1 mixture of toluene and *n*-heptane. Afterwards, the rods had to be dipped into a third tank, which was a 95–5% mixture of dichloromethane and methanol. That organic medium proved suitable to develop the resin fraction whereas the asphaltene fraction was left on the lower end of the rods. Details of bitumen composition were listed in Table 3.

2.4. Empirical characterization

Penetration tests for bitumens were performed according to the standard procedure (ASTM D946) [36]. The bitumen consistency was evaluated by measuring the penetration depth (531/2-T101, Tecnotest, Italy) of a stainless steel needle of standard dimensions under determinate charge conditions (100 g), time (5 s) and temperature (25 °C).

2.4.1. Boiling tests

Boiling tests were performed on aggregates with size ranging from 8 mm to 12 mm. The aggregate is a stone having acid chemical nature (quartz porphyry). The boiling test procedure used in this study was according to ASTM D3625 [31]. In particular, the sample was placed in boiling water for 10 min and then cooled to room temperature; the water decanted and the sample let dry on

Table 2
Chemical composition of the powdered aggregate (sample PT) by SEM-EDS analysis; LOI: Loss on ignition.

%wt	SiO ₂	TiO ₂	Al ₂ O ₃	Fe ₂ O ₃	MnO	MgO	CaO	Na ₂ O	K ₂ O	P ₂ O ₅	LOI	Sum
PT	70.04	0.54	13.35	3.60	0.25	0.58	1.11	3.00	5.89	0.16	1.49	100.00

a paper towel. The degree of bitumen coverage in% was rated by visual observation. A lighted magnifying glass was used to examine samples. The average of the ratings was rounded to the nearest 5% (see Table 4).

2.5. Rheological characterization

Rheological tests on bitumen samples were carried out using a controlled shear stress rheometer (SR5, Rheometric Scientific, USA) equipped with a parallel plate geometry (gap 2.0 ± 0.1 mm, diameter 25 mm for the samples analyzed within the temperature range 20–150 °C) and a Peltier system (±0.1 °C) for temperature control. Bitumen exhibits aspects of both elastic and viscous behaviours and is thus called visco-elastic material. The Dynamic Shear Rheometer (DSR) is a common tool used to study the rheology of asphalt binders at high and intermediate temperatures. Operatively, a bitumen sample is sandwiched between two parallel plates, one standing and one oscillatory. The oscillating plate is rotated accordingly with the sample and the resulting shear stress is measured. The linear viscoelastic regime of both pristine and modified bitumen was checked through the determination of the complex shear modulus G^* in the regime of small-amplitude oscillatory shear [26,37,38]. The complex modulus can be divided into two components, a real part and imaginary part [32]:

$$G^* = G'(\omega) + i G''(\omega)$$

The frequency dependent functions $G'(\omega)$ and $G''(\omega)$ are the in-phase (storage) modulus and the out-of-phase (loss) modulus, respectively, being i the imaginary unit of the complex number. $G'(\omega)$ is a measure of the reversible, elastic energy, while $G''(\omega)$ represents the irreversible viscous dissipation of the mechanical energy [39]. Both the storage and loss moduli are related to each other through the phase angle δ defined by:

$$\tan\delta = G''(\omega)/G'(\omega)$$

Aimed at investigating the material phase transition, temperature sweep tests were performed at 10 Hz increasing temperature from 25 °C to 130 °C at 1 °C/min and applying the proper stress values to guarantee linear viscoelastic conditions at all tested temperatures. The adopted heating rate was a suitable compromise between the experimental times and an acceptable accuracy of data.

2.6. Chemical and mineralogical analysis of the aggregate

The petrographic analysis of the aggregate chosen as tested stone material (sample PT), was performed by polarized light microscopy with a Zeiss-Axioskop 40 microscope. The qualitative mineralogical composition of the aggregate was studied using a Bruker D8 Advance X-ray powder diffractometer (XRPD) with Cu-K α radiation, operating at 40 kV and 40 mA. Powder diffraction data were collected in the range 3–60° 2 θ in steps of 0.02° 2 θ (step time 0.4 s). The EVA software program (DIFFRACplus EVA) was used to identify the mineral phases in each X-ray powder spectrum, by comparing experimental peaks with PDF2 reference patterns. The major chemical composition of the sample PT was performed on pressed powder by scanning electron microscopy with energy-dispersive X-ray spectroscopic microanalyses (SEM-EDS), using a FEI Quanta 200 instrument equipped with an EDAX Si with Li detector (see Tables 1 and 2).

Table 3
Group composition of the pristine bitumen.

SAMPLE	Area% (± 0.1)
Saturated	3.8
Aromatics	51.3
ResinsAsphaltenes	21.5 23.4

Table 4
Percentage of bitumen coating retained (boiling test) for both pristine and modified bitumens.

Sample	% coating after boiling ± 5
Pristine bitumen	<5%
Bitumen + 1% LCS	80%
Bitumen + 3% LCS	75%
Bitumen + 1% LCL	90%
Bitumen + 3% LCL	85%

2.7. Contact angle measurements

Measurements of contact angle between binder and aggregate surface were performed by using an automated pendant drop tensiometer (FTA200, First Ten Angstroms, USA) equipped with the *fta32 v2.0* software. Details of this apparatus are given by Biresaw et al. [40].

Contact angles were measured by fitting a mathematical expression to the shape of the drop and then calculating the slope of the tangent to the drop at the liquid-solid-vapor (LSV) interface line.

The instrument comprises an automated pump that can be fitted with various sizes of syringes and needles to allow for software control of pendant drop formation and of sinusoidal variations in the drop volume or surface area.

All experiments were carried out at room temperature (22 ± 1 °C). Briefly, three drops of each sample, either pristine or modified hot bitumen (150 °C), were laid with the help of a needle on the inert stones, which were previously cut to obtain a smooth surface, washed with water and left to dry at r.t. for 24 h (step 1). Then, samples were kept for 10 min at a temperature 25–30 °C higher than the softening point of bitumen determined through the Ring-and-Ball Test, R&B [41] (step 2).

Finally, the very same samples were immersed in distilled water for 2 h at a temperature 5 °C lower than the R&B of bitumen (step 3).

Contact angle data averaged over three measurements each sample, have been collected in Table 5 as differences between measurements carried out after step 3 and step 2, respectively, ($\Delta \text{angle} = \text{angle}_{\text{step3}} - \text{angle}_{\text{step2}}$).

3. Results and discussion

The mineralogical composition of the crushed stone used for the boiling tests was confirmed by the petrographic study in thin section (see Table 1). The minerals present in the sample, in order of decreasing abundance, were quartz (Qtz), plagioclase (Pl), orthoclase (Or), biotite (Bt) and chlorite (Chl). The sample PT was a magmatic acid effusive rock with porphyritic structure and anisotropic texture. The matrix was microcrystalline. In the sample were present, as phenocrysts, the same minerals detected by XRPD analysis; in addition to the previous minerals, it was possible to observe also opaque minerals. Quartz was the most abundant mineral (Fig. 1a). The plagioclase appeared altered to sericite (Fig. 1b) and the orthoclase was strongly kaolinized. Its chemical (Table 2) and petrographic composition allowed to classify the rock as a rhyolitic ignimbrite.

Bitumen was characterized by the SARA method and four different groups were individuated: Saturates, Aromatics, Resins and

Asphaltenes (SARA). We recall here that according to the current accepted colloidal model for bitumen, asphaltene molecules rich in resins as peptizing agents self-assembly into micellar-like structures dispersed into the continuous phase composed mainly by the saturate and aromatic oil fractions (maltene) [42–44].

The SARA content of the pristine bitumen was determined (See Materials and Methods) and the results are shown in Table 3.

Then, the adhesion efficiency of the binder onto aggregate surfaces was determined by boiling water tests according to ASTM D3625 [31], and the results compared to contact angle measurements [28,30].

The boiling water test is an empirical method useful to evaluate the asphalt resistance against water penetration. This qualitative test provides a subjective evaluation of the stripping, which represents fundamentally the loss of adhesion between the asphalt and aggregate. Operatively, the inert stone was coated either with pristine bitumen as a reference or with bitumen mixed with increasing amount of LCS (LCL) within the range 1–3 wt%.

Table 4 collects the percentage of asphalt coating retained (% of bitumen coverage onto inert stones after immersion in boiling water) for pristine bitumen and bitumen mixed with either powdery phospholipids (LCS) or liquid mixture of phospholipids (LCL).

However, in order to decrease the error limits of the boiling water test, recent investigations demonstrated the feasibility of modern surface analysis techniques such as the contact angle method, to obtain a quantitative and more accurate evaluation of the bitumen adhesion capacity [12,30].

Since an efficient wettability is correlated with lower contact angles, a remarkable decrease of contact angle difference (Δangle) could be observed in correspondence of bitumen samples pre-mixed with either LCS 3 wt% (12.8°) and even lower with LCL 3 wt% (2.7°) compared to pristine bitumen (35.3°). The latter was almost unaffected by addition of 1 wt% of both types of additives (see Table 5). We deduce that a minimum amount of LCL (3 wt%) can result very efficient in lowering the interfacial energy between the aggregate and the binder. Presumably, higher amounts of LCL would provide similar results of the contact angle as a typical property played by an efficient adhesion promoter. Therefore it can be argued that the adhesive bond at bitumen-aggregate interface may be favored by the better dispersivity provided by the food grade emulsifier added in its liquid form. A similar effect, though less pronounced, can be also detected for bitumen modified with phospholipids added in form of solid powder.

Concerning the mechanical behaviour, an understanding of the rheological properties of asphalt binders is essential for predicting the end-use performance of these materials [45]. Materials that are able to return to their original shape after the removal of stress are known as elastic materials.

The stress-strain behaviour of these materials are time-dependent and are characterized by their elastic G' and viscous G'' moduli. On the contrary, some materials dissipate the input energy, which leads to permanent deformation.

Two important parameters are obtained from DSR tests on bitumen: G^* the complex modulus and δ the phase angle. These parameters can be used to characterize both viscous and elastic behaviour of the binder. The dependence of these quantities on the temperature gives rise to the so-called time cures. As the temperature increases or frequency decreases, bitumen begins to lose the majority of its G' behaviour and starts to behave as a viscous fluid. As such, $\tan \delta$ will diverge and G'' becomes dominant. Thus, the limiting temperature in correspondence of which $\tan \delta \rightarrow \infty$ identifies the sol-transition temperature t^* where viscous behaviour is highly predominant over elastic behaviour. Inverting the experimental conditions, as the temperature decreases or the frequency is increased, bitumen will behave like an elastic solid and then

Table 5
Relative contact angles as a function of different percentage of additives.

	Pristine bitumen	Bitumen + 1% LCS	Bitumen + 3% LCS	Bitumen + 1% LCL	Bitumen + 3% LCL
(Δ angle) $\pm 0.1^\circ$	35.3	35.3	12.8	32.5	2.7

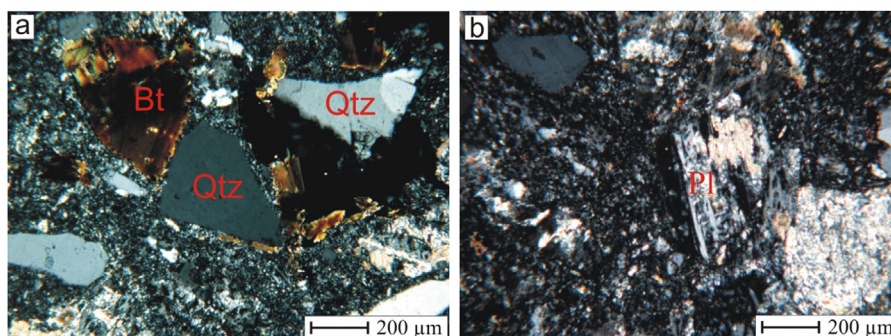


Fig. 1. Micro-photos of the aggregate (sample PT) under crossed polarizers. a) Biotite and quartz inside sample PT; b) Weathered plagioclase inside sample PT.

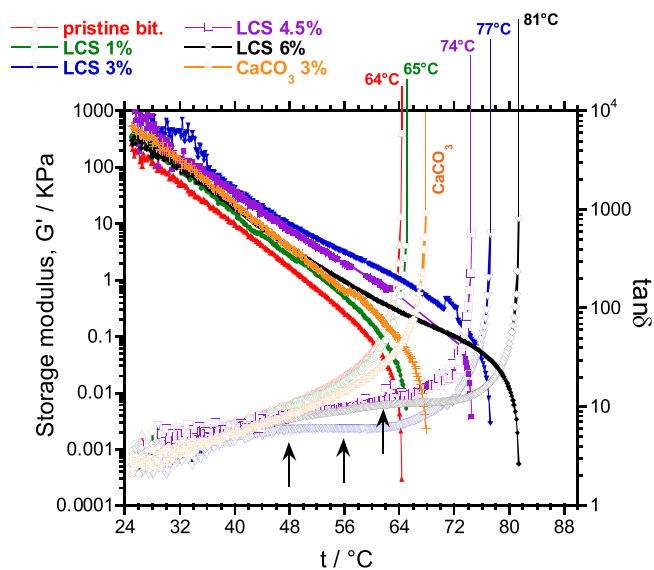


Fig. 2. Semi-log plot of temperature ramp tests for the pristine and modified bitumens formulated with 1–6 wt% of phospholipids added as solid powder dispersion (LCS). The effect of an inert filler CaCO_3 (3 wt%) was also determined. Left axis: storage modulus, G' . Right axis: loss tangent $\tan\delta$, the asymptotic value of which identifies the sol-transition temperature t^* indicated on the topside of the figure. Arrows indicate an extended interval of temperatures wherein $\tan\delta$ is independent of t (see text for details).

$\tan\delta$ will approach zero with G' providing the dominant contribution. Therefore, materials with higher storage moduli have greater ability to recover from deformation, and material with higher loss moduli have greater ability to resist deformation at prescribed frequency.

Fig. 2 illustrates the time cure tests of both the pristine and bitumens modified with LCS, to compare the rheological response of the tested systems. The effect of an inert filler CaCO_3 (3 wt%) was also determined. As a general trend, the loss tangent increased and the storage modulus decreased as the temperature increased.

However, the addition of phospholipids to bitumen in form of solid powder dispersion (LCS) provided a pronounced hardening effect for additive amounts in the range 3–4.5 wt%, manifested by a shift of the sol-transition temperature t^* observed at higher temperature values compared to unmodified bitumen.

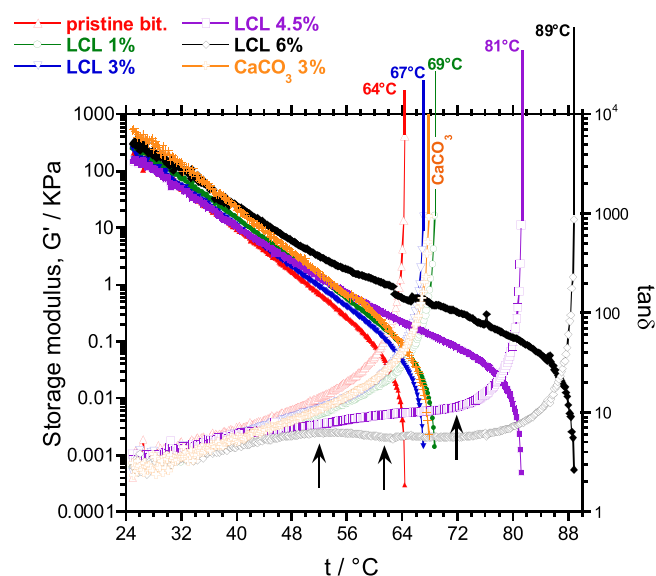


Fig. 3. Semi-log plot of temperature ramp tests for the pristine and modified bitumens formulated with 1–6 wt% of phospholipids added as liquid dispersion (LCL). The effect of an inert filler CaCO_3 (3 wt%) was also determined. Left axis: storage modulus, G' . Right axis: loss tangent $\tan\delta$, the asymptotic value of which identifies the sol-transition temperature t^* indicated on the topside of the figure. Arrows indicate an extended interval of temperatures wherein $\tan\delta$ is independent of t (see text for details).

Time cure curves acquired for unmodified bitumen (both G' and $\tan\delta$) were almost unaffected by the presence of both the inert filler (CaCO_3) and LCS 1 wt%. However, an upward trend of G' curves was observed starting from LCS 3 wt%, which was also reflected by a correspondent flattened behaviour of the loss tangent extending over a wide range of temperature before to diverge toward its limiting value t^* . That peculiar mechanical response may be ascribed to a sort of viscoelastic buffering effect induced above a threshold amount of LCS dispersed into bitumen.

A similar behaviour, though with noticeable differences, was also recorded for bitumen samples modified with phospholipids added in liquid state (LCL). Indeed on heating, t^* was reached at even higher values compared to the LCS modified system and, obviously, to the neat bitumen (see Fig. 3). Here, both the effects of inert filler (CaCO_3) and LCL were found almost coincident in the narrow range 1–3 wt%. Remarkably, a more pronounced increase of t^* was

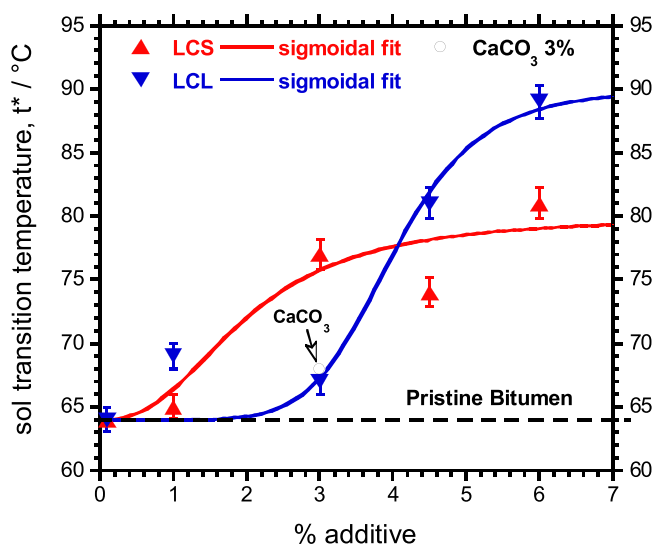


Fig. 4. Sol-transition temperature t^* determined through time cure tests, as a function of phospholipid content (% additive) mixed in form of solid powder dispersion (LCS: upward apex red triangles) or as liquid dispersion (LCL: downward apex blue triangles). t^* for the unmodified bitumen (64°C dashed horizontal line) is shifted to 68°C after addition of the inert filler CaCO_3 (empty circle). Red (LCS) and blue (LCL) solid lines represent the best non-linear fits to equation 1) (see text for details). (For interpretation of the references to colour in this figure legend, the reader is referred to the web version of this article.)

observed for LCL >3 wt% where the correspondent $\tan\delta$ curves (LCL 4.5 and 6 wt%) showed a wide interval of flatness prior to tip up toward the respective sol-transition temperatures.

To better emphasize the differences between LCS and LCL modified systems, the next Fig. 4 illustrates the asymptotic t^* vs additive contents (wt%). Both series of data followed sigmoidal trends as evidenced by the solid curves derived through non-linear fits to the expression:

$$t^* = t_0^* + \frac{t_s^* - t_0^*}{1 + \left(\frac{x}{x_c}\right)^{-\alpha}} \quad (1)$$

Here $t_0^* = 64^\circ\text{C}$ corresponded to the sol-transition temperature of neat bitumen while the saturation temperature value t_s^* , the critical amount of additive x_c and the exponent α were adjustable parameters.

The efficiency as modifier agent could be easily identified in the bitumen samples mixed with LCL rather than with LCS, as evidenced by the steepest increase of t^* connected to the former additive ($t_s^* = 90^\circ\text{C}$, $x_c = 4$ wt%, $\alpha = 7$) in comparison to the latter ($t_s^* = 80^\circ\text{C}$, $x_c = 2$ wt%, $\alpha = 3$). The higher performance of LCL was qualitatively in accord with both the percentage of bitumen coating retained (boiling test, Table 4) and contact angle data (Table 5).

Indeed, the same $\Delta t^* = 17^\circ\text{C}$ as a difference between sol-transition temperatures of neat (64°C) and modified bitumens (81°C), was obtained by adding either 4.5 wt% LCL or 6 wt% LCS, with a reasonable economical convenience in favor of the former. The observed difference between liquid and powdered forms of those food grade additives may be interpreted in term of partial (LCS) and complete (LCL) miscibility of phospholipids in the heterogeneous continuous phase of the binder, which is composed mainly by the saturate and aromatic oil fractions (maltene). However, other physicochemical effects might be also considered, deserving an in-depth investigation in a subsequent study.

4. Conclusions

In this study, we have undertaken a systematic investigation on the effects played by commercial food grade phospholipids used as additives for bitumen, in order to obtain a two-fold benefit of improving the high temperature mechanical properties and enhancing its adhesion efficiency onto mineral aggregate surfaces. From the analysis of boiling tests, contact angle and time cure rheological measurements; we were able to confirm the positive role of phospholipids acting both as adhesion promoters and as rheological modifiers. We also found that bitumen modified with phospholipids added in liquid state (LCL) provided better results than the analogous solid powdered form (LCS). In particular, a minimum amount of LCL 3 wt% has been turned suitable to improve the percentage of bitumen coating retained after boiling and consequently decrease the contact angle between binder and tested stone. Similar results have been obtained for bitumens modified with slightly higher amounts of LCS than LCL. Those differences, confirmed also by time cure rheological tests, have been ascribed to different miscibility properties manifested by both liquid and solid forms of food grade additives, once mixed to the binder. We think that this study could promote an alternative research field devoted to demonstrate the usefulness of natural additives in the formulation of sustainable asphalt pavements.

Acknowledgements

The authors thank the Loprete Costruzioni Stradali SRL (Italy) for supplying the bitumen and Porfido Trentino SRL for furnishing the stone materials.

References

- [1] O.E. Briscoe, *Asphalt Rheology: Relationship to Mixture*, ASTM Spec. Publ. 941, American Society for Testing and Materials, Philadelphia, PA, 1987.
- [2] T.F. Yen, G.V. Chilingarian, *Asphalthenes and Asphalts*, Elsevier, New York, 1994.
- [3] S. Rozeveld, E. Shin, A. Bhurke, L. France, L. Drzal, Network morphology of straight and polymer modified asphalt cements, *Microsc. Res. Technol.* 38 (1997) 529–543.
- [4] D. Lesueur, The colloidal structure of bitumen: consequences on the rheology and on the mechanisms of bitumen modification, *Adv. Colloid Interface Sci.* 145 (2009) 42–82.
- [5] L. Loeber, G. Muller, J. Morel, O. Sutton, Bitumen in colloid science: a chemical, structure and rheological approach, *Fuel* 77 (1998) 1443–1450.
- [6] M.E. Labib, Asphalt-aggregate interactions and mechanisms for water stripping, *Fuel* 37 (1992) 1472–1481.
- [7] T.W. Kennedy, Prevention of water damage in Asphalt in Mixtures, in: B.E. Ruth (Ed.), *Evaluation and Prevention of Water Damage to Asphalt Pavement Materials Asphalt*, American Society for Testing and Materials Philadelphia, PA, USA, 1985, pp. 119–133.
- [8] U. Bagampadde, U. Isacsson, B.M. Kiggundu, Classical and contemporary aspects of stripping in bituminous mixtures *Road Materials and Pavement Design*, vol. 5, 2004, pp. 7–45.
- [9] M. Huurman, L. Mo, M.F. Woldekidan, R.N. Khedoe, J. Moraal, Overview of the LOT meso mechanical research into porous asphalt ravelling *Advanced Testing and Characterization of Bituminous Materials*, vol. 1, CRC Press, Taylor & Francis Group, 2009, pp. 507–517.
- [10] R. Kluttz, E. Jellema, M. Woldekidan, M. Huurman, Highly modified bitumen for prevention of winter damage in OGFCs, in: *Airfield and Highway Pavement*, 2013, pp. 1075–1087, <http://dx.doi.org/10.1061/9780784413005.090>.
- [11] C. Oliviero Rossi, A. Spadafora, B. Teltayev, G. Izmailova, Y. Amerbayev, V. Bortolotti, Polymer modified bitumen: rheological properties and structural characterization, *Colloids Surf. A: Physicochem. Eng. Aspects* 480 (2015) 390–397.
- [12] C. Oliviero Rossi, P. Caputo, N. Baldino, F.R. Lupi, D. Miriello, R. Angelico, Effects of adhesion promoters on the contact angle of bitumen-aggregate interface, *Int. J. Adhes. Adhes.* 70 (2016) 297–303.
- [13] J. Shen, S.N. Amirhanian, F. Xiao, B. Tang, Influence of surface area and size of crumb rubber on high temperature properties of crumb rubber and modified binders, *Constr. Build. Mater.* 23 (2009) 304–310.
- [14] N.S. Mashaan, M.R. Karim, Investigating the rheological properties of crumb rubber modified bitumen and its correlation with temperature susceptibility, *Mater. Res.* 16 (2013) 116–127.

- [15] H.U. Bahia, D. Perdomo, P. Turner, Applicability of Superpave Binder Testing protocols to modified binders, *Transp. Res. Rec.* 1586 (1995) 16–23.
- [16] C.D. Whiteoak, *The Shell Bitumen Handbook*, Shell Bitumen, Surrey, UK, 1990.
- [17] J.O. Levin, K. Andersson, C. Hallgren, Exposure to low molecular polyamines during road paving, *Ann. Occup. Hyg.* 38 (1994) 257–264.
- [18] N.M. Katamine, Phosphate waste in mixtures to improve their deformation, *J. Transp. Eng.* 126 (2000) 382–389.
- [19] N. Baldino, D. Gabriele, C. Oliviero Rossi, L. Seta, F.R. Lupi, P. Caputo, Low temperature rheology of polyphosphoric acid (PPA) added bitumen, *Constr. Build. Mater.* 36 (2012) 592–598.
- [20] F. Xiao, S. Amirkhanian, H. Wang, P. Hao, Rheological property investigations for polymer and polyphosphoric acidmodified asphalt binders at high temperatures, *Constr. Build. Mater.* 64 (2014) 316–323.
- [21] I. Kodrat, D. Sohn, S.A.M. Hesp, Comparison of polyphosphoric acid-modified asphalt binders with straight and polymer-modified materials, *Transp. Res. Rec. J. Transp. Res. Board* 1998 (2007) 47–55.
- [22] D. Liu, F. Ma, Soybean phospholipids, in: D. Krezhova (Ed.), *Recent Trends for Enhancing the Diversity and Quality of Soybean Products*, InTech, 2011, ISBN: 978-953-307-533-4.
- [23] L. Galantini, N.V. Pavel, Collective diffusion and self-diffusion coefficients comparison to separate interactions and micellar size effects on ionic micelle diffusivities: cylindrical micelles of sodium taurodeoxycholate, *J. Chem. Phys.* 118 (2003) 2865–2872.
- [24] L. Galantini, M.C. di Gregorio, M. Gubitosi, L. Travaglini, J.V. Tato, A. Jover, F. Mejjide, V.H. Soto Tellini, N.V. Pavel, Bile salts and derivatives: rigid unconventional amphiphiles as dispersants, carriers and superstructure building blocks, *Curr. Opin. Colloid Interface Sci.* 20 (2015) 170–182.
- [25] R. Angelico, C. Oliviero Rossi, L. Ambrosone, G. Palazzo, K. Mortensen, U. Olsson, Ordering fluctuation in a shear-banding wormlike micellar system, *Phys. Chem. Chem. Phys.* 12 (2010) 8856–8862.
- [26] R. Angelico, S. Amin, M. Monduzzi, S. Murgia, U. Olsson, G. Palazzo, Impact of branching on the wormlike micelles viscoelasticity, *Soft Matter* 8 (2012) 10941–10949.
- [27] R. Angelico, L. Gentile, G.A. Ranieri, C. Oliviero Rossi, Flow induced structures observed in a viscoelastic reverse wormlike micellar system by magnetic resonance imaging and NMR velocimetry, *RSC Adv.* 6 (2016) 33339–33347.
- [28] D.Y. Kwok, A.W. Neumann, Contact angle measurements and criteria for surface energetic interpretation Contact Angle Wettability and Adhesion, vol. 3, 2003, pp. 117–159.
- [29] Q.-Y. Xiao, L.-Y. Wei, A precise evaluation method for adhesion of asphalt aggregate, *Int. J. Pavement Res. Technol.* 2 (2009) 270–274.
- [30] C. Oliviero Rossi, P. Caputo, N. Baldino, E.I. Szerb, B. Teltayev, Quantitative evaluation of organosilane-based adhesion promoter effect on bitumen-aggregate bond by contact angle test, *Int. J. Adhes. Adhes.* 72 (2017) 117–122.
- [31] American Society for Testing and Materials, Standard Practice for Effect of Water on Bituminous-Coated Aggregate Using Boiling Water ASTM D3625 96 (2005).
- [32] G.C. Hurley, B.D. Prowell, Evaluation of potential processes for use in warm asphalt mixes, *J. Assoc. Asphalt Paving Technol.* 75 (2006) 41–85.
- [33] R. Karlsson, U. Isacson, Material-related aspects of asphalt recycling, state-of-the-art, *J. Mater. Civil Eng.* 18 (2006) 81–92.
- [34] J. Read, D. Whiteoak, in: R.N. Hunter (Ed.), *The Shell Bitumen Handbook*, fifth edition, Thomas Telford Publishing, London, 2003.
- [35] S. Yoon, S. Durgashanker Bhatt, W. Lee, H.Y. Lee, S.Y. Jeong, J.-O. Baeg, C. Wee Lee, Separation and characterization of bitumen from Athabasca oil sand, *Korean J. Chem. Eng.* 26 (2009) 64–71.
- [36] ASTM Standard, Standard for Penetration-Graded Asphalt Cement for Use in Pavement Construction, D946-82, ASTM International, West Conshohocken, PA, 2005.
- [37] F.E. Antunes, L. Coppola, D. Gaudio, I. Nicotera, C. Oliviero, Shear rheology and phase behaviour of sodium oleate/water mixtures colloids and surfaces A: Physicochemical and engineering aspects colloids and surfaces A: Physicochemical and engineering, *Phys. Chem. Chem. Phys.* 297 (2004) 95–104.
- [38] R. Angelico, M. Carboni, S. Lampis, J. Schmidt, Y. Talmon, M. Monduzzi, S. Murgia, Physicochemical and rheological properties of a novel monoolein-based vesicle gel, *Soft Matter* 9 (2013) 921–928.
- [39] L. Coppola, L. Gentile, I. Nicotera, C. Oliviero Rossi, G.A. Ranieri, Evidence of formation of ammonium perfluorononanoate/2H₂O multilamellar vesicles: Morphological analysis by rheology and rheo-2H NMR experiments, *Langmuir* 26 (2010) 19060–19065.
- [40] G. Biresaw, Z.S. Liu, S.Z. Erhan Investigation of the surface properties of polymeric soaps obtained by ring-opening polymerization of epoxidized soybean oil, *J. Appl. Polym. Sci.* 108 (2008) 1976–1985.
- [41] American Society for Testing and Materials D3695 Standard test method for softening point of bitumen (Ring-and-Ball Apparatus) 1998 Annual Books of ASTM Standards, Volume V04.04, Philadelphia, PA, 19103-1187.
- [42] S.J. Andersen, K.S. Birdi, Aggregation of asphaltenes as determined by calorimetry, *J. Colloid Interface Sci.* 42 (1991) 497–502.
- [43] E.Y. Sheu, D.A. Storm, Colloidal properties of asphaltenes in organic solvents, in: E.Y. Sheu, O.C. Mullins (Eds.), *Asphaltenes: Fundamentals and Applications*, Plenum Press, New York City, 1995, Chap.1.
- [44] E.B. Sirota, Physical structure of asphaltenes, *Energy Fuels* 19 (2005) 1290–1296.
- [45] N. Baldino, D. Gabriele, F.R. Lupi, C. Oliviero Rossi, P. Caputo, T. Falvo, Rheological effects on bitumen of polyphosphoric acid (PPA) addition, *Constr. Build. Mater.* 40 (2013) 397–404.


Chapter 6

Article

^1H -NMR Spectroscopy: A Possible Approach to Advanced Bitumen Characterization for Industrial and Paving Applications

Article

¹H-NMR Spectroscopy: A Possible Approach to Advanced Bitumen Characterization for Industrial and Paving Applications

Cesare Oliviero Rossi ^{1,*} , Paolino Caputo ¹, Giuseppina De Luca ^{1,*}, Loredana Maiuolo ¹, Shahin Eskandarsefat ² and Cesare Sangiorgi ²

¹ Department of Chemistry and Chemical Technologies, University of Calabria, Ponte P. Bucci, Arcavacata di Rende, 87036 Cosenza, Italy; paolino.caputo@unical.it (P.C.); maiuolo@unical.it (L.M.)

² DICAM-Roads, Department of Civil, Chemical, Environmental and Materials Engineering, University of Bologna, V.le Risorgimento 2, 40136 Bologna, Italy; shahin.eskandarsefat@unibo.it (S.E.); cesare.sangiorgi4@unibo.it (C.S.)

* Correspondence: cesare.oliviero@unical.it (C.O.R.); giuseppina.deluca@unical.it (G.D.L.)

Received: 8 January 2018; Accepted: 31 January 2018; Published: 2 February 2018

Abstract: Bitumen has unique chemo-mechanical properties, and for this reason, it is today one of the main constituents of many industrial products beside its common use in highway pavements construction. While the excellent rheological properties of bitumens have been investigated by means of different techniques, much remains to be known about the intrinsic properties of this complex material. It is therefore important to investigate its structure and properties from a closer point of view, towards possible useful modifications of the neat material. The present research developed a technique to investigate the composition of bitumens using Thin Layer Chromatography (TLC) to separate the different fractions, and Nuclear Magnetic Resonance (NMR) spectroscopy to assess and quantify the aliphatic hydrogen part with respect to the aromatic part. To achieve a comprehensive understanding of the chemical composition of the materials, Proton Nuclear Magnetic Resonance (¹H-NMR) analysis was conducted in solution, using CCl₄ as solvent, on three different neat bitumens and on their asphaltene and maltene fractions. The combined application of TLC and ¹H-NMR spectroscopy enables the advanced characterization of bitumens supplied from different sources or obtained from different processes. This further allows addressing the use of specific modifications according to the bitumen final applications.

Keywords: bitumen; chemo-mechanical properties; Thin Layer Chromatography (TLC); Nuclear Magnetic Resonance (NMR) spectroscopy

1. Introduction

1.1. Background

Bitumen, as one of the materials obtained from crude oil, is a viscoelastic material, which is remarkably soluble in carbon disulfide (CS₂) and holds adhesive and waterproofing properties. From the chemical point of view, bitumen contains approximately 80% carbon, 15% hydrogen and the remaining part consists of two types of atoms: heteroatoms and metals [1]. Considering the chemical composition, it is highly dependent on the source (crude oil) and on the refinery process, which contribute to its unique chemical and physical properties [2]. Although in this context chemistry of bitumen has been considered as a key parameter in fundamental understanding of bitumen characterization, the knowledge about such a complex material is still limited. Bitumen is typically constituted of two main groups of compounds: (a) asphaltenes, defined as *n*-heptane-insoluble and toluene-soluble part,

which are complex mixtures of high molecular weight hydrocarbons present in a percentage ranging between 5% and 25% by weight, consisting mainly of condensed aromatic compounds, as well as oxygen, nitrogen, sulfur and metals; and (b) maltenes, as soluble part in *n*-heptane, can in turn be subdivided into saturates, aromatics, and resins, which, together with the asphaltenes, are known as SARA fractions [3]. While asphaltenes have the highest polarity, saturates are the least polarized molecules following the aromatics and resins, which rank in between the two extremes. Several former studies have indicated that the relative amount of bitumen fractions considerably affect both the physical and mechanical properties. It has been found that, while the polar fraction directly affects the elastic phase, the presence of non-polar fraction contributes to the viscous behavior of bitumen [4]. Therefore, a better understanding of the structural characteristics and composition of the various fractions is of utmost importance in the industrial use of these complex mixtures to apply appropriate methodologies to adapt their chemical-physical properties in a controlled manner [5,6].

Since the bitumen fractions obviously determine the bitumen mechanical properties and characteristics, several attempts have been made to analyze the bitumen composition and to fractionate the bitumen compounds. Beside Atomic Force Microscopy (AFM) images and Fourier Transform-Infrared Spectroscopy (FT-IR) analysis, recently Nuclear Magnetic Resonance (NMR) spectroscopy has been found to be a practically efficient and reliable technique for complex material characterization such as bitumen [7,8]. It is worth underlining that the NMR has become one of the most powerful tools for probing in all states of matter. The technique in isotropic solution is commonly used for the characterization of synthetic or natural compounds, while structural and conformational information on even large-sized molecules can be obtained in anisotropic media through the anisotropic NMR observables, such as the residual dipolar couplings (RDCs) [9–12].

Nowadays, the NMR technique is also well known as an analytical technique for qualitative and quantitative study, at molecular level, of complex mixtures. Compared to the conventional analysis, NMR spectroscopy does not need the pre-treatment of samples that could considerably reduce the time consuming process of their preparation. In addition, since the amount of solvent that is used and the waste generation is minimum, the technique is considered environmentally friendly [13]. The superiority of this technique is the ability to simultaneously investigate several components of the mixture with a single ^1H -NMR spectrum and to evaluate the relative amount of the aliphatic and aromatic hydrogens portion in the mixture [8,14,15].

On the other hand, the separation technique to prepare a sufficient sample for NMR analysis can be a challenge. Among the proposed conventional methods to separate the bitumen fractions, Thin Layer Chromatography (TLC) and Liquid Chromatography (LC), known as qualitative and quantitative techniques in many fields such as organic, inorganic analytic and physical chemistry are commonly used [16–19].

TLC, compared to LC, requires milligram size samples, less solvent, and no deasphaltenization before the analysis, which makes it a rapid and affordable separation technique for bitumen [20]. It is worth mentioning that, despite the successfully employed TLC method for bitumen fractionation, the key point to obtain well-defined and separated spots is to select a stationary phase and an appropriate solvent or even mixed compound [21].

1.2. Objectives

Since the properties of bitumen and its use largely depend on its chemical composition, it is clear that significant improvements would result from a better understanding of the material at its molecular level. Starting with the difficulties highlighted in the characterization of chemical composition of bitumen, this research aimed to suggest and develop a new methodology for characterizing this complex mixture of organic compounds by combining the separation of the individual fractions via TLC with the high resolution ^1H -NMR technique. Note that TLC was selected considering all benefits of this technique compared to LC. Moreover, since conventional bitumens are primarily used in road

pavements and the modification of their mechanical properties is often required in any field, a deeper knowledge of bitumen composition would be of outermost importance.

Therefore, the main goal of this work was the characterization of three commercial bitumens, with different degrees of penetration (traditional penetration test), using the $^1\text{H-NMR}$ spectra recorded on the neat bitumen and on their fractions obtained through silica preparative TLC.

2. Materials and Methods

The bitumens used in this work are three commercial ones having penetrations ranging between 70 and 220 dmm (one penetration unit = 0.1 mm, Table 1). Penetration value test on bitumen is a measure of hardness or consistency of bituminous material. A 70/100 grade bitumen indicates that its penetration value lies between 70 and 100. Penetration value is the vertical distance traversed or penetrated by the point of a standard needle into the bituminous material under specific conditions of load, time and temperature. This distance is measured in one tenths of a millimeter. The two soft bitumens having the same class of penetration (160/220) have similar physical properties, while they have different origins and are processed by different techniques. They were selected to ascertain whether their chemical compositions are equal or different [22]. In the literature, it has been shown that, while two bitumens have the same softening point and penetration grade, they may show significant difference from the chemical point of view [22,23]. In addition, a 70/100 paving grade bitumen was also investigated to understand the effects of different bitumen processing on bitumen fundamental chemical properties.

Table 1. Fundamental physical properties of bitumens.

Measured Properties	Standard	Unit	Paving Grade	Paving Grade	Industrial
			70/100	160/220	160/220
Penetration at 25 °C	EN 1426	0.1 mm	70–100	160–220	170
Softening point (R&B)	EN 1427	°C	43–51	35–43	35–43
Flash point	EN 2592	°C	≥230	≥220	271
Solubility	EN 12592	% (m/m)	≥99	≥99	≥99
Mass change at 163 °C	EN 12607-1	%	≤0.8	≤1	≤1
Retained penetration	EN 1426	%	≥46	≥37	≥37
Increase in softening point	EN 1427	°C	≤9	≤11	≤12

The diagram shown in Figure 1 illustrates the main methodology followed in this research. In the first phase, $^1\text{H-NMR}$ spectra were recorded on untreated bitumen samples and on asphaltene and maltene fractions separated from the three bitumens using *n*-pentane as a solvent, with a slightly modified method compared to the commonly used one. The separation procedure is explained later.

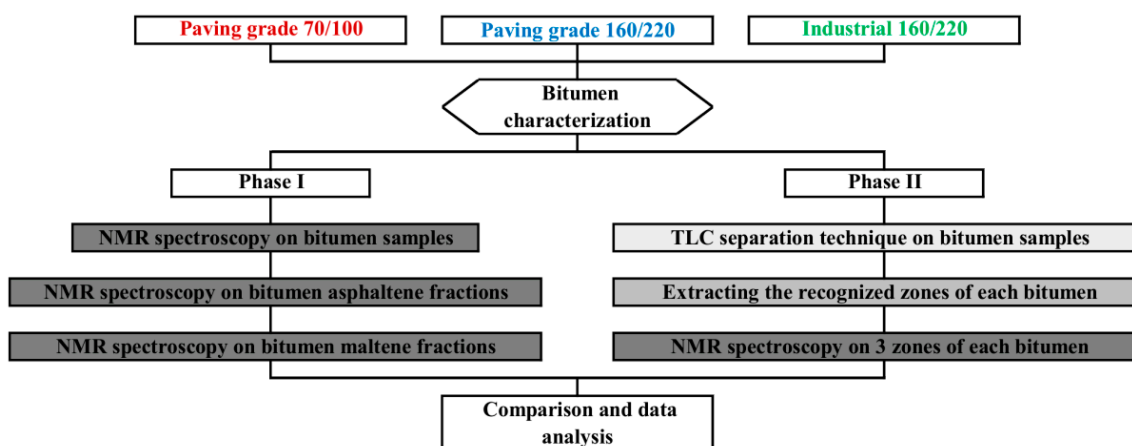


Figure 1. Research scheme.

In the second phase, the $^1\text{H-NMR}$ spectroscopy was applied to the separated zones extracted from each bitumen by preparative TLC.

3. Experimental Work

3.1. Bitumen Separation Techniques

In the present research, two different separation techniques have been used to separate test bitumens into fractions and prepare samples for the following analysis: the conventional method and Thin Layer Chromatography (TLC). It is worth mentioning that TLC was applied as qualitative and quantitative technique for bitumen fractions analyses using a ternary mixture of Methanol/Tetrahydrofuran/Chloroform (3:3:4 *v/v/v*) as solvent.

3.1.1. Asphaltenes and Maltenes Separation (Modified Conventional Method)

In a vessel, a volume in milliliters of CHCl_3 was combined to a corresponding amount in grams of bitumen (e.g., 3 g of bitumen for 3 mL of CHCl_3) and the mixture was carefully dissolved. Then, a volume of *n*-pentane forty times the CHCl_3 volume was added to the solution, which was left in dark for two hours, mixing occasionally. Finally, the precipitated asphaltenes were filtered in a funnel with paper filter by vacuum (Whatman 42 ashless). The residue was washed several times with *n*-pentane until solvent became colorless. The filter paper was dried in oven at 80 °C for three hours and successively the residue of the solvent was removed in vacuum for two hours. The filtrate, containing maltene portion, was evaporated to dryness with a rotary evaporator under reduced pressure and the residual solvent removed under vacuum pump.

3.1.2. Thin Layer Chromatography (TLC)

TLC separation technique was performed on Merck glass plates (silica gel coated with fluorescent indicator F254; gel thickness: 0.25 mm and 1 mm for qualitative and quantitative analysis, respectively), with MeOH/THF/ CHCl_3 mixture (3:3:4 *v/v/v*) as eluent [24]. Preliminary tests on neutral alumina plates and silica gel plates were performed to select the stationary phase. The results confirmed a higher separation of bitumen samples by silica gel as stationary phase. Noteworthy, given that the bitumen stiffness and mechanical properties are related to the asphaltene content, the method has been applied for both bitumens with asphaltene and deasphaltized bitumens. Dichloromethane (DCM) was used to solubilize the sample by mixing 0.04–0.05 g of bitumen to the amount of DCM needed to provide a homogenous solution (Figure 2A). The performed procedure is illustrated in Figure 2 and consists of some steps. Firstly, all prepared samples were spotted on the silica gel plate with a pipette as spotter (Figure 2B,C). Subsequently, the plate was placed in a glass eluent container (separation chamber) until the solvent rises through 90% of the plate (Figure 2D,E). Finally, the plate was removed from separation chamber and exposed to the UV lamp, Shortwave 254 nm (Figure 3). The visualization under ultraviolet (UV) light is surely the most used revelation technique to check molecules with chromophore groups and, for this reason, we chose to use it to observe the separated spots.

Figure 3 shows three main zones (A, B and C) visualized under UV lamp that were separated by scraping off the silica with a scraper and transferring it to three flasks respectively. Methanol (100 mL) was added to each flask, the flasks were swirled for 30 min, and the contents were allowed to sediment. The supernatant solution was pipetted off and centrifuged. This procedure was repeated three times for each sample using same volume of methanol, and the combined extracts were evaporated to dryness in vacuo. Using this procedure, we obtained the three separated fractions as thick mass.

Considering the complex composition of bitumen, in this first phase, we only hypothesized that Zone A (red frame) should match with the asphaltene fraction of bitumen, considering the absence of this spot in preliminary TLC tests on bitumen samples without asphaltene. Subsequently, all separated fractions have been analyzed by $^1\text{H-NMR}$ technique.

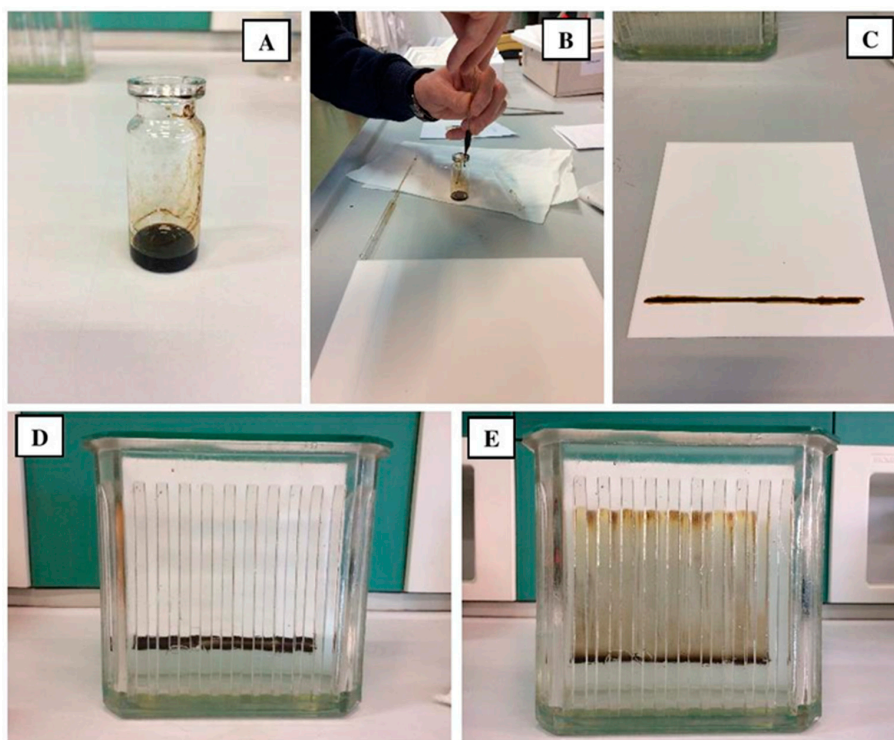


Figure 2. TLC technique procedure in chronology (A–E).

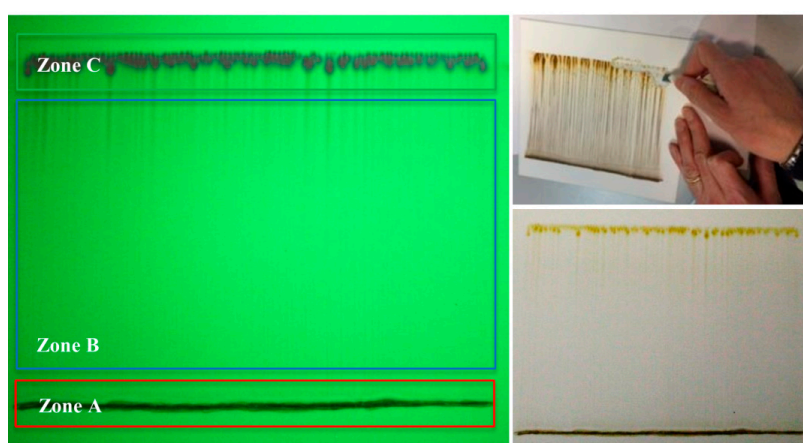


Figure 3. Separated spots on silica gel plate (160/220 Industrial bitumen sample). Three distinguished zones visualized under UV irradiation at 254 nm on the left and the scratching the zones on the top of right.

3.2. Nuclear Magnetic Resonance Spectroscopy (NMR)

The ^1H -NMR spectra were recorded at room temperature on a high-resolution Bruker Avance 500 MHz spectrometer (11.74 T) (Bruker, Rheinstetten, Germany) equipped with a 5 mm TBO probe (Triple Resonance Broadband Observe) and a standard variable-temperature unit BVT-3000. Each sample was prepared using CCl_4 as a solvent to prevent any overlapping of protonic signal due to the solvent. The ^1H -NMR experiments were performed using 20 mg of bitumen diluted in 0.5 mL of CCl_4 . Typical ^1H -NMR signal positions are reported in Table 2 commonly used for NMR data interpretation. If the protons associated to the heteroatoms are neglected, the NMR spectrum is characterized by five types of proton groups: aromatic protons (H_{ar} ; 6–9 ppm), olefinic protons (H_{ol} ;

4–6 ppm), alpha-alkyl protons (H_{α} ; 2–4 ppm), alkyl protons, primarily the methylene protons which are β or farther from the aromatic ring (H_{β} ; 1–2 ppm) and the methyl protons in the γ position or farther from the aromatic ring (H_{γ} ; 0.5–1 ppm). The fractions of asphaltenes, maltene and products obtained from TLC were used to prepare the NMR samples, using for each sample ≈ 20 mg of substance and 0.5 mL of CCl_4 as solvent.

Table 2. Types of protons and chemical shift assignments [25].

Parameter	Chemical Shift	Type of Protons
H_{ar}	6.0–9.0	Aromatic hydrogen
H_{ol}	4.0–6.0	Olefinic hydrogen
H_{α}	2.0–4.0	Aliphatic Hydrogen on C_{α} to aromatic rings
H_{β}	1.0–2.0	Aliphatic Hydrogen on C_{β} and the CH_2 beyond the C_{β} to aromatic rings
H_{γ}	0.5–1.0	Aliphatic Hydrogen on C_{γ} and the CH_3 beyond the C_{γ} to aromatic rings

4. Results and Discussion

Due to the complex nature of bitumen and difficulties in distinguishing the discernible differences in the bitumens with similar physical properties, a comprehensive analysis requires detailed integration of chromatographic and spectroscopic data. In the context, it was shown that, for discriminating the differences of various bitumens, the understanding of structural and functional entities in asphaltene is playing a key role. It was found that asphaltene from different bitumens have different structural characteristics [22]. For this reason, in the present research, the $^1\text{H-NMR}$ analysis was conducted on both asphaltene and maltene fractions along with the bitumen samples. The $^1\text{H-NMR}$ spectra of the analyzed bitumens including neat samples, asphaltene, and maltene fractions are shown in Figures 4–6. All three spectra show a very similar distribution of signals: two strong absorption peaks at 0.85 and 1.25 ppm, which correspond to proton on methyl and methylene groups, respectively; and some other large bands at 2.3–3.8 ppm and at 5.8–8.5 ppm that correspond to alkyl proton on C_{α} and to aromatic protons, respectively. It should be noted that, in all spectra, no signal in the 4.5–6 ppm region is recorded, typically the olefinic region, which means that the amount of olefinic hydrocarbons, although present, is negligible. The four regions selected for each spectrum were integrated and normalized to get the fractional proton distributions directly from the integration curve. The fractional proton distributions of the three bitumen samples are given in Table 3.

Table 3. Fractional proton distribution of the three bitumens obtained from the $^1\text{H-NMR}$ spectra reported in Figures 4, 5 and 6a.

Bitumen	Hydrogen Distribution ± 0.05			
	H_{ar}	H_{α}	H_{β}	H_{γ}
Paving 70/100	8.00	3.86	64.38	23.73
Paving 160/220	8.32	3.80	64.19	23.66
Industrial 160/220	4.82	16.10	61.07	18.00

Comparing the values of hydrogen distribution reported in Table 3, it can be observed that the two paving bitumens have a similar distribution of hydrogen types, while the distribution corresponding to the industrial bitumen is very different from the first two. In detail, the area corresponding to the aromatic zone is nearly the same in the first two samples (8.00% and 8.32%), while it is markedly lower in the last one (4.82%). On the contrary, the industrial bitumen is characterized by a high percentage of aliphatic protons compared to the other bitumens (95.17% vs. $\approx 91.90\%$), most of them corresponding to aliphatic hydrogens in α relative to aromatic rings, since, as can be seen in Table 3, the hydrogen percentage H_{α} , relating to the sample of industrial bitumen is much larger than the other two samples (16.10% vs. $\approx 3.8\%$). This means that the nature of the compounds of the first two samples is similar,

and rather different from the third sample. It should be here reminded that, while the second paving grade bitumen and the industrial bitumen have the same classification grade, they originated from two different processes, which affect their final chemical compositions.

In the next stage, for each bitumen, the fractions of maltene and asphaltene extracted using the mentioned procedure were analyzed. Thereafter, each fraction was dissolved in CCl_4 and the $^1\text{H-NMR}$ spectrum was recorded for the provided samples. The $^1\text{H-NMR}$ spectra of Maltene and Asphaltene fractions are reported respectively in Figures 4b, 5b and 6b and in Figures 4c, 5c and 6c, while, in Table 4, fractional proton distributions of each samples are reported. Observing the results of $^1\text{H-NMR}$ analysis (Table 4), it is evident, as expected, that a higher percentage of aromatic hydrogen is present in the asphaltene fractions for all samples. Comparing the results for the asphaltene fractions, extracted from the three bitumens, it can be noted that the samples from the two bitumens with the same grade present a similar distribution of aromatic and aliphatic hydrogens ($\approx 19\%$ and $\approx 81\%$, respectively), while the distribution of aliphatic hydrogen type is rather different. On the contrary, asphaltenes extracted from the paving bitumen (70/100) were characterized by a lower percentage of aromatic hydrogens. These data seem to point to a similar chemical composition for the asphaltene samples obtained from the two bitumen with the same degree of penetration and a different chemical composition for the asphaltene deriving from the paving bitumen (70/100).

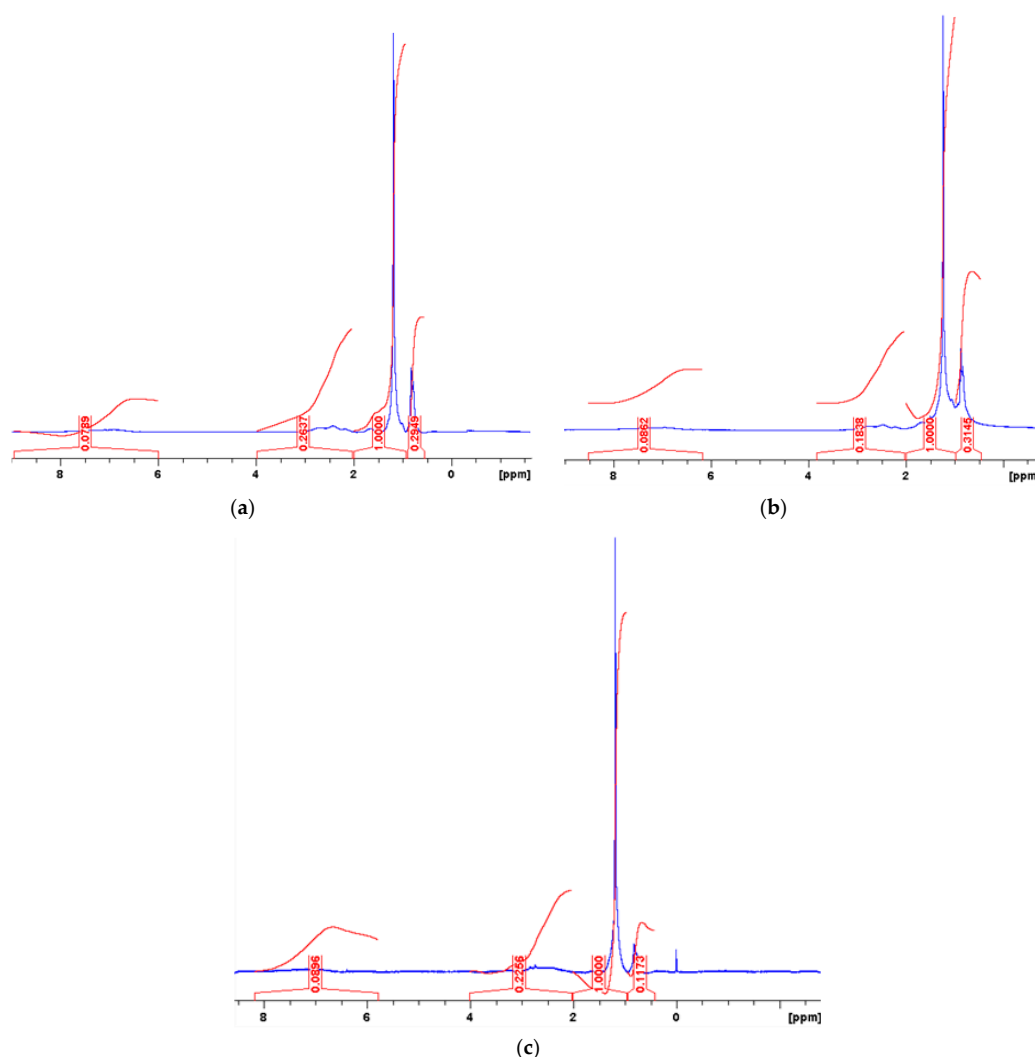


Figure 4. The $^1\text{H-NMR}$ spectra of Paving 70/100 bitumen in CCl_4 : (a) neat bitumen; (b) maltene fraction; and (c) asphaltene fraction.

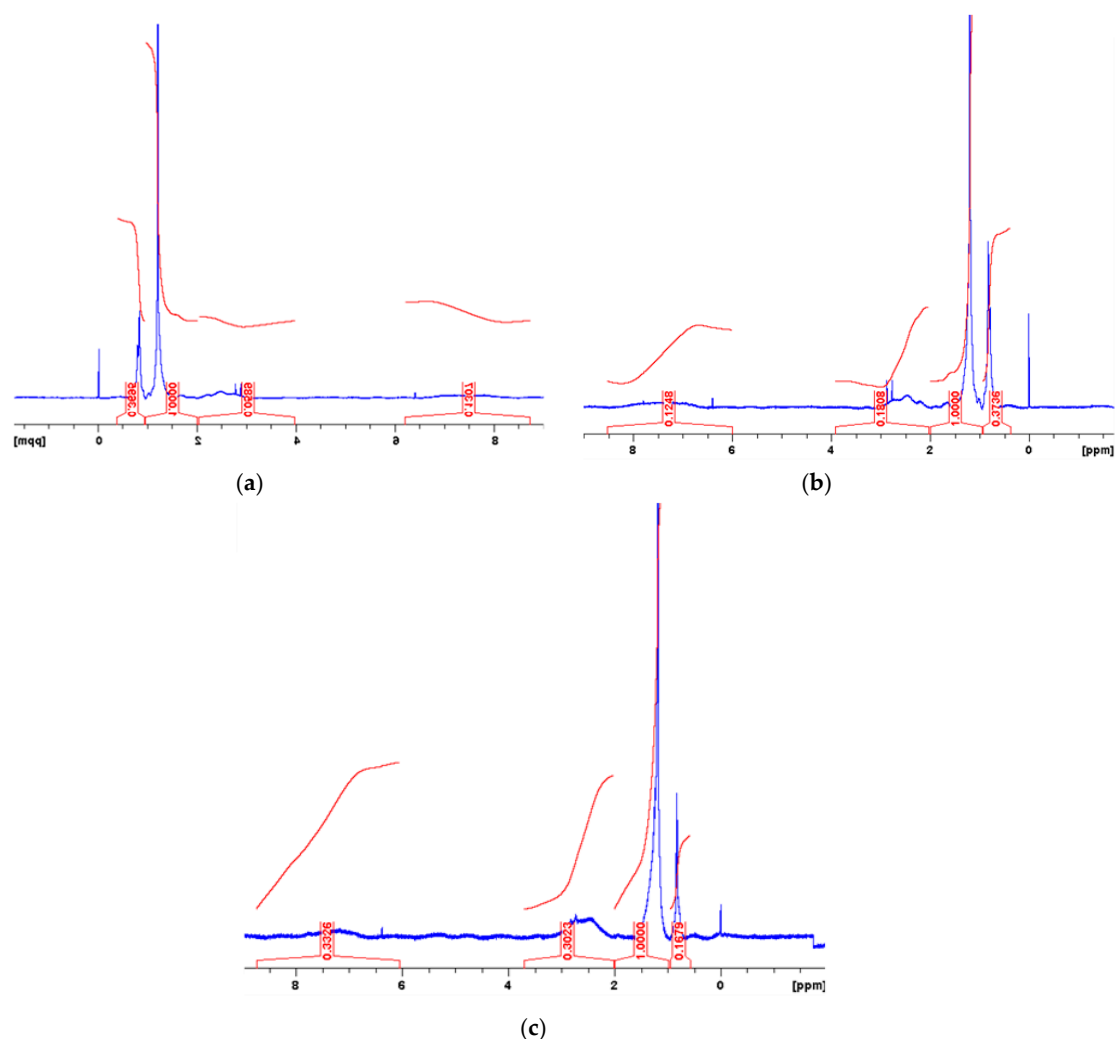


Figure 5. The ^1H -NMR spectra of Paving 160/220 bitumen in CCl_4 : (a) neat bitumen; (b) maltene fraction; and (c) asphaltene fraction.

Table 4. Fractional proton distribution of the maltene and asphaltene fractions obtained from the ^1H -NMR spectra reported in Figure 4b,c, Figure 5b,c and Figure 6b,c.

Bitumen	Hydrogen Distribution of Maltenes ± 0.05				Hydrogen Distribution of Asphaltenes ± 0.05			
	H_{ar}	H_{α}	H_{β}	H_{γ}	H_{ar}	H_{α}	H_{β}	H_{γ}
Paving 70/100	4.49	12.34	64.01	19.16	14.25	15.75	61.80	8.19
Paving 160/220	7.43	11.77	60.55	20.24	18.30	16.77	55.47	9.31
Industrial 160/220	7.54	11.61	61.00	19.86	19.58	8.19	60.79	11.44

Moreover, the NMR data on the maltene fraction extracted from the two bitumens with high penetration show almost equal distribution of aromatic and aliphatic hydrogens, while the maltene sample from the paving bitumen 70/100 presents a lower aromatic percentage if compared to the other samples (4.49% vs. $\approx 7\%$). The results obtained on maltene and asphaltene fractions provided a better understanding of bitumens detailed characteristics needed for developing methods to improve their properties. For example, adding suitable substances, it will be possible to increase or decrease the aromatic percentage that could be the key to modulate the viscosity of bitumen. Considering the bitumen complex system, the resins (intermediate polarity compounds) play a crucial role in the mechanical properties and in general on the bitumen performance properties [26].

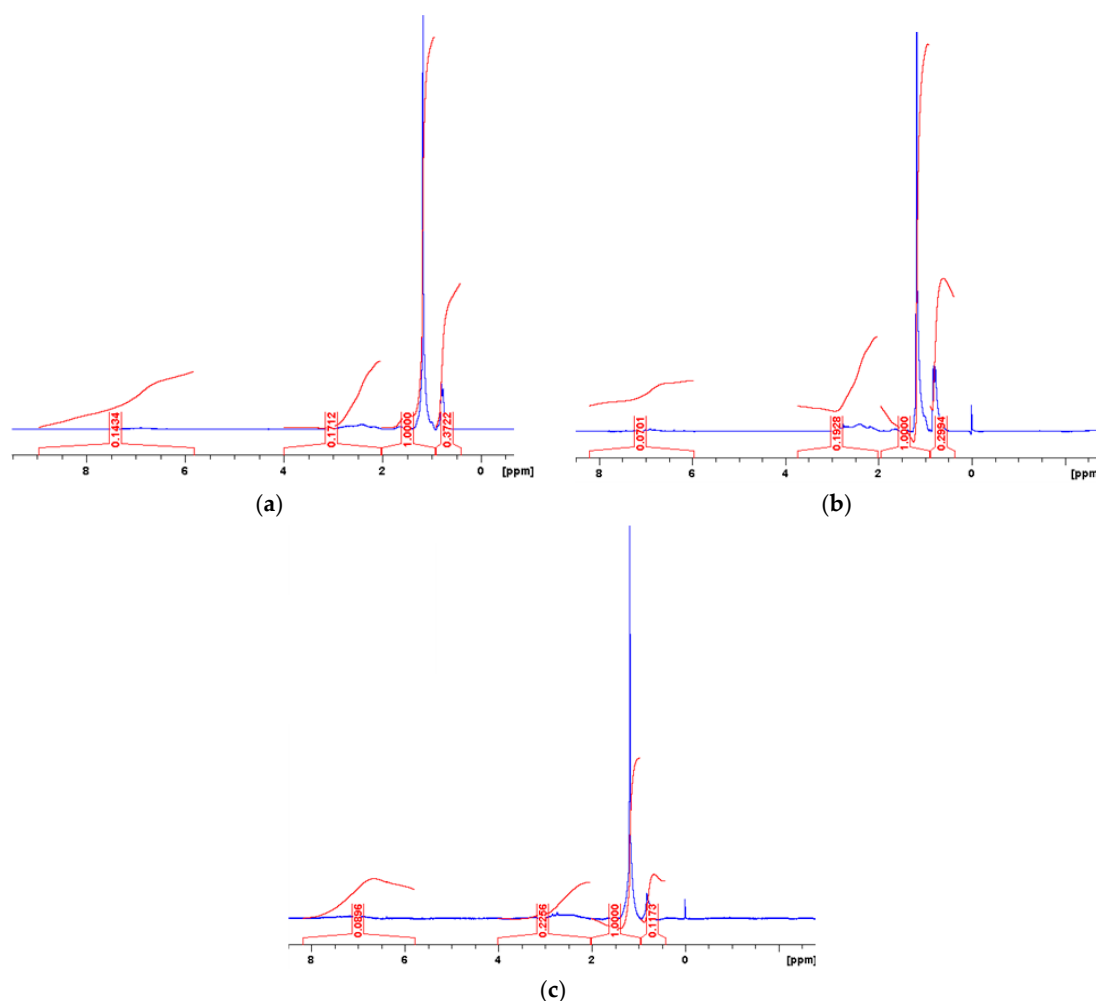


Figure 6. The ^1H -NMR spectra of Industrial 2 160/220 bitumen in CCl_4 : (a) neat bitumen; (b) maltene fraction; and (c) asphaltene fraction.

As mentioned earlier, for understanding the needed additives/modifiers to alter the characteristics of bitumens for specific uses, it is required to fractionate the bitumen with a preparative TLC and to analyze the obtained zones by NMR. The recognized three zones included: the C zone (on the top) should contain the apolar parts, i.e., the maltenes; the B zone is where the molecules with medium polarity are present; and the A zone, the lower spot, includes highly polar molecules. The B zone and A zone together should count for all the asphaltenes present in the sample. Table 5 lists the fractional proton distribution of the three zones obtained from the spectra reported in Figures 7–9. As it can be seen, data on hydrogens distribution confirm the hypothesis: the distribution related to zone C is similar in all samples to that found for maltenes extracted according to the classical procedure results (see Table 4). The hydrogens distribution of zone B is of particular interest: paving grade 70/100 and 160/220 bitumen samples are both characterized by a high percentage of aromatic hydrogen (22.47% and 32.19%, respectively) and by the presence of olefinic peaks in the aliphatic region. Moreover, the broad band of aromatic hydrogen was replaced by a fine structure of well-defined aromatic zones and with not much overlapping peaks. This probably means that, for these two bitumens, zone B is characterized by the presence of simple polyaromatic compounds that originate a fine structure. Instead, the sample of Industrial bitumen presents only aliphatic hydrogen, which corresponds to proton on methyl and methylene groups and no appreciable line/band at the aromatic zone.

Table 5. Fractional proton distribution of various zones scratched from the three bitumens by preparative TLC obtained from the ¹H-NMR spectra reported in Figures 7–9.

Bitumen	Hydrogen Distribution of Zone C ±0.05				Hydrogen Distribution of Zone B ±0.05			
	H _{ar}	H _α	H _β	H _γ	H _{ar}	H _{ol} /H _α	H _β	H _γ
Paving70/100	3.48	7.80	62.27	26.45	22.47	8.97/13.46	53.86	9.34
Paving 160/220	8.49	7.30	58.73	25.47	32.19	11.95 H _{ol}	45.91	9.94
Industrial 160/220	8.75	13.48	60.73	17.04	-	-	92.62	7.38
Bitumen	Hydrogen Distribution of Zone A ±0.05				Hydrogen Distribution of Zones B + A ±0.05			
	H _{ar}	H _α	H _β	H _γ	H _{ar}	H _{ol} /H _α	H _β	H _γ
Paving70/100	17.43	14.38	55.53	12.66	19.17	17.69	52.27	10.57
Paving 160/220	5.27	3.24	77.36	14.13	18.73	7.59	61.64	12.03
Industrial 160/220	6.07	8.23	71.86	13.84	-	-	-	-

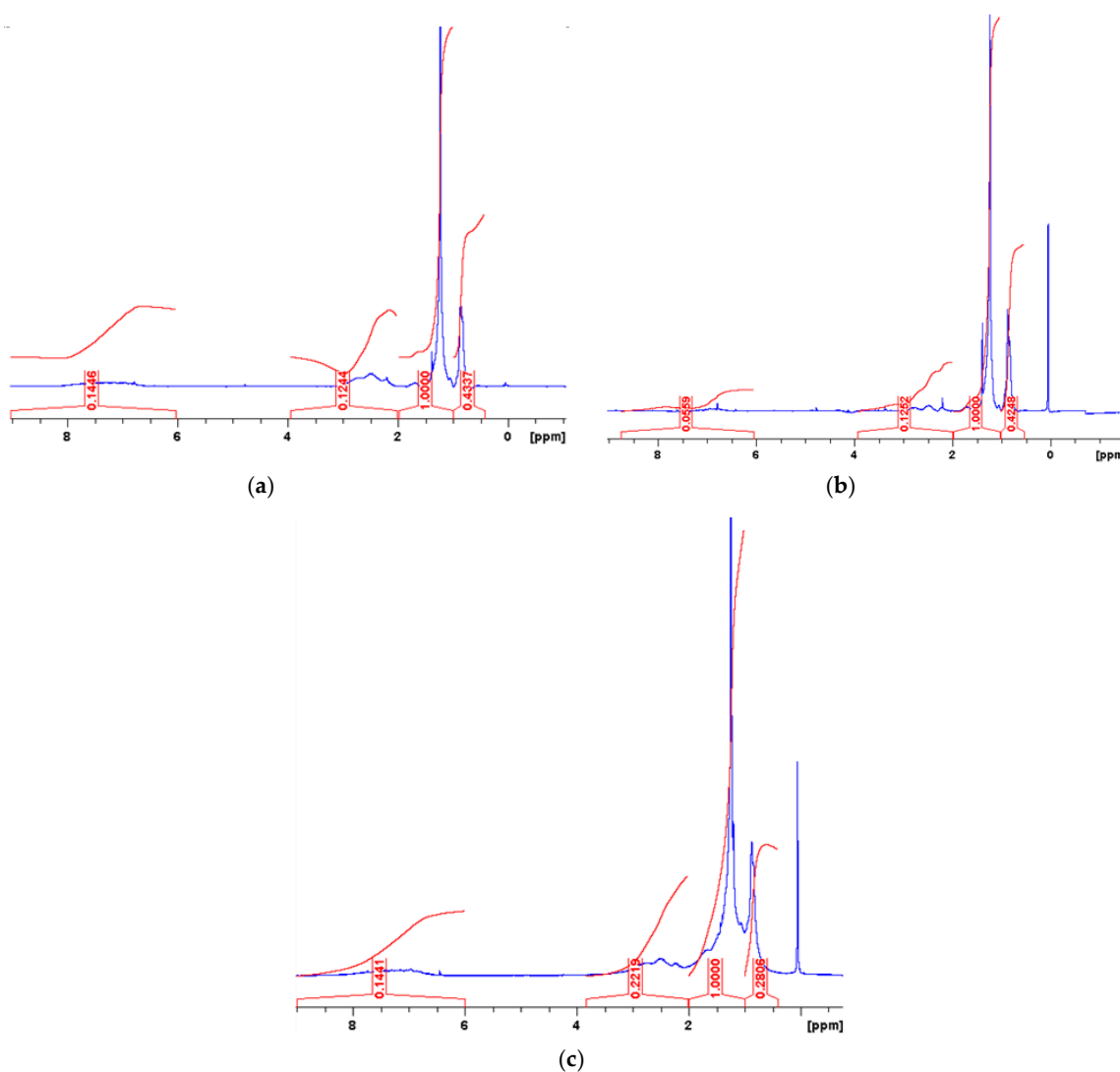


Figure 7. The ¹H-NMR spectra of zone C obtained through a preparative TLC for the three bitumens: (a) paving 160/220; (b) paving 70/100; and (c) industrial 160/220.

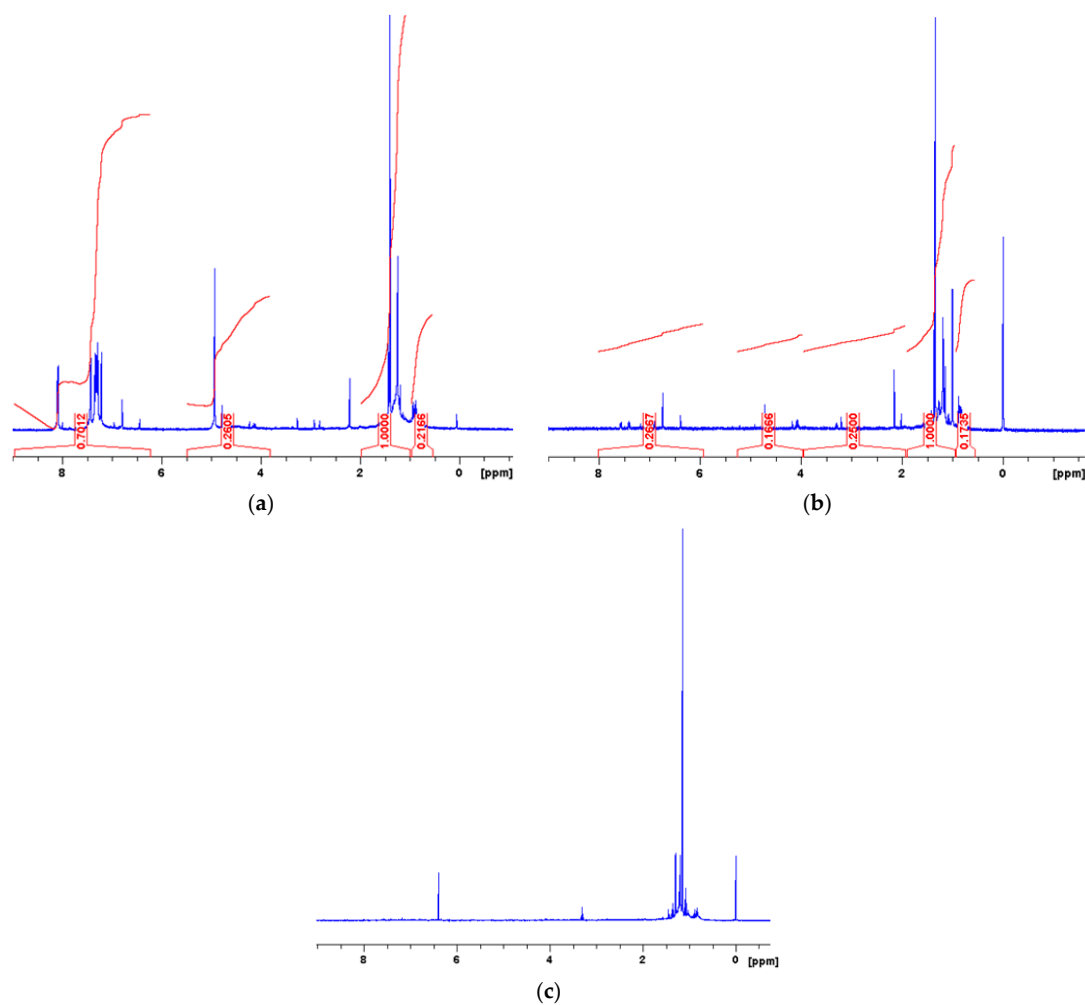


Figure 8. The ^1H -NMR spectra of zone B obtained through a preparative TLC for the three bitumens: (a) paving 160/220; (b) paving 70/100; and (c) industrial 160/220.

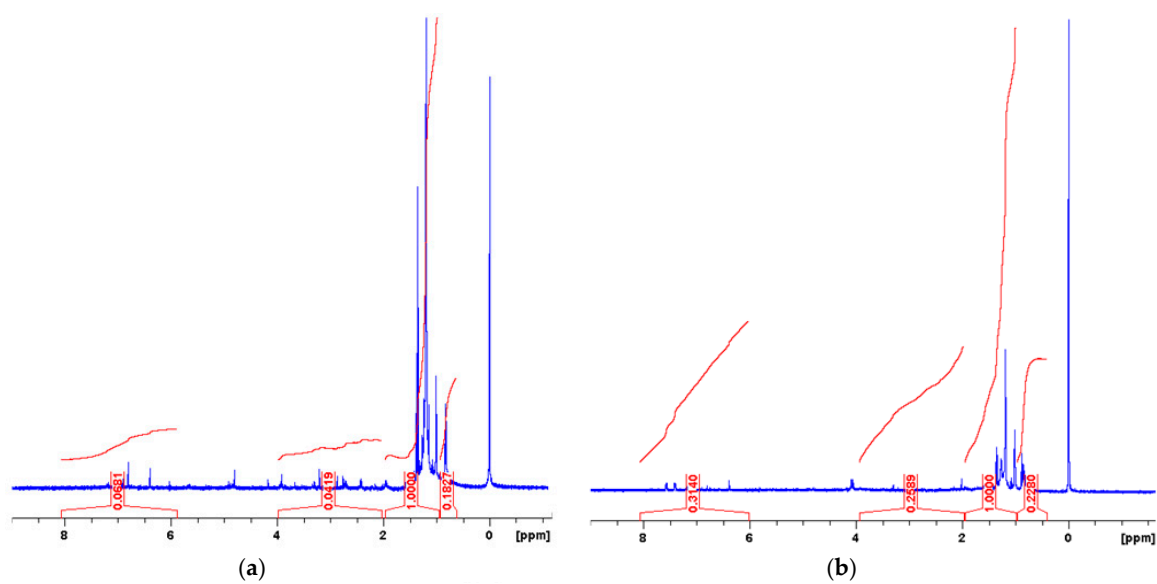


Figure 9. Cont.

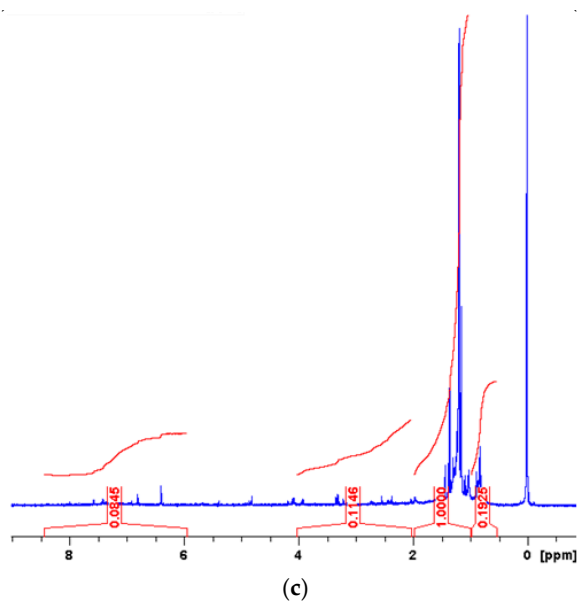


Figure 9. The ^1H -NMR spectra of zone A obtained through a preparative TLC for the three bitumens: (a) paving 160/220; (b) paving 70/100; and (c) industrial 160/220.

In the last zone A (the lower spot), the samples of the bitumen with the same grade showed a similar distribution of hydrogen, with the aliphatic part predominating with respect to the aromatic part, while the sample of the 70/100 bitumen is characterized by a higher percentage of aromatics than the others. It should be noted that, in Table 5, the distribution of H_{ar} and H_{ol}/H_{α} hydrogen of zone B for the industrial bitumen is not reported. The reason for the missing data is due to an ^1H experimental spectrum of this zone that does not present significant signals for these hydrogens. Important information can be extracted from Table 5; once again, the paving bitumen is poor in aromatic hydrogens and this lack can be found in both the maltene and resins. The NMR data suggest adding aromatic oils and aromatic surfactant-based mixtures to the paving bitumen to have chemical affinity similar to the industrial bitumen. This chemical affinity is very important for practical applications, e.g., solubility of polymers additives.

5. Conclusions and Remarks

The need for deeper insights into the characterization of bituminous materials used in industrial and infrastructural applications cast the basis for the presented research. Beyond the traditional rheo-mechanical analysis of bitumens, a deeper characterization is needed for today's multi-functional products introduced in both industry and road infrastructures. In this research, it was shown that the combined use of TLC technique and ^1H -NMR spectroscopy is a feasible approach to distinguish between different bitumens even with similar physical and rheological properties.

In light of the presented achievements, the following conclusions can be made:

- Asphaltene and maltene fractions of bitumens can be successfully separated by means of TLC techniques and be used for further characterization tests in the laboratory.
- The choice of solvents determination, mobile phases and support material are crucial to obtain a consistent separation of the binder components.
- ^1H -NMR provides a wider perspective on the chemical characteristics of the various binders than traditional SARA analysis.
- Although within the proposed technique unconventional laboratory work is required, the obtained data provide a comprehensive understanding on the chemo-mechanical nature of the binders.

- The acquired knowledge will be at the basis of any prospective alteration/modification of binders for commercial purposes.

The described general findings are based on the laboratory study reported in this paper. Any other investigation into the use of coupled TLC and $^1\text{H-NMR}$ methodologies may differ with changes in the bituminous material's characteristics. A consistent database should be created and disseminated for further scientific upgrades.

Author Contributions: All authors contributed equally to this work.

Conflicts of Interest: The authors declare no conflict of interest.

References

1. Asphalt Institute. *Superpave Asphalt Binder Specification (SP-1)*, 3rd ed.; Asphalt Institute: Lexington, KY, USA, 2003.
2. Read, J.; Whiteoak, D. *The Shell Bitumen Handbook*, 5th ed.; Thomas Telford Publishing: London, UK, 2003.
3. Handle, F.; Harir, M.; Fussl, J.; Koyun, A.N.; Grosseegger, D.; Hertkorn, N.; Eberhardsteiner, L.; Hofko, B.; Hospodka, M.; Blab, R.; et al. Tracking Aging of Bitumen and Its Saturate, Aromatic, Resin, and Asphaltene Fractions Using High-Field Fourier Transform Ion Cyclotron Resonance Mass Spectrometry. *Energy Fuels* **2017**, *31*, 4771–4779. [[CrossRef](#)]
4. Robertson, R.E. *Chemical Properties of Asphalts and Their Relationship to Pavement Performance*; Strategic Highway Research Program National Research Council: Washington, DC, USA, 1991.
5. Gentile, L.; Filippelli, L.; Oliviero Rossi, C.; Baldino, N.; Ranieri, G.A. Rheological and H-NMR Spin-Spin relaxation time for the evaluation of the effects of PPA addition on bitumen. *Mol. Cryst. Liq. Cryst.* **2012**, *558*, 54–63. [[CrossRef](#)]
6. Baldino, N.; Gabriele, D.; Oliviero Rossi, C.; Seta, L.; Lupi, F.R.; Caputo, P.; Falvo, T. Rheological effects on bitumen of polyphosphoric acid (PPA) addition. *Constr. Build. Mater.* **2013**, *40*, 397–404. [[CrossRef](#)]
7. Masson, J.-F.; Leblond, V.; Margeson, J. Bitumen morphologies by phase-detection atomic force microscopy. *J. Microsc.* **2006**, *221*, 17–29. [[CrossRef](#)] [[PubMed](#)]
8. Nciri, N.; Song, S.; Kim, N.; Cho, N. Chemical Characterization of Gilsonite Bitumen. *J. Pet. Environ. Biotechnol.* **2014**, *5*, 1000193. [[CrossRef](#)]
9. Aroulanda, C.; Celebre, G.; De Luca, G.; Longeri, M. Molecular ordering and structure of quasi-spherical solutes by liquid crystal NMR and Monte Carlo simulations: The case of norbornadiene. *J. Phys. Chem. B* **2006**, *110*, 10485–10496. [[CrossRef](#)] [[PubMed](#)]
10. Celebre, G.; Concistrè, M.; De Luca, G.; Longeri, M.; Pileio, G. Intrinsic information content of NMR dipolar couplings: A conformational investigation of 1,3-butadiene in a nematic phase. *ChemPhysChem* **2006**, *7*, 1930–1943. [[CrossRef](#)] [[PubMed](#)]
11. De Luca, G.; Longeri, M.; Pileio, G.; Lantto, P. NMR spectroscopy investigation of the cooperative nature of the internal rotational motions in acetophenone. *ChemPhysChem* **2005**, *6*, 2086–2098. [[CrossRef](#)] [[PubMed](#)]
12. Maltsev, A.S.; Grishaev, A.; Roche, J.; Zasloff, M.; Bax, A. Improved Cross Validation of a Static Ubiquitin Structure Derived from High Precision Residual Dipolar Couplings Measured in a Drug-Based Liquid Crystalline Phase. *J. Am. Chem. Soc.* **2014**, *136*, 3752–3755. [[CrossRef](#)] [[PubMed](#)]
13. Majid, A.; Pihillagawa, I. Potential of NMR spectroscopy in the characterization of non-conventional oils. *J. Fuels* **2014**, 390261. [[CrossRef](#)]
14. Nciri, N.; Kim, N.; Cho, N. New insights into the effects of styrene-butadiene-styrene polymer modifier on the structure, properties, and performance of asphalt binder: The case of AP-5 asphalt and solvent deasphalting pitch. *Mater. Chem. Phys.* **2017**, *193*, 477–495. [[CrossRef](#)]
15. Poveda, J.; Molina, D.; Pantoja-Agreda, E. $^1\text{H-}$ and $^{13}\text{C-NMR}$ structural characterization of Asphaltenes from vacuum residua modified by Thermal cracking. *J. Oil Gas Altern. Energy Sources* **2014**, *5*, 49–60. [[CrossRef](#)]
16. Maiuolo, L.; Bortolini, O.; De Nino, A.; Russo, B.; Gavioli, R.; Sforza, F. Modified N,O-Nucleosides: Design, Synthesis, and Anti-tumour Activity. *Aust. J. Chem.* **2014**, *67*, 670–674. [[CrossRef](#)]
17. De Nino, A.; Bortolini, O.; Maiuolo, L.; Garofalo, A.; Russo, B.; Sindona, G. A sustainable procedure for highly enantioselective organocatalyzed Diels-Alder cycloadditions in homogeneous ionic liquid/water phase. *Tetrahedron Lett.* **2011**, *52*, 1415–1417. [[CrossRef](#)]

18. Lee, H.-J.; Koung, F.-P.; Kwon, K.-R.; Kang, D.-I.; Cohen, L.; Yang, P.-Y.; Yoo, H.-S. Comparative Analysis of the Bufonis Venenum by Using TLC, HPLC, and LC-MS for Different Extraction Methods. *J. Pharmacopunct.* **2012**, *15*, 52–65. [[CrossRef](#)] [[PubMed](#)]
19. Dolowy, M.; Pyka, A. Chromatographic Methods in the Separation of Long-Chain Mono- and Polyunsaturated Fatty Acids. *J. Chem.* **2015**, 120830. [[CrossRef](#)]
20. Masson, J.-F.; Price, T.; Collins, P. Dynamics of bitumen fractions by Thin-Layer Chromatography/Flame Ionization detection. *Energy Fuels* **2001**, *15*, 955–960. [[CrossRef](#)]
21. Dunn, K.; Chilingarian, G.V.; Yen, T.F. *Bitumens: Liquid Chromatography*; Academic Press: Cambridge, MA, USA, 2000.
22. Christopher, J.; Sarpal, A.S.; Kapur, G.S.; Krishna, A.; Tyagi, B.R.; Jain, M.C.; Jain, S.K.; Bhatnagar, A.K. Chemical structure of bitumen-derived asphaltene by nuclear magnetic resonance spectroscopy and X-ray diffractometry. *Fuel* **1996**, *75*, 999–1008. [[CrossRef](#)]
23. Oyekunle, L.O. Certain Relationships between Chemical Composition and Properties of Petroleum Asphalts from Different Origin. *Oil Gas Sci. Technol. Rev. IFP* **2006**, *61*, 433–441. [[CrossRef](#)]
24. Preethi, J.; Harita, B.; Rajesh, T. Review on Thin Layer Chromatography. *J. Formul. Sci. Bioavailab.* **2017**, *1*, 1–4.
25. Zander, M.; Marsh, H.; Rodríguez-Reinoso, F. Chemistry and properties of coal-tar and petroleum pitch. In *Sciences of Carbon Materials*; Marsh, H., Rodríguez-Reinoso, F., Eds.; Universidad de Alicante, Secretariado de Publicaciones: Alicante, Spain, 2000; pp. 205–257.
26. Çubuk, M.; Gürü, M.; Kürşat Çubuk, M. Improvement of bitumen performance with epoxy resin. *Fuel* **2009**, *88*, 1324–1328. [[CrossRef](#)]



© 2018 by the authors. Licensee MDPI, Basel, Switzerland. This article is an open access article distributed under the terms and conditions of the Creative Commons Attribution (CC BY) license (<http://creativecommons.org/licenses/by/4.0/>).




Chapter 7

Article

Effects of Natural Antioxidant Agents on the Bitumen Aging Process: An EPR and Rheological Investigation

Article

Effects of Natural Antioxidant Agents on the Bitumen Aging Process: An EPR and Rheological Investigation

Cesare Oliviero Rossi ¹ , Paolino Caputo ¹, Saltanat Ashimova ¹, Antonio Fabozzi ²,
Gerardino D'Errico ^{2,3,*}  and Ruggero Angelico ^{3,4,*} 

¹ Department of Chemistry and Chemical Technologies, University of Calabria,

I-87036 Arcavacata di Rende (CS), Italy; cesare.oliviero@unical.it (C.O.R.); paolino.caputo@unical.it (P.C.);
salta_32@mail.ru (S.A.)

² Department of Chemical Sciences, University of Naples Federico II, Complesso di Monte S. Angelo,
via Cinthia, I-80126 Naples (NA), Italy; antonio.fabozzi@unina.it

³ CSGI (Center for Colloid and Surface Science), Via della Lastruccia 3, I-50019 Sesto Fiorentino (FI), Italy

⁴ Department of Agricultural, Environmental and Food Sciences, University of Molise, Via De Sanctis,
I-86100 Campobasso (CB), Italy

* Correspondence: gerardino.derrico@unina.it (G.D.); angelico@unimol.it (R.A.); Tel.: +39-081-674245 (G.D.);
+39-0874-404649 (R.A.)

Received: 24 July 2018; Accepted: 15 August 2018; Published: 19 August 2018



Featured Application: Additives obtained from natural waste materials could effectively reduce the hardening effect of bitumen aging in road pavements by exerting an effective antioxidant protection.

Abstract: Bitumen aging is the major factor contributing to the deterioration of the road pavement. Oxidation and volatilization are generally considered as the most important phenomena affecting aging in asphalt paving mixtures. The present study was carried out to investigate whether various antioxidants provided by natural resources such as phospholipids, ascorbic acid as well as lignin from rice husk, could be used to reduce age hardening in asphalt binders. A selected bituminous material was modified by adding 2% *w/w* of the anti-aging natural additives and subjected to accelerated oxidative aging regimes according to the Rolling Thin Film Oven Test (RTFOT) method. The effects of aging were evaluated based on changes in sol-gel transition temperature of modified bitumens measured through Dynamic Shear Rheology (DSR). Moreover, changes of Electron Paramagnetic Resonance (EPR) spectra were monitored on the bituminous fractions asphaltene and maltene separated by solvent extraction upon oxidative aging. The phospholipids-treated binder exhibited the highest resistance to oxidation and the lowest age-hardening effect compared to the other tested anti-oxidants. The combination of EPR and DSR techniques represents a promising method for elucidating the changes in associated complex properties of bitumen fractions promoted by addition of free radical scavengers borrowed by green resources.

Keywords: bitumen; antioxidant agent; rheology; electron paramagnetic resonance

1. Introduction

In asphalt industry, the term *aging* identifies the process of deterioration of bitumen due to the occurrence of oxidation mechanisms and progressive loss of volatile components. This alteration occurs over time and causes a change in the chemical, physical, colloidal and rheological properties of the bitumen itself, affecting the useful life of the road pavement as aging tends to make the binder more fragile and therefore the conglomerate more prone to cracking [1]. The aging process

is strongly linked to the thermal susceptibility of bitumen and evolves depending on two main factors: the original crude oil and the production process. The bitumen oxidation process is extremely complex. Because of the varied and complex molecular composition, it is unthinkable to isolate and identify the individual species obtained as a result of oxidation. However, understanding the mechanisms by which it takes place is of fundamental importance as it represents the main factor responsible for the hardening of road pavements and therefore of irreversible changes in the physical properties of the binder. Despite the impossibility of isolating the single oxidized components, the main functional groups have been identified. These include predominantly ketones and sulfoxides, accompanied by dicarboxylic anhydrides and dicarboxylic acids in much smaller concentrations [2]. As described by Petersen [3], the oxidation mechanism can be divided into two sequential phases. The primary or short-term aging, which occurs in the phase of production of bituminous mixes and during the paving phase of the bituminous conglomerates, and secondary or long-term aging, which manifests with increasing the pavement service life. Besides, the field aging of asphalt pavements must also be considered, and a number of studies have attempted to characterize the aging viscoelastic properties of asphalt mixtures such as dynamic modulus at different aging times and pavement depths, to account for the effects of long-term aging and non-uniform field aging in the pavement depth [4,5]. Primary aging is a process of short temporal duration, compared to the secondary one and is generated during the mixing phase of the binder with the aggregates and the process of spreading and compacting [6]. Inevitably, the main consequences due to primary aging concern the variation of the chemical composition, caused mainly by oxidation processes. Bitumen storage, even for a long time, does not generate important changes in the consistency of the binder due to the limited access of oxygen. During mixing, transport and spreading of the conglomerate, the thin film bitumen is instead exposed to high temperature and atmospheric oxygen; the resulting chemical changes translate into obvious physical changes. In particular, there is a substantial reduction of the aromatic fraction together with the increase in the content of resins and asphaltenes [7,8]. The saturated content remains substantially unchanged due to the relatively low reactivity of the components in question. The changes in the chemical composition determine an increase in the average size of the molecules present (with increase in molecular weight) accompanied by a hardening of the bitumen [9]. The addition of antioxidant compounds to a bituminous aggregate is therefore a good strategy to increase its durability and prevent deterioration.

Many studies have appeared in the specific literature about the addition of various additives to the bitumen, with the aim to evaluate their antiaging performances. Several organic and inorganic compounds have been tested to improve the aging resistance of bitumen and, hence, its durability in the asphalt mix [10–15]. For example, Banerjee et al. [16] tested Sasobit, Rediset, Cecabase, and Evotherm, of which the first additive is a Fischer–Tropsch paraffin and the other antioxidants are synthetic. Further applications can be found in a recent comprehensive review of aging of asphalt paving materials with focus on antioxidant additives [17]. However, a few studies deal with the application of natural additives or byproducts rich in antioxidants as free radical scavengers to protect bituminous materials from oxidation phenomena [18–20]. The antioxidant properties of many raw materials borrowed from renewable natural resources have yet to be tested such as, e.g., the polyunsaturated fatty components of natural phospholipids. The application of cheap and environmentally friendly anti-aging additives to virgin bitumen would enjoy the double advantage of using sustainable and renewable compounds and at same time reducing the carbon footprint of the products of asphalt industries according to the circular economy's recommendations.

The objective of the present work is to investigate whether the addition to bitumen of antioxidant agents obtained by natural resources improves its resistance towards short artificial aging by Rolling Thin Film Oven Test (RTFOT). The research design is accomplished by investigating the effects of the aging process on both the mechanical response of binders by running Dynamic Shear Rheology (DSR) tests, and the free radical content detected by Electron Paramagnetic Resonance (EPR) spectroscopy on asphaltene and maltene bituminous fractions. The experimental approach is sketched in the flowchart

of Figure 1. Bitumen manifests EPR spectra due to organic radicals [21–23] the signal shape of which is susceptible to changes in the oxidative state, and vanadyl ions VO^{2+} [24] associated with porphyrin species, which instead appear to be unaffected by oxidative treatments. Here we will focus our attention on the two most representative components present in the bitumen, namely, asphaltenes and maltenes [25]. The former are macromolecular compounds, comprising polyaromatic nuclei linked by aliphatic chains or rings of various lengths and sometimes by functional groups [26]. A peculiar characteristic of petroleum asphaltenes is the presence of stable free radicals, well detectable by EPR, associated with a non-localized π system of electrons stabilized by resonance. Maltene represents the bitumen fraction soluble in n-pentane, which in turn can be split into saturates, aromatics (also apolar aromatics), and resins (also polar aromatics) [27]. The results of the present work show that it is possible to draw useful anti-aging additives from renewable sources capable to reduce the age-hardening effect and concomitantly protect bitumen against oxidative aging.

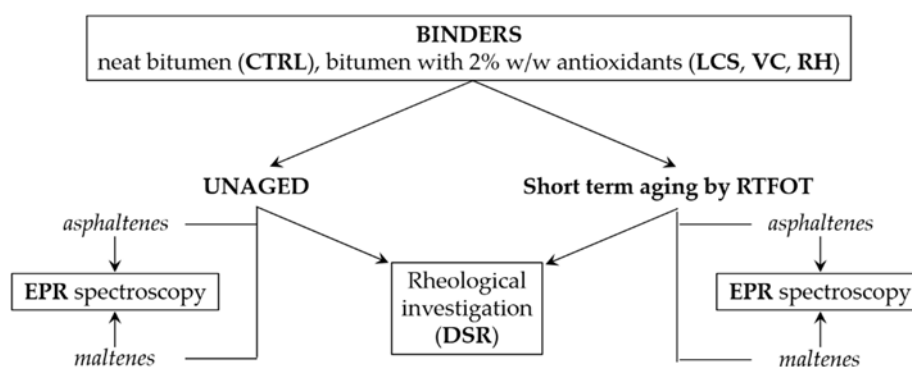


Figure 1. Flowchart of the experimental approach. The tested binders both neat bitumen as control CTRL, and bitumen modified with 2% *w/w* of natural antioxidants, namely, a mix of phospholipids (LCS), Vitamin C (VC) and rice husk (RH), are subjected to artificial thermal treatment by Rolling Thin Film Oven Test (RTFOT). Then, Dynamic Shear Rheological (DSR) tests carried out on artificially aged binders are compared to those performed on aliquots of unaged samples. A parallel EPR study is performed on both the asphaltene and maltene fractions obtained, respectively, from unaged binders and bitumens subjected to short-term aging by RTFOT.

2. Materials and Methods

2.1. Sample Preparation

A light brown bitumen (penetration grade 50/70), produced in Saudi Arabia and kindly supplied by Loprete Costruzioni Stradali (Terranova Sappo Minulio (RC), Italy), was used as base asphalt binder to test the effectiveness of natural compounds selected as anti-aging additives. The natural antioxidant additives selected for the present research were: (a) commercial mix of phospholipids in form of light yellow powder (hereafter LCS) provided by Kimical srl (Rende (CS), Italy); (b) Vitamin C, also known as ascorbic acid (hereafter VC) provided by Sigma-Aldich (Milano, Italy); (c) rice husk (hereafter RH) obtained from producers located in Mantova, Italy. The raw RH was first washed with distilled water and dried at 60 °C and then ground for 10 min in an electric mixer and sieved with 0.5 mm sieve to get fine powder prior mixing with bitumen. Three aliquots of the starting bitumen were first heated at 140–160 °C and then mixed with 2% by weight (*w/w*) of LCS, VC and RH, respectively. A fourth aliquot of the same bitumen source was used as reference (hereafter, CTRL). Each compound was separately added to bitumen, under vigorous stirring at the temperature of 150 °C and the stirring was maintained for a period of 30 min. Once the mixing procedure was finished, each of the resulting bitumen mixtures was separately poured into small sealed containers and then stored in a darkened thermostat at 25 °C to preserve morphology.

2.2. Bitumen Separation

Both unaged and artificially aged bituminous samples, either modified with antioxidants or not, were subjected to an experimental procedure based on the bitumen separation by n-pentane extraction according to the American Society for Testing Materials (ASTM) Standard method 4124 [28]. In details, 10 g ca. of bitumen were weighed into a 2 L Erlenmeyer flask and 300 mL ca. of n-pentane were added. A good dispersion of the bitumen was assured through vigorous stirring. The flask was then heated to 90 °C and kept at that temperature for about 1–2 h. Afterwards, the bottle was left overnight for cooling and sedimentation of solid fraction. The next day, the dispersion was filtered through a Büchner-funnel (Whatman 42 ashless) and the insoluble phase, called asphaltene phase, was collected and stored. Then, the n-pentane soluble maltene phase, appearing as a viscous liquid, was obtained after the solvent had been removed by evaporation under reduced pressure. In Table 1 the percentages of asphaltene collected from the unaged and aged samples are reported.

Table 1. The weight percentages of asphaltene fraction obtained from crude bitumen (CTRL) and bitumen modified with LCS, VC and RH additives, both unaged and subjected to artificial aging.

Sample	Asphaltene (% <i>w/w</i>)	
	Unaged	Aged
CTRL	26.8	34.2
Bitumen + LCS	29.2	32.8
Bitumen + VC	28.2	35.3
Bitumen + RH	29.5	35.7

2.3. Aging Test

In order to study the effects of aging in the laboratory, the method known as Rolling Thin Film Oven Test (RTFOT) [29,30] was adopted to simulate the short-term aging of asphalt binders that would occur during the hot-mixing process. The apparatus consists essentially of an internal double-wall furnace, in which the hot air circulates conveyed by an internal fan at the test temperature of 163 °C. The test consists in subjecting a thin layer of bitumen, ~1.25 mm, to a hot air jet for 75 min. Each modified bitumen, plus a reference binder free of additives, was divided into two aliquots, of which only one was subjected to the process of artificial aging. Both sets of aliquots were subsequently separated into the respective fractions of asphaltene and maltene by extraction in n-pentane, which were finally characterized through Dynamic Shear Rheology (DSR) and Electron Paramagnetic Resonance (EPR) spectroscopy tests (see the flowchart of the experimental approach in Figure 1).

2.4. Dynamic Shear Rheology (DSR)

Temperature sweep (time cure) rheological tests were performed to analyze the mechanical response of modified bitumens vs. CTRL upon artificial aging process. Experiments were carried out using a controlled shear stress rheometer (SR5, Rheometric Scientific, Piscataway, NJ, USA) equipped with a parallel plate geometry (gap 2.0 ± 0.1 mm, diameter 25 mm) and a Peltier system (± 0.1 °C) for temperature control. Bitumen exhibits aspects of both elastic and viscous behaviors and is thus classified as a visco-elastic material [31,32]. DSR is a common technique used to study the rheology of asphalt binders at high and intermediate temperatures [33,34]. Operatively, a bitumen sample was sandwiched between two parallel plates, one standing and one oscillatory. The oscillating plate was rotated accordingly with the sample and the resulting shear stress was measured. The linear viscoelastic regime of both the reference free of additives (CTRL), and modified bitumens was checked by preliminary stress sweep tests. The temperature sweep tests were performed within the range 25–80 °C with ramp 1 °C/min in heating by applying the proper stress values to guarantee linear viscoelastic conditions at all tested temperatures. During the tests a periodic sinusoidal displacement at

constant frequency of 1 Hz was applied to the sample and the resulting sinusoidal force was measured in terms of amplitude and phase angle as the loss tangent ($\tan \delta$). RSI Orchestrator[®] software was used to determine the complex modulus (G^*), storage (G') and loss (G'') moduli, phase angle (δ) or $\tan \delta = G''/G'$. More details about the mechanical characterization can be found elsewhere [35].

2.5. Electron Paramagnetic Resonance (EPR) Spectroscopy

Nine GHz EPR (X-band) spectra were recorded on a Bruker Elexys E-500 spectrometer (Bruker, Rheinstetten, Germany). Capillaries containing the samples were placed in a standard 4 mm quartz sample tube containing light silicone oil for thermal stability. The temperature of the sample was regulated at 25 °C and maintained constant during the measurement by blowing thermostated nitrogen gas through a quartz Dewar. The protocol of EPR testing is sketched in Figure 2. The instrumental settings were as follows: sweep width, 120 G; resolution, 1024 points; modulation frequency, 100 kHz; modulation amplitude, 1.0 G; time constant, 20.5 ms. From preliminary power saturation tests, r.f. power levels 0.203 and 0.40 mW selected, respectively, for asphaltene and maltene fractions, were found to be sufficiently low to avoid saturation effects. Several scans, typically 4–16, were accumulated to improve the signal-to-noise ratio. Linewidths were measured from first-derivative curves (peak-to-peak). The spin concentration could be estimated by taking the ratio of area of the sample to that of a standard containing a known number of radicals. Therefore, the concentration of paramagnetic centers in both the asphaltene and maltene fractions of bituminous specimens were obtained by double integration of the experimental first-derivative spectrum and compared with EPR spectrum of a known amount of a MgO-MnO solid solution used as standard [36,37] (spin density = 6.83×10^{15} spin/g). The g -value (Landé factor) was determined from the condition $h\nu = g\beta B_r = g_s\beta B_s$, from which $g = g_s B_s / B_r$ where ν is the frequency of the used microwave radiation, β the Bohr magneton for electron, $g_s = 1.9810$ is the g -value for the standard [38,39], B_s and B_r are the magnetic field values of standard and sample, respectively.

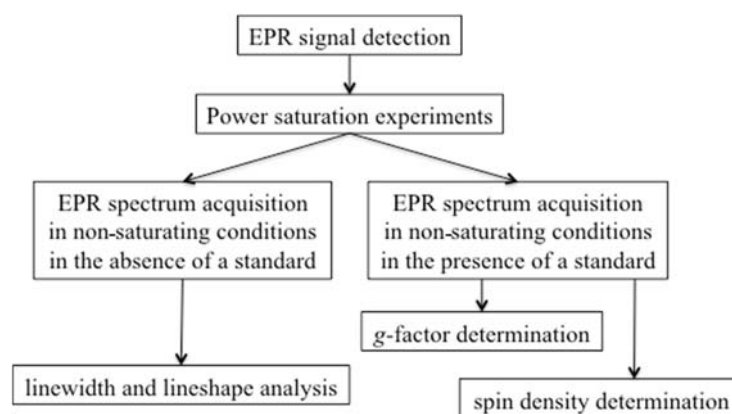


Figure 2. Flowchart of the Electron Paramagnetic Resonance (EPR) test protocol. The preliminary power saturation experiments are necessary to determine the power of the incident microwave beam to be used in the following steps.

3. Results and Discussion

3.1. Mechanical Behavior

Two important parameters are obtained from DSR tests on bitumen: the complex modulus, G^* , and the phase angle, δ . These parameters can be used to characterize both viscous and elastic behavior of the binder [40]. The dependence of these quantities on the temperature gives rise to the so-called time cures. As the temperature increases or frequency decreases, bitumen begins to lose the majority of its elastic behavior (the storage modulus, $G' = G^* \cos \delta$, decreases) and starts to behave as a viscous fluid

(the loss modulus, $G'' = G^* \sin \delta$, increases). Thus, the limiting temperature in correspondence of which $\tan \delta \rightarrow \infty$ identifies the viscoelastic-sol transition temperature T_{TR} above which viscous behavior is highly predominant over elastic mechanical contribution. Figure 3 shows the time cure curves for virgin bitumen and bitumens modified with antioxidant additives and compared to analogous measurements performed after the aging process (RTFOT). Through data interpolation the asymptotic value of $\tan \delta$ intercepts the temperature axis and identifies T_{TR} . Actually, in Figure 3 the temperature difference $\Delta T = T_{TR}(\text{aged}) - T_{TR}(\text{unaged})$ can be read in each graph while the histogram of Figure 4 illustrates a direct comparison of ΔT for all the investigated samples.

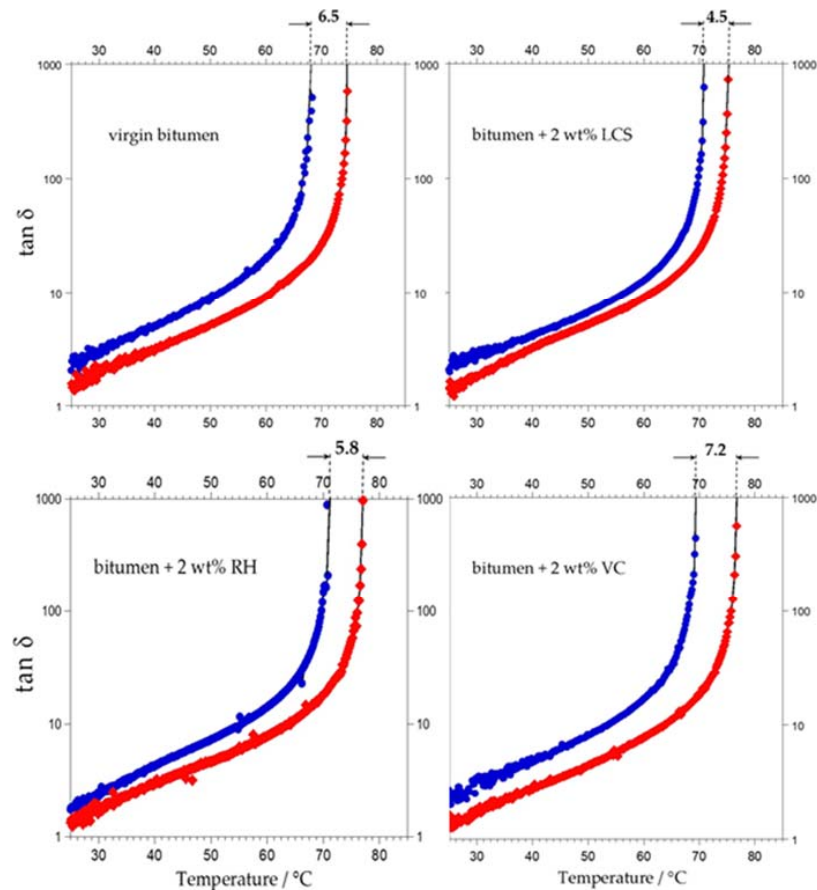


Figure 3. Time cure curves for virgin bitumen and bitumens modified with 2% *w/w* of LCS, RH and VC antioxidant additives, respectively. The increments of viscoelastic-sol transition temperature between aged (red symbols) and unaged (blue symbols) samples are indicated on the top axis of each graph.

Upon addition of 2% *w/w* of anti-oxidants a slight increase of T_{TR} is observed for unaged samples, 69.4 $^{\circ}\text{C}$ (VC), 70.6 $^{\circ}\text{C}$ (LCS) and 71.2 $^{\circ}\text{C}$ (VC) compared to virgin bitumen 68.1 $^{\circ}\text{C}$. The shift ΔT (± 0.2 $^{\circ}\text{C}$ as estimated error) of T_{TR} recorded upon heating treatment respect to the same unaged sample is an indication of an increase in hardening consistency of bitumen, which in turn can be correlated to the oxidation degree occurred in the material. Aging significantly changes both the chemical and physical properties of asphalts, which results in lower elasticity and higher stiffness. In absence of additive a shift of T_{TR} towards higher temperatures has been observed with $\Delta T_{CTRL} = 6.5$ $^{\circ}\text{C}$. Then, the following sequence of ΔT values has been detected for bitumen supplemented with inhibitors of free radicals: $\Delta T_{LCS} = 4.5$ $^{\circ}\text{C}$, $\Delta T_{RH} = 5.8$ $^{\circ}\text{C}$ and $\Delta T_{VC} = 7.2$ $^{\circ}\text{C}$. Those data clearly indicate a superior performance manifested by LCS in retarding oxidative hardening compared to the other tested antioxidants. Hitherto, the use of raw mixtures of natural phospholipids has been confirmed to be a powerful method to increase both the adhesion properties of bitumen [34] and its mechanical

resistance to the action of thermal shocks [41]. Here, the discover of anti-aging properties of LCS adds another advantage of using these green compounds as multi-functional additives to enhance the bitumen performances. The presence of polyunsaturated fatty components in phospholipids providing carbon sites susceptible of oxidation may be responsible for the observed antioxidant activity [42] as it will be also confirmed by the analysis of EPR spectra.

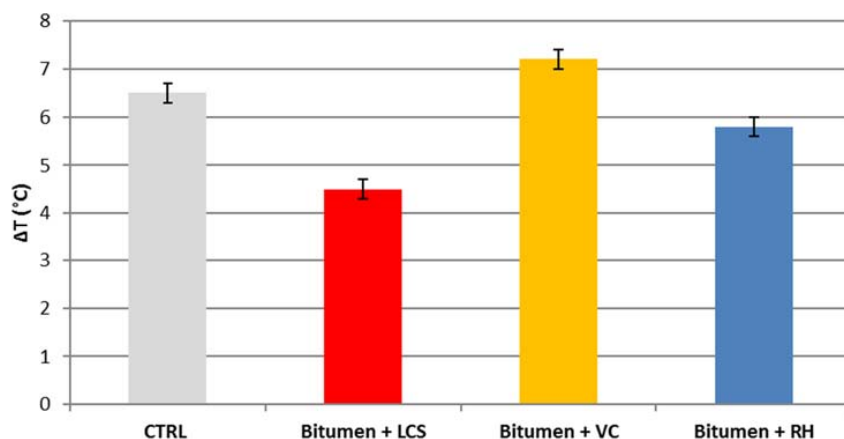


Figure 4. Comparison of $\Delta T = T_{TR}(\text{aged}) - T_{TR}(\text{unaged})$ for the series of investigated samples.

3.2. EPR Spectroscopy Investigation

EPR measurements clearly confirm the presence of unpaired electrons in all the investigated systems, according to previous studies [22,43]. The X-band EPR spectra of the bituminous signals consist of two non-overlapping EPR signals, one centered at about 3480 G due to vanadyl ions (spin 7/2), and the second in a range between 3510 and 3530 G associated to organic radicals (see Figure 5 for the asphaltene fractions).

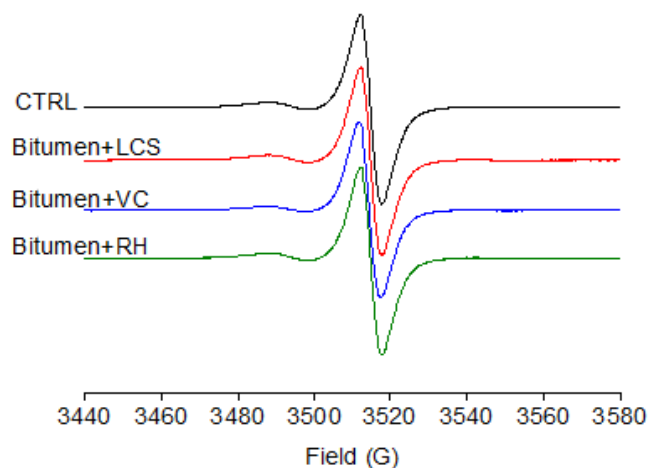


Figure 5. X-band EPR spectra of unaged asphaltene samples mixed with 2% *w/w* of antioxidants registered at room temperature. CTRL indicates the control sample with no antioxidant added.

A complete set of spectra acquired for both the asphaltene and maltene fractions is illustrated in Figure S1 of Supplementary Material. Free radicals associated with non-localized π system, stabilized by resonance in polyaromatic centers, can be studied by EPR spectroscopy owing to the influence of the environment on the radical magnetic properties. Therefore, various parameters can be derived from the analysis of spectra, furnishing different pieces of information, sometimes complementary, sometimes partially overlapping.

3.2.1. The g -Factor

The g -factor (or Landé factor) indicates the magnetic field of resonance (position in the spectrum); it is a parameter sensitive to the chemical environment of the unpaired electron, i.e., to the specific features of the orbital in which it is localized.

The g -factor increases in the presence of heteroatoms, owing to their contribution to the electron molecular orbital. In fact, the heteroatoms shift g to values higher than 2.0023 corresponding to free electron [44]. For all the asphaltene samples, whether unaged or aged, the peak assigned to organic radical gives $g = 2.0027$ – 2.0028 (see Table S1 in Supplementary Material) very close to the free electron value, thus indicating that if present in these radicals, heteroatoms are not likely to participate in the molecular orbital of the unpaired electron to any significant degree. Even for maltene samples, the Landé factor remains substantially constant in the range 2.0025–2.0029 (see Table S1 in Supplementary Material) comparable with that obtained for asphaltene. A weak reduction has been found only in the case of maltene fraction isolated from CTRL upon RTFOT treatment ($2.0028 \rightarrow 2.0025$). The effects of the oxidation process are in fact more evident on the reference system free of antioxidants, which inevitably favors the aggregation and condensation of adjacent units, forming more complex structures. The latter are accompanied by an increase in the level of aromaticity responsible for the shift of g -factor towards lower values. Finally, the g -value for the signal of the vanadyl group does not undergo any variation as a result of the oxidation process for both asphaltene (2.0018–2.0019) and maltene (2.0011–2.0014) fractions analyzed (see Table S1 in Supplementary Material). This condition is in accordance with the fact that in the primary aging process simulated by heat treatment the vanadyl group is not involved in any way.

3.2.2. The Spin Density

Spin concentration is a measure of the number of unpaired electrons in a given amount of sample. Overall, the EPR results show that the spin density of the maltene fraction, in both unaged and aged samples, is around 5% of that determined in the asphaltene phase. This is a further confirmation that the main contribution to the organic radicals detected in bitumen samples comes from unpaired electron in non-localized π system stabilized by resonance in extended polyaromatic macromolecules.

Interestingly, natural antioxidant additives affect the bitumen spin density even in the absence of the aging treatment, just as an effect of mixing. This is specifically true for LCS, the addition of which results in a lower radical content in the asphaltene fraction, ascribable to an effective scavenging action (see Figure 6).

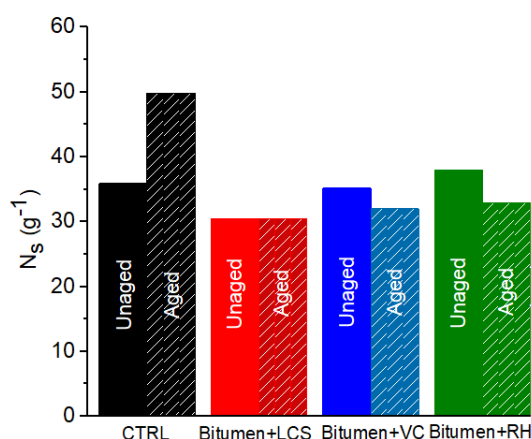


Figure 6. Spin density of asphaltene samples mixed with 2% w/w of antioxidants, as determined from the X-band EPR spectra registered at room temperature. CTRL indicates the control sample with no antioxidant added. Full bars: unaged samples; striped patterned bars: samples artificially aged through the Rolling Thin Film Oven Test (RTFOT) method.

The RTFOT treatment causes a significant increase of the spin density in the CTRL asphaltene sample, and, to a lower extent, in the corresponding maltene fraction. This indicates aging causes an increase in the average size of the polyaromatic asphaltene molecules, thus resulting in a further stabilization of the unpaired electrons in the extended π systems.

The anti-aging effect of natural antioxidant additives can be evidenced by observing the differences in concentration relative to the aged CTRL. In fact, upon the aging treatment, the addition of LCS, VC and RH leads to a reduction in the density of free radicals in asphaltene fraction of 39%, 36% and 34%, respectively (see Table 2).

Table 2. Concentrations of paramagnetic centers N_s determined in asphaltene and maltene fractions obtained both from unaged bituminous samples and after artificial aging through RTFOT. Relative concentration differences with respect to the aged CTRL have been also indicated in brackets.

Sample	Organic Radical Density N_s in 10^{17} Spins \cdot g $^{-1}$			
	Asphaltene		Maltene	
	Unaged	Aged	Unaged	Aged
CTRL	35.9	49.8	2.27	2.68
Bitumen + LCS	30.5	30.5 (39%)	1.92	1.27 (53%)
Bitumen + VC	35.2	32.0 (36%)	1.79	1.36 (49%)
Bitumen + RH	38.0	32.9 (34%)	1.96	2.23 (17%)

In particular, among all the additives tested, LCS is the only one able not only to lower the free radical content of the asphaltenic component in response to the heat treatment to which the bitumen is subjected, but also to keep the spin density unchanged before and after aging stress. The relative antioxidant effect recorded on the maltene fraction is much more pronounced compared to the aged CTRL, showing a strong reduction in the concentration of paramagnetic radicals for bitumens modified, respectively, with LCS (53%) and VC (49%) while the effect of RH is somewhat weaker (17%).

3.2.3. Linewidth and Lineshape

The width of an EPR band is inversely proportional to the lifetime of the absorbing species in its excited state. It depends on the interaction between the unpaired electrons and their surroundings; the greater the interaction, the wider the band. Moreover, for complex and chemically heterogeneous samples, spectrum broadening could be the result of unresolved hyperfine structure; in bitumen samples, broadening of EPR signals due to unpaired electrons delocalized in aromatic π systems could arise from the hyperfine coupling with the adjacent aromatic H atoms [45].

The spectral linewidth is generally quantified by measuring, in gauss (G), the peak-to-peak distance (H_{pp}) of the first-derivative curve, which is the experimental output of the instrument. The (H_{pp}) values determined for the examined samples, collected in Table 3, show that, overall, the linewidth of the organic radical signal is only marginally affected by both aging and antioxidant addition. This indicates that both the molecular structure and the supramolecular organization of the sample do not change. Perusal of the table only reveals a slight narrowing for asphaltene in the presence of the LCS additive, thus suggesting reduced local interactions.

Further information can be obtained from the analysis of the EPR signal lineshape. In general, it is affected by the unresolved hyperfine structure and the anisotropic effects and is classified as either Lorentzian or Gaussian. EPR lines have a trend toward a more Lorentzian character with increasing aromaticity [46]. However, radical species with different relaxation behaviors give rise to independent narrow absorptions, which yield a Gaussian-shaped envelope [46]. The accordance with one lineshape rather than another can be estimated by evaluating the ratio R_n of H_n to H_{pp} where H_n is the width at the position $1/n$ of the peak-to-peak height of the first-derivative curve. For $n = 5$, the expected R_5 values for a Lorentzian and Gaussian lineshape are 1.72 and 1.17, respectively [46].

The peak-to-peak separations of the asphaltene and maltene EPR derivative signals (H_{pp}) and the lineshape ratio $R_5 = H_5/H_{pp}$ are reported in Table 3. It is observed that for both the series of unaged and aged asphaltenic samples, the reference parameter R_5 remains almost constant and intermediate between Lorentzian and Gaussian lineshape, implying that the core size of the polyaromatic clusters remains essentially unchanged upon thermal treatment.

Table 3. Peak-to-peak separation of the derivative peak (H_{pp}) and lineshape parameter (R_5) of EPR spectra of asphaltene and maltene fractions obtained both from unaged bituminous samples and after artificial aging through RTFOT.

Sample	Asphaltene				Maltene			
	H_{pp} (G)		R_5		H_{pp} (G)		R_5	
	Unaged	Aged	Unaged	Aged	Unaged	Aged	Unaged	Aged
CTRL	6.2	5.8	1.4	1.5	5.4	4.9	1.5	1.5
Bitumen + LCS	5.9	5.6	1.4	1.5	5.2	5.3	1.5	1.3
Bitumen + VC	5.9	5.8	1.4	1.4	5.6	5.4	1.4	1.4
Bitumen + RH	5.7	5.7	1.5	1.4	5.7	5.6	1.4	1.4

An exception of this feature regards the unaged sample modified with RH additive, in correspondence of which a significant increment of R_5 is recorded compared to the asphaltene samples of the same series. Considering the maltene fraction, calculated R_5 data are slightly scattered compared to asphaltene, though manifesting the same intermediate character of the signal lineshape. Only for the sample supplemented with LCS a marked Gaussian tendency is observed in response to the aging treatment. In this case, this tendency is probably due to the presence of radical species characterized by quite different (less homogeneous) relaxation times, leading to independent absorptions.

3.2.4. Saturation Curves

Analysis of saturation curves of asphaltene samples shows a typical homogeneous saturation trend, as shown in Figure 7, characterized by the presence of a maximum followed by a decrease of the signal, which indicates the onset of spin saturation process. The homogeneous saturation trend is generally observed when a given set of spins is exposed to the same net magnetic field and has a uniform distribution in space. In fact, decrease of amplitude with increasing microwave power is characteristic for free radicals homogeneously located in the sample. Homogeneous saturation occurs when all free radical spins behave as a single spin system with the same relaxation behavior. In other words, the energy absorbed from the microwave field is distributed to all the spins and thermal equilibrium of the spin is maintained through resonance.

The observed homogeneous saturation is in agreements with the molecular structure of asphaltenes, which can be visualized as polycondensates of a multicomponent system made up of individual molecules of aromatics, paraffins, naphthenics, macrocyclics, and heterocyclics characterized by extensive conjugation and wide electronic delocalization. As illustrated in Figure 7, all the saturation curves are affected neither by the presence of additives nor by the aging process.

Analogous tests have been carried out on maltene samples isolated from both CTRL and bitumen modified with LCS, VC and RH additives, respectively. The correspondent power saturation curves, shown in Figure 8, manifest a definitely more complex trend.

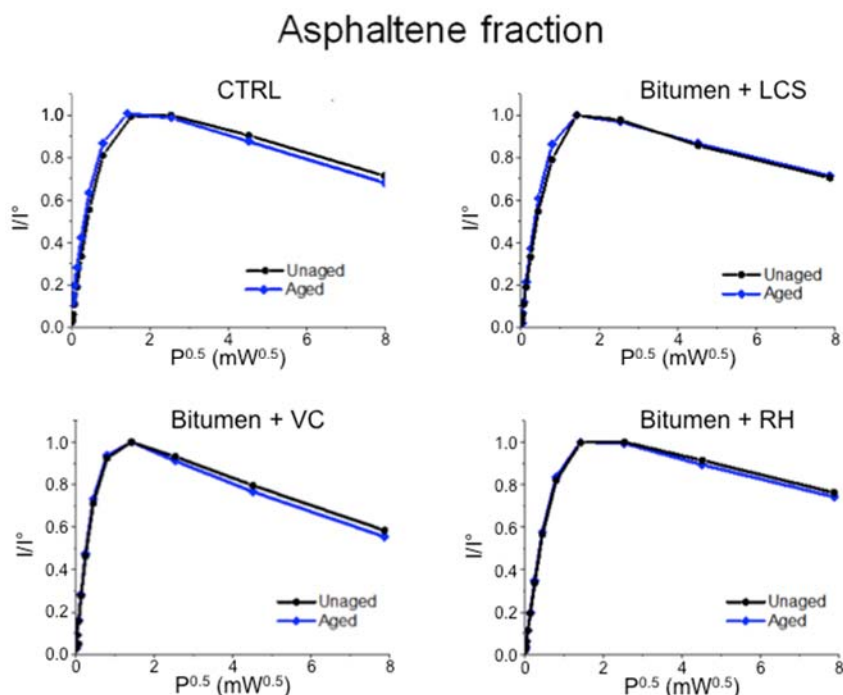


Figure 7. Power saturation profiles for asphaltene samples mixed with 2% *w/w* of antioxidants, as determined from the X-band EPR spectra registered at room temperature. CTRL indicates the control sample with no antioxidant added. Black lines, full circles: unaged samples; blue lines, full diamonds: samples artificially aged through the RTFOT method.

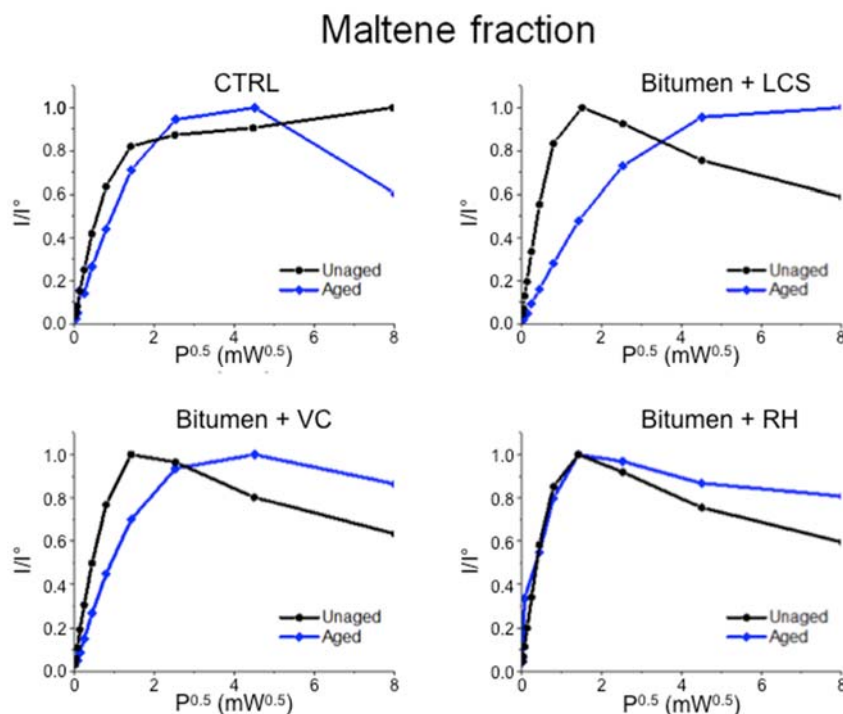


Figure 8. Power saturation profiles for maltene samples mixed with 2% *w/w* of antioxidants, as determined from the X-band EPR spectra registered at room temperature. CTRL indicates the control sample with no antioxidant added. Black lines, full circles: unaged samples; blue lines, full diamonds: samples artificially aged through the RTFOT method.

Maltene phase free of antioxidants shows a heterogeneous trend characterized by the absence of a maximum, which becomes homogeneous by following the simulated aging process in the laboratory, (see Figure 8). This circumstance may occur because aging of bitumen promotes a progressive increase of aromaticity accompanied by a consequent decrease in mass of saturated oils and resins [1]. The presence of antioxidant agents imparts an inversion of trend shown by the reference, i.e., from homogeneous to heterogeneous saturation upon RTFOT treatment. This aspect might be a consequence of a reduced oxidability of the organic matrix due to the antioxidant activity, the efficiency of which qualitatively increases along the series $RH < VC < LCS$.

4. Conclusions

The effectiveness of natural compounds as anti-aging additives in the reduction of age-hardening effect and concomitant bitumen protection against oxidative aging was evaluated by measuring the rheological properties and EPR spectra of asphalt binders in unaged samples and after artificial thermal treatment. Addition of phospholipids turned out to be beneficial in minimizing the shift of viscoelastic-sol transition temperature towards higher values in temperature sweep rheological tests, which is a typical fingerprint of bitumen hardening in response to oxidative phenomena. The apparent scavenging action manifested by phospholipids was confirmed by a lower radical content detected in the asphaltene fraction compared to the reference system as observed by EPR results. An increase of heterogeneity of distribution of radicals in maltene fractions was inferred by the power saturation profiles determined from the X-band of EPR spectra upon addition of natural anti-aging compounds. However, that effect was more pronounced in presence of phospholipids, in a minor degree for vitamin C and even less for rice husk, thus indicating a greater aging inhibitory effect promoted by the former additive. The present study confirmed the usefulness of considering green compounds from renewable resources of reduced carbon footprint as anti-aging additives for bituminous materials.

Supplementary Materials: The following are available online at <http://www.mdpi.com/2076-3417/8/8/1405/s1>, Figure S1: X-band EPR spectra of asphaltene and maltene fractions obtained from bitumen samples mixed with 2% w/w of antioxidants, Table S1: Landé factor (g) of EPR signals of asphaltene and maltene fractions obtained both from unaged bituminous samples and after artificial aging through RTFOT.

Author Contributions: Conceptualization, C.O.R., G.D. and R.A.; Methodology, C.O.R. and G.D.; Validation, P.C. and A.F.; Formal Analysis, C.O.R., S.A., R.A. and G.D.; Investigation, P.C., S.A. and A.F.; Resources, C.O.R. and G.D.; Data Curation, R.A., P.C. and A.F.; Writing-Original Draft Preparation, R.A.; Writing-Review & Editing, G.D.; Visualization, G.D. and R.A.; Supervision, C.O.R.; Project Administration, C.O.R.

Funding: This work was financially supported by KimiCal s.r.l. (Rende, Italy).

Acknowledgments: Marcellino D'Avino is gratefully acknowledged for technical support in EPR experiments.

Conflicts of Interest: The authors declare no conflict of interest.

References

1. Read, J.; Whiteoak, D. *The Shell Bitumen Handbook*, 5th ed.; Thomas Telford: London, UK, 2003; ISBN 10:072773220X.
2. Petersen, J.C.; Glaser, R. Asphalt oxidation mechanisms and the role of oxidation products on age hardening revisited. *Road Mater. Pavement Des.* **2011**, *12*, 795–819. [[CrossRef](#)]
3. Petersen, J.C. A dual sequential mechanism for the oxidation of petroleum asphalts. *Pet. Sci. Technol.* **1998**, *16*, 1023–1059. [[CrossRef](#)]
4. Ling, M.; Luo, X.; Gu, F.; Lytton, R.L. Time-temperature-aging-depth shift functions for dynamic modulus master curves of asphalt mixtures. *Constr. Build. Mater.* **2017**, *157*, 943–951. [[CrossRef](#)]
5. Ling, M.; Luo, X.; Gu, F.; Lytton, R.L. An inverse approach to determine complex modulus gradient of field-aged asphalt mixtures. *Mater. Struct.* **2017**, *50*, 138. [[CrossRef](#)]
6. Lu, X.H.; Isacsson, U. Effect of ageing on bitumen chemistry and rheology. *Constr. Build. Mater.* **2002**, *16*, 15–22. [[CrossRef](#)]

7. Mastrofini, D.; Scarsella, M. The application of rheology to the evaluation of bitumen ageing. *Fuel* **2000**, *79*, 1005–1015. [[CrossRef](#)]
8. Zaidullin, I.M.; Petrova, L.M.; Yakubov, M.R.; Borisov, D.N. Variation of the Composition of Asphaltenes in the Course of Bitumen Aging in the Presence of Antioxidants. *Russ. J. Appl. Chem.* **2013**, *86*, 1070–1075. [[CrossRef](#)]
9. Airey, G.D. State of the art report on ageing test methods for bituminous pavement materials. *Int. J. Pavement Eng.* **2003**, *4*, 165–176. [[CrossRef](#)]
10. Ouyang, C.F.; Wang, S.F.; Zhang, Y.; Zhang, Y.X. Improving the aging resistance of asphalt by addition of zinc dialkyldithiophosphate. *Fuel* **2006**, *85*, 1060–1066. [[CrossRef](#)]
11. Feng, Z.G.; Yu, J.Y.; Zhang, H.L.; Kuang, D.L. Preparation and properties of ageing resistant asphalt binder with various anti-ageing additives. *Appl. Mech. Mater.* **2011**, *71–78*, 1062–1067. [[CrossRef](#)]
12. Apeageyi, A. Laboratory evaluation of antioxidants for asphalt binders. *Constr. Build. Mater.* **2011**, *25*, 47–53. [[CrossRef](#)]
13. Zhao, Z.J.; Xu, S.; Wu, W.F.; Yu, J.Y.; Wu, S.P. The aging resistance of asphalt containing a compound of LDH and antioxidant. *Petrol. Sci. Technol.* **2015**, *33*, 787–793. [[CrossRef](#)]
14. Dessouky, S.; Ilias, M.; Park, D.W.; Kim, I.T. Influence of antioxidant-enhanced polymers in bitumen rheology and bituminous concrete mixtures mechanical performance. *Adv. Mater. Sci. Eng.* **2015**, *2015*, 214585. [[CrossRef](#)]
15. Kassem, E.; Khan, M.S.; Katukuri, S.; Sirin, O.; Muftah, A.; Bayomy, F. Retarding aging of asphalt binders using antioxidant additives and copolymers. *Int. J. Pavement Eng.* **2017**. [[CrossRef](#)]
16. Banerjee, A.; de Fortier Smit, A.; Prozzi, J.A. The effect of long-term aging on the rheology of warm mix asphalt binders. *Fuel* **2012**, *97*, 603–611. [[CrossRef](#)]
17. Sirin, O.; Paul, D.K.; Kassem, E. State of the Art Study on Aging of Asphalt Mixtures and Use of Antioxidant Additives. *Adv. Civ. Eng.* **2018**, *2018*, 3428961. [[CrossRef](#)]
18. Calabi-Floody, A.; Thenoux, G. Controlling asphalt aging by inclusion of byproducts from red wine industry. *Constr. Build. Mater.* **2012**, *28*, 616–623. [[CrossRef](#)]
19. Nahi, M.H.; Kamaruddin, I.; Napiah, M. The utilization of rice husks powder as an antioxidant in asphalt binder. *Appl. Mech. Mater.* **2014**, *567*, 539–544. [[CrossRef](#)]
20. Gawel, I.; Czechowski, F.; Kosno, J. An environmental friendly anti-ageing additive to bitumen. *Constr. Build. Mater.* **2016**, *110*, 42–47. [[CrossRef](#)]
21. Yen, T.F.; Erdman, J.G.; Saraceno, A.J. Investigation of the nature of free radicals in petroleum asphaltenes and related substances by electron spin resonance. *Anal. Chem.* **1962**, *34*, 694–700. [[CrossRef](#)]
22. Chang, H.-L.; Wong, G.; Lin, J.R.; Yen, T.F. Electron spin resonance study of bituminous substances and asphaltenes. In *Asphaltenes and Asphalts*, 1st ed.; Yen, T.F., Chilingarin, G.V., Eds.; Elsevier Science: Amsterdam, The Netherlands, 2000; Volume 2, pp. 229–280. ISBN 9780080868998.
23. Masmoudi, H.; Rebufa, C.; Raffi, J.; Permanyer, A.; Kister, J. Spectroscopic study of bituminous oxidative stress. *Spectrochim. Acta A Mol. Biomol. Spectrosc.* **2004**, *60*, 1343–1348. [[CrossRef](#)] [[PubMed](#)]
24. Premovic, P.I.; Tonsa, I.R.; Pajovic, M.T.; Lopez, L.; Monaco, S.L.; Dordevic, D.M.; Pavlovic, M.S. Electron spin resonance study of the kerogen/asphaltene vanadyl porphyrins: Air oxidation. *Fuel* **2001**, *80*, 635–639. [[CrossRef](#)]
25. Merino-Garcia, D.; Shaw, J.; Carrier, H.; Yarranton, H.; Goual, L. Petrophase 2009 panel discussion on standardization of petroleum fractions. *Energy Fuels* **2010**, *24*, 2175–2177. [[CrossRef](#)]
26. Sirota, E.B. Physical structure of asphaltenes. *Energy Fuels* **2005**, *19*, 1290–1296. [[CrossRef](#)]
27. Lesueur, D. The colloidal structure of bitumen: Consequences on the rheology and on the mechanisms of bitumen modification. *Adv. Colloid Interface Sci.* **2009**, *145*, 42–82. [[CrossRef](#)] [[PubMed](#)]
28. American Society for Testing and Materials. *Standard Test Methods for Separation of Asphalt into Four Fractions*; ASTM D4124-01; ASTM: West Conshohocken, PA, USA, 2001.
29. American Association of State Highway and Transportation Officials. *Standard Method of Test for Effect of Heat and Air on a Moving Film of Asphalt Binder (Rolling Thin-Film Oven Test)*; AASHTO T-240; AASHTO: Washington, DC, USA, 2009.
30. British Standards Institution. *Bitumen and Bituminous Binders—Determination of the Resistance to Hardening under Influence of Heat and Air—RTFOT Method*; EN 12607-1:2007; British Standards Institution: London, UK, 2007. [[CrossRef](#)]

31. Barnes, H.A.; Hutton, J.F.; Walters, K. *An Introduction to Rheology*, 1st ed.; Elsevier Science: Amsterdam, The Netherlands, 1989; ISBN 0444871403.
32. Olsson, U.; Börjesson, J.; Angelico, R.; Ceglie, A.; Palazzo, G. Slow dynamics of wormlike micelles. *Soft Matter* **2010**, *6*, 1769–1777. [[CrossRef](#)]
33. Rossi, C.O.; Spadafora, A.; Teltayev, B.; Izmailova, G.; Amerbayev, Y.; Bortolotti, V. Polymer modified bitumen: Rheological properties and structural characterization. *Colloids Surf. A Physicochem. Eng. Aspects* **2015**, *480*, 390–397. [[CrossRef](#)]
34. Rossi, C.O.; Caputo, P.; Loise, V.; Miriello, D.; Taltayev, B.; Angelico, R. Role of a food grade additive in the high temperature performance of modified bitumens. *Colloids Surf. A Physicochem. Eng. Aspects* **2017**, *532*, 618–624. [[CrossRef](#)]
35. Antunes, F.E.; Gentile, L.; Rossi, C.O.; Tavano, L.; Ranieri, G.A. Gels of Pluronic F127 and nonionic surfactants from rheological characterization to controlled drug permeation. *Colloids Surf. B Biointerfaces* **2011**, *87*, 42–48. [[CrossRef](#)] [[PubMed](#)]
36. Cordischi, D.; Occhiuzzi, M.; Dragon, R. Quantitative EPR Spectroscopy: Comparison between primary standards and application to MgO-MnO and α -Al₂O₃-Cr₂O₃ solid solutions. *Appl. Magn. Reson.* **1999**, *16*, 427–445. [[CrossRef](#)]
37. Muñoz-García, A.B.; Sannino, F.; Vitiello, G.; Pirozzi, D.; Minieri, L.; Aronne, A.; Pernice, P.; Pavone, M.; D'Errico, G. Origin and electronic features of reactive oxygen species at hybrid zirconia-acetylacetonate interfaces. *ACS Appl. Mater. Interfaces* **2015**, *7*, 21662–21667. [[CrossRef](#)] [[PubMed](#)]
38. Yordanov, N.D.; Gancheva, V.; Pelova, V.A. Studies on some materials suitable for use as internal standards in high energy EPR dosimetry. *J. Radioanal. Nucl. Chem.* **1999**, *240*, 619–622. [[CrossRef](#)]
39. Krauss, I.R.; Imperatore, R.; De Santis, A.; Luchini, A.; Paduano, L.; D'Errico, G. Structure and dynamics of cetyltrimethylammonium chloride-sodium dodecylsulfate (CTAC-SDS) catanionic vesicles: High-value nano-vehicles from low-cost surfactants. *J. Colloid Interface Sci.* **2017**, *501*, 112–122. [[CrossRef](#)] [[PubMed](#)]
40. Baldino, N.; Gabriele, D.; Lupi, F.R.; Rossi, C.O.; Caputo, P.; Falvo, T. Rheological effects on bitumen of polyphosphoric acid (PPA) addition. *Constr. Build. Mater.* **2013**, *40*, 397–404. [[CrossRef](#)]
41. Rossi, C.O.; Ashimova, S.; Calandra, P.; De Santo, M.P.; Angelico, R. Mechanical resilience of modified bitumen at different cooling rates: A rheological and atomic force microscopy investigation. *Appl. Sci.* **2017**, *7*, 779. [[CrossRef](#)]
42. Sugino, H.; Ishikawa, M.; Nitoda, T.; Koketsu, M.; Juneja, L.R.; Kim, M.; Yamamoto, T. Antioxidative activity of egg yolk phospholipids. *J. Agric. Food Chem.* **1997**, *45*, 551–554. [[CrossRef](#)]
43. Mamin, G.V.; Gafurov, M.R.; Yusupov, R.V.; Gracheva, I.N.; Ganeeva, Y.M.; Yusupova, T.N.; Orlinkii, S.B. Toward the asphaltene structure by electron paramagnetic resonance relaxation studies at high fields (3.4 T). *Energy Fuels* **2016**, *30*, 6942–6946. [[CrossRef](#)]
44. Calemme, V.; Iwanski, P.; Nali, M.; Scotti, R.; Montanari, L. Structural characterization of asphaltenes of different origins. *Energy Fuels* **1995**, *9*, 225–230. [[CrossRef](#)]
45. Montanari, L.; Clericuzio, M.; Del Piero, G.; Scotti, R. Asphaltene radicals and their interaction with molecular oxygen: An EPR probe of their molecular characteristics and tendency to aggregate. *Appl. Magn. Reson.* **1998**, *14*, 81–100. [[CrossRef](#)]
46. Kwan, C.L.; Yen, T.F. Electron spin resonance study of coal by linewidth and lineshape analysis. *Anal. Chem.* **1979**, *51*, 1225–1229. [[CrossRef](#)]





A New Green Rejuvenator: Evaluation of Structural Changes of Aged and Recycled Bitumens by Means of Rheology and NMR

Cesare Oliviero Rossi¹(✉), Paolino Caputo¹, Valeria Loise¹,
Saltanat Ashimova^{1,2}, Bagdat Teltayev², and Cesare Sangiorgi³

¹ Department of Chemistry and Chemical Technologies,
University of Calabria, 87036 Arcavacata di Rende, CS, Italy
{cesare.oliviero, polino.caputo,
valeria.loise}@unical.it, salta_32@mail.ru

² Kazakhstan Highway Research Institute,
Nurpeisova Str., 2A, Almaty 050061, Kazakhstan

³ DICAM-Roads, Department of Civil, Chemical, Environmental and Materials
Engineering, University of Bologna, V.le Risorgimento 2, 40136 Bologna, Italy
cesare.sangiorgi4@unibo.it

Abstract. The functionality of a green additive, acting as bitumen rejuvenator was considered in the presented experimental work. The additive's effects on aged bitumen have been investigated through advanced rheological and NMR-relaxometry measurements. Bitumen ageing encompasses volatilization and oxidation which enable changes in the material molecular structure. Volatilization occurs mainly at high temperatures during production, transport and laying of the asphalt concrete. The oxidation, also caused by atmospheric oxygen and UV radiation, leads to an increased fragility and development of cracks in the asphalt layer. Fresh, aged, and doped recycled bitumens were tested. Rheology and NMR have been used to assess the structural differences between the bitumens and to understand the role of the proposed additive. A real rejuvenator helps to rearrange the colloidal structure of the oxidized bitumen, thus recreating one similar to the fresh bitumen. As a novel approach to bitumen characterisation, an inverse Laplace transform of the NMR spin-echo decay (T₂) was here applied.

Keywords: Bitumen · Rejuvenator · Nuclear Magnetic Resonance
Rheology

1 Introduction

Bitumen's organic complex are easily oxidized during paving and pavement service life, especially under thermal and/or ultraviolet radiation (UV) conditions (Hu et al. 2018). In general, an aged bitumen has higher reprocessing temperature because some of the aromatic components and resins, which are responsible for a certain grade of mobility, are oxidized to asphaltenes and reduced to saturates. Hence asphaltene micelles become larger so that the fluidity of the system is reduced. Compared with virgin bitumen, the aged bitumen is more brittle and has worse relaxation characteristics that make it

vulnerable to cracking (Baldino et al. 2012). Once removed and processed, bituminous layers become Reclaimed Asphalt Pavement (RAP), which contains valuable asphalt binder and aggregates (Baldino et al. 2017). Over the past decades, researchers have conducted many investigations on the use of RAP materials in the production of recycled asphalt. As a result, rejuvenators are a solution that can be utilized to restore RAP binder properties towards its original state (Dinis-Almeida et al. 2016; Zaumanis et al. 2014). Today, rejuvenators play a crucial role in bitumen recycling methods aiming to an optimized performance of the reclaimed bitumen. Nevertheless, the rejuvenator affects are still not well understood and especially its impact on bitumen's supramolecular structure arrangement has not been fully investigated.

This research describes the physical-chemical characteristics of a new green rejuvenator, using the potentiality of Nuclear Magnetic Resonance (NMR) techniques to identify the main effect of chemicals on the regeneration process of the aged bitumen. The vegetable oils are a common flux for bitumen and many times, the flux of oil action has been mistakenly considered as regenerating operation. This confusion arises from the fact that oils simply soften the hard bitumen to match the macroscopic mechanical parameters according to specific requirements.

2 Experimental Work

2.1 Chemicals, Materials and Sample Preparation

A 100/130 pen virgin bitumen was sourced from Kazakhstan and supplied by Highway Research Institute (Almaty, Kazakhstan). The Vegetable Flux Oil (VO) and the green rejuvenator (HR) were provided by KimiCal s.r.l. (Rende, Italy).

The transformed bitumen was prepared with a high shear mixing homogenizer (IKA model, USA). Firstly, bitumen was heated up to 150 ± 5 °C until it fully flowed, then a given part of HR or VO (2% of the weight) was added to the melted bitumen under a high-speed shear of 400 to 600 rpm/min. Subsequently, the mixture was kept under mechanical stirring at 150 °C for 10 min in a closed beaker to avoid any oxidation process. After mixing, the resulting bitumen was poured into a sealed container and stored in a dark chamber at 25 °C to retain the obtained morphology. The in-service aging of the base bitumen was simulated with the Pressure Aging Vessel (PAV) according to the AASHTO/ASTM T179 standard.

All the prepared mixtures are listed and labelled in the paper as follows: Virgin bitumen: Sample A, PAV bitumen: Sample B, PAV bitumen + 2 wt% VO: Sample C and PAV bitumen + 2 wt% HR: Sample D.

2.2 Rheology, NMR Tests and Inverse Laplace Transform (ILT)

The rheological behavior at different temperatures was investigated by a Dynamic Shear Rheometer (DSR) time cure test at 1 Hz with a ramp rate of 1 °C/min (from 25 °C to 120 °C) within the linear viscoelastic range of the binders.

Relaxation experiments were performed by means of a purposely-built NMR equipment that operates at a proton frequency of 15 MHz. Those experiments were

done at temperatures lower than 15 °C which correspond to the respective temperature transition from viscoelastic to liquid (the temperature is chosen in order to standardize the structure of all samples). Inhomogeneity of field and surface effects usually causes the T_2 relaxation times to vary in the sample (Oliviero Rossi et al. 2015). The T_2 parameter is the spin-spin relaxation time as the relaxation relates to the exchange of energy only among spins and not with the surrounding environment. Hence, if inside the sample a continuous distribution of relaxation time exists, the amplitude A_n of the n^{th} echo in the echo train is given by:

$$A_n = A_0 \int_0^{\infty} P(T_2) e^{-2n\tau/T_2} dT_2 \quad (1)$$

where A_0 is a constant, τ is the half echo time and $P(T_2)$ is the ILT of the unknown function that fits the echo amplitude curve. Furthermore, $P(T_2)$ can be agreed upon as a distribution of rate (inverse of time) constant. $P(T_2)$ can be related to probability density function (PDF) accounting different macro-structures that compose the bitumen binder (Oliviero Rossi et al. 2015). In this work, ILT computation was performed by means of UpenWin (Bortolotti et al. 2009).

3 Results and Discussion

Rheology temperature-sweep tests were performed to collect information on the structural changes induced by temperature, trying to define a transition temperature range better than usual empirical tests (i.e. Ring and Ball) (Baldino et al. 2013). The elastic modulus (G') is continuously monitored during a temperature ramp at a constant heating rate (1 °C/min) and at a frequency of 1 Hz (Fig. 1). The transition temperature is evidenced when G' is plotted as a function of temperature. The initial trend is almost linear with temperature, when the material mainly behaves like a viscoelastic system. The subsequent decrease occurs in correspondence of the transition towards a liquid-like behavior (G' plot disappears).

The aged bitumen (sample B) shows much higher transition temperatures than the unaged fresh material (Romera et al. 2006). This effect is due to an increased fraction of asphaltenes resulted from oxidation processes of the soft unsaturated organic part. The higher asphaltene fraction causes a hardening of the bitumen and higher inner connectivity, if compared to the less dense and weaker network of the virgin bitumen where the asphaltene domains are less connected. Both additives shift at lower temperatures the transitions from the viscoelastic to the liquid material. HR which is a surfactant, shows a stronger effect. Authors believe that its presence might reduce the associative interactions amid the asphaltene particles by interposition between them and the maltenes. As a result, the colloidal network can be weakened, which in turn may correspond to a reduction of the transition temperature.

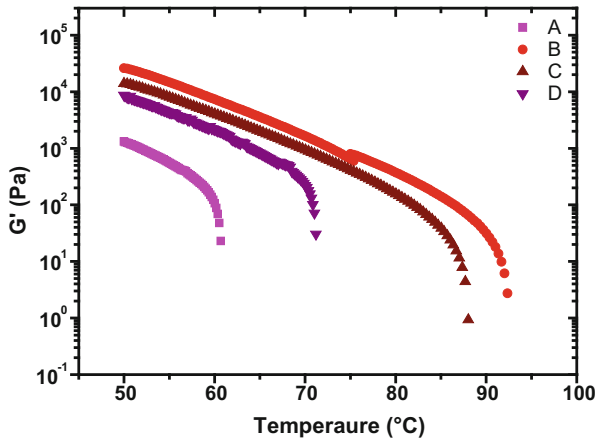


Fig. 1. Semi-log plot of high temperature ramp test for the A, B, C and D samples

3.1 NMR Study

The ILT analysis of the NMR echo signal decay was used to obtain the T2 relaxation time distributions. This technique allows finding the PDF distribution which associates to relaxation times that correspond to unrelated molecular aggregates inside the samples (Gentile et al. 2012). Results are presented in Fig. 2, where the time relaxation distributions PDFs are plotted as a function of the relaxation time. The T2 relaxation time distribution shows two peaks. The shorter T2 times correspond to more rigid supra-molecular aggregates, ascribed to asphaltenes, while longer T2 times are attributed to maltene fractions. For the virgin bitumen, one peak falls around 10 ms and it is due to asphaltene fraction; while the one centered at around 100 ms refers to maltenes.

The ILT of the aged bitumen again exhibits two peaks shifted towards shorter times and present very characteristic shapes. This more likely indicates a gradually increase of the material rigidity with the oxidation process. In particular, the asphaltene peaks are now closer to 1 ms for the aged bitumen. The hard consistency of the samples is strongly affected by the aging processes. During the oxidative aging, the concentration of polar functional groups becomes sufficiently high to immobilize an excessive number of molecules through intermolecular association. What is more, the molecules or molecular agglomerates lose sufficient mobility to flow past one another under thermal or mechanical stresses. The resulting embrittlement of the asphalt makes it susceptible to fracturing or cracking and resistant to healing. This presence of two peaks also supports the colloidal model of the bitumen. All experiments are performed at temperatures lower than 15 °C which is the respective temperature transition from solid to liquid (the temperature is chosen in order to standardize the structure of all samples). On the other hand, it is evident that the addition of VO and HR to the aged bitumen results in the asphaltene peaks shift to longer T2 times. The HR sample shows time distributions similar to the virgin bitumen, although VO simply shifts the distribution to longer times evidencing only its softening action.

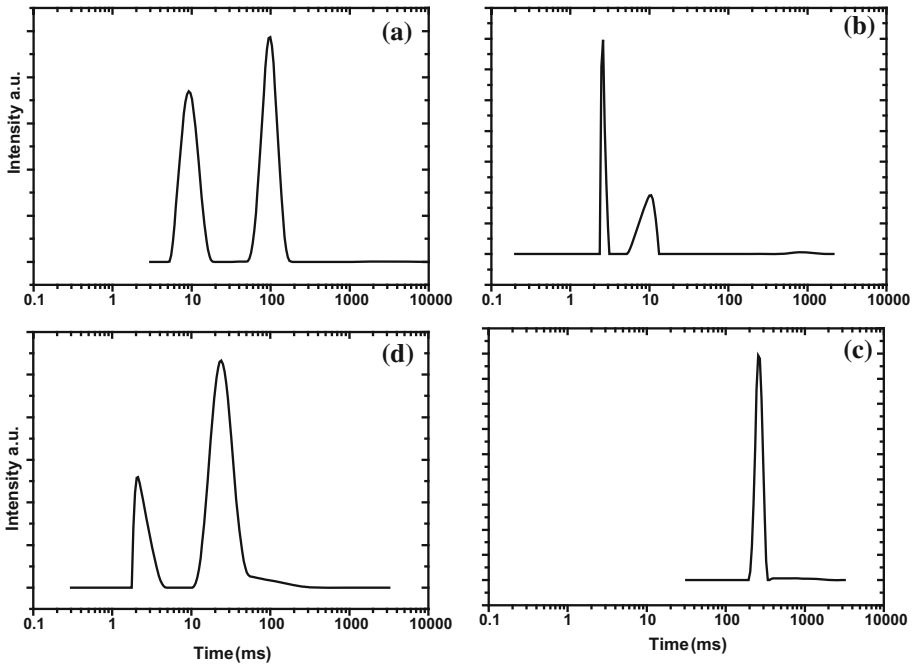


Fig. 2. ILT relaxation time distributions of bitumen samples at 15 °C lower than transition temperature (solid-liquid) determined by dynamic temperature ramp test experiment for each sample

4 Conclusions

This work shows the effectiveness of the HR additive in restoring both bitumen rheological (DSR) and physical (NMR) properties. This green additive tends to restore the mechanical properties of the oxidized bitumen. Moreover, the article aims to demonstrate the importance of testing the regenerated bitumen using structural techniques in order to distinguish between fluxed bitumen and real regenerated compound. Thus, bituminous systems can have alike macroscopic (ring and ball) or rheological properties, but unique supra-molecular structure. The bitumen with flux can be mistakenly considered as a real regenerated one according to the ring and ball test or to other simple rheological investigations.

References

- Baldino, N., Gabriele, D., Lupi, F.R., Oliviero Rossi, C., Caputo, P., Falvo, T.: Rheological effects on bitumen of polyphosphoric acid (PPA) addition. *Constr. Build. Mater.* **40**, 397–404 (2013)
- Baldino, N., Gabriele, D., Oliviero Rossi, C., Seta, L., Lupi, F.R., Caputo, P.: Low temperature rheology of polyphosphoric acid (PPA) added bitumen. *Constr. Build. Mater.* **36**, 592–596 (2012)

- Baldino, N., Oliviero Rossi, C., Lupi, F.R., Gabriele, D.: Rheological and structural properties at high and low temperature of bitumen for warm recycling technology. *Colloid Surf. A* **532**, 592–600 (2017)
- Bortolotti, V., Brown, R.J.S., Fantazzini, P.: *UpenWin: a software to invert multi-exponential relaxation decay data*. Distributed by the University of Bologna (2009)
- Dinis-Almeida, M., Castro-Gomes, J., Sangiorgi, C., Zoorob, S.E., Lopes Afonso, M.: Performance of warm mix recycled asphalt containing up to 100% RAP. *Constr. Build. Mater.* **112**, 1–6 (2016)
- Gentile, L., Filippelli, L., Oliviero Rossi, C., Baldino, N., Ranieri, G.A.: Rheological and H-NMR spin-spin relaxation time for the evaluation of the effects of PPA addition on bitumen. *Mol. Cryst. Liq. Cryst.* **558**, 54–63 (2012)
- Hu, J., Wu, S., Liu, Q., García Hernández, M., Wang, Z., Nie, S., Zhang, G.: Effect of ultraviolet radiation in different wavebands on bitumen. *Constr. Build. Mater.* **159**, 479–485 (2018)
- Oliviero Rossi, C., Spadafora, A., Teltayev, B., Izmailova, G., Amerbayev, Y., Bortolotti, V.: Polymer modified bitumen: rheological properties and structural characterization. *Colloid Surf. A* **480**, 390–397 (2015)
- Romera, R., Santamaria, A., Peña, J.J., Muñoz, M.E., Barral, M., Garcia, E., Jañez, V.: Rheological aspects of the rejuvenation of aged bitumen. *Rheol. Acta* **45**, 474–478 (2006)
- Zaumanis, M., Mallick, R.B., Poulidakos, L., Frank, R.: Influence of six rejuvenators on the performance properties of Reclaimed Asphalt Pavement (RAP) binder and 100% recycled asphalt mixtures. *Constr. Build. Mater.* **71**, 538–550 (2014)

Chapter 9

Effect of high water salinity on the bitumen adhesion properties modified with a smart additive.

Noemi Baldino^{†*}, Ruggero Angelico[‡], Paolino Caputo[□], Domenico Gabriele[†] and Cesare Oliviero
Rossi[□]

[†]Department of Information, Modeling, Electronics and System Engineering, (D.I.M.E.S.)
University of Calabria, Via P. Bucci, Cubo 39C, I-87036 Rende (CS), Italy.

[‡]Department of Agricultural, Environmental and Food Sciences (DIAAA), University of Molise,
Via De Sanctis, Campobasso (CB) 86100, Italy; angelico@unimol.it

[□]Department of Chemistry and Chemical Technologies, University of Calabria, Arcavacata di
Rende (CS) 87036, Italy.

Corresponding author

Dr. Noemi Baldino

Department of Information, Modeling, Electronics and System Engineering (D.I.M.E.S.)

Via P. Bucci – Cubo 39C University of Calabria

I-87036 Arcavacata di Rende (CS), Italy

Email: noemi.baldino@unical.it

Tel. +39 0984 494011; Fax +39 0984 494009

Abstract

Dynamic interfacial tensions between bitumen with three different additives and aqueous salt solution were measured to investigate the salt water effect on the adhesion properties on asphalt in sea areas. In addition, contact angle and boiling water tests were performed to understand the salt effect better. Three different surfactants were used in this work to obtain modified bitumen solutions: a cationic, a nonionic organosilane surfactant and a primary alkyl amine surfactant. Generally, for all the added molecules, the salt had a pejorative effect on the adhesion properties even if the organosilane surfactant looked likely to have the best performance and then it was tested at different salt concentrations. All the dynamic interfacial results were studied and analyzed thanks to the Ward-Torday model and the Graham and Phillips approach, obtaining information about diffusion rate and the potential unfolding/rearrangement phenomena of adsorbed asphaltenes and additives.

Keywords Interfacial tension, salt water, bitumen, interfacial rheology, adhesion promoter.

Introduction

Asphalt roads subjected to salt exposure in coastal areas or salt de-icing in cold regions may suffer serious structural damage with considerable costs for the restoration of the road surface [1, 2]. In fact, seawater can easily invade asphalt pavement structure and salt will be left on the surface of pavement after evaporation. The salt accumulated on the surface of asphalt pavement can cause damage to the asphalt material due to erosion and crystal formation after dehydration. Meanwhile, the durability of roads exposed to winter maintenance practices relies on sodium chloride, the world's most commonly used de-icing salt, which is known to trigger pavement damaging mechanisms. De-icing salt with snow invaded into asphalt concrete will accelerate freeze-thaw

damage and cause the destruction of asphalt pavement. A possible solution to overcome this problem would be to use bitumen modified with smart organic additives capable of rendering the interfacial properties unaltered to the action of salt effect. From the chemical point of view, bitumen is defined as a naturally occurring mixture of hydrocarbons, which may also include compounds of sulfur, nitrogen, oxygen (heteroatoms), metals and other elements [1, 3]. The most commonly occurring components found in crude oils are based on fractions of saturates, aromatics, resins and asphaltenes (SARA-fractions) [4], the latter compounds being also considered active species at the oil-water interface⁵. Other interfacial active components present in a crude oil are naphthenic acids, which refer to an unspecific mixture of different types of carboxylic acids, including both acyclic and aromatic acids [6, 7]. It has been observed that the interfacial tension (IFT) of a pure hydrocarbon versus brine system increases with salt concentration; however, when a small amount of surfactant is present, the IFT can further decrease with salinity[8-10]. The IFT also varies with the type of hydrocarbons. Hence, the interfacial tension of crude oil versus reservoir brine depends on type and concentration of hydrocarbons, salts, and surfactants present in the system. The IFT also depends on temperature and pressure. However, the effect of the aqueous phase chemistry on asphaltenes and interfacial film properties is not yet well understood. While there is considerable data in the literature on the IFT of systems of pure hydrocarbons, surfactants, and water, there is little data on the effect of salt concentration on IFT. It has been reported that, for most crude oils, the interfacial tension decreases with an increase in the salt content [11, 12]. The presence of salt reduces the IFT of the system by accelerating the diffusion rate of surfactant monomers from aqueous phase to oil-water interface, hence enhances the adsorption rate and intensity of monomers at the interface [13-15].

For example, alkali has been used as an injecting fluid which further reacts with the natural acids present in crude oil and forms natural surface acting agents [16, 17].

To the best of our knowledge, a good strategy to make bitumen less prone to be negatively affected by the presence of salt is still lacking in the current research. Therefore, the purpose of the present

study is to benchmark three types of bituminous formulations on the basis of the ability to maintain their adhesive properties unchanged towards the negative side-effect of salt (NaCl). To estimate the strength of adhesion onto the same stony material, the boiling water test was used whose results were compared to contact angle and dynamic interfacial tension measurements.

The selected additives were represented by 1) a cationic surfactant consisting of a quaternary ammonium and a halide ion as a counterion, 2) a non-ionic surfactant carrying an organosilane head group and 3) a primary alkylamino surfactant. In order to distinguish the effect of surfactant–electrolyte interactions from effects caused by the surface active crude oil components, equivalent measurements were conducted for bitumen without added surfactant.

The specificity of the present investigation compared to other analogous studies published in the specific literature, consists with the fact that the tested surfactants were pre-mixed into the crude oil phase rather than the aqueous phase, as reported by the totality of the works focusing on the effects of salinity and surfactants on the adhesion properties of the water / crude oil interface.

Materials and Methods

A. Samples preparation

The twice-distilled water used throughout all the experiments was obtained from a Milli-Q purification system (Millipore, USA), and it was checked for contaminants before each experiment, measuring the surface tension of the buffer solution at the air/water interface at room temperature. No aqueous solution with a surface tension other than the value commonly accepted in the literature (72 - 73 mN/m at 20° C) was used [18]. The salt aqueous solutions were prepared adding NaCl (Sigma Aldrich, 99.8% purity) at concentrations 1, 3 and 6 wt/wt %, respectively. Light brown bitumen, produced in Saudi Arabia and supplied by Total SpA (Italy), having the composition reported in Table 1, was divided into four aliquots one of which used as a control “Bit(ctrl)”. The remaining three fractions were mixed separately with the following additives at 0.1 wt/wt %: a

cationic surfactant (CTAB, CetyTrimetylAmmonium Bromide, from Sigma Aldrich - additive A), a nonionic organosilane (P2KA[®] from Kimical srl, Italy - additive B) mainly used as adhesion promoter, and a primary alkyl amine surfactant (from Sigma, Milan additive - C). The resulting mixtures were identified, respectively, with “Bit(A)”, “Bit(B)” and “Bit(C)”. Because bitumen at room temperature is a black visco-elastic material, it was necessary to reduce the bitumen viscosity to allow the interfacial tension measurements to be taken by a pendant drop tensiometer. Then the bitumen was diluted at 20 wt/wt % in soybean oil (SO) furnished by Baldini srl (Italy), obtaining what is generally called fluxed bitumen (henceforth “Bit-SO”) [19].

Sample	Area % (± 0.1)
Saturated	3.8
Aromatics	51.3
Resins	21.5
Asphaltenes	23.4

Table1. Group composition of the pristine bitumen.

The stone materials were natural mineral chips and were kindly furnished by the laboratory of civil engineering of Prof. R. Vaiana, University of Calabria (Italy).

B. Interfacial tension and Contact angle measurements

Axisymmetric Drop Shape Analysis (ADSA) was used to obtain interfacial tension γ (mN/m) and contact angle α by using an automated pendant drop tensiometer (FTA200, First Ten Angstroms, USA) equipped with the fta32 v2.0 software. Details of this apparatus are given by Biresaw et al. [20]. All the experiments were carried out at room temperature ($22 \pm 1^\circ$ C), placing the aqueous solutions in a 100 ml glass Hamilton syringe (1710TLL) equipped with a 20 Gauge stainless steel

needle, and forming the bituminous drops in a rectangular quartz cuvette (5 ml) containing the desired phase according to Seta et al.[18]. Thus, ca. 8 μ l drop volume of bituminous material was used in every test in order to measure γ values independent of the drop size and the drop profile was monitored up to a maximum time of 70 min to guarantee a quasi-equilibrium γ_{eq} value, when possible. For some systems, a quick decay of γ vs. time was observed without reaching a true γ_{eq} , owing to the rapid detachment of the drop. The control Bit-SO was subjected to dynamic γ measurements in contact with both pure water (Bit-SO / PW) and salt water at 6 wt/wt % of NaCl (Bit-SO / SW-6%), respectively. Likewise, the bituminous mixtures modified by adding 0.1 wt/wt % of additives, were diluted to 20 wt/wt % in SO and classified as “Bit(A)-SO”, “Bit(B)-SO” and “Bit(C)-SO”, respectively. They were subjected to analogous measurements to verify the effect of the additive on γ in the presence of both PW and SW with 6 wt/wt % of salt, respectively. In particular, Bit(B)-SO was also tested with aqueous solutions at different NaCl contents, namely, SW-1% and SW-3%. Contact angles α at the three-phase contact line (inert stone/Bit(X)/air, with X = ctrl, A, B and C), were measured by fitting a mathematical expression to the shape of the drop and then calculating the slope of the tangent to the drop at the liquid-solid-vapor (LSV) interface line. All experiments were carried out at room temperature (22 ± 1 °C) and according to the protocol described in detail previously [21]. Contact angles, averaged over three measurements for each sample, are illustrated in Table 2.

Sample	% coating after boiling ± 5		Contact angle α (°)	
	PW	SW-6%	PW	SW-6%
Bit(ctrl)	5	< 5	n.d.*	n.d.*
Bit(A)	20	5	n.d.*	n.d.*
Bit(B)	90	85	61.3 \pm 1.3	38.9 \pm 4.0

Bit(C)	95	60	37.5±0.4	51.1±2.2
--------	----	----	----------	----------

*After boiling, deposited bituminous sample was lost due to absence of adhesion onto the stones.

Table 2. Percentage of bitumen coating retained after boiling test, respectively, in pure water (PW) and salt water at 6 wt/wt % of NaCl (SW-6%) for pristine bitumen, Bit(ctrl), and bitumen modified with additives A, B and C. The latter two columns report a comparison between the contact angle measured after boiling tests in PW and SW-6 wt%, respectively.

C. Boiling water test

Boiling tests were performed by using mineral aggregates with size ranging from 8 mm to 12mm. The boiling test procedure applied in this study was according to ASTM D3625 [22]. The stones were characterized by double chemical nature (50 wt % acid based- and 50 wt % basic based-stones) corresponding to the composition usually found in most asphalt cements. In detail, hot mixtures of bitumen and stones were prepared and then left to cool for at least 12 h before being divided into pairs of equal portions by weight. They were boiled for 10 min, one portion in distilled water and the other in salt water at 6 wt/wt % of NaCl. Then, they were left to cool to r.t., the water left to settle and the samples spread to dry on a paper towel. The degree of bitumen coverage in % was rated by visual observation. An illuminated magnifying glass was used to examine samples. The average of the ratings was rounded to the nearest 5%. The results are illustrated in Table 2.

Results and Discussion

Transient interfacial tension (IFT)

The variation of interfacial tension, γ , with time is known as dynamic interfacial tension (IFT) [23, 24]. When an aqueous-based solution is placed in contact with an opposing phase such as a crude oil, a finite time is required for the water-insoluble polar components and surface active species to diffuse, adsorb at the interface, and reach the equilibrium value [25]. In particular, for the investigated systems the decay of IFT as a function of molecular diffusion and time-dependent reorganization at the interface can give information on the role played by different additives at pure-water (PW) or salt-water (SW) interfaces as well as on the effect of surfactant active species present in bitumen diluted with soybean oil (Bit-SO), eventually. For most of the examined systems, a true plateau value of IFT, *viz.* adsorption equilibrium, could not be observed owing to the premature detachment of the drop.

Figures 1-3 illustrate the surface tension time-dependence for the different systems analyzed. Figure 1 shows the decrease of IFT for the control in the absence of additives (Bit-SO) in contact with pure water and salt water (6 wt/wt % of NaCl), respectively. For the former system, a decrease of γ with time is observed from 24 mN/m at $t = 0$ until the equilibrium value 5.9 mN/m, whereas the effect of salinity promotes a more rapid decay from 15 mN/m towards a pseudo-equilibrium value of 3 mN/m.

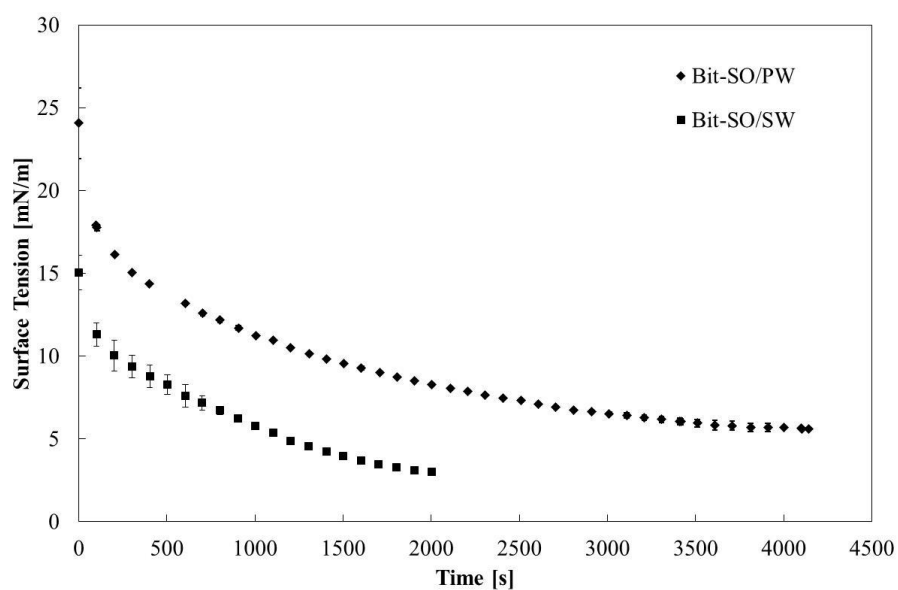


Figure 1. Dependence of dynamic surface tension on the interface age for bitumen diluted with soybean oil (Bit-SO) in contact with pure water (PW) and salt water (SW, 6 wt/wt % of NaCl), respectively.

Figure 2 illustrates the decrease of IFT observed for Bit-SO in the presence of different additives premixed in the bituminous fluid. For both PW (Figure 2A) and SW (Figure 2B) contact interfaces, the trend $\gamma_C < \gamma_A < \gamma_B < \gamma_{ctrl}$ is always respected, where the shortest time-range (< 30 s) is detected in the presence of additive C, *viz.* alkyl amine surfactant, owing to the very rapid detachment of the droplet from the needle.

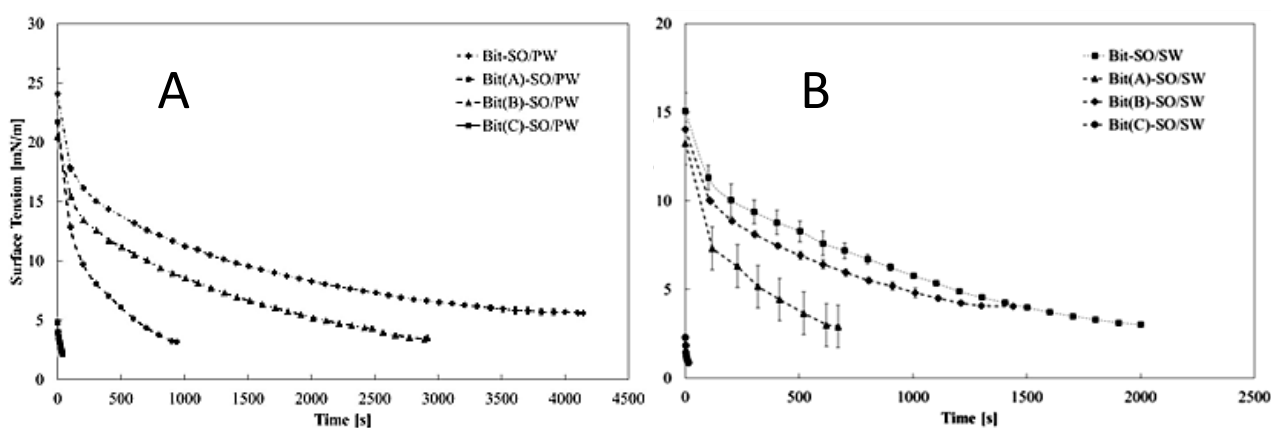


Figure 2. Surface tension decays for bitumen premixed with three different additives and diluted with soybean oil: Bit(A)-SO, Bit(B)-SO and Bit(C)-SO in contact, respectively, with pure water PW (A) and salt water SW at 6 wt/wt % of NaCl (B). The Data for the control system in the absence of additives (Bit-SO) are shown for comparison. Different axis scales are displayed for both the plots.

Moreover, a direct comparison between both series of measurements (Figure 2A vs. 2B) reveals that the presence of salinity is able to induce a more pronounced and rapid reduction of all measured

surface tension values (note the different scales adopted for the axes of both graphs). Then, a further investigation was carried out to test the dependence of transient IFT on the concentration of water salinity. This effect was checked only for Bit(B)-SO, that is, the bitumen-additive combination that has been proved to be the most performing oil-wettable binder of inert stones after immersion in salt water, as will be illustrated below. Figure 3 shows that with increasing the NaCl concentration in the aqueous phase in contact with Bit(B)-SO, the kinetics process of approaching the asymptotic IFT value becomes increasingly steep to such an extent that the drop detaches from the needle at the highest percentage of salt (see Figure 3).

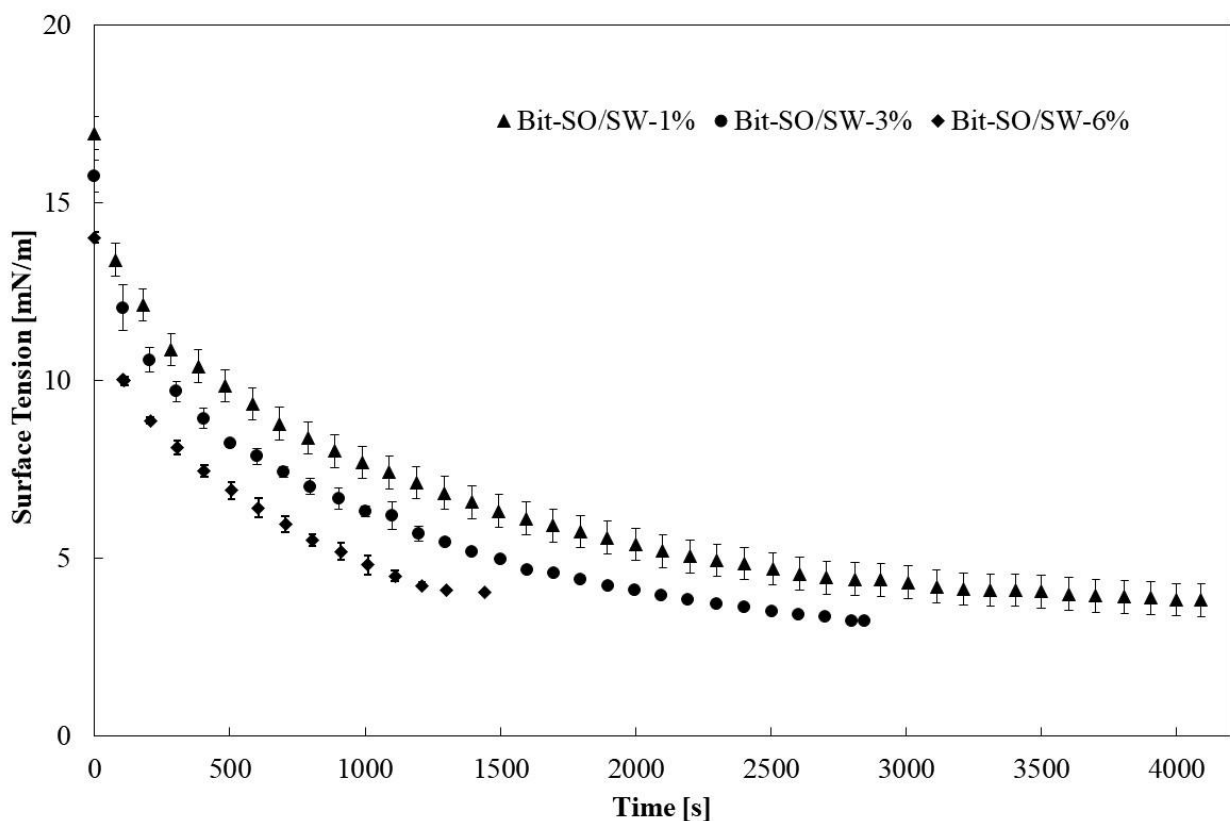


Figure 3. IFT trend for bitumen premixed with additive B (nonionic organosilane surfactant) and diluted with soybean oil, Bit(B)-SO, in contact with salt water (SW) at different NaCl concentrations 1, 3 and 6 wt/wt %, respectively.

Boiling test and contact angle measurements

The boiling tests and three-phase contact angles crude oil-stone-air, were determined to evaluate the effect of preconditioning in boiling salt water (SW) at 6 wt/wt % NaCl on the adhesion properties of both the pristine binder Bit(ctrl) and the bituminous samples modified, respectively, with additives A, B and C. A parallel study was carried out using pure water (PW) as a reference test.

Regarding the boiling test, the percentage of bitumen coverage onto the stones after immersion in boiled SW for 10 min, decreased in the order Bit(B) > Bit(C) >> Bit(A) \approx Bit(ctrl), as shown in Table 2. In relative terms, by comparing both the treatments in PW and SW, bitumen modified with the nonionic P2KA[®], Bit(B), yielded superior performance respect to the sample modified with the alkylamino surfactant, Bit(C). Concerning the three-phase contact angle, a noticeable result was found again with Bit(B), for which the effect of salt water led to an increase in the oil-wettability onto the stones ($\Delta\alpha = -22.4^\circ$), where $\Delta\alpha = \alpha_{SW} - \alpha_{PW}$. While an opposite tendency ($\Delta\alpha = +13.6^\circ$) occurred for the sample with the type C additive, as illustrated in Figure 4. For Bit(A) as well as the control without additives Bit(ctrl), the measurement of contact angle failed due to a total absence of adhesion onto the stones, regardless of PW or SW as aqueous contact phase.

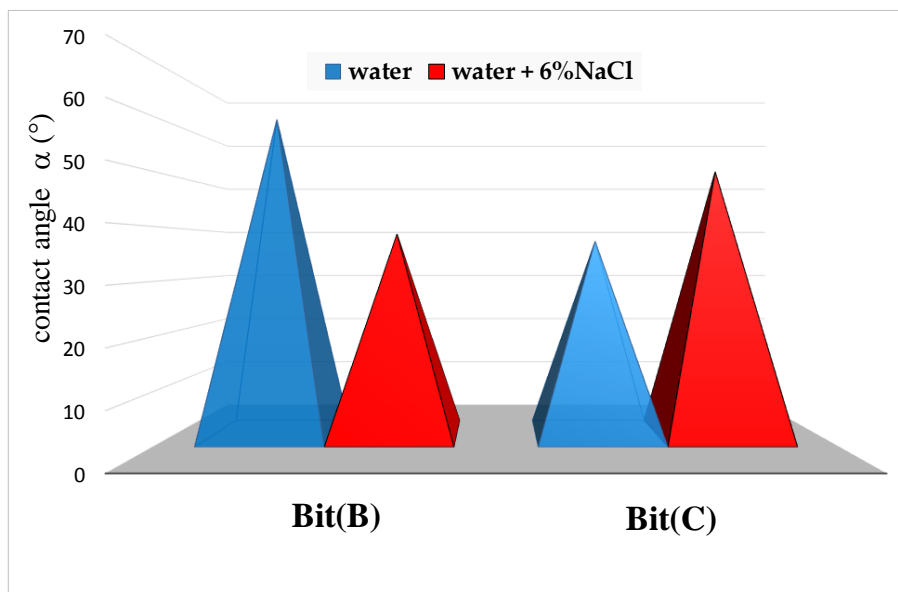


Figure 4. Change of contact angle α at interface, Bit(X)-stone-air, for X = B and C additives after soaking in distilled water and salt water (6 % NaCl), respectively.

General Discussion

The time dependence of interfacial tensions, IFT, between the crude oil, diluted with soybean oil SO, and either distilled water or water + NaCl (6 wt/wt %), was measured with the pendant drop technique in order to investigate the effect of the tested additives premixed in bitumen on the dynamics of interfacial tension, IFT. First, it should be noted that the bitumen components themselves exhibit a certain degree of surface activity. For instance, there is a lot of scientific literature about the effect of asphaltene (the bituminous polar fraction soluble in aromatic solvents comprising polyaromatic nuclei linked by functional groups), on the IFT although is still not well understood (see, e.g. ref. [5] and references therein). Some authors found that asphaltenes do not have effect at the interface as surfactants [26], while others have confirmed that they are able to adsorb at the water-oil interface, lowering the IFT in the same manner as surfactants [6, 27, 28]. In addition, both resins (the bituminous fraction soluble in aliphatic solvents) and asphaltenes have been found to exert synergistic effects [29, 30].

For our control system, i.e., in the absence of additives, the results shown in Figure 1 confirm that NaCl has a pronounced effect on the IFT. The dissociation of acidic components (e.g. naphthenic acids) present in pristine bitumen is enhanced by the presence of electrolytes in water, which in turn leads to a further accumulation of ionic species at the interface and, hence, a concomitant reduction of surface energy is observed, in agreement with other studies in the literature [23, 31]. The decrease of surface energy arises from a reduction in electrostatic repulsion due to the screening effect of NaCl, because salt provides additional counterions surrounding the interface and accelerates the diffusion of surface active components from the bulk to the interface [14]. This dynamic behaviour prior to an eventual equilibrium can be driven by several mechanisms, including migration to the interface controlled by molecular diffusion, adsorption and reorientation at the interface, and exchange of surface active components between the bulk immiscible phases [18, 32, 33]. For instance, in crude oil systems, it has been reported that after rapid diffusion of asphaltenes to the interface, a long reorganization phase with a progressive build-up of multilayers occurs [34, 25]. The relative rates of the various steps ultimately decide the profile for the dynamic interfacial tension. Such a kinetic process has been widely described by the Ward-Tordai model in many applications [18, 36-38]. Then, at low surface pressure, the Ward-Tordai modified equation [39] can be used to describe the diffusion process of the different species:

$$\pi = C_0 K T \left(\frac{D_{dif} \cdot t}{\Pi} \right)^{\frac{1}{2}} \quad (1)$$

where π is the interfacial pressure at any time t , C_0 is the bulk concentration of surface-active species, K is the Boltzmann constant, T the absolute temperature, D_{dif} the diffusion coefficient and Π the Pi Greco value. When plotting the interfacial pressure as a function of $t^{1/2}$, a diffusion rate (k_D) can be obtained [18, 40]. Typical trends of surface pressure, π , at the pure water interface for

crude oil diluted in soybean oil (Bit-SO/PW) and bitumen modified by adding 0.1 wt/wt % of additive B, Bit(B)-SO/PW, are shown in Figure 5.

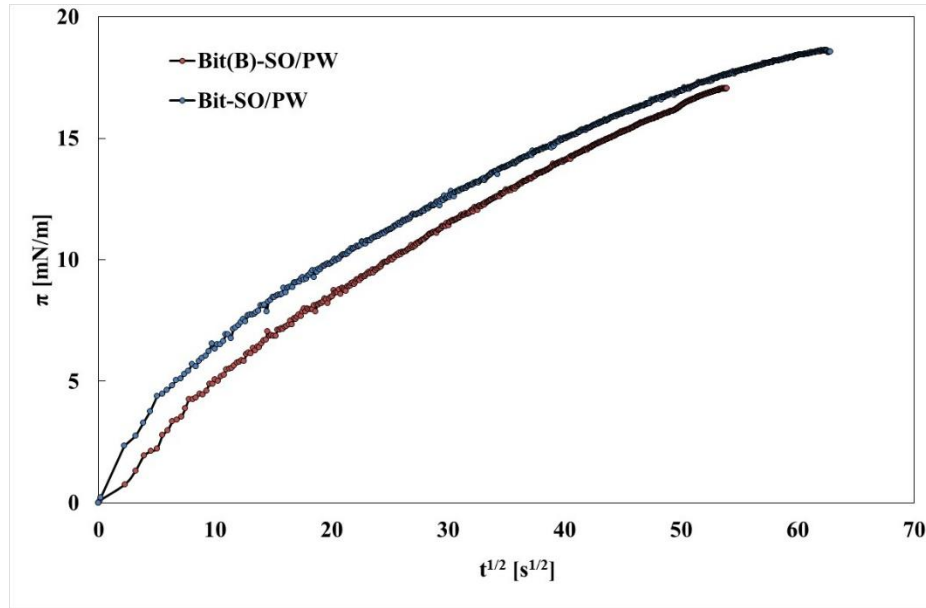


Figure 5. Temporal evolution of surface pressure, π , at the crude oil-PW interface for the systems Bit(B)-SO and Bit-SO, respectively. Data are reported as a function of square root of time, $t^{1/2}$, according to Eq. (1). Error bars are not reported to make the figure more readable; the standard error was computed over three repetitions and was lower than 10%.

In accordance with the literature on biopolymer interfacial behavior [18, 38, 41], the unfolding/rearrangement phenomena of adsorbed asphaltenes and additives were evaluated by a semi-empirical first-order equation, determining the rate constant, k_i :

$$\ln \frac{\pi_f - \pi_t}{\pi_f - \pi_0} = k_i t \quad (2)$$

Where π_f , π_0 and π_t are the surface pressure at the end of the adsorption process, at $t = 0$ and at any time t , respectively. The application of Eq. (2) can evidence, depending on the specific system, the potential presence of two linear regions with different slopes: the first one is related to the

molecular adsorption, whereas the second is related to the rearrangement of adsorbed molecules [16- 18].

Therefore, two different kinetic constants (k_{ads} and k_{rear}) associated, respectively, with the adsorption and rearrangement phenomena, were evaluated by applying Eq. (2) to our systems where possible, and the results are reported in Table 3.

The diffusion rates (k_D) are reported in Table 3, and they were computed from data at low surface pressure ($\pi < 10$), corresponding to the initial period where the diffusion of the additives and/or asphaltenic compounds may constitute the predominant phenomenon. For the control system without additives, it is possible to observe that the presence of NaCl in water enhances the migration of surface active compounds at the interface as evident from the higher value of k_D and from the reduction of the diffusion time (t_{diff}), value up to which the pressure is less than 10 mN/m [25]. For the considered reference system (Bit-SO), the salt effect is reflected in an increase of both k_{ads} and k_{rear} values as well. As discussed before, an increase in the diffusion velocity in the presence of electrolytes can be attributable to a higher dissociation of acidic components, which in turn is responsible for the enhanced IFT reduction observed for the sample in contact with salt water. The presence of salt is able to provide additional counterions at the interface in much higher concentrations than H^+ ions present in pure water, thus avoiding large differences between the bulk and interfacial pH, and promoting the dissociation of acidic components.

Sample	k_D (mN/m s ^{-0.5})	t_{diff} (s)	k_{ads} (s ⁻¹)·10 ³	k_{rear} (s ⁻¹) 10 ³
Bit-SO/PW	0.348±0.003	650±1	1.05±0.10	3.2±0.1
Bit-SO/SW	0.525±0.001	45±1	1.45±0.17	5.1±0.1
Bit(A)-SO/PW	0.801±0.002	164±1	3.05±0.10	6.0±0.1
Bit(A)-SO/SW	0.504±0.023	232±3	4.70±0.10	23.9±0.9

Bit(B)-SO/PW	0.356±0.020	635±50	1.05±0.10	3.4±0.4
Bit(B)-SO/SW	0.245±0.003	1258±19	-	-
Bit(C)-SO/PW	0.435±0.017	40±1	-	-
Bit(C)-SO/SW	0.429±0.024	12±4	-	-
Bit(B)-SO/PW – 1%	0.260±0.001	1162±44	1.2±0.1	3.1±0.3
Bit(B)-SO/PW – 3%	0.263±0.007	1180±220	2.1±0.1	2.7±0.2

Table 3. Diffusion (k_D), adsorption (k_{ads}) and rearrangement (k_{rear}) rates calculated from Eqs.(1)-(2) for the crude oil systems diluted with soybean oil (SO) with or without additives A, B and C in contact with either pure water (PW) or salt water at 6 wt/wt % of NaCl (SW). Further data have been derived for Bit(B)-SO at different salt concentrations (1 and 3 wt/wt %).

Influence of additives on the oil-water IFT

When the tested additives are used, IFT values are found to be highly decreased compared to those of pristine bitumen in contact with either pure water or brine. However, looking at the behavior of the sample with C additive, *viz.*, the surfactant carrying a protonable amino group in its polar head, it is observed that k_D remains unaffected by the presence of electrolytes in the water phase. Moreover, since IFT decreases from low initial values (4.8 and 2.3 mN/m for PW and SW, respectively, at $t = 0$), a premature and rapid detachment of the drop from the needle is observed for Bit(C)-SO in contact with either PW or SW. Accordingly, the kinetic parameters associated with slower relaxation processes, such as adsorption (k_{ads}) and rearrangement (k_{rear}), could not be determined by Eq. (2). The fast kinetic decay can be explained in terms of ionic couples produced by acid-base reactions between naphthenic acids and the weak basic groups of surfactant C monomers. This would make the effect of salinity on the IFT reduction less relevant than expected.

Indeed, rapid formation at the interface of organic salts or other supramolecular structures as micelles/complexes [42] would lead to a more efficient screening of the electrostatic repulsion than the case previously discussed for the reference system (Bit-SO/SW). The ability manifested by additive C to significantly lower the oil-water IFT, regardless of the presence or absence of salt, indicates that the oil wettability of inert stones would be somewhat altered, as confirmed by boiling tests and contact angle data illustrated in Table 3, which definitively represents an undesirable effect. As concerns the samples with the additives A and B, respectively, quaternary ammonium chloride surfactant and a nonionic organosilane, a different behaviour is observed. Both the samples show a decrease in the diffusion rate with a corresponding increment of t_{diff} when the salt is added to the system. Moreover, for the sample with additive B in the presence of salt water, the diffusion is the only step during our observation time. Evidently, the presence of organosilane surfactant could favor a better dispersion of asphaltenic aggregates with consequent reduction of their average dimensions, which in turn would increase the rate of initial adsorption process controlled by diffusion. However, the most striking result comes from the change of the three-phase contact angle after inert stones wetted by Bit(B), were subjected to the action of hot salt water compared to hot pure water. Indeed, a variation of $\Delta\alpha = -22.4^\circ$ promoted by the addition of the organosilane P2KA[®] to bitumen, well underlines the beneficial effect of this additive in increasing the wettability of crude oil onto rocks, even in extreme conditions caused by the contact with very salty water. Since it is assumed that electrolytes do not interact with a nonionic surfactant, a less ionic character of the interface, owing to the supposed presence of organosilane, could give rise to a thickening of the electric double layer thus working in the opposite direction compared to additive A (no oil wetting at all), and in a minor extension to C ($\Delta\alpha = +13.6^\circ$ in Figure 4). As can be observed in Table 3, the diffusion rate increments with increasing salt concentration (Figure 3), as expected, and for the system with only 1 % wt/wt of salt, a small difference between the pure and salt interface is detected during the rearrangement in an adsorption period. By increasing the salt level, the adsorption rate doubles, even if no increment is observed in the rearrangement velocity. And at the

end, when the salt quantity reaches 6 % wt/wt only the diffusion period is observable. The peculiar adhesion properties triggered by P2KA[®] once mixed in very low amounts to bitumen have also been ascertained in recent published works [21, 43] and reviews [44].

Conclusion

Experimental investigations were conducted to elucidate the performance of some types of additives mixed to bitumen in tiny amounts, in order to search for the best adhesion performances onto stones in contrast to the deleterious action of water with high salinity. Dynamic interfacial tension measurements demonstrated that the effect of water salinity on the surface energy can be noticeably influenced by the type of additive mixed to crude oil. In particular, the additive carrying an amino group in its polar head was able to reduce the water-crude oil interface very fast and made stones less oil-wet than the organosilane-based additive, a well-tested adhesion promoter, which instead showed an improved oil-wettability once in contact with salt water. The use of a quaternary ammonium chloride surfactant gave an even worst result, making the stone material completely not oil-wet after the treatment in hot salt water.

For practical cases, where it is desirable or required that the addition of adhesion promoters does not significantly alter the wettability properties of bitumen when subjected to the action of salt water, the organosilane-based additive confirms its fulfilment of this requirement.

Acknowledgements

Acknowledgments are due to Dr. Olga Mileti for the rheological measurements.

References

1. Feng, D. C.; Yi, J. Y.; Wang, D. S.; Chen, L. L., Impact of salt and freeze-thaw cycles on performance of asphalt mixtures in coastal frozen region of China. *Cold Reg. Sci. Technol.* (2010) 62 (1), 34-41.
2. Hassan, Y.; El Halim, A. O. A.; Razaqpur, A. G.; Bekheet, W.; Farha, M. H., Effects of runway deicers on pavement materials and mixes: Comparison with road salt. *Transp. Eng. J. ASCE* (2002) 128 (4), 385-391.
3. ASTM, A. D., Standard Terminology Relating to Petroleum, Petroleum Products, and Lubricants. In *Annual Book of Standards, A.S.f.T.a. Materials*, for, A. S.; Materials, T. a., Eds. Philadelphia, PA, 2005.
4. Speight, J. G., Part 1: History and Terminology. In *The Chemistry and Technology of Petroleum*, Raton, B., Ed. CRC press: 2014; pp 3-174.
5. Langevin, D.; Argillier, J. F., Interfacial behavior of asphaltenes. *Adv. Colloid Interface Sci* (2016) 233, 83-93.
6. Havre, T. E.; Sjoblom, J.; Vindstad, J. E., Oil/water-partitioning and interfacial behavior of naphthenic acids. *J. Dispersion Sci. Technol.* (2003) 24 (6), 789-801.
7. Hutin, A.; Argillier, J. F.; Langevin, D., Mass Transfer between Crude Oil and Water. Part 1: Effect of Oil Components. *Energy Fuels* (2014) 28 (12), 7331-7336.
8. Heimenz, P. C.; Rajagopalan, R., *Principles of Colloid and Surface Chemistry*. 3rd ed.; New York, 1997.
9. Cai, B. Y.; Yang, J. T.; Guo, T. M., Interfacial tension of hydrocarbon plus water/brine systems under high pressure. *J. Chem. Eng. Data* (1996) 41 (3), 493-496.
10. Prosser, A. J.; Franses, E. I., Adsorption and surface tension of ionic surfactants at the air-water interface: review and evaluation of equilibrium models. *Colloids Surf., A* (2001) 178 (1-3), 1-40.
11. Lashkarbolooki, M.; Ayatollahi, S.; Riazi, M., Effect of Salinity, Resin, and Asphaltene on the Surface Properties of Acidic Crude Oil/Smart Water/Rock System. *Energy Fuels* (2014) 28 (11), 6820-6829.

12. Tichelkamp, T.; Teigen, E.; Nourani, M.; Oye, G., Systematic study of the effect of electrolyte composition on interfacial tensions between surfactant solutions and crude oils. *Chem. Eng. Sci.* (2015) 132, 160-165.
13. Al-Sahhaf, T.; Elkamel, A.; Ahmed, A. S.; Khan, A. R., The influence of temperature, pressure, salinity, and surfactant concentration on the interfacial tension of the N-octane-water system. *Chem. Eng. Commun.* (2005) 192 (5), 667-684.
14. Bai, J. M.; Fan, W. Y.; Nan, G. Z.; Li, S. P.; Yu, B. S., Influence of Interaction Between Heavy Oil Components and Petroleum Sulfonate on the Oil-Water Interfacial Tension. *J. Dispersion Sci. Technol.* (2010) 31 (4), 551-556.
15. Kumar, S.; Mandal, A., Studies on interfacial behavior and wettability change phenomena by ionic and nonionic surfactants in presence of alkalis and salt for enhanced oil recovery. *Appl. Surf. Sci.* (2016) 372, 42-51.
16. Dong, M.; Wu, Y.; Li, A., Sweep Efficiency Improvement by Alkaline Flooding for Pelican Lake Heavy Oil. In *Canadian Unconventional Resources Conference*, Society of Petroleum Engineers: Canada, 2011.
17. Samanta, A.; Ojha, K.; Mandal, A., Interactions between Acidic Crude Oil and Alkali and Their Effects on Enhanced Oil Recovery. *Energy Fuels* (2011) 25 (4), 1642-1649.
18. Seta, L.; Baldino, N.; Gabriele, D.; Lupi, F. R.; De Cindio, B., The effect of surfactant type on the rheology of ovalbumin layers at the air/water and oil/water interfaces. *Food Hydrocolloids* (2012) 29 (2), 247-257.
19. Guarin, A.; Khan, A.; Butt, A. A.; Birgisson, B.; Kringos, N., An extensive laboratory investigation of the use of bio-oil modified bitumen in road construction. *Constr. Build. Mater.* (2016) 106, 133-139.
20. Biresaw, G.; Liu, Z. S.; Erhan, S. Z., Investigation of the surface properties of polymeric soaps obtained by ring-opening polymerization of epoxidized soybean oil. *J. Appl. Polym. Sci.* (2008) 108 (3), 1976-1985.
21. Oliviero Rossi, C.; Caputo, P.; Baldino, N.; Lupi, F. R.; Miriello, D.; Angelico, R., Effects of adhesion promoters on the contact angle of bitumen-aggregate interface. *Int. J. Adhes. Adhes.* (2016) 70, 297-303.

22. 96, A. D., Standard Practice for Effect of Water on Bituminous-Coated Aggregate Using Boiling Water. 2005.
23. Farooq, U.; Simon, S.; Tweheyo, M. T.; Oye, G.; Sjoblom, J., Interfacial Tension Measurements Between Oil Fractions of a Crude Oil and Aqueous Solutions with Different Ionic Composition and pH. *J. Dispersion Sci. Technol.* (2013) 34 (5), 701-708.
24. Kelesoglu, S.; Meakin, P.; Sjoblom, J., Effect of Aqueous Phase pH on the Dynamic Interfacial Tension of Acidic Crude Oils and Myristic Acid in Dodecane. *Journal of Dispersion Science and Technology* (2011) 32 (11), 1682-1691.
25. Dukhin, S. S.; Kretzschmer, G.; Miller, R., *Dynamics of Adsorption at Liquid Interfaces*. 1st Edition ed.; Elsevier Science: Amsterdam, The Netherlands, 1995; Vol. 1.
26. Buckley, J. S.; Fan, T. G., Crude oil/brine interfacial tensions. *Petrophysics* (2007) 48 (3), 175-185.
27. Mohamed, R. S.; Ramos, A. C. S.; Loh, W., Aggregation behavior of two asphaltenic fractions in aromatic solvents. *Energy Fuels* (1999) 13 (2), 323-327.
28. Yarranton, H. W.; Alboudwarej, H.; Jakher, R., Investigation of asphaltene association with vapor pressure osmometry and interfacial tension measurements. *Ind. Eng. Chem. Res.* (2000) 39 (8), 2916-2924.
29. Varadaraj, R.; Brons, C., Molecular origins of heavy oil interfacial activity part 1: Fundamental interfacial properties of asphaltenes derived from heavy crude oils and their correlation to chemical composition. *Energy Fuels* (2007) 21 (1), 195-198.
30. Varadaraj, R.; Brons, C., Molecular origins of heavy crude oil interfacial activity part 2: Fundamental interfacial properties of model naphthenic acids and naphthenic acids separated from heavy crude oils. *Energy Fuels* (2007) 21 (1), 199-204.
31. Alves, D. R.; Carneiro, J. S. A.; Oliveira, I. F.; Facanha, F.; Santos, A. F.; Dariva, C.; Franceschi, E.; Fortuny, M., Influence of the salinity on the interfacial properties of a Brazilian crude oil-brine systems. *Fuel* (2014) 118, 21-26.
32. Berg, J. C., Thermodynamics of interfacial. In *An Introduction to Interfaces and Colloids: The Bridge to Nanoscience*, Co, W. S. P.; Ltd, P., Eds. 2009.
33. Diamant, H.; Andelman, D., Kinetics of surfactant adsorption at fluid/fluid interfaces: Non-ionic surfactants. *Europhys. Lett.* (1996) 34 (8), 575-580.

34. Bauget, F.; Langevin, D.; Lenormand, R., Dynamic surface properties of asphaltenes and resins at the oil-air interface. *J. Colloid Interface Sci.* (2001) 239 (2), 501-508.
35. Freer, E. M.; Radke, C. J., Relaxation of asphaltenes at the toluene/water interface: Diffusion exchange and surface rearrangement. *J. Adhes.* (2004) 80 (6), 481-496.
36. Beverung, C. J.; Radke, C. J.; Blanch, H. W., Protein adsorption at the oil/water interface: characterization of adsorption kinetics by dynamic interfacial tension measurements. *Biophys. Chem.* (1999) 81 (1), 59-80.
37. Rane, J. P.; Harbottle, D.; Pauchard, V.; Couzis, A.; Banerjee, S., Adsorption Kinetics of Asphaltenes at the Oil-Water Interface and Nanoaggregation in the Bulk. *Langmuir* (2012) 28 (26), 9986-9995.
38. Zhang, S.; Zhang, L.; Lu, X.; Shi, C.; Tang, T.; Wang, X. G.; Huang, Q. X.; Zeng, H. B., Adsorption kinetics of asphaltenes at oil/water interface: Effects of concentration and temperature. *Fuel* (2018) 212, 387-394.
39. Camino, N. A.; Perez, O. E.; Sanchez, C. C.; Patino, J. M. R.; Pilosof, A. M. R., Hydroxypropylmethylcellulose surface activity at equilibrium and adsorption dynamics at the air-water and oil-water interfaces. *Food Hydrocolloids* (2009) 23 (8), 2359-2368.
40. Baldino, N.; Mileti, O.; Lupi, F. R.; Gabriele, D., Rheological surface properties of commercial citrus pectins at different pH and concentration. *LWT--Food Sci. Technol* (2018) 93, 124-130.
41. Graham, D. E.; Phillips, M. C., Proteins at liquid interfaces: III. Molecular structures of adsorbed films *J. Colloid Interface Sci.* 1979, 70, 12 .
42. Zhao, S.; Huang, B. S.; Shu, X.; Woods, M., Comparative evaluation of warm mix asphalt containing high percentages of reclaimed asphalt pavement. *Constr. Build. Mater.* (2013) 44, 92-100.
43. Rossi, C. O.; Caputo, P.; Baldino, N.; Szerb, E. I.; Teltayev, B., Quantitative evaluation of organosilane-based adhesion promoter effect on bitumen-aggregate bond by contact angle test. *Int. J. Adhes. Adhes.* (2017) 72, 117-122.
44. Rossi, C. O.; Teltayev, B.; Angelico, R., Adhesion Promoters in Bituminous Road Materials: A Review. *Appl. Sci.* (2017) 7 (5), 10.

Chapter 10

Effect of additives on the structural organization of asphaltene aggregates in bitumen

Pietro Calandra^{1,*}, Paolino Caputo², Maria Penelope Santo³, Lorena Todaro⁴,
Vincenzo Turco Liveri⁴, Cesare Oliviero Rossi^{2,*}

¹CNR-ISMN, National Council of Research, Institute for the Study of Nanostructured Materials, Via Salaria km 29.300, Monterotondo Stazione (RM), Italy

²Department of Chemistry and Chemical Technologies, University of Calabria, 87036 Arcavacata di Rende (CS), Italy; tel./fax. +39 0984492045

³Department of Physics and CNR-Nanotec, University of Calabria, via Bucci 31C, 87036 Rende (CS), Italy

⁴University of Palermo - Dept. STEBICEF - Parco d'Orleans II, Palermo, Italy, retired

* Correspondence: pietro.calandra@ismn.cnr.it (P.C.); cesare.oliviero@unical.it (C.O.R.); tel. +39 06 90672409 (P.C.); +39 0984 492045 (C.O.R.);

ABSTRACT:

Bitumens are composite materials whose complex organization hinders the rational understanding of their relationships between composition, structure and performances. So, research attempting to shed more light in this field is required. In this work Wide Angle X ray Scattering (WAXS) has been used to explore the influence of six opportunely chosen additives on the bitumen structure with the aim to ultimately correlate the findings with the bitumen performances. Diagnostic fingerprints have been observed in the WAXS profile: asphaltenes form stuck of about 18 Å and constituted by about 6 asphaltene units on average. Such stuck are, in turn, organized at higher levels of complexity forming anisotropic aggregates of about 200 Å × 28 Å which, again, are assembled to form micrometer-size elongated aggregates characterized by the so-called bee-structure. The structural effects of the six opportunely chosen additives (Organosilane, Polyphosphoric, Phospholipids, Acetamidophenol, Oleic Acid, octadecylamine) have been pointed out and, corroborated by AFM images, have been correlated with the rheological behavior and justified at the microscopic level: additive with an apolar nature are preferentially located in the maltene phase weakening asphaltene inter-clusters interactions and softening the bitumen, whereas, on the contrary more polar additives act in opposite directions. Peculiar behavior have been unveiled in the case of amphiphilic additive due to the simultaneous presence, within their molecular architecture, of both polar and apolar moieties. The knowledge of the detailed effect of appropriately chosen additives on the nanoscopic and

mesoscopic structure and their correlation with the rheological properties constitute the first step for opening the door to the piloted design of new bitumens with desired properties for *ad-hoc* uses.

KEYWORDS:

bitumen, surfactant, additives, stability, AFM, WAXS, structure

1. INTRODUCTION

Asphalts concretes are well known materials used for road pavement throughout the world.

They are biphasic systems manufactured by mixing macro-meter sized inorganic particles called aggregates (93-96 % w/w, size from microns to millimeters) with the bitumen, which is an organic high-viscosity viscoelastic binding agent which is itself a composite system constituted by nano-meter sized aggregates of polar molecules (asphaltenes) dispersed in a more apolar continuous phase of saturated paraffins, aromatic oils and resins called maltene^{1,2}.

For the optimization of the material overall performances, actions have been mainly directed to the improvement of the mechanical and chemical properties of the bitumen by means of opportune additives. For example, aggression of environmental chemicals or simple ageing can oxidize some of the organic components so that the increase in polar functional groups can cause immobilization of an excessive number of polar molecules and ultimately bitumen embrittlement. In this case the final asphalt is susceptible to fracturing or cracking after thermal or mechanical stresses so one chemical action of an additive is to tune the red-ox state of the polar molecules contained in the bitumen to avoid this degrading process. Another beneficial action of an additive can be adhesion promotion: in this case the additive acts on the inorganic/organic interfacial tension thus better dispersing the inorganic particle among the bitumen matrix, an effect which can be also directed to the stabilization of eventual supramolecular aggregates (mainly made by asphaltene) formed in the maltene phase^{3,4}. For this reason, such compounds are also called "antistripping agents".

In doing so, a rheological description of the materials is often given and an empirical approach is always followed to optimize the performances within a chosen temperature range^{5,6} for convenient use^{7,8}.

This is probably due, in our opinion, to the always urgent need of improving performances for applicative purposes so that basic research, highlighting the specific intermolecular interactions and the molecular organization at the base of the observed behavior has been sometimes overlooked. As consequence, there is still lack of information on how many additives affect the supra-molecular structure and its distribution in the bituminous colloidal network and how this can reflect to the overall material properties, making the relationship between molecular interactions and the final material structure/properties (which is ultimately the final objective of physical chemistry) still quite vague.

To face this problem the fact that bitumens are characterized by intermolecular associations at different length-scales (asphaltene molecules are aggregated to form stacks by self-interactions and these aggregates are stabilized by polar resins due to their amphiphilic chemical nature and the overall structures are then dispersed in a paraffin-like apolar matrix) must be first recognized. These characteristics render this material a truly complex system with different levels of complexity, each of them potentially showing emerging properties arising from the opportune organization of the molecules. For this reason, an approach based on the complex systems theory is necessary.

Then It must be also pointed out that asphaltenes are not classified using their molecular structure, but they are defined traditionally on the basis of the procedure required to extract them from heavy oils⁹. Consequently, asphaltene is a not well defined mixture of constituents so, for an effective study, the general viewpoint of their overall assembly becomes more important than the detailed chemical speciation of the various molecules involved. Given the recent progresses in the field of comprehension of the intermolecular self-assembly in complex systems¹⁰ the approach of the present paper is to apply the same approach also to these complex materials. In this way, the results can be more easily transferred to other bitumens/asphalts.

Regarding the additive role, it can exert its effect at the inorganic/organic interface or, at a lower level of complexity, within the maltene/asphaltene aggregates, whereas a redox additive works at the chemical state of the single polar molecules i.e. at an even lower level of complexity. Another mechanism exerted by the additive is the formation of a network inside the maltene giving elasticity to the bitumen¹¹ or a simple

change of physical phase transition with fluxing at higher temperature while conferring rigidity at lower ones¹².

As regards the additive chemical nature, selected polymers have been used (low-density polyethylene, ethylene-vinyl-acetate, SBS-polyphosphoric acid (PPA), Elvaloy etc)¹³ as well as smaller molecules falling in the categories of organosilane and phospholipids¹⁴ or paraffinic synthetic waxes, derivate of fatty amines and surfactants¹⁵, antioxidants¹⁶ etc.

Due to the general description of the bitumen performances in rheological terms (penetration index, softening point, ductility, viscosity), and due to the lack of detailed knowledge of the supramolecular assembly characterizing the bitumen structure at the various levels of complexity, a rational correlation of the bitumen structure with its performances is missing. Scattering experiment, and in particular X-ray scattering ones, are advisable to probe the structure from the Å to the meso-scale but the bitumen complex organization has hindered such detailed structural study. The structural investigation has been therefore generally carried out by Atomic Force microscopy (AFM)¹⁷, by Confocal Laser Scanning Microscopy¹⁸, by optical microscopy¹⁹ and fluorescence Microscopy²⁰ but all these methods were used to probe the micro-scale (not going deeper to the nano-scale) and the surface. Attempts at gaining information on the nano-scale structure of the bulk have been limited and the result remained quite hypothetical.³⁹ Even the “colloidal structure” is just empirically derived by the contents of aromatics, resins, asphaltenes and saturates²¹.

The aim of this work is to shed light on the inter-molecular self- assembly characterizing the bitumen and how this can be affected by some selected additives in order to correlate the changes the structural features to the rheological properties. To do so, Wide Angle X-ray Scattering (WAXS), Atomic Force Microscopy (AFM) and rheological measurements have been carried out on bare and additivated bitumens. Six additives have been selected: three of them (Organosilane (P2KA), Polyphosphoric Acid (PPA) and phospholipids (LCS) have been already used in the recent literature^{22,23,24} and the other three (Acetamidophenol, Oleic Acid, octadecylamine) have been used to expand the knowledge in this field and with the aim of prediction of their performances. We have chosen these molecules because they possess, within their molecular architecture simultaneously both a polar part and an apolar one at different extents.

This confers a certain amphiphilicity, so we expect that the polar part can strongly interact with the asphaltene (polar) part of the bitumen and the additive apolar one (alkyl chain) could better interact with the apolar part of the maltene. This would render an additive quite effective and interesting effects are expected. Moreover, the choice of these molecules as additives answers the need for cheap chemicals, since they are commercially available at low cost. The last criterion followed to choose the additive studied in this work is their stability. It is well ascertained that these molecules are stable even at critical operating conditions of an asphalt and in sample preparation (150 ± 10 °C, see experimental part).

Industrial companies involved in the production of bitumen modifiers are strongly interested in the understanding of the modifier mechanism of action in order to design future and *ad-hoc* additives. Consequently, the acquired information will be the base of any prospective alteration/modification of binders for commercial purposes.

2 EXPERIMENTAL PART

2.1 Materials

The bitumen was kindly supplied by Loprete Costruzioni Stradali (Terranova Sappo Minulio, Calabria, Italy) and was used as fresh reference sample. It was produced in Italy and the crude oil was from Saudi Arabia. Its penetration grade (50/70) was measured by the usual standardized procedure (ASTM D946)²⁵ in which a standard needle (531/2-T101, Tecnotest, Italy) is loaded with a weight of 100 g and the length traveled into the bitumen specimen is measured in tenths of a millimeter for a known time (5s), at fixed temperature (25°C). The bare bitumen was added by:

- Organosilane (P2KA), provided by KimiCal S.r.l. (Rende, Italy)
- Polyphosphoric Acid (PPA) provided by Sigma Aldrich (Milano, Italy).
- Phospholipids (LCS) were provided by Somercom S.r.l. (Catania, Italy)
- Acetamidophenol, provided by Sigma Aldrich (Milano, Italy). and used without further purification
- Oleic Acid, purchased by Sigma Aldrich (Milano, Italy) and used without further purification
- octadecylamine provided by Sigma Aldrich (Milano, Italy).

2.2 Sample preparation

Although different additives are generally used at different concentrations, the aim of this work is to compare the effects of the various additives on the bitumen structure and properties, so the additive concentration has been kept the same for all the sample and equal to 2% w/w to maximize the effect. This concentration is also used by other authors²⁶. Weighted amount of additives were added separately to a fully flowing hot bitumen (150 ± 10 °C) and stirred at 500–700 rpm by a mechanical stirrer (IKA RW20, Königswinter, Germany) for 30 min at the same temperature to allow homogenization of the blend. Our previous studies showed that such conditions assure the preparation of homogeneous samples: at lower rpm samples homogenization is not effective, while above 700 rpm the bitumen can become oxidized with consequent change in the rheological properties. This method is quite standard: this is our inner protocol according to our experience

but also other authors use analogous procedure when the bitumen is mixed with similar additives²⁷.

After mixing, the resulting bitumen was poured into a small sealed can and then stored in a dark chamber at 25 °C to retain the desired morphology. Due to the sensitivity of such kind of materials to the annealing time¹⁴, and due to the comparative spirit of our work, we took care that all our samples had the same temperature cooling rate ($5^{\circ}\text{C min}^{-1}$) and annealing time (15min).

A standard additive-free bitumen sample was used as reference.

2.3 Saturates, Aromatics, Resins and Asphaltenes (S.A.R.A.) determination

The latroscan MK 5 Thin Layer Chromatography (TLC) was used for the chemical characterization of bitumen by separating it into the four fractions foreseen by the standard S.A.R.A. method: Saturates, Aromatics, Resins and Asphaltenes²⁸. During the measurement, the separation took place on the surface of silica-coated rods. The detection of the amount of different groups was performed according to the flame ionization. The sample was dissolved in peroxide-free tetrahydrofuran solvent to reach a 2% (w/v) solution. Saturated components of the sample were developed in *n*-heptane solvent while the aromatics in a 4:1 mixture of toluene and *n*-heptane. Afterwards, the rods had to be dipped into a third tank, which was

a 95 to 5 % mixture of dichloromethane and methanol. That organic medium proved suitable to develop the resin fraction whereas the asphaltene fraction was left on the lower end of the rods.

2.4 Wide Angle X-Ray Scattering (WAXS)

Wide Angle X-Ray Scattering (WAXS) measurements were carried out at 25°C by a Philips diffractometer (PW1050/39 X Change), equipped with a copper anode (Cu $K\alpha$, wavelength $\lambda=1.5418 \text{ \AA}$). The apparatus worked in a $\theta/2\theta$ configuration operating at 40 kV and 30 mA. Spectra in the 2°-80° scan range of 2θ were acquired with a scan rate of 0.2°/s and a count time of 25 s/step. Due to the complex nature of the material it can be expected that exposure to radiation and consequent heating can influence the structure of samples. For this reason, we have checked by preliminary tests that in our experimental conditions WAXS data acquisition does not involve any structural modification thus ruling out sample degradation/modification during measurements.

2.5 Rheological Tests

Isothermal oscillatory rheological tests at constant temperature $t = 25 \text{ }^\circ\text{C}$, were carried out by dynamic stress-controlled rheometer (SR5, Rheometric Scientific, Piscataway, NJ, USA) equipped with a parallel plate geometry (gap $2.0 \pm 0.1 \text{ mm}$, diameter 25 mm). Temperature was controlled by a Peltier element ($\pm 0.1 \text{ }^\circ\text{C}$). The complex shear modulus G^* was measured in the regime of small-amplitude oscillatory shear^{29,30}.

For viscoelastic materials, G^* is split into a real and imaginary part i.e. $G^* = G' + i G''$ ²⁵, where the real and imaginary parts define the in-phase (storage) and the out-of-phase (loss) moduli, respectively. G' is a measure of the reversible, elastic energy, while G'' represents the irreversible viscous dissipation of the mechanical energy³¹. Their ratio is related to the phase angle δ according to $\tan \delta = G''/G'$.

These quantities are all frequency-dependent. In our experiments, after preliminary stress-sweep tests, the frequency was kept fixed at 1 Hz and proper stress values were applied to guarantee linear viscoelastic conditions

2.6 Atomic Force Microscopy (AFM)

Atomic Force Microscopy (AFM) was carried out by a Nanoscope VIII, Bruker microscope operating in tapping mode. In tapping mode, the cantilever oscillates close to its resonance frequency (150kHz). Since the cantilever oscillates up and down, the tip is contacting the sample surface intermittently. When the tip is brought close to the surface, the vibration of the cantilever is influenced by the tip–sample interaction. In particular, shifts in the phase angle of vibration of the cantilever, implying energy dissipation in the tip–sample ensemble, are due to the specific mechanical properties of the sample. For measurements, cantilevers with elastic constant of 5N/m and 42N/m have been used. Antimony doped silicon probes (TAP150A, TESPA-V2, Bruker) with resonance frequencies 150 kHz and 320 kHz, respectively, and nominal tip radius of curvature 10 nm were used. Phase images were acquired simultaneously with the topography.

3 DATA ANALYSIS

3.1 Saturates, Aromatics, Resins and Asphaltenes (S.A.R.A.) determination

Pristine bitumen was characterized by the S.A.R.A. method to assess the concentration of the four different portions: Saturates, Aromatics, Resins and Asphaltenes. According to the Micellar Model, the overall material has to be intended as asphaltene molecules rich in resins as peptizing agents aggregated into micellar-like structures and dispersed into the continuous phase composed mainly by the saturated and aromatic oil fractions (maltene)³². The results are shown in Table 1.

Table 1. Group composition of the pristine bitumen.

Fraction	abundance w/w % (± 0.1)
Saturates	3.8
Aromatics	51.3
Resins	21.5
Asphaltenes	23.4

In a standard bitumen, the asphaltenes are the main component to bitumen fractional composition and constitute 5 to 25% of the total mass and this fraction is the dominant component controlling hardness of the bitumen, it consists of a very complex mixture with a large variation in size, polarity and functional groups. This percentage of asphaltenes is typical of the 50/70 grade bitumen.

3.2 Wide Angle X-Ray Scattering (WAXS) spectra

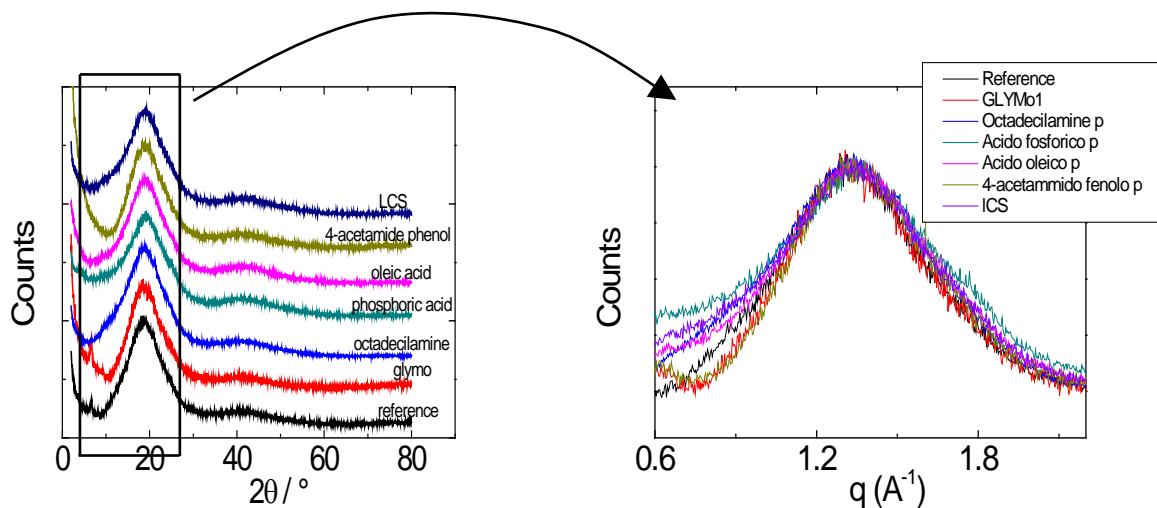


Fig. 1: Wide Angle X-ray Scattering profiles of the studied samples. The spectra are vertically shifted for clarity sake.

The wide angle X-ray scattering (WAXS) profiles of the investigated samples are shown in Fig. 1 (left panel).

Three features are clearly visible:

1. a tiny but sharp peak below 10°
2. a prominent broad band centered at 20°
3. a weak and broad band around 42° .

The presence of peaks in a wide range of scattering angles is a first indication that there are different characteristic distances belonging to various atomic and molecular organizations of different levels of complexity. Let's analyze and comment each of these signals separately.

3.2.1 WAXS range 30-50 °

In the 30-50° range, a low-intensity broad band is present around 42°. The position of the center corresponds, according to the Bragg law

$$d = \frac{\lambda}{2 \sin \theta} \quad (\text{eq.1})$$

(where d is the interplanar distance, θ is the scattering angle and λ is the wavelength of the incident radiation 1.5418 Å) to a characteristic distance (d) of 2.2 Å. This value could be somewhat affected by the presence of the tail of the more intense contribution around 20°. However, this distance can be surely attributed to some particular interatomic distance within the molecules making part of the scattering aggregates. More specifically, the distance of 2.2 Å is in the range of the typical distance between non-adjacent carbons reported for polycyclic aromatic compounds³³. This distance is schematically depicted in Fig. 2. Since it refers to an intra-molecular distance, it is found to be independent on the additive nature due to the fact that it cannot change the molecular structure of the bitumen components.

3.2.2 WAXS range 10°<2θ<30°

In the range 10-30°, the most evident feature of the whole scattering profile occurs, i.e. an intense and broad band centered around 2θ=20° and corresponding, according to the Bragg relation (eq. 1), to a repetition distance d of about 4.7 Å. This value must be attributed to an intermolecular distance: we have already ascertained that in alkyl-based fluids a broad band around 2θ=20° can be attributed to a typical intermolecular distance of 4.4-4.7 Å^{34,35,36,37}. This distance is typical in the conventional liquid (disordered) state and can be seen as the first shell lateral distance typical of the conventional liquid state³⁸.

This peak, as reported by Tanaka et al.³⁹, can be shifted to higher angles (up to about 26°) in case of aromatic compounds giving the so-called *graphene* band and due to a characteristic lateral distance of

about 3.6 Å. Due to the simultaneous presence of both aliphatic and aromatic compounds in the bitumen it can be expected that the observed band is the not-resolved superposition of these two contribution. Interestingly, as seen in Fig. 1 (right panel) where these bands are compared after normalization at the same height for clarity sake, slight changes in the band shape is observed when changing the additive. This is the first hint that the additive can change the asphaltene intermolecular self-assembly by changing the asphaltene or the alkyl domains sizes or structural order.

3.2.3 WAXS range $2 < 2\theta < 10^\circ$

In the range 2-10° it is present a tiny peak which reveals the occurrence of a supra-molecular aggregation. This peak can be associated to a repetition distance between one asphaltene local aggregate and its neighboring one³⁹, suggesting the presence of aggregates of asphaltene aggregates, in accordance with a model of a complex system with different levels of complexity. For this scattering signal both position and intensity were found to be even more dependent on the added additive, with respect to the band centered around 20°. This is a clear indication that the additive, whilst exerting a slight influence on asphaltene domains, as revealed by the slight changes in the band around 20°, exerts instead a marked influence on the cluster-cluster assembly hold up by weaker interactions. Such interactions may be considered as weaker than the asphaltene-asphaltene self-interactions and-competitive with those of the polar resins in the maltene phase. The change of the peak position will therefore show the specific influence of the additive on the mutual interactions among asphaltenes aggregates.

3.2.4 WAXS range $2\theta < 2^\circ$

In the low-angles range of the WAXS spectrum the fractal aggregation of the supra-aggregates of asphaltene clusters can be explored. The auto-similarity in the 1-100 nm range is predicted by the model reported by TANAKA and can be highlighted by a linear trend in the log-log plot of the scattered intensity vs. q (where q is the scattering vector defined as $q = 4\pi \sin\theta / \lambda$) which is shown in Fig. 3. The fractal

dimension can be derived by analyzing the power-law regime of the scattering intensity $I(q) \approx q^{-\alpha}$ where the exponent α is related to the fractal dimension D of the scattering structure^{40,41}.

Due to the limit of the q -range window explored in WAXS, no detailed structural information beyond 50 Å can be accessible, where the indication of some structure has been unveiled and for which Small Angle X-Ray Scattering experiments are better suitable⁴²

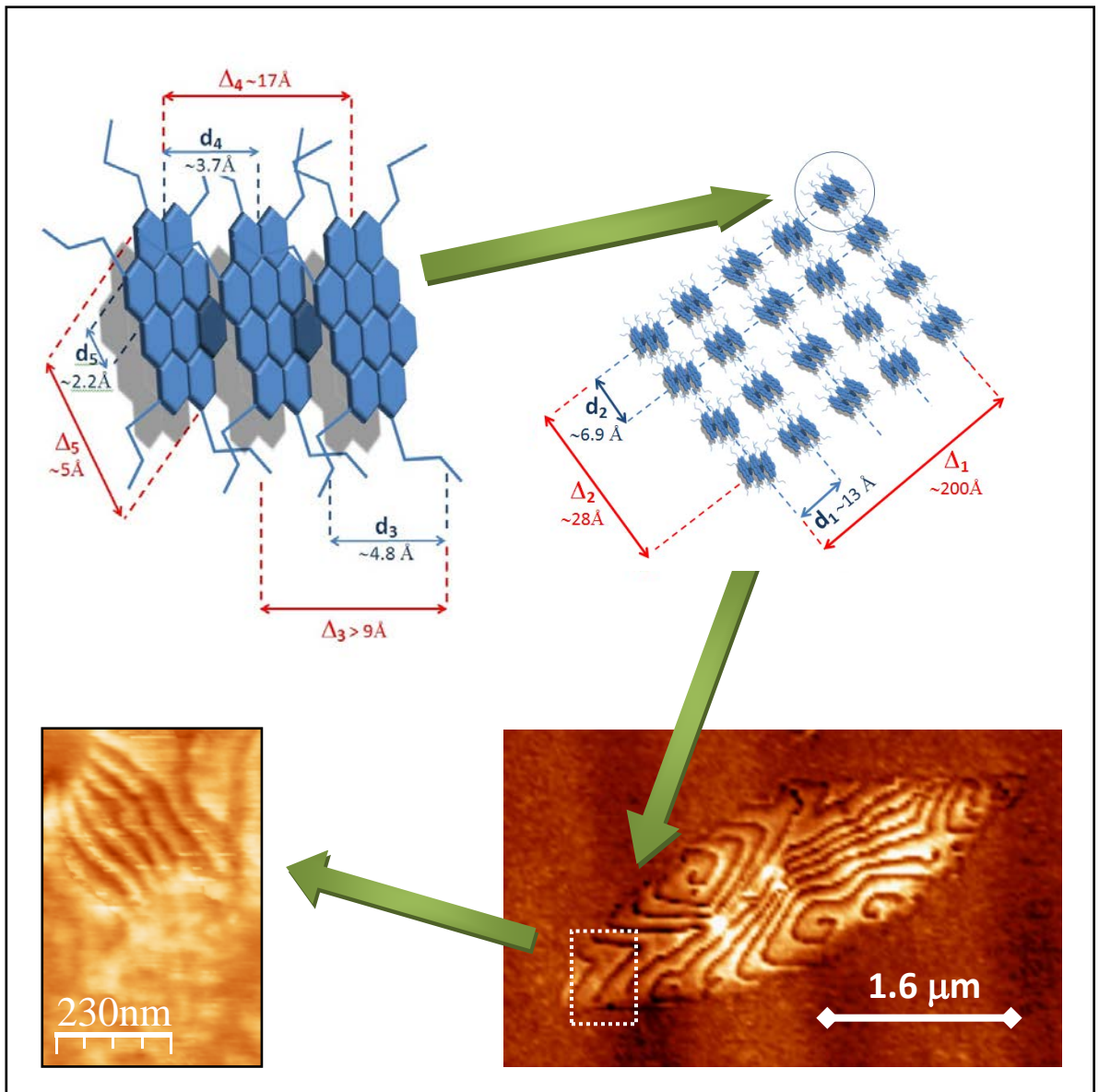


Fig. 2: representative scheme of the bitumen structure with the corresponding quantities derived by WAXS and AFM.

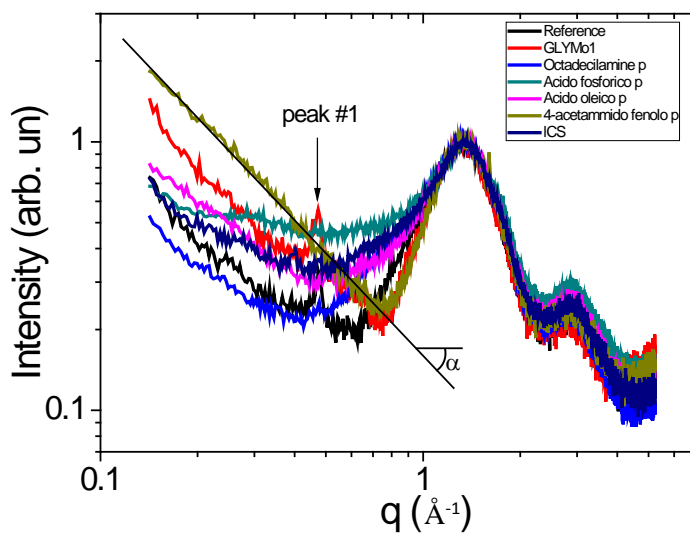


Fig. 3: log-log plot of the scattering profile

3.2.5. WAXS spectra fitting and results

Due to the presence of two scattering signals merging in one broad band centered around 20° and due to its partial overlap with the band centered around 42° , a fitting procedure in the whole range $10\text{-}50^\circ$ range has been used to unveil the single contributions of all of the signals. For this reason we initially used three bell-shaped curves: one for modeling the intermolecular lateral distance between alkyl chains (at 20°), another one for the graphene band at 26° and the last one for the intra-molecular distance-related band at 42° .

Interestingly, we found that three curves did not adequately describe the WAXS profile especially the most prominent band around 20° giving a discrepancy on its left side in the range $10\text{-}12^\circ$. Therefore we were forced to assume that another WAXS signal must be included in this region so we used a fourth band in our fitting procedure. With four curves the fitting had, instead, excellent quality and a representative fitting result is shown in Fig. 4 together with the signal labelling. This result suggested us to take into account for another inter-cluster distance in addition to the aforementioned ones. We used Lorentzian curves because of their better capability to reproduce the sharp tips of the prominent band at 20° but fitting with Gaussian curves gave similar results.

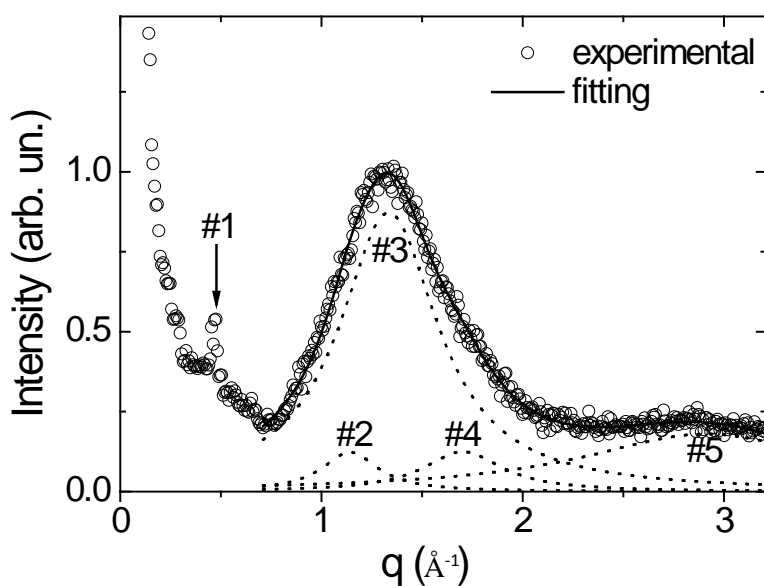


Fig. 4: representative fitting result of the WAXS profile with four Lorentzian curves

It must be noted that we fitted the WAXS intensity as a function of q for a more convenient derivation of the physical quantities below described. The fitting parameters are reported in table 1: among these, the center of the band (q_{MAX}) and the Full Width at Half Maximum (FWHM) are of particular interest since they give the repetition distance (d) and the ordering parameter Δ according to the equations

$$\Delta = \frac{2\pi}{FWH} \quad (\text{eq. 2})$$

$$d = \frac{2\pi}{q_{MAX}} \quad (\text{eq. 3})$$

where the values of q_{MAX} and of FWHM are given in unities of scattering vector q . Δ can be taken as an indicator of the order present in the sample. Its meaning is the distance at which the order is lost as a consequence of the finite size of scattering domain. Wider widths imply loosening of the order at shorter distances giving smaller Δ values.

The derived parameters d and Δ are also collected in table 1.

A perusal of Table 1 allows a detailed interpretation of the structural features of bitumen and of the effects due to the various additives addition. In particular:

- Regarding the band due to the intra-molecular distance the obtained FWHM value of about 1.27 \AA^{-1} gives a Δ value of about 5 \AA . Its relative area (25%) is in agreement with S.A.R.A. determination which highlights that the asphaltene fraction is 27%. The correlation distance can be therefore safely considered as an estimation of the asphaltene orientation-averaged size.
- Regarding the graphene band, its FWHM of 2.85 \AA^{-1} gives a Δ value of about 18 \AA . Considering the interplanar distance of 3.7 \AA the asphaltene stacks turn out to be made of about $6 (\Delta/d + 1)$ asphaltene units on average. In this case however, it cannot be excluded the presence of different chemical species contributing to this scattering signal further contributing to band broadening, so the derived Δ value and consequently mean the number of asphaltene units per cluster, have to be considered as a lower limit.
- Regarding the alkyl-alkyl lateral distance the WAXS signal is centered around 1.3 \AA^{-1} giving a repetition distance of 4.8 \AA whereas the FWHM of 0.69 \AA^{-1} gives a Δ value of 9 \AA . It must be pointed out that the band

is usually broad not only because of the reduced size of the scattering domain but also because of a polydispersion in the characteristic distance as a consequence of the disordered (fluidic) nature of the domain. So, the derived Δ value has to be considered as a lower limit.

- regarding the Lorentian in the low- q range, it must be noted that its intensity is generally low and gives a repetition distance of 6.9 Å which is consistent with the sum of the asphaltene plane extension (about 5 Å) plus the alkyl part (few Å) The scattering correlation distance is 28 Å. Meaning that the order is lost at short distance. Due to the weak interactions involved in keeping assembled the asphaltene clusters together along this direction, confirmed by the marked effect of additive presence, here it can be claimed that the order is lost mainly as a consequence of the disordered (fluidic) nature of the domain which gives a marked polydispersity in the characteristic distances, rather than the markedly reduced size of an internally ordered scattering domain,

- regarding the peak around 1 \AA^{-1} it is quite sharp and gives a repetition distance of 13 Å and a correlation length of 200 Å,

- regarding the lowest q -range trend, surprisingly, as shown in Fig. 3 the pristine bitumen does not show linear trend in a sufficiently wide q range, therefore the presence of fractal structure can be ruled out. The rising up of the scattering intensity at lower q values is therefore to be attributed rather to a size polydispersion of the scattering domains.

All these structural information are depicted schematically in Fig. 2.

3.2.6 additive effects

As to additive effects, the following clues can be derived from WAXS data:

d_5 and Δ_5 are characteristic of asphaltene so their values, as observed, are not additive dependent.

d_4 and d_3 were found to be almost independent on the presence of additive, meaning that the asphaltene-asphaltene interactions are quite strong both in the aromatic and in the alkyl parts. On the contrary, both Δ_4 and Δ_3 slightly change with the additive, meaning that the additive can perturb the building up of asphaltene clusters. In particular the addition of polar additives can more efficiently perturb the packing of

asphaltene alkyl parts with reduction of the Δ_3 value whereas it seems to act in the opposite way for the aromatic part (increase of Δ_4)

Lateral Interactions between asphaltene clusters are probed by d_2 and Δ_2 which are characteristic of a signal very weak in the neat bitumen but significant in the additivated bitumens. The effect of the additive is a general decrease of the scattering domains and its order. For this structural feature, polar additives and amphiphilic ones can reduce more the ordering parameter, as expected for interactions between aggregates of polar molecules which are expected to be of a polar type.

Interesting is the case of d_1 and Δ_1 . It refers to the longest distance between aggregates of asphaltene aggregates. This structure can extend to long distances even up to dozens of nanometers. The value, as for the Δ_2 value, is reduced by the presence of the additive.

By all the above observation it can be concluded that the additive is located in the maltene phase, and its effects are of lower strength than asphaltene-asphaltene interactions but of higher intensity with respect to their aggregates-aggregates interactions. In any case their interactions are competitive with those present in the maltene phase.

The additive addition does not generally change the fact that there is an inherent polydispersity of aggregates of aggregates. The only additive triggering fractal aggregation of asphaltenes clusters is 4-acetamido-phenol. For the sample 4-acetamidophenol-additivated bitumen, the fractal dimension is 1.2, as derived by the power-law regime of the scattering intensity $I(q) \approx q^{-\alpha}$, i.e. very close to unit suggesting an uni-directional growth of the supra-aggregates of asphaltene clusters, in accordance with the model by Tanaka. For all the other samples, a more isotropic structuring is instead present. The disappearance of the peak #1 for the 4-acetamidophenol-additivated bitumen and the maintaining of the scattering #2 in a situation of uni-directional growth of asphaltene aggregates, confirms our hypothesis that scattering signals #1 and #2 refer to two perpendicular directions of growth of the aggregate made of asphaltene clusters.

3.3 Atomic Force Microscopy

Atomic Force Microscopy has been used to analyze the topography of the samples. The topography and phase images usually match. In the pristine bitumen, elongated clusters of 1-2 μm , with a rippled interior with few nanometers edges and dispersed in a quite uniform matrix, can be clearly seen, as shown in the lower part of Fig. 2 and as already observed by Oliviero Rossi et al.¹⁴. These aggregates can be safely considered to be made of asphaltene clusters at different levels of aggregation, in accordance with the clues obtained by WAXS data which suggests a hierarchical aggregation pattern and in accordance with previous observations⁴³. AFM probes lengthscales larger than those explored by WAXS and suggests that asphaltene self-assembly gives, at high levels of aggregations, particles with a prolate ellipsoid shape which can extend up to thousands of nm. In the presence of additives, this feature is generally maintained, although with small variations in size and shape which somehow reflect the changes occurring at shorter lengthscales and highlighted by WAXS data analysis. More precisely, the decrease in Δ_1 and Δ_2 observed when the additive is added to the pristine bitumen, reflects also the decrease in size of the micro-meter sized clusters observed by AFM. Moreover, as shown in Fig. 5 where some representative AFM Phase images are reported, it is suggested also a certain losing of the well-defined ellipsoidal shape of the particles in the bitumen when an additive is used. It must be noted that in the extreme case of acetamidophenol-additivated bitumen, where the disappearance of d_1 is observed, the cluster observed by AFM are almost disappeared. All these considerations lead to the conclusion that the structure in the nano-scale is somehow correlated to that at the meso-scale.

SAMPLE	peak #1 (spectrum)					peak #2 (by fitting)					peak #3 (by fitting)					peak #4 (by fitting)					peak #5 (by fitting)				
	q _{max1}	d1	FWHM1	Int.	Δ1	q _{max2}	d2	FWHM2	%2	Δ2	q _{max3}	d3	FWHM3	%3	Δ3	q _{max4}	d4	FWHM4	%4	Δ4	q _{max5}	d5	FWHM5	%5	Δ5
No additive	0.48	13.2	0.02	med	220	0.91	6.88	0.23	0.8	28	1.32	4.77	0.69	71.0	9.17	1.70	3.69	0.36	2.85	17.6	2.91	2.16	1.27	25	5.0
P2KA	0.47	13.4	0.03	med	190	1.14	5.51	0.34	4.7	18	1.33	4.73	0.60	58.2	10.5	1.70	3.70	0.48	6.70	13.1	2.91	2.16	1.51	30	4.2
PPA	0.26	24.0	0.10	low	190	0.75	8.35	1.09	24	5.8	1.37	4.60	0.70	47.9	8.98	1.77	3.56	0.29	2.46	21.7	2.95	2.13	1.36	26	4.6
LCS	0.40	15.7	0.03	low	195	0.66	9.51	1.02	18	6.2	1.35	4.65	0.71	57.7	8.80	1.75	3.59	0.25	1.65	24.9	2.95	2.13	1.27	23	4.9
octadecylamine	0.48	13.1	0.42	low	180	0.79	7.93	0.67	7.8	9.4	1.34	4.70	0.74	71.6	8.55	1.73	3.63	0.21	1.18	29.9	2.92	2.15	1.09	20	5.8
oleic acid	0.38	16.4	0.05	low	125	0.50	12.5	0.83	11	7.5	1.34	4.69	0.73	62.8	8.61	1.73	3.63	0.31	1.78	20.6	2.95	2.13	1.25	24	5.0
4-acetamidophenol	---	---	---	absent	---	1.08	5.82	0.28	2.9	22	1.32	4.76	0.55	50.1	11.5	1.65	3.81	0.51	13.3	12.3	2.89	2.17	1.55	34	4.1

Table 1: WAXS peaks parameters and quantities derived by eqs 2 and 3.

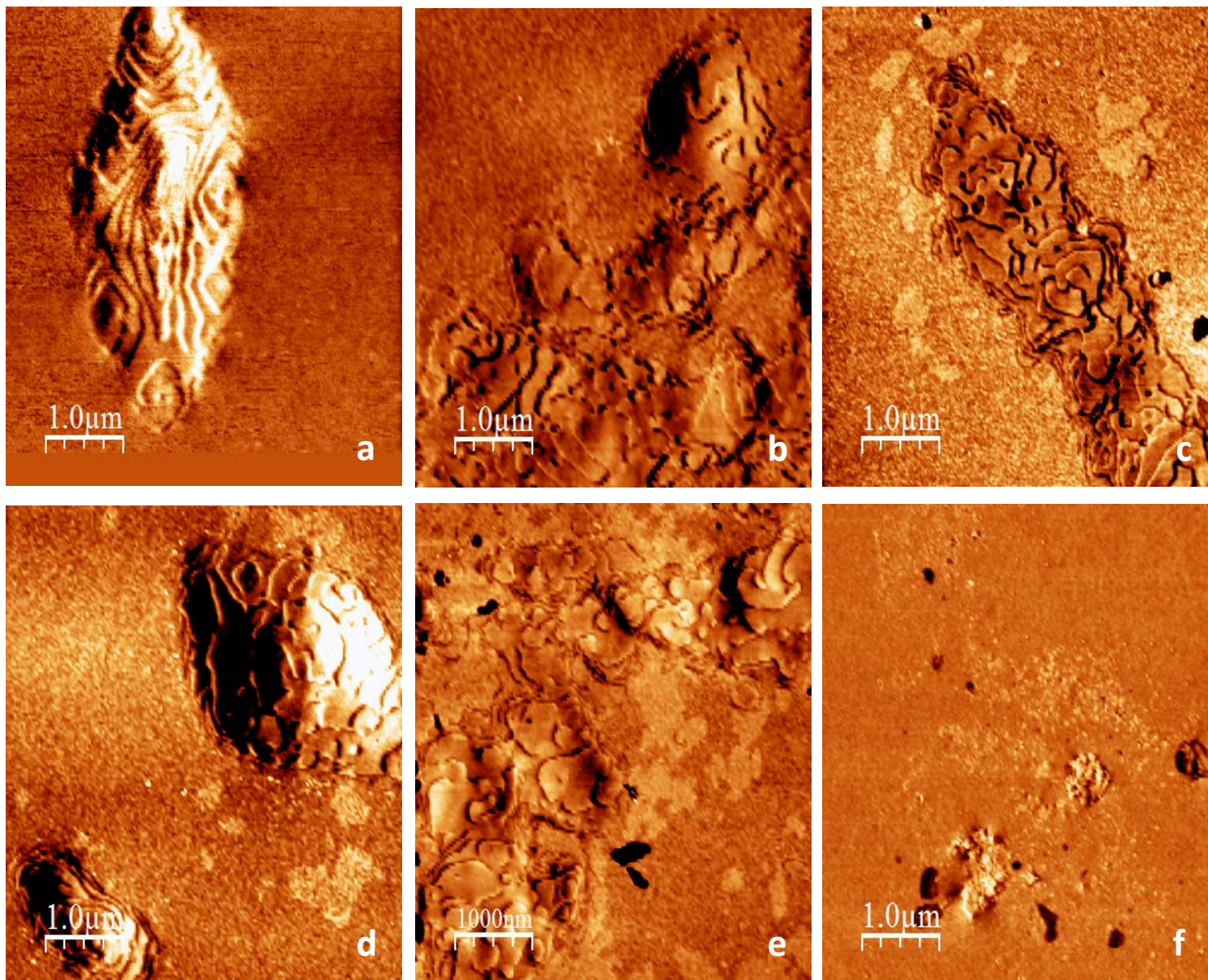


Fig. 5: AFM Phase images of the pristine bitumen (a) as compared to some representative additivated ones (b, P2KA; c, PPA; d, LCS; e, oleic acid; f, 4-acetamidophenol)

3.4 Rheology

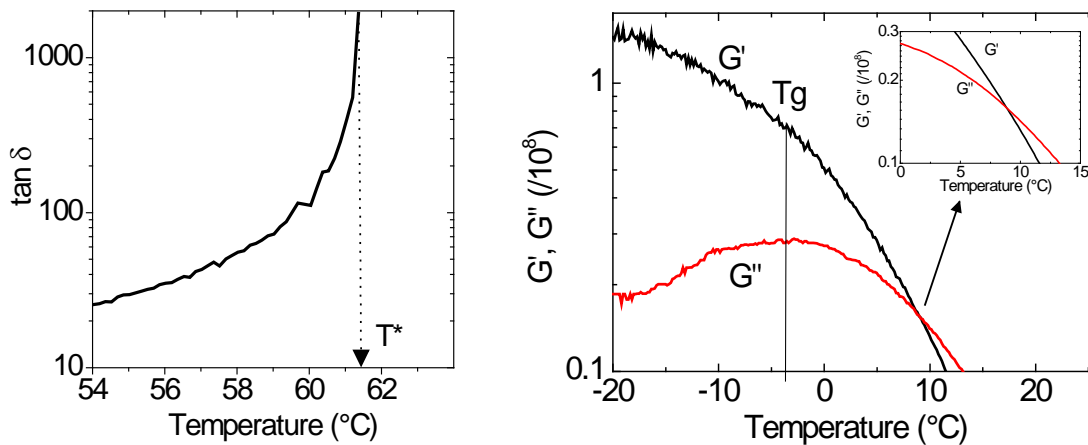
Although several empirical techniques for characterizing mechanical and rheological properties of bitumen have been developed⁴⁴, small amplitude oscillatory rheometry is a fundamental technique that uses specific specimen geometries and instruments, allowing systematic and mathematical interpretation of the results. In fact, the data obtained during a test include the complex modulus G^* , which is a measure of the total energy required to deform the specimen and is defined as:

$$|G^*|^2 = G'^2 + G''^2$$

where G' is the elastic modulus (or storage modulus), a measure of the energy stored in the material during an oscillation, and G'' is the viscous modulus (or loss modulus), a measure of energy dissipated as heat.

The temperature dependence of the experimental G' , G'' measured at 1Hz can give several information. First of all, the value of G' at 25°C ($G' @25^\circ\text{C}$) can be immediately seen and is representative of the mechanical property (rigidity) of the material. This value changes in the presence of additives. Moreover, when temperature is increased the material is progressively softened so that at a certain point $\tan \delta$ diverges. The typical behavior of $\tan \delta$ as a function of temperature is reported in Fig. 6 (left panel) where the trend for the neat bitumen is shown as representative. The temperature at which the $\tan \delta$ diverges (T^*) is just the temperature at which $\tan \delta$ reaches very high values of >1000 . This has the physical meaning of being a temperature at which the binder almost behaves as a Newtonian fluid. From the microscopic point of view it can be intended as the temperature at which the thermal motion is sufficiently high to completely destroy the interacting network made by the above described complex structure. Consequently, at T^* no storage of energy can be afforded by the sample so the storage modulus G' drops. Another interesting characteristic is the presence of a glass transition at lower temperatures. Such transition is always accompanied by a drop in G' and a concomitant maximum in G'' . The maximum in G'' can be safely taken as the temperature of the transition (T_g). Moreover, at lower temperatures the samples exhibit a viscoelastic response typical of strong gel-like materials where $G' > G''$ reaching a glassy modulus; with increasing temperature, and above the glass transition, G' decreases faster than G'' so that a crossover temperature (T_{cross} , where G' equals G'') is shown: for higher temperatures the samples have a

pseudoplastic fluid. T_{cross} is therefore the transition temperature at which the sample changes from solid-like (rigid, with a response mainly elastic) to viscoelastic material (with a higher mechanical response). The typical behavior of G' and G'' as a function of temperature is reported in Fig. 6 (right panel) for the sample additivated with LCS chosen as representative.



ig.6: $\tan \delta$ (left panel) and G^* (right panel) as a function of temperature 446

Table 2: Data derived from the analysis of rheological tests.

ADDITIVE	$G' @ 25^\circ\text{C}$ (Pa)	T^* ($^\circ\text{C}$)	T_g ($^\circ\text{C}$)	Activation energy η^* (kJ mol^{-1})
none	267000	61.4	-4	121
P2KA	151000	57.6	-6	120
PPA	430000	111	-26	96
LCS	129000	70.5	-4	112
octadecylamine	120000	60.4	-6	115
oleic acid	130000	56.7	-11	116
4-acetamidophenol	387000	61.3	-6	105

Finally, the effect of temperature allows the Arrhenius analysis. When conducting a temperature sweep experiment (increasing temperature while maintaining steady oscillatory strain and frequency), the activation energy E_a may be calculated over a limited temperature range by substituting the complex

viscosity (η^* , the ratio of G^* to frequency i.e. $\eta^* = G^*/\omega^{45}$) and absolute temperature (T) in the Arrhenius equation:

$$\eta^* = A \exp\left(\frac{E_a}{RT}\right) \quad (\text{eq. 4})$$

where A is the pre-exponential factor and R is the gas constant, $8.314 \text{ J K}^{-1} \text{ mol}^{-1}$. E_a is proportional to the slope of the line in the Arrhenius plot of $\ln \eta^*$ versus $1/T$.

Since η^* represents the resistance to flow under oscillatory shear conditions, E_a represents the activation energy to overcome for flowing to occur. Whereas the measurement of G' and G'' yields information on the strength of the intermolecular network in bitumen, E_a quantitates how quickly the structure degrades with heating.

The E_a values are consistent with the other derived quantities. G' @25°C, T^* , and T_g and E_a values are reported in table 2.

By perusal of the data it can be seen that organic molecules characterized by an alkyl chains and apolar (LCS, octadecylamine, oleic acid, P2KA) tend to lower the rigidity of the bitumen. This effect can be interpreted as a consequence of the lowering of the inter-clusters interactions exerted by the additive which, with their mostly apolar nature, preferentially tend to soften the maltene matrix. It can be claimed that such organic molecules are located within the maltene matrix. On the contrary, PPA, which has an acidic and consequently polar nature, leads to an opposite effect (induces an increase in G') probably due to their polar interactions with the asphaltene clusters. For such molecule a direct interactions with the polar groups of asphaltene is expected. Its effect on the bitumen structure is exerted on the size of the supra-aggregates made by clusters of asphaltene cluster: both $\Delta 1$ and $\Delta 2$ are lower revealing a reduced size of such supra-aggregates. Moreover the d_1 and d_2 values are higher, indicating that the density of its building blocks (the asphaltene clusters) is lower. The resulting structural effect is to increase the number and density of supra-aggregates and therefore the overall maltene/asphaltene interface which in turn gives enhanced G' . The findings are in agreement with a previous paper²³, where, by a deep rheological analysis, it was observed that the PPA reduces micellar aggregate size increasing the surface to volume ratio and that these structures are connected in a sort of network.

These clues also explain the results by Y. Edwards et al. who found a high stiffening effect when adding commercial wax or polyphosphoric to bitumen in a wide range of temperatures, without furnish any correlation with the structure of the system^{46,47}.

In this case the effect of PPA appears more pronounced than that observed in previous investigations^{48, 4, 23}. We attribute this phenomenon to the strong reactivity of the PPA on this particular bitumen making the precise characterization of temperature of transitions not completely reproducible. However, it must be pointed out that PPA general behavior of strongly decreasing T_g and strongly increasing T^* is confirmed.

Accordingly, 4-acetamidophenol, through its polar atoms, has also the effect of increasing G' although at a minor extend due a less polar nature than PPA. For this molecule the overall interface increase is exerted by its fractal structure formed by the uni-directional disposition of asphaltene clusters.

These effects of the additives have their repercussions also in the value of T^* : P2KA, octadecilamine and oleic acid lower the T^* value and PPA increases it. Generally, the additive effect on $G'@25^\circ\text{C}$ is correlated with that on T^* . The eventual slight deviation of LCS which slightly lowers $G'@25^\circ\text{C}$ but slightly increases T^* can be justified by the different behavior with temperature of this molecule with respect to the other additives. The T_g is usually comprised by -4°C and -10°C revealing a not marked effect of the additive, with the only exception of PPA for which a quite low T_g has been found (-26°C). This particularly low value is in accordance with the peculiar rheological properties of PPA-additivated bitumens⁴⁸. The activation energy for flowing to occur is of the order of a hundred kJ mol^{-1} . PPA tends to lower it to about 96 kJ mol^{-1} consistently with its marked effect on the structure. Acidic additives seem to increase the rigidity and lower the activation energy: it can be argued that the acidic additives interacts with the asphaltene clusters tending to increase their inter-particles interactions thus smoothing the potential well during their flow in the interpretation of the two-wells potential (Arrhenius) model for the viscosity. As for octadecilamine, oleic acid and 4-acetamidophenol, they generally lower the activation energy. Since these molecules have both polar and apolar parts within their molecular architecture, they can be considered as moderate amphiphilic. So, they are expected to act as weak surfactants binding the asphaltene clusters by their polar moiety and interacting with the maltene phase via their apolar tails. This justifies their effect in lowering the activation energy of flow.

4 CONCLUSIONS

Wide Angle X-ray Scattering (WAXS) and Atomic Force Microscopy (AFM) measurements have permitted to investigate the details of the complex structure of bare and six addivated bitumens. The results have pointed out that this technique is well suited for the study of such systems highlighting the presence of asphaltene stacks of about 18 Å, in turn organized at higher levels of complexity forming anisotropic aggregates of about 200 Å × 28 Å which, again, are assembled to form micrometer-size elongated aggregates characterized by the so-called bee-structure. Also, WAXS analysis has permitted to show the influence of the various additives (Organosilane, Polyphosphoric, Phospholipids, Acetamidophenol, Oleic Acid, octadecylamine at constant content of 2% wt/wt) on this structure and on the rheological properties. The additive effects have been attributed mainly to their preferential localization in the maltene phase or close to the asphaltene cluster, depending on the additive polarity, leading to a change of overall asphaltene/maltene interfacial area with final repercussions on the rigidity (G').

Interestingly, 4-acetamidophenol was found to maintain unaltered the characteristic distance of its building blocks, but, triggering a 1D fractal aggregation of asphaltene clusters, it confers high rigidity through the consequent enhanced asphaltene/maltene interfacial area.

The present study, giving knowledge of the detailed effects of additives on the nanoscopic and mesoscopic structure of the bitumen, constitute through the correlation with the rheological properties, the first step for opening the door to the piloted design of new bitumens with desired properties for *ad-hoc* uses.

ACKNOWLEDGEMENTS

Financial support from "MERA VIGLIE" Project, POR CALABRIA FESR-FSE 2014-2020 is gratefully acknowledged.

REFERENCES

- ¹ Rozeveld, S.; Shin, E.; Bhurke, A.; France, L.; Drzal, L. Network morphology of straight and polymer modified asphalt cements. *Microsc. Res. Tech.* **1997**, *38*, 529–43.
- ² Lesueur D. The colloidal structure of bitumen: Consequences on the rheology and on the mechanisms of bitumen modification. *Adv. Colloid. Interface Sci.* **2009**, *145*, 42–82.
- ³ Filippelli, L.; Gentile, L.; Oliviero Rossi, C.; Ranieri, G. A.; Antunes, F. E. Structural change of bitumen in the recycling process by using rheology and NMR. *Industrial & Engineering Chemistry Research* **2012**, *51*, 16346–16353.
- ⁴ Gentile, L.; Filippelli, L.; Oliviero Rossi, C.; Baldino, N.; Ranieri, G. A. Rheological and H-NMR spin–spin relaxation time for the evaluation of the effects of PPA addition on bitumen. *Molecular Crystals and Liquid Crystals* **2012**, *558(1)*, 54–63.
- ⁵ Hurley, G. C.; Prowell, B. D. Evaluation of potential processes for use in warm mix asphalt. *Journal of the Association of Asphalt Paving Technologists* **2006**, *75*, 41–90.
- ⁶ Silva, H. M. R. D.; Oliveira, J. R. M.; Ferreira, C. I. G.; Pereira, P. A. A. Assessment of the performance of warm mix asphalts in road pavements. *International Journal of Pavement Research and Technology* **2010**, *3*, 119–127.
- ⁷ Hakseo, K.; Soon-Jae, L. Rheology of warm mix asphalt binders with aged binders. *Construction and Building Materials* **2011**, *25*, 183–189.
- ⁸ Jamshidia, A.; Hamzaha, M. O. Performance of warm mix asphalt containing Sasobit®: State-of-the-art. *Construction and Building Materials* **2013**, *38*, 530–553.
- ⁹ Altgelt, K. H.; Boduszynski, M. M. *Composition and Analysis of Heavy Petroleum Fractions*; Marcel Dekker: New York, **1994**; Chapter 2
- ¹⁰ Calandra, P.; Caschera, D.; Turco Liveri, V.; Lombardo, D. How self-assembly of amphiphilic molecules can generate complexity in the nanoscale. *Colloids and Surfaces A: Physicochemical and Engineering Aspects* **2015**, *484*, 164-183.
- ¹¹ Lu, I.; Isacson, U. Influence of styrene-butadiene-styrene polymer modification on bitumen viscosity. *Fuel* **1997**, *76(14–15)*, 1353-1359.
- ¹² Y. Edwards Influence of Waxes on Bitumen and Asphalt Concrete Mixture Performance. *Road Materials and Pavement Design* **2009**, *10(2)*, 313-335. DOI: 10.1080/14680629.2009.9690197)
- ¹³ Senise, S.; Carrera, V.; Navarro, F. J.; Partal, P. Thermomechanical and microstructural evaluation of hybrid rubberised bitumen containing a thermoplastic polymer. *Construction and Building Materials* **2017**, *157*, 873-884
- ¹⁴ Oliviero Rossi, C.; Ashimova, S.; Calandra, P.; De Santo, M. P., Angelico, R. Mechanical Resilience of Modified Bitumen at Different Cooling Rates: A Rheological and Atomic Force Microscopy Investigation *Applied Science* **2017**, *7(8)*, a.n. 779; doi:10.3390/app7080779
- ¹⁵ Remišová, E.; Holý M. Changes of Properties of Bitumen Binders by Additives Application. *IOP Conf. Series: Materials Science and Engineering* **2017**, *245*, 032003. doi:10.1088/1757-899X/245/3/032003

-
- ¹⁶ Abdullin, A. I.; Idrisov, M. R.; Emelyanycheva, E. Improvement of thermal-oxidative stability of petroleum bitumen using "overoxidation-dilution" technology and introduction of antioxidant additives. *Petroleum Science and technology* **2017**, *35(18)*, 1859-1865.
- ¹⁷ Jäger, A.; Lackner, R.; Eisenmenger-Sittner, C.; Blab, R. Identification of Microstructural components of bitumen by means of Atomic Force microscopy (AFM). *Proc. PAMM Appl. Math. Mech.* **2004**, *4*, 400-401]
- ¹⁸ Handle, F.; Füssl, J.; Neudl, S.; Grosseegger, D.; Eberhardsteiner, L.; Hofko, B.; Hospodka, M.; Blab, R.; Grothe, H. The bitumen microstructure: a fluorescent approach. *Materials and Structures.* **2016**, *49*, 167-180
- ¹⁹ Zhang, F.; Hu, C.; Zhang, Y. Influence of poly(phosphoric acid) on the properties and structure of ethylene-vinyl acetate-modified bitumen, *Journal of Applied Polymer Science* **2018**, *135*, 46553]
- ²⁰ Xu, X.; Yu, J.; Xue, L.; Zhang, C.; He, B.; Wu, M.; Structure and performance evaluation on aged SBS modified bitumen with bi- or tri- epoxy reactive rejuvenating system *Construction and building materials*, **2017**, *151*, 479-486
- ²¹ Kuang, D.; Ye, Z.; Yang, L.; liu, N.; Lu,Z.; Che, H. "Effect of Rejuvenator Containing Dodecyl Benzene Sulfonic Acid (DBSA) on Physical Properties, Chemical Components, Colloidal Structure and Micro-Morphology of Aged Bitumen" *Materials* **2018**, *11(8)*, 1476; <https://doi.org/10.3390/ma11081476>]
- ²² Oliviero Rossi, C.; Caputo, P.; Baldino, N.; Szerb, E. I.; Teltayev, B. Quantitative evaluation of organosilane-based adhesion promoter effect on bitumen-aggregate bond by contact angle test. *International Journal of Adhesion & Adhesives* **2017**, *72*, 117–122.
- ²³ Baldino, N.; Gabriele, D.; Lupi, F. R.; Oliviero Rossi, C.; Caputo, P.; Falvo, T. Rheological effects on bitumen of polyphosphoric acid (PPA) addition. *Construction and Building Materials* **2013**, *40*, 397–404.
- ²⁴ Cesare Oliviero Rossi, Caputo, P.; Loise, V.; Miriello, D., Teltayev, B.; Angelico, R. Role of a food grade additive in the high temperature performance of modified bitumens. *Construction and Building Materials* **2012**, *36*, 592–596.
- ²⁵ Read, J.; Whiteoak, D. *The Shell Bitumen Handbook*, 5th ed.; Hunter, R.N., Ed.; Thomas Telford Publishing: London, UK, 2003
- ²⁶ Zhang, J., Liu, G.; Xu, L.; Pei, J. Effects of WMA Additive on the Rheological Properties of Asphalt Binder and High Temperature Performance Grade. *Advances in Materials Science and Engineering*, **2015**, Article ID 467891, 7 pages <http://dx.doi.org/10.1155/2015/467891>
- ²⁷ Shaffie, E.; Arshad, A. K.; Alisibramulisi, A.; Ahmad, J.; Hashim, W.; Abd Rahman, Z.; Jaya, R.P. Effect of mixing variables on physical properties of modified bitumen using natural rubber latex. *International Journal of Civil Engineering and Technology.* **2018**, *9(7)*, 1812–1821, Article ID: IJCIET_09_07_193
- ²⁸ Yoon, S.; Durgashanker Bhatt, S.; Lee, W.; Lee, H. Y.; Jeong, S.Y.; Baeg, J.-O.; Wee Lee, C. Separation and characterization of bitumen from Athabasca oil sand. *Korean J. Chem. Eng.* **2009**, *26*, 64-71.
- ²⁹ Remišová, E.; Zatkalíková, V.; Schlosser F. Study of Rheological Properties of bituminous binders in middle and high temperatures . *Civil and Environmental Engineering* **2016**, *12(1)*, 13-20 DOI: 10.1515/cee-2016-0002.
- ³⁰ H. A. Barnes, J. F. Hutton, K.Walters, *An introduction to rheology*. Amsterdam: Elsevier Science; **1989**.

-
- ³¹ Antunes, F.; Gentile, L.; Rossi, C.O.; Tavano, L.; Ranieri, G.A. Gels of Pluronic F127 and nonionic surfactants from rheological characterization to controlled drug permeation. *Colloids Surf. B Biointerfaces* **2011**, *87*, 42–48.
- ³² Sheu, E. Y.; Storm, D. A. Colloidal properties of asphaltenes in organic solvents. *Asphaltenes: Fundamentals and Applications*, E.Y. Sheu, O.C. Mullins (Eds), Plenum Press, New York City **1995**, Chap.1
- ³³ Charlesby, A.; Finch, G. I.; Wilman H. The diffraction of electrons by anthracene. *Proc. Phys. Soc.* **1939**, *51*, 479-528.
- ³⁴ Calandra, P.; Turco Liveri, V.; Ruggirello, A. M.; Licciardi, M.; Lombardo D.; Mandanici, A. Anti-Arrhenian behaviour of conductivity in octanoic acid–bis(2-ethylhexyl)amine systems: a physico-chemical study. *Mater. Chem. C* **2015**, *3*, 3198-3210.
- ³⁵ Calandra, P.; Mandanici, A.; Turco Liveri, V.; Self-assembly in surfactant-based mixtures driven by acid–base reactions: bis(2-ethylhexyl) phosphoric acid– n-octylamine systems. *RSC Adv.* **2013**, *3*, 5148–5155.
- ³⁶ Calandra, P.; Turco Liveri, V.; Riello, P.; Freris, I.; Mandanici A. Self-assembly in surfactant-based liquid mixtures: Octanoic acid/Bis(2-ethylhexyl)amine systems. *J. Coll. Interf. Sci.* **2012**, *367*, 280–285.
- ³⁷ Calandra, P.; Ruggirello, A. M., Mele, A.; Turco Liveri, V. Self-assembly in surfactant-based liquid mixtures: Bis(2-ethylhexyl)phosphoric acid/bis(2-ethylhexyl)amine systems. *J. Coll. Interf. Sci.* **2010**, *348*, 183–188.
- ³⁸ Nagana Gowda, G. A.; Chen, H.; Khetrapal, C. L.; Weiss, R. G. Amphotropic Ionic Liquid Crystals with Low Order Parameters. *Chem. Mater.* **2004**, *16*, 2101-2106.
- ³⁹ Tanaka, R.; Sato, E.; Hunt, J. E.; Winans, R. E.; Sato, S.; Takanoashi, T. Characterization of Asphaltene Aggregates Using X-ray Diffraction and Small-Angle X-ray Scattering. *Energy & Fuels* **2004**, *18*, 1118-1125.
- ⁴⁰ Glatter, O.; Kratky, O. *Small-Angle X-ray Scattering*; Academic Press: London, **1982**.
- ⁴¹ Schmidt, P. W. In: *The Fractal Approach to Heterogeneous Chemistry: Surface, Colloids, Polymers*; Avnir, D., Ed.; Wiley: Chichester, U.K., **1989**.
- ⁴² Dickie J.P; Yen, T.F. Macrostructures of the Asphaltic Fractions by Various Instrumental Methods” *Analytical Chem.* **1967**, *39(14)*, 1847-1852
- ⁴³ Tanaka, R.; Hunt, J. E.; Winans, R. E.; Thiyagarajan, P.; Sato, S.; Takanoashi, T. Aggregates Structure Analysis of Petroleum Asphaltenes with Small-Angle Neutron Scattering. *Energy Fuels* **2003**, *17*, 127-134.
- ⁴⁴ Yousefi A.A. Rubber-Modified Bitumens. *Iran. Polym. J.* 2002, *11(5)*, 303-309
- ⁴⁵ Macosko, C.W. *Rheology: Principles, Measurements, and Applications*” **1994** Wiley Publishing USA ISBN: 978-0-471-18575-8
- ⁴⁶ Edwards,Y.; Tasdemir, Y.; Isacssonc, U. Rheological effects of commercial waxes and polyphosphoric acid in bitumen 160/220 – high and medium temperature performance. *Construction and Building Materials*, **2007**, *21*, 1899-1908.
- ⁴⁷ Edwards,Y.; Tasdemir, Y.; Isacssonc, U. Rheological effects of commercial waxes and polyphosphoric acid in bitumen 160/220—low temperature performance. *Fuel*, **2006**, *85*, 989-997.

⁴⁸ Baldino, N.; Gabriele, D.; Oliviero Rossi, C.; Seta, L.; Lupi, F.R.; Caputo, P. Low temperature rheology of polyphosphoric acid (PPA) added bitumen. *Constr. Build. Mater.* **2012**, 36, 592–598.

Chapter 11

A new eco friendly rejuvenator and differentiation between a real rejuvenator and a softener for bitumens by means NMR techniques

Abstract: The potentialities of a new low cost, non-toxic and eco-friendly biocompatible additive on aged bitumen are explored for the first time as bitumen rejuvenator, by means of advanced rheological and NMR measurements. Fresh, aged, and doped aged bitumen have been investigated. The structural differences between the types of bitumen were assessed in order to understand the role of the proposed additive. As a novel approach to observe the real rejuvenating effect of the potential additive, an inverse Laplace transform of the NMR spin-echo decay (T_2) was applied. The new rejuvenator helps rearrange the structure of the aged bitumen (aiming at the original one), thus restoring the requested workability and elasticity of the binder.

Keywords: Aged Bitumen, Rejuvenator, Rheological properties, ILT, Nuclear Magnetic Resonance (NMR) spectroscopy

1. Introduction

The main use of bitumen is as a binder for mineral aggregates to produce asphalt mixes. Aging and adverse climatic events cause severe degradation phenomena and require the pavement replacement after a certain time in use [1]. However, the waste asphalt mixture contains valuable asphalt binder. The aged bitumen from this reclaimed asphalt pavement has a lower penetration and is more viscous than when first mixed [2].

The regeneration methods employed include the addition of fresh binder, softer than those typically used to produce hot mixes, or the use of some vegetable oils [3]. However, often the action of the vegetable oil only softens hard bitumen bringing it to match the macroscopic mechanical parameters, but does not have a regenerating action. Indeed, as is well known, the mechanism of bitumen aging, high temperatures used during production, storage, transport and laying (Short-Term Aging), involves volatilization and oxidation reactions of complex organic compounds in the bitumen, which lead to changes in the molecular structure [4]. Moreover, the aging process continues throughout the service life of the road pavement by oxidation processes also caused by atmospheric oxygen and UV radiation (Long-Term Aging) [5]. Oxidation leads to an increased fragility and, consequently, a decreased fatigue resistance involving the development of cracks in the asphalt layer [6,7]. Therefore, the regeneration of the aged bitumen is erroneously correlated with balancing penetration and softening point or viscosity.

A real rejuvenator modifies the chemical and physical structure of aged bitumen while reducing the rigidity of the bitumen [8]. Thus, rejuvenators can be used to restore the aged binder properties to its original state, playing a crucial role in the bitumen recycling method, by ensuring the reusing of aged bitumen and a good performance of the reclaimed bitumen.

Unfortunately, the rejuvenator mixtures have significant variability in terms of physical and chemical properties [9], and their behaviour and especially their action on the supramolecular structure arrangement of the bitumen is not well known yet [10].

The bitumen can be depicted as a colloidal model where asphaltenes (dispersed phase) and maltenes (continuous phase) are the constituents in bituminous materials [11]. Using this model, the present research study describes the physical chemical characteristics of a new green rejuvenator (HR) developed during our research activity, focusing on the understanding of the physical–chemical interactions between a real regenerating substance and a simple vegetable oil (VO) and bitumen. Two different bitumen's were employed and, in an attempt to have more data, two different aging acknowledged methods were used for the bitumen [12].

URL: <http://mc.manuscriptcentral.com/rmpd> Email: TRMP-peerreview@journals.tandf.co.uk

The rejuvenator HR is prepared by a direct reaction between oleic acid and urea, both low cost and green materials. All the prepared mixtures are listed and labelled in Table 1. Labels are indicating the samples which will be carried forward throughout the text.

Table 1: Investigated Samples

Kazak bitumen: Penetration grade 100/130	As made
Base bitumen	Sample KA
PAV bitumen	Sample KB
PAV bitumen + 2wt% VO	Sample KC
PAV bitumen + 2wt% HR	Sample KD
Arabia Saudi bitumen: Penetration grade 50/70	As made
Base bitumen	Sample SA
RTFOT bitumen	Sample SB
RTFOT bitumen+ 2wt% VO	Sample SC
RTFOT bitumen+ 2wt% HR	Sample SD

All the bitumens were characterized by rheological tests and NMR. The inverse Laplace transform to the spin-echo decay (T_2) was carried out. Thus, the efficiency of the NMR technique as an effective technique to highlight the difference between a flux agent (softener) and a real rejuvenator will be highlighted.

2. Experimental

2.1. Chemicals and materials

Two independent virgin bitumens from different sources are tested in this work: one with a penetration grade 100/130, produced in Kazakhstan and supplied by Kazakhstan Highway Research Institute (Almaty, Kazakhstan) and the second one with a penetration grade 50/70 sourced from Saudi Arabia and supplied by Loprete Costruzioni Stradali (Terranova Sappo Minulio, Reggio Calabria, Italy). The Vegetable Flux Oil (VO) was provided by Kimical SRL (Rende, Italy), Oleic acid and Urea were provided by Sigma Aldrich (Milan, Italy).

2.2 Sample preparations

The modified bitumen was prepared by using a high shear mixing homogenizer (IKA model, USA). Firstly, bitumen was heated up to $150 \pm 5^\circ\text{C}$ until it flowed fully, then a given part of HR or VO (2%

of the weight of the base bitumen) was added to the melted bitumen under a high-speed shear mixer of 400 to 600 rpm/min. Furthermore, the mixture was kept under mechanical stirring at 150°C for 10 minutes in a closed beaker to avoid oxidation. After mixing, the resulting bitumen was poured into a small sealed can and then stored in a dark chamber thermostated at 25°C to retain the obtained morphology.

Urea was added to Oleic acid previously heated to 140°C. The mixture was further stirred for 3 hours. During this time, the colour changed from pale yellow to dark brown. At the end of the reaction, the warming was stopped and the mixture was stirred until cooling. The final product, recovered without any work-up or treatment, it resulted in a liquid form without the presence of precipitates. There is no carcinogenic risk of each component and it can be carried safely by operators.

Our research group remains at the disposition of interested parties for any technical advice on how to use the HR range for regeneration of aged bitumen.

2.2.1 Aging

RTFOT method (Saudi Arabia bitumen): According to ASTM D2872-04, the simulation of bitumen aging is carried out with Rolling Thin-Film Oven Test (RTFOT) [7]. Accordingly, a moving film of bitumen was heated in an oven for 85 min at 163°C. The aging of bitumen is determined from changes in its physical and rheological properties, as measured before and after the oven treatment.

In this article, the same procedure (i.e. the RTFOT) was lengthened up to 225 min to acquire an ideal bitumen with a penetration grade 30/45, therefore making a quite-stiff material (sample SB, see Table 2) in order to simulate a different aging process with separated SARA fractions [13]. **PAV method** (Kazakhstan bitumen): With the Pressure Aging Vessel (PAV), the bitumen was simulated to in-service aging of the base bitumen after 5 to 10 years [7]. The binder was subjected to high pressure and heat for 20 hours to give the effect of long-term oxidative aging. The apparatus was made up of a stainless-steel pressure container with encased band heaters and its own pressure and heat controls. A platinum resistance thermometer measures the internal test temperature to $\pm 0.1^\circ\text{C}$. Selectable test temperatures (standard 90/100/110°C) are controlled with a precision of $\pm 0.2^\circ\text{C}$. Pressure is monitored by transducer and controlled at 2.1 ± 0.1 MPa. Temperature and pressure calibration were executed. The procedure was referenced according to AASHTO/ASTM T179.

2.2.2 Asphaltene determination

Asphaltenes were isolated from bitumens in the manner described elsewhere. [14]

2.3 Empirical Characterization.

The bitumen softening temperature (R&B T, ring and ball temperature) is determined with the ring and ball test (ASTM Standard D36) [15, 16].

The bitumen consistency was evaluated by measuring the penetration depth (of a stainless-steel needle of standard dimensions under determinate charge conditions (100 g), time (5 s) and temperature (25 °C), according to the standard procedure (ASTM D946) [15, 16].

2.4 Rheological characterization

Dynamic Shear Rheological (DSR) measurements on bitumen samples were carried out using a controlled shear stress rheometer (SR5, Rheometric Scientific, USA) equipped with a parallel plate geometry (gap 2 mm, $\phi = 25$ mm within the temperature range 25-150 °C, gap 2 mm, $\phi = 8$ mm within the temperature range from 25 to -20 °C) and a Peltier system (± 0.1 °C) for temperature control. Dynamic experiments were performed within the linear viscoelastic region where measured material features are independent of the amplitude of applied load and are the only function of microstructure of material [17, 18].

Aimed at investigating the material phase transition, temperature sweep tests were performed at 1 Hz with heating rate 1°C/min and applying the proper stress values to guarantee linear viscoelastic conditions (previously determined by stress sweep tests) at all tested temperatures.

More details about the mechanical characterization can be found elsewhere [19]

2.5 NMR measurement and Inverse Laplace Transform (ILT).

Relaxation experiments were effected at 15°C lower than transition temperature (sol-liquid) each where each sample underwent a dynamic temperature ramp test experiment by means of a custom- built NMR instrument that operates at a proton frequency of 15 MHz.

A CPMG sequence with an interpulse time of 160 μ s provided the T_2 decay signal. The CPMG signals were made up of 400 echoes, with 128 averages, which provided a signal-to-noise level of circa 500 [20]. Heterogeneity usually causes the T_2 relaxation time to vary all over the sample, surface relaxation effects other than magnetic field in homogeneities [21]. Therefore, in general the obtained NMR signal is analyzed in terms of sum exponentials, or, more realistically, allowing a continuous distribution of relaxation times to be observed [22]. Hence, if there is a continuous distribution of relaxation time inside the sample, the amplitude A_n of the n^{th} echo in the echo train is given by:

$$A_n = A_0 \int_0^{\infty} P(T_2) e^{-2n\tau/T_2} dT_2 \quad (1)$$

where A_0 is a constant, τ is the half echo time and $P(T_2)$ is the ILT of the unknown function that fits the echo amplitude curve. Moreover, $P(T_2)$ can be seen to be a distribution of rate (inverse of time) constant. Expressly, a probability density function (PDF) which, in addition, could explain the different macro-structures composing the bitumen binder [23].

In this paper, ILT computation was operated by means of UpenWin, which is a Windows software written in C++ and released by the University of Bologna, which implements the UPEN algorithm [24]. UPEN allows obtaining distributions of relaxation time without multiple peaks which does not require separation by the data to prevent physical misinterpretation of data [25].

3. RESULTS AND DISCUSSION

3.1 Mechanical behaviour

The hard consistency of the samples is strongly affected by aging processes. This is as a result of the oxidized aged bitumen. During the oxidative aging, the concentration of polar functional groups becomes high enough to render inactive an excessive number of molecules through intermolecular association. Furthermore, the molecules or molecular agglomerates lose enough mobility to flow past one another under thermal or mechanical stress. The resulting embrittlement of the asphalt makes it susceptible to fracturing or cracking and resistant to healing. After that, the penetration depth decreases according to the additives content and the aging steps as long as on the contrary, the softening points escalate. Finally, the viscoelastic-liquid transition temperatures step-up with the aging process.

Using standardized tests, the penetration depth (PN), softening point (R&B) and the asphaltene content were determined (Table 2).

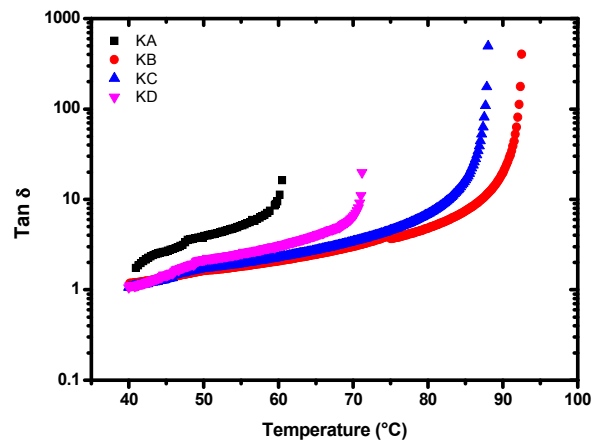
Table 2. Physical chemical parameters of investigated samples

Sample	PN (mm) Penetration depth ± 1	R&B (°C) Softening point ± 1	X_A (wt%) Asphaltene content ± 0.5	T (°C) transition ± 0.1
Sample KA	110	44	32.9	60,7
Sample KB	47	59	35.6	124,7
Sample KC	57	49	31.3	88,0
Sample KD	60	52	32.1	71,2
Sample SA	60	51	26.8	70,0
Sample SB	19	62	39.0	84,9
Sample SC	27	59	33.9	78,2
Sample SD	24	56	34.6	79,0

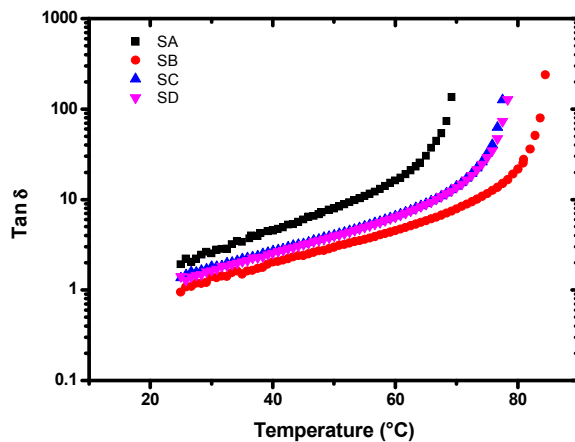
Although each bitumen displays a unique role, a good correlation exists between bitumen hardness and asphaltenes content for each of the investigated bitumens. Some points can be inferred from the data in Table 2. The asphaltenes fraction seems to be the dominant component that is controlling hardness of the bitumen. The asphaltene content increases with the aging step. These empirical data do not allow distinguishing the real efficiency of the rejuvenator.

3.2. Rheology

Rheology temperature-sweep experiments have been exploited to obtain some information on the structural changes induced by temperature, trying to better define a transition temperature range. In fact, in this experiment, the evolution of the loss tangent ($\tan\delta$) is monitored continuously during a temperature ramp at a constant heating rate ($1^\circ\text{C}/\text{min}$) and at a frequency of 1 Hz. In Figure 1, the time cure tests of Kazak and Saudi bitumens are shown.



a)



b)

Fig. 1. Semi-log plot of high temperature ramp test for a) KA; KB; KC and KD and b) SA, SB, SC and SD. Left axis: loss tangent, $\tan \delta$.

The transition temperature is evidenced when the loss tangent ($\tan \delta$) is plotted as a function of temperature. The initial trend is almost linear with temperature, when the material mainly behaves like a viscoelastic system. The subsequent sharp increase occurs in correspondence to the transition toward a liquid-like behaviour ($\tan \delta$ diverges). Even though the typical trend is quite similar for the different samples, a discrepancy in transition temperatures is clearly obtained.

The aged bitumens (samples KB and SB) show much higher transition temperatures than the fresh material. This effect is due to an increased fraction of asphaltenes resulted from oxidation of the soft unsaturated organic part. This asphaltene enrichment causes a stronger rigidity and connectivity when compared to the less dense network of the virgin bitumen where the asphaltene domains are poorly connected to each other.

Both VO and HR induce a shift toward lower transition temperatures from the viscoelastic to the liquid regime compared to the aged bitumen (Table 2). In another way, they also inflate the values of loss tangent, thus establishing the system more viscous than the simply aged binder. For the Kazak system, on the contrary of VO, the additive HR has an enormous effect in terms of loss of rigidity. This additive possesses an amphiphilic nature. We believe that this behaviour might reduce the associative interactions between the asphaltene particles by interposing itself between the asphaltenes and the maltenes. This phenomenon might be alike to the one found in the deactivation of hydrophobic cross-links in hydrophobically modified polymers by surfactants [24].

As a result, the colloidal network can be weakened, which in turn may express a rise to a lowering of the transition temperature.

For the Saudi system, both VO and HR influence a shift toward lower transition temperatures, but in this case VO and HR present very similar trends of $\tan \delta$. This phenomenon endures a typical situation where the analysis of the mechanical properties alone is not enough to distinguish between flux effect and regeneration effect.

In Figure 2, the temperature sweep experiments at low temperatures are presented

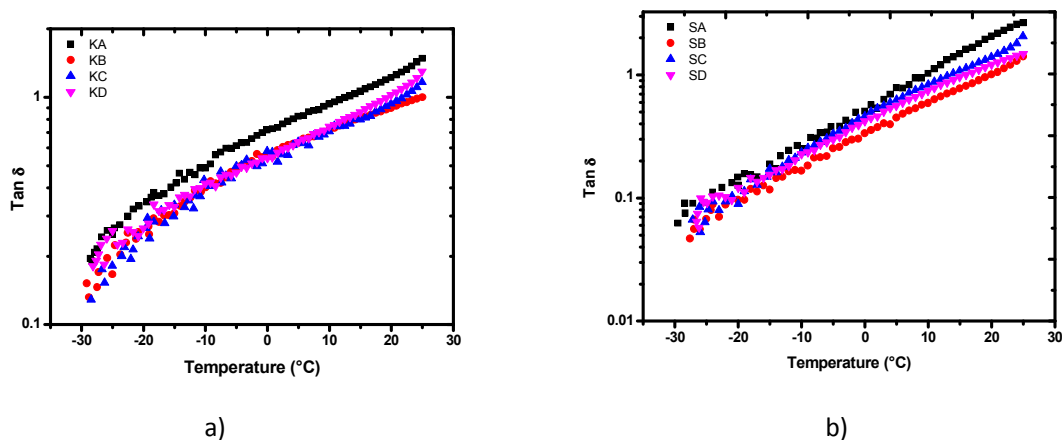


Fig. 2. Semi-log plot of low temperature ramp test for the samples a) KA; KB; KC and KD and b)SA; SB; SC and SD. Left axis: loss tangent, $\tan \delta$

Similar trends of $\tan \delta$ are observed for two kind of bitumens. The neat bitumens (KA and SA) are softer, whilst the aged (KB and SB) bitumens are harder. Considering the doped samples, the bitumen containing VO and HR reveal higher $\tan \delta$ than aged ones. The dynamic mechanical analysis at low temperature reproduces what we observed at higher temperature where it is impossible to distinguish the effect of VO and HR.

3.3 NMR study

The Inverse Laplace Transform (ILT) analysis of the NMR echo signal decay has been implied to achieve the T_2 relaxation time distributions. This technique allows finding the PDF distribution which associates with relaxation times that correspond to unrelated molecular aggregates inside the samples. The results are presented in Figures 3a and 3b, where the plots are the distribution PDF as a function of the relaxation time for the K and S bitumens are shown.

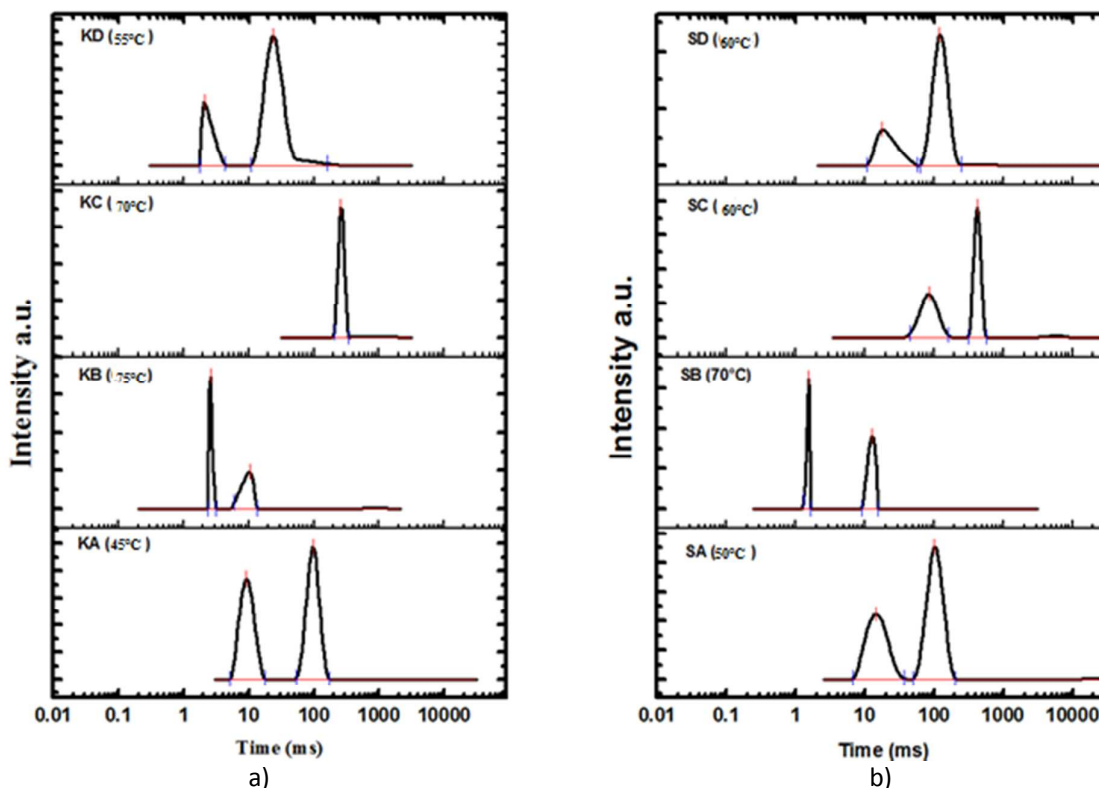


Fig. 3. ILT relaxation time distributions of K(a) and S (b) bitumen samples measured at the temperature of 15°C lower than transition temperature (sol-liquid) determined by dynamic temperature ramp test experiment for each sample

The T_2 relaxation time distribution exhibits two peaks. The shorter T_2 times (10ms) correspond to more rigid supra-molecular aggregates, hence they are attributed to asphaltenes, while longer T_2 times (100 ms) to maltene fraction. This finding supports the colloidal model of the bitumen. In fact, if the polar fluid model suggested by Anderson [26] was applicable to our system, the ILT result would demonstrate a sole broad peak referred to as a continuous T_2 time. All experiments are applied at temperature lower than 15°C which is the respective temperature transition from solid to liquid (the temperature is chosen in order to standardize the structure of all the samples).

The ILT of the aged bitumen again discloses two shifted peaks toward shorter times (more potent effect as the aging step is increased) and present profoundly distinctive shapes. This probably indicates a gradual rise of the materials rigidity with the on-going oxidation process. In particular, the asphaltene peaks are now close to 1 ms for the aged S and K bitumens.

The addition of VO and HR to the aged bitumen shift the asphaltene peaks to longer T_2 times compared with the aged bitumen. Moreover, analysing the graphics in detail, evidence of differences in the action of the two additives emerges clearly. A single peak with a higher time is the representation KC sample. This is the confirmation of the flux action of this additive and its action on the high penetration grade bitumen. Remarkably, HR and neat bitumen have similar

distribution profiles and relaxation time values, evidencing the real rejuvenator character of this additive.

For the Saudi system, the same differences between the action of the VO and HR are observed. While the addition of VO simply shifts the distribution forward a more extensive time evidencing just its softening action, the sample containing HR represents the same time distribution as the fresh bitumen.

Conclusions

This article shows the effectiveness of the HR additive for regenerating bitumen, acting as rejuvenator. This green additive is obtained by a simple method from two low-cost and eco-friendly precursors. HR tends to restore the mechanical properties of the oxidized bitumen, acting on the structure of the bitumen, having a restructuring effect on the altered colloidal network of the aged bitumen binder.

In the present work, we once more contributed to supporting the colloidal view of the bitumen structure. Moreover, the article demonstrates the necessity of testing the regenerated bitumen using structural techniques in order to distinguish between bitumen with flux or a real regenerating. Thus, bituminous systems can have like macroscopic (ring and ball) or rheological properties but unique supramolecular structure.

As expected, the fluxing action of VO reduces the temperature transitions for both systems. This can be explained by an increase of the maltene part, and we could call it “Solvent effect”. In the case of Saudi bitumen, the bitumen with flux can be mistakenly considered as a real regenerating according to the ring and ball test or rheological investigations. However, using the ILT analysis of the NMR echo signal decay, distinction between a real rejuvenator and a simple softener can be made.

References

- [1] Hofko B., Cannone Falchetto A., Grenfell J., Huber L., Lu X., Porot L., Poulidakos L. D., You Z., “Effect of short-term ageing temperature on bitumen properties”, *Road Materials and Pavement Design*, Vol. 18, 2017, p. 108-117
- [2] Bearsley S. R., Haverkamp R. G., “Age Hardening Potential of Tall Oil Pitch Modified Bitumen”, *Road Materials and Pavement Design*, Vol. 8, 2007, p. 467-481

- [3] Simonen M., Blomberg T., Pellinen T., Makowska M., Valtonen J., “Curing and ageing of biofluxed bitumen: a physicochemical approach”, *Road Materials and Pavement Design*, Vol. 14, 2013, p. 159-177
- [4] Quin Q, Schabron J.F, Boysen R.B, Farrar M.J. “Field aging effect on chemistry and rheology of asphalt binders and rheological predictions for field aging”, *Fuel*, Vol. 121, 2014, p. 86-94
- [5] Hu J., Wu S., Liu Q., García Hernández M., Wang Z., Nie S., Zhang G. “Effect of ultraviolet radiation in different wavebands on bitumen”, *Constr. Build. Mater.*, Vol. 159, 2018, p. 479-485
- [6] Baldino N, Gabriele D, Oliviero Rossi C, Seta L, Lupi F.R, Caputo P. “Low temperature rheology of polyphosphoric acid (PPA) added bitumen”, *Constr. Build. Mater.*, Vol. 36, 2012, p. 592-596
- [7] J-P Planche “Insights into binder chemistry, microstructure, properties relationships—usage in the real world”, *Asphalt Pavements*, Edited By Kim Y. R., CRC Press, 2014
- [8] Yu X., Zaumanis M., dos Santos S., Poulidakos L.D., “Rheological, microscopic, and chemical characterization of the rejuvenating effect on asphalt binders”, *Fuel*, Vol. 135, 2014, p. 162-171
- [9] Moghaddam T. B., Baaj H., “The use of rejuvenating agents in production of recycled hot mix asphalt: A systematic review”, *Constr. Build. Mater.*, Vol. 114, 2016, p.805-816
- [10] Król J. B., Kowalski K. J, Niczke L, Radziszewski P., “Effect of bitumen fluxing using a bio- origin additive and a rejuvenator”, *Constr. Build. Mater.*, Vol. 114, 2016, p. 194-203
- [11] Jin L., Xiaosheng H., Yuzhen Z., Meng X., “Bitumen Colloidal and Structural Stability Characterization” *Road Materials and Pavement Design*, Vol. 10, 2009, p. 45-59
- [12] Grilli A, Iorio Gnisci M, Bocci M., “Effect of ageing process on bitumen and rejuvenated bitumen”, *Constr. Build. Mater.*, Vol. 163, 2017, p. 474-481

[13] Baldino N, Oliviero Rossi C, Lupi F. R, Gabriele D., “Rheological and structural properties at high and low temperature of bitumen for warm recycling technology”, *Colloid and Surface A*, Vol. 532, 2017, p. 592-600

[14] Oliviero Rossi C, Caputo P, De Luca G, Maiuolo L, Eskandarsefat S, Sangiorgi C., “¹H-NMR spectroscopy: A possible approach to advanced bitumen characterization for industrial and paving applications”, *Appl. Sci.*, 2018.

[15] Altgelt K. H, Boduszynski M.M., “Composition and Analysis of Heavy Petroleum Fractions”, Marcel Dekker Inc., New York 1994.

[16] Oliviero Rossi C, Caputo P, Loise V, Miriello D, Teltayev B, Angelico R., “Role of a food grade additive in the high temperature performance of modified bitumens”, *Colloid and Surface A*, Vol. 532, 2017, p. 618-624

[17] Barnes H. A, Hutton J.F, Walters K. “An introduction to rheology”. Amsterdam, Elsevier Science, (1989).

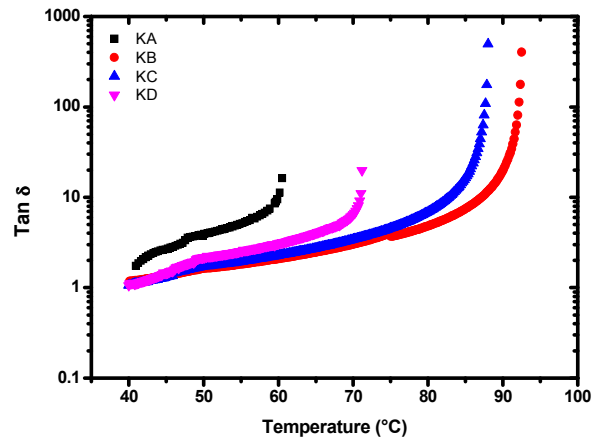
[18] Jansen J.C, Macchione M, Oliviero Rossi C, Mendichi R, Ranieri G.A, Drioli E., “Rheological evaluation of the influence of polymer concentration and molar mass distribution on the formation and performance of asymmetric gas separation membranes prepared by dry phase inversion”, *Polymer*, Vol. 46, 2005, p.11366-11379

[19] Lupi, F.R., Shakeel, A., Greco, V., Oliviero Rossi C., Baldino, N., Gabriele, D., “A rheological and microstructural characterisation of bigels for cosmetic and pharmaceutical uses”, *Materials Science and Engineering: C*, Vol. 69, 2016, p. 358-365

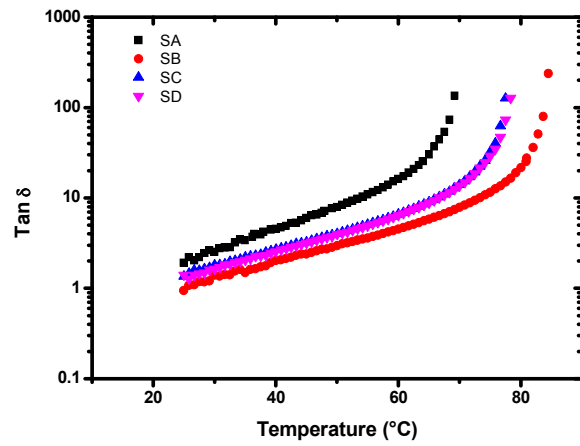
[20] Carr H.Y., Purcell E. M., “Effects of Diffusion on Free Precession in Nuclear Magnetic Resonance Experiments”, *Phys. Rev.*, Vol. 94, No. 3, 1954, p. 630-638

[20] Bilardo U., Borgia G. C., Bortolotti V., Fantazzini P., Mesini E., “Magnetic resonance lifetimes as a bridge between transport and structural properties of natural porous media”, *Journal of Petroleum Science and Engineering*, Vol. 5, 1991, p. 273-283

- [21] Gentile L., Filippelli L., Oliviero Rossi C., Baldino N., Ranieri G.A., “Rheological and H- NMR spin-spin relaxation time for the evaluation of the effects of PPA addition on bitumen”, *Mol. Cryst. Liq. Cryst.*, Vol. 558, 2012, p. 54-63
- [22] Muhammad A., Azeredo R.B.D.V., “¹H NMR spectroscopy and low-field relaxometry for predicting viscosity and API gravity of Brazilian crude oils – A comparative study”, *Fuel*, Vol. 130, 2014, p. 126-134
- [23] Bortolotti V., Brown R. J. S., Fantazzini P., “UopenWin: a software to invert multi-exponential relaxation decay data”, Distributed by the University of Bologna, villiam.bortolotti@unibo.it, 2009.
- [24] Oliviero Rossi C, Spadafora A, Teltayev B, Izmailova G, Amerbayev Y, Bortolotti V., “Polymer modified bitumen: Rheological properties and structural characterization”, *Colloid and Surface A*, Vol. 480, 2015, p. 390-397
- [25] Antunes F. E., Marques E. F., Miguel M. G., Lindman B., “Polymer–vesicle association”, *Adv Colloid Interface Sci.*, Vol. 147–148, 2009, p. 18-35
- [26] Christensen D. W., Anderson D. A., “Rheological evidence concerning the molecular architecture of asphalt cements”, *Proc. Chemistry of Bitumen 2*, Rome 1991, p. 568–595.



a)



b)

Fig. 1. Semi-log plot of high temperature ramp test for a) KA; KB; KC and KD and b) SA, SB, SC and SD. Left axis: loss tangent, $\tan \delta$.

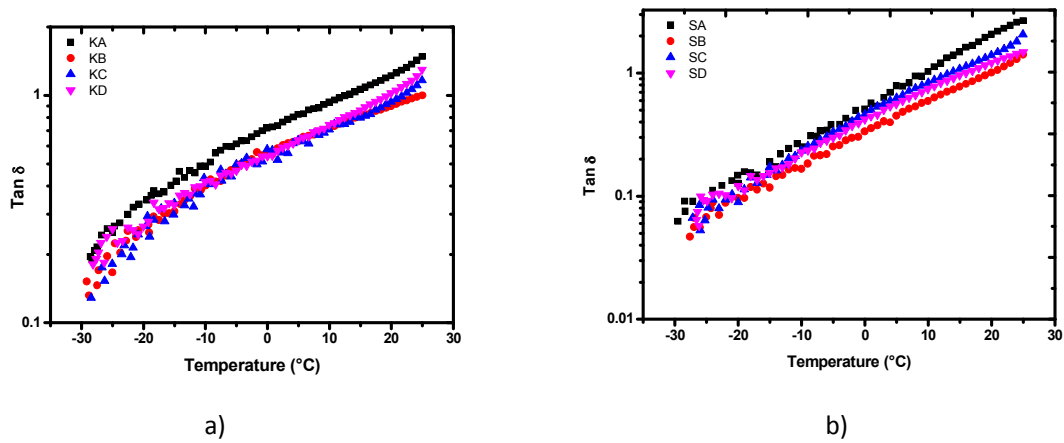


Fig. 2. Semi-log plot of low temperature ramp test for the samples a) KA; KB; KC and KD and b)SA; SB; SC and SD. Left axis: loss tangent, $\tan \delta$

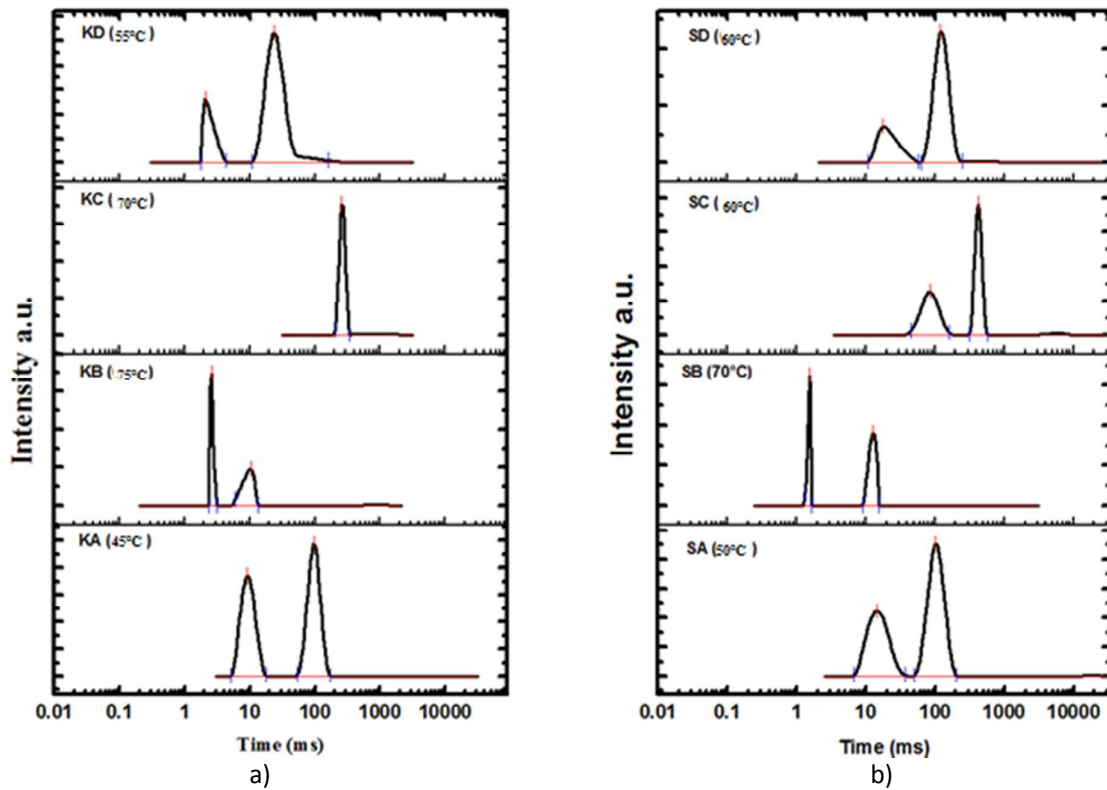


Fig. 3. ILT relaxation time distributions of K(a) and S (b) bitumen samples measured at the temperature of 15°C lower than transition temperature (sol-liquid) determined by dynamic temperature ramp test experiment for each sample

Table 1: Investigated Samples

Kazak bitumen: Penetration grade 100/130		As made
Base bitumen		Sample KA
PAV bitumen		Sample KB
PAV bitumen + 2wt% VO		Sample KC
PAV bitumen + 2wt% HR		Sample KD
Arabia Saudi bitumen: Penetration grade 50/70		As made
Base bitumen		Sample SA
RTFOT bitumen		Sample SB
RTFOT bitumen+ 2wt% VO		Sample SC
RTFOT bitumen+ 2wt% HR		Sample SD

Table 2. Physical chemical parameters of investigated samples

Sample	PN (mm) Penetration depth ± 1	R&B (°C) Softening point ± 1	X_A (wt%) Asphaltene content ± 0.5	T (°C) transition ± 0.1
Sample KA	110	44	32.9	60,7
Sample KB	47	59	35.6	124,7
Sample KC	57	49	31.3	88,0
Sample KD	60	52	32.1	71,2
Sample SA	60	51	26.8	70,0
Sample SB	19	62	39.0	84,9
Sample SC	27	59	33.9	78,2
Sample SD	24	56	34.6	79,0